## *Morphometric and immunohistochemical studies on mechanosensory innervation of the muscle spindle*

Abdulaziz Alamri

# MORPHOMETRIC AND IMMUNOHISTOCHEMICAL STUDIES ON MECHANOSENSORY INNERVATION OF THE MUSCLE SPINDLE

A thesis presented in candidature for the

Degree of Doctor of Philosophy

By

Abdulaziz Alamri, BS.MLS. (Riyadh)

SCHOOL OF BIOLOGY AND BIOMEDICAL SCIENCES

UNIVERSITY OF DURHAM UK



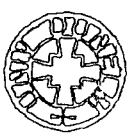



DURHAM 2004

# Abstract

The purpose of this thesis is to study aspects of the function of the primary sensory endings of muscle spindles using morphometric and immunohistochemical techniques. For morphometry the right tenuissimus muscles of three adult cats, whose right hind limbs were fixed with the hip and knee flexed at various acute angles, have been compared with the corresponding muscles from the fully extended left hind limbs of the same animals. The aim of this project is a better understanding of morphometric changes in the muscle spindle including intrafusal fibre diameter, sarcomere length, and (in particular) changes in the primary nerve endings in response to passive stretch. Immunohistochemical studies of the calcium-binding protein, calretinin, and immunogold labelling for glutamate were also carried out on the primary nerve endings as detailed below.

All the work reported in this thesis was carried out in the School of Biological and Biomedical Sciences, at the University of Durham.

## This thesis is divided into five chapters

Chapter one is an introduction to the structure and innervation of the muscle spindle and tendon organ, discussing briefly the presence of calretinin and glutamate in muscle spindle nerve endings. This provides general introduction and background to the work.

Chapter two describes the deformation of the nerve endings in the muscle spindle when the cat tenuissimus muscle is subjected to different degrees of flexion of the hip and knee on the experimental side, the control side being extended so that the angles between the hip

and the knee were approximately equal in the each case. For rapid and optimum fixation, both sides were perfused with fixative solution.

The results show morphometric changes in the experimental muscles compared with the controls in terms of diameter, sarcomere length, and sensory nerve terminal deformation. Muscle fibres in the experimental (flexed) side have a greater diameter, and shorter sarcomeres, with nerve endings more indented into the intrafusal fibres, compared with those on the extended, control side. Nuclei of the equatorial region in both the experimental and control muscles differed in arrangements of nuclei and their outline.

Chapter three discusses the calcium-binding proteins, with the emphasis on calretinin and its distribution in the nerve endings of rat muscle spindles and tendon organs as shown by histochemical examination of rat soleus muscle. The calretinin distribution was evident in the primary endings of both $bag_1$ and $bag_2$ fibres and also in the primary endings of the chain fibres, although no secondary endings or tendon organs were observed.

Chapter four describes quantitative immunological study carried out on the muscle spindle of the cat tenuissimus muscle to assess the comparative level of glutamate –like immunoreactivity in the equatorial region of the primary nerve endings, and their associated intrafusal fibres, were all found to show less glutamate –LI compared with the secondary nerve endings and their associated intrafusal fibre, but not the intrafusal fibre nuclei.

In chapter five the results are summarised, and possible further studies outlined.

# Table of Contents

# List of figures

## Chapter one



## Chapter two



## Chapte three



## Chapter four

# List of Tables

## Chapter three



## Chapter four

# List of charts

## Chapter two



## Chapter four

# Glossary and abbreviations

**Chapter two**

C866.LHS.A.B1

A – The side of section.

B1- $bag_1$.

C- Control

LHS-Left hand side.

E866.RHS.A.B1

A- Side of section.

B1-$bag_1$

C-the semi-cord.

E-experimental.

Extra-extrafusal.

Intra- intrafusal.

I –Inside radius

Mus.L muscle length

O- Outside radius

RHS- Right hand side

Sarc.Ex length of external sarcomere

Sarc.In length of internal sarcomere

Std.Dev- standard deviation.

**Chapter four**

Ext-fus-extrafusal

Glut-Glutamate

Mus- muscle

Nr-nerve

Nuc-nucleus

Prim-primary

Prim-nerve-end. Primary nerve endings.

Prim-intr-mus. Primary intrafusal muscle.

Prim-intr-nuc. Primary intrafusal nucleus.

Sec-nerve-end. Secondary nerve endings.

Sec-intr-mus. Secondary intrafusal muscle.

Sec-intr-nuc. Secondary intrafusal nucleus.

# Acknowledgements

In accomplishing this work I would like to express my gratitude to my Supervisor, Dr R. W Banks, for his constant advice, guidance and encouragement throughout the experimental phase of this study.

I also wish to thank Dr. Dave Hyde for his help and introduction to the use of Photoshop program. And my gratitude goes to Mrs. A. C. Richardson for introducing me to the electron microscope, histological techniques, and the use and application of different computer programs. My thanks are due to Mr. P. Sydney for his photographic assistance, to Mrs Heather Russell for her help with the English manuscript, and her meticulous editing. I am indebted to my family for their encouragement and support especially my wife for her encouragement and patience, throughout the period of my study. Finally I am indebted to the Saudi National Guard who was responsible for the financing and support of my scholarship.

# CHAPTER ONE

## 1. General Introduction

## Definition of the muscle spindle

Mechanoreceptors are sensory receptors which generate nerve impulses when they, or adjacent tissues, are deformed by mechanical forces such as touch, pressure (including blood pressure), vibration stretch and itch. Muscle spindles are mechanoreceptors that are sensitive to muscle length and to changes in muscle length (Marieb 2001). The muscle spindle of the frog was first noted and described by Weismann, in 1861. They are also named neuromuscular spindles by Ruffini (1893). They occur in the somatic muscles of tetrapod vertebrates and consist of bundles of small (intrafusal) muscle fibres laying in parallel with ordinary (extrafusal) muscle fibres.

A typical muscle spindle in a cat hind limb muscle consists of a 7 to 10 mm long bundle, of six to nine muscle fibres; it is richly vascularized, partly encapsulated (generally around the middle third) and innervated by a spindle nerve that leaves a nearby intramuscular nerve trunk to enter the equatorial region of the intrafusal bundle. (Banks and Barker, 2004)

## 1.2 Number and types of spindle unit

It may be estimated that the human body possesses approximately 50,000 spindles (based in data in Voss 1971). They are usually concentrated in the region where the nerve enters its associated muscle and around the subdivisions of the intramuscular nerves. They also appear to be more common among those extrafusal fibres with a high proportion of oxidative (slow oxidative; SO and fast oxidative-glycolytic; FOG) types (Gregor, 1904; Yellin, 1969). However, these features are not necessarily independent of each other.

Spindles can occur as a single unit, or in various combinations as groups or in close association with tendon organs. A single encapsulated receptor with its sensory and motor innervations is termed a spindle unit, which stresses the functional significance of this organ. Spindle units can be linked in series, when they are referred to as tandem spindles (Cooper and Daniel, 1956). They may also be combined in pairs, in which the intrafusal bundles either remain separately encapsulated or equatorially share a common capsule (Banks and Emonet-Dénand, 1996).

A spindle complex may be formed when many spindle units are linked together in tandem and compound fashion, as has been shown in the cat neck and intervertebral muscles (Richmond and Abrahams, 1975; Bakker and Richmond, 1981, 1982). The standard spindle unit comprises one $bag_1$ fibre, one $bag_2$ fibre, and about six chain fibres. However composition of any of these three types of intrafusal fibre may vary: for example, the presence of more than one $bag_2$ or the absence of the $bag_1$ fibre may be noted, most commonly in certain tandem spindle units (Barker and Ip, 1961).

## 1.3 Structure of the adult muscle spindle

The cat muscle spindle is the source of most of the studies of the structure and behaviour of mammalian spindles. The cat is a very suitable animal for experimental study because of its highly developed motor control system.

### 1.3.1. The capsule

The capsule is composed of an outer portion and a thin inner component, or axial sheath. The outer capsule consists of several layers of concentrically arranged cells enclosing the so-called periaxial space, which contain a highly viscous gel containing glycosaminoglycan hyaluronate (Brzezinski 1961; Fukami, 1986). The outer portion of

the capsule is continuous with the perineurium of the sensory nerves that supply the spindle, and like the perineurium, is made up largely of very thin flat epithelial cells connected by tight junctions (Low, 1976).

These junctions are presumably located in the inner layers of the capsule, since horseradish peroxidase (HRP) flooded directly onto the living spindle penetrates the outer layers but fails to enter the periaxial space (Kennedy and Yoon 1979); however, some leakage occurs into the poles through the open end of each capsule sleeve which indicate that the capsule tight junction prevents it elsewhere (Dow, Shinn and Ovalle 1980)

So these tight junctions act as a barrier to the diffusion of substances into the periaxial space (Kennedy *et al.*, 1979). Numerous collagen fibrils are found on the outer surface of the capsule and between all the cellular layers. The number of cell layers in the outer capsule diminishes as the capsule narrows toward its poles. They end in a single layer, usually with the end of the chain fibres closely investing the bag fibres that pass beyond it. Small blood vessels are commonly found on the outer layers of the capsule and capillaries may be enclosed between layers of the capsule (Banks and James 1973). In the rabbit these spindle capillaries are separate from those supplying the extrafusal muscle fibres and differ from them in being larger and having intercellular tight junctions. This is also the case with capillaries supplying intramuscular nerves (Kennedy and Yoon 1979). In the equatorial region, some fibrocytes from the innermost capsular layer cross the periaxial space obliquely to join other cells of the same type, thus forming the axial sheath and endomysial cells enclosing the intrafusal muscle fibres. These cells have no basement membrane, have terminal-bar tight junctions at their adjoining edges, and form more or less complete envelopes around each intrafusal muscle fibre at the equator. Towards the ends of the periaxial space, the covering becomes less complete, to enclose two or more intrafusal muscle fibres in each

compartment. Myelinated axons, collagen fibrils, loose strands of basal lamina and elastic fibres are found between these thin cellular layers.

### 1.3.2 Structure of the intrafusal fibres.

Three types of intrafusal fibre are distinguishable in mammals (Ovalle and Smith 1972; Banks, Harker and Stacey, 1977). In the cat, for example, there are usually two large nuclear-bag fibres, so called because of the central accumulation of nuclei that can be seen in a transverse section of the fibres close to the point where the fluid space is widest. In addition there are usually three to five thinner intrafusal fibres, about half the length of the nuclear-bag fibres, termed nuclear-chain fibres, because they have a single row of nuclei in the equatorial region. Each fibre is subdivided into an equatorial, two juxta-equatorial and two polar regions, which are clearly distinguishable. According to a widely accepted definition, zone A is a sensory region that includes the equatorial and both juxta-equatorial zones, whereas zone B is the intracapsular and zone C the extracapsular part of the polar regions (Boyd and Gladden, 1985; Barker and Banks, 1994). All three type of fibre become thinner as they pass through the equatorial region, but those fibres that extend well into region C tends to become thickest in this region. The presence of a secondary ending, adjacent to the primary, results in the bag fibres undergoing a marked increase in diameter at the sites where they receive secondary terminals (Banks *et al*, 1982). Nuclear-bag fibres are of two types, differing in their histochemical, ultratructural, and mechanical properties. They were first termed $bag_1$ and $bag_2$ fibres on the basis of histochemical differences (Ovalle and Smith 1972) and also termed dynamic nuclear-bag fibres $bag_1$, and static nuclear-bag fibres $bag_2$ on the basis of mechanical differences (Boyd *et al.*, 1975). In frozen sections of tenuissimus

muscle static $bag_2$ fibres usually form the longest nuclear bag, with a mean polar length of 2,947 μm for $bag_2$, 2760 μm for $bag_1$ and 1231μm for typical chains (Kucera 1982).

Nuclear-chain fibres are usually about half the diameter of the nuclear-bag fibres and they can be categorized into three types long -chain fibres, typical- chain fibres and intermediate -chain fibres. Typical-chain fibres are intracapsular, whereas long-chain and intermediate-chain fibres are not (Kucera 1980). At the polar regions intrafusal fibres are completely filled with myofibrils and possess peripheral nuclei. The fibres display a characteristic arrangement of myofibrils; they are large and confluent, the sarcoplasmic reticulum is poorly developed; and mitochondria are small and rare.

Histochemically, intrafusal fibres are similar to extrafusal fibres in varying according to fibre type, but differ from them in showing regional variation. The mammalian intrafusal muscle fibre types can be distinguished histochemically: for example, mATPase treatment after acidic and alkaline pre-incubation reaction is routinely used to classify muscle fibres and different types of intrafusal muscle fibre differ in their possession of various isoforms of the myosin heavy chain (MHC), reflected by differences in ATPase activity. It has been shown that $bag_1$ contain slow-tonic MHC, whereas $bag_2$ fibres contain slow-twitch MHC and chain fibres are characterized by fast-twitch and neonatal MHC (Kucera, Walro and Gorza, 1992).

Structural differences between intrafusal fibres have been revealed by light microscopy and subsequently confirmed by electron microscopy. For example there are more elastic fibres around the intrafusal fibres than around the extrafusal fibres, and they are more numerous around $bag_2$ fibres than around chain fibres. Elastic fibres anchor the spindle at each end to the elastic-fibre network between extrafusal muscle fibres. When the elastic fibres pass through the spindle, they branch to form smaller fibres, which travel alongside the muscle fibres, or within intercellular spaces in the inner and outer capsules (Landon, 1966a; Cooper and Daniel, 1967; Cooper and Gladden, 1974).

It has been revealed that the bag fibres have peg-like projections on their surface over a length of 300 to 400μm on either side of the primary region. Each projection slants towards the equator and appears to serve as an anchoring point for elastic fibres originating from the opposite pole. These attachments are strongly believed to enhance the elastic properties of the primary region (Banks, 1983)

### 1.3.3 Structural differences between intrafusal muscle fibre types

The main ultra structural features of intrafusal muscle fibres are as follows. Transverse sections of the polar regions of bag fibres are characterized by ill-defined myofibrils. These myofibrils are tightly packed together, with little interfibrillar sarcoplasm, and contain few sarcoplasmic organelles (glycogen, mitochondria and sarcoplasmic reticulum elements). The polar region of chain fibres, by contrast, has discrete myofibrilar units with abundant interfibrillar containing various sarcoplasmic organelles (Merrillees, 1960; Landon, 1966a; Ovalle, 1971). In the cat, numerous prominent elastic fibres surround the $bag_2$ fibres in its polar regions, whereas those associated with $bag_1$ fibres are few in number (Gladden, 1976).

Electron microscopy has shown the presence of a single M line at all points along nuclear chain fibres and in all regions of the $bag_2$ fibres except for the equatorial region this distinct single M line is absent in all regions of the $bag_1$ fibres except for the extra capsular region, though a faint double M line may be present (Banks and James 1975, Banks *et al.*, 1977 and Barker *et al.*, 1976).

## 1.4 Sensory innervation

The sensory endings overlie the middle of the nuclear bag and nuclear chain fibres, and occupied small channels that are partially indented into the intrafusal fibre and run transversely to the fibre.

### 1.4.1 Primary ending

Each muscle spindle is supplied by a large thick afferent sensory fibre, known as a group Ia axon, which enters the spindle near the equator of the capsule. Within the periaxial space the axon divides into several branches to form the terminal branches (sensory endings) on the densely nucleated equatorial regions of the three types of intrafusal muscle fibre (the nuclear bags, myotubes, and nuclear chains). These terminals are known as the primary ending (Fig 1.1).

Occasionally, two axons enter the same spindle to terminate around bag fibres (Barker, 1974). Some cat spindles can be innervated by two Ia axons, referred to as double primaries (Banks, Baker and Stacey, 1982) (Fig 1-1). It was also found that some rabbit spindles contained two separately innervated primary endings, the endings lying side-by-side or end-to-end. (Banks, 1973)

The terminals appear to consist of spirals, half rings and a few complete rings (Ruffini 1898). In a reconstruction study of the form and distribution of cat tenuissimus muscle spindles Banks (1986) found that all ring features on the intrafusal muscle fibres were open; they do not fuse with each other (as previously thought); rather, they wind once around an intrafusal fibre before abutting against themselves.

Chain fibres have more spirals than bag fibres. $Bag_1$ and $bag_2$ can be distinguished from each other by comparing their terminal supply. $Bag_1$ fibres have more bands per unit

length and hence more contact area. This may have to do with the role of $bag_1$ as dynamic bag fibres. (Fig. 1.1) (Banks and Barker, 2004)

$Bag_1$ and $bag_2$ fibres receive more terminals than chain fibres and an association between nucleation and innervation can be observed. However, the terminals on chain fibres, although less numerous, may supply more than one chain fibre (Adal, 1969). Chain fibres may also have regions of close apposition; these two features may account for the contraction of the chain fibres as a group in response to a motor stimulation (Boyd, 1976).The fact that the primary-ending terminals vary in their appearance and domains on different intrafusal fibres suggest that they are competing with each other for a limited amount of suitable contact area on the intrafusal fibres. Ultrastructural studies carried out on rat lumbrical muscles by Merrillees (1960) and Landon (1966b) showed that the axon terminals lie in shallow grooves on the surface of the muscle fibres; they are devoid of Schwann cells and are covered by the basal lamina of the intrafusal fibres. The terminals on bag fibres, especially those of the $bag_1$ fibres usually bulge outwards from the surface of the muscle fibres. In the study that forms the basis of this thesis, the degree of the prominence of the nerve endings was used as an indicator of the deformational changes in the primary nerve endings when comparing the experimental with the control muscles.

In contrast to terminals on the bag fibres, those on the chain fibres are usually more indented and flattened (Barker, 1974; Banks, 1986). When a terminal wraps around two or three adjacent muscle fibres a sensory cross-terminal would be formed (Adal, 1969). Although these sensory cross-terminals occur more often between chain fibres, they are sometimes found between a chain and a bag fibre (Barker 1974; Banks, Barker and Stacey, 1982; Kucera, Walro and Reichler, 1988), and between a $bag_1$ and a $bag_2$ fibre (Diwan and Milburn 1986; Walro and Kucera, 1987).

### 1.4.2 Secondary endings

The secondary-ending terminals are supplied by afferents that are thinner than group Ia axons and are known as group II axons. They usually enter the spindle together with the primary afferent (Fig 1-1).

The termination of the secondary endings varies according to the degree of complexity of the spindle. Some simple spindles have no secondary endings at all, whereas others tend to have between one and five on average (six at most); they may be found only on one side of the primary ending or running to both sides.

Those secondary endings nearer to the primary endings seem to have larger group II axons and more terminals on nuclear bag fibres than those farther toward the pole (Boyd and Smith, 1984). Secondary-ending innervation is usually distributed to all three types of intrafusal fibre but restriction to one or two intrafusal fibres is found in the more polar position. Secondary terminals supplying chain fibres are generally thinner, more dispersed and more irregular than primary terminals (Banks and Barker, 2004).

Information regarding the sensory innervation of the rat muscle spindle is relatively sparse for both axons and terminals compared with sensory innervation of the cat and rabbit this is because of the difficulty of staining rat nerve endings with silver and of teasing muscle when using an impregnation method. Similarly, calretinin immunohistochemical staining of rat soleus muscle spindle was not easy: the tissue was delicate and difficult to handle.

## 1.5 The motor innervation

The motor innervation of the mammalian muscle spindle takes place at the spindle poles and involves two types of motor system: the first is a fusimotor (γ) system which is exclusively intrafusal the second is a skeletofusimotor (β) system in which intrafusal and extrafusal muscle fibres share a common innervation, as in non-mammalian spindles (Fig1-1).

The motor innervation consists of a diffuse multiterminal trial ending and two types of plate known as $p_1$ and $p_2$. These endings can be distinguished by their shape or length or by their location and there are differences in the complexity of their subneural apparatus (Barker, Stacey and Adal, 1970; Barker, 1974; Banks, Barker and Stacey, 1985; Walro and Kucera, 1985a, b; Kucera and Walro. 1987a, b; Kucera, Walro and Reichler, 1988a).

### 1.5.1 Types of fusimotor endings

1.5.1.1 *The β innervation, $p_1$ plates*: the $p_1$ plate is the terminal of an axon derived from a collateral branch of a β axon. Its shape is usually tapering, but occasionally may be knob-like or ring –shaped; it is often found in the polar regions either just before or just after the muscle fibres pass out of the capsule. In cat spindles, $p_1$ plates were usually found to innervate bag fibres (Barker, Stacey, and Adal, 1970). The $p_1$ plate is longer than, but similar to, an extrafusal endplate and has a nucleated sole plate and a Doye`re eminence.

By using the glycogen-depletion method, it became clear that β axons in cat spindles innervated the $bag_1$ fibre or the long-chain fibre (Barker et al. 1977; Jami et al. 1978, 1979). A study of 15 spindles from rat lumbrical muscle, serially sectioned to give

transverse 1μm-thick sections has demonstrated that of seven β axons each terminating on one intrafusal fibre, five terminated on the $bag_1$ fibres and two on chain fibres (Walro and Kucera, 1985b).

1.5.1.2 *the γ innervation, $p_2$ plates*: The $p_2$ plates of cat are much longer and more elaborate than $p_1$ and extrafusal plates. Their location in cat spindles is like that of $p_1$ plates. It has been reported that, in cat spindles 90% of $p_2$ plates were located on bag fibres and 10% on chain fibres (Barker, Stacey and Adal 1970). These structures are knob-like axon terminals, lacking a nucleated soleplate and Doye're eminence. In rabbit spindles, the $p_2$ plate has been described as claw like, and distributed to bag fibres only (Barker, Stacey and Adal 1970).

1.5.1.3 *The γ innervation, trail ending*: The trail ending is a long branched ending, so named because the preterminal branches travel for relatively long distances within the spindle before terminating. It is located mainly at the intracapsular and juxta-equatorial regions. Non-myelinated trail fibres are sometimes found to participate in the trail innervation of cat muscle spindles. Trail endings may overlap with secondary endings, and both trail and sensory axon terminals may sometimes occur side by side on the same muscle fibre. Trail endings have been found to be distributed to both bag and chain fibres (Barker, 1974; Banks, Barker and Stacey, 1985) (Fig 1-1).

FIGURE1-1Digramic illustration of the structure and innervation of mammalian muscle spindles, as exemplified by the cat tenuissimus muscle.

a. The encapsulated bundle of intrafusal muscle fibres that constitute a spindle. b. The equatorial region and part of one pole illustrating the descriptive regions A, B, C and innervation by Ia and II sensory and β and γ motor axons. ex.m.f. = extrafusal muscle fibres; FG/FOG = fast glycolytic or fast oxidative-glycolytic muscle fibre; SO = slow oxidative muscle fibre. c. Sensory innervation comprising a primary ending and an $S_1$ secondary ending, in this instance. The distribution of the total terminal contact area of a primary ending is about 35% $bag_1$, 25% $bag_2$, 40% chains; of an $S_1$ secondary 10% $bag_1$, 20% $bag_2$, 70% chains. d. Nuclear-bag and nuclear-chain intrafusal muscle fibres showing nucleation in primary and $S_1$ secondary regions. e,f. Motor innervation of a typical pole (e). The most common variation (f) is for static and dynamic β axons to participate in the motor innervation. Some spindles receive a nonvascular autonomic innervation. a-d depict features drawn to the scale of average dimensions; c, d are based on reconstructions, e, f are schematic diagrams. (Reproduce from the muscle spindle review by Robert W. Banks and David Barker).

Figure 1.1 Diagram illustration of the structure and innervation of mammalian muscle spindles, as exemplified by the cat tenuissimus muscle from Banks and Barker (2004).

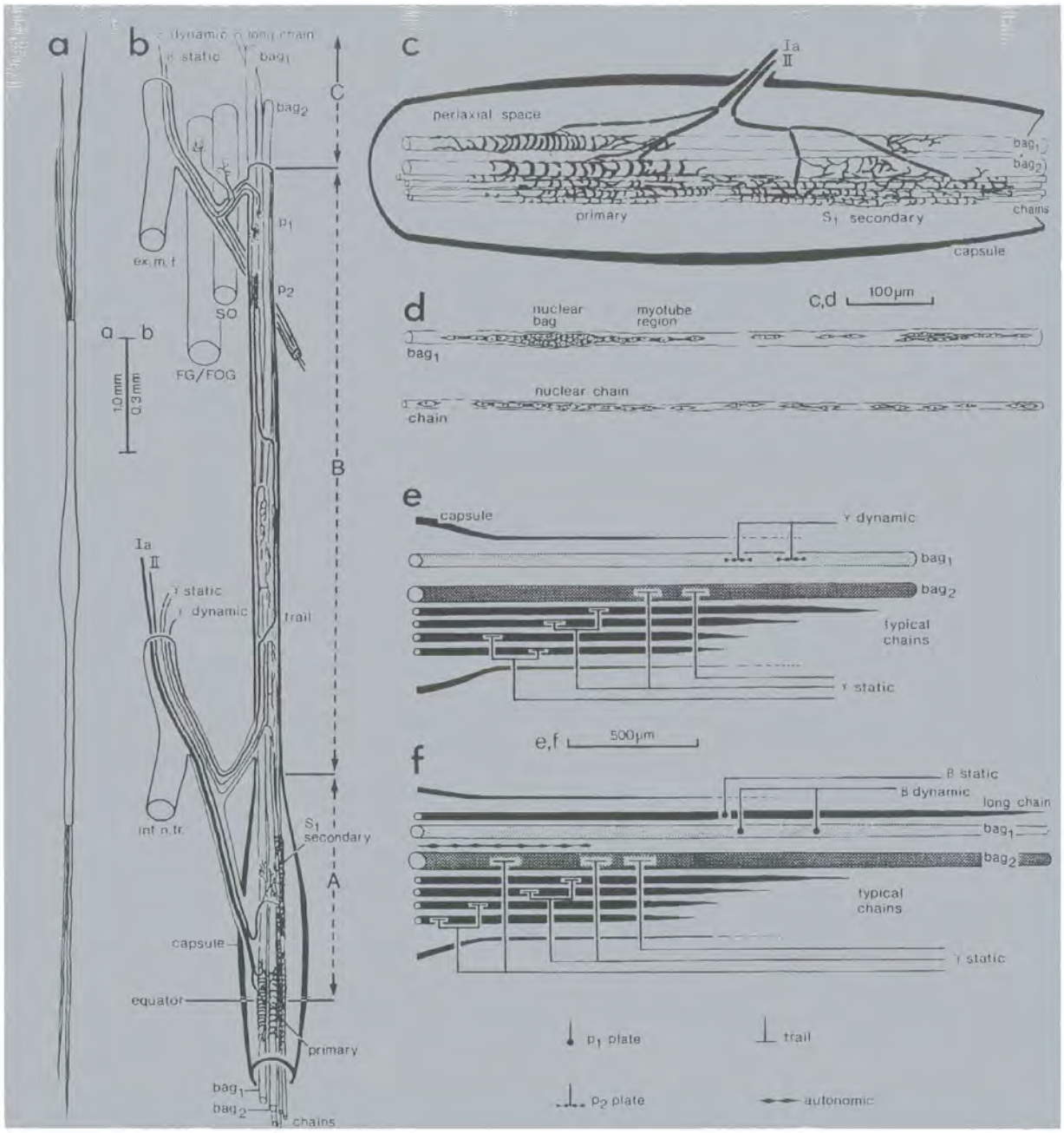

## 1.6 Initiation of sensory nerve impulses.

I a study on frog muscle spindle local depolarization of the nerve terminals appeared when the muscle was stretched, as well as the impulses in the sensory nerve axon (Katz 1950). Treatment of the preparation with procaine prevented the production of impulses though it did not affect the maintained depolarization. It has also been noticed that the degree of depolarisation increases with increasing stretch, and the impulse frequency in the sensory nerve is linearly proportional to the extent of the local depolarization. (Aidley. 1998) All these results led to the conclusion that the local depolarization is an intermediate link between the stimulus and the action potentials in the sensory nerve fibre (Katz 1950). This local depolarization is called the receptor potential (Davis, 1961). Receptor potentials, which have been defined as potential changes induced by action of the sensory stimulus, have since been recorded from a wide variety of receptor cells or sensory nerve endings. The receptor potential size is usually proportional to the intensity of the stimulus. So it is regarded as a graded potential change, not an all-or-nothing one.

This graded receptor potential is thought to be set up in the terminal branches of the sensory neuron, where it usually arises when the sensory stimulus induces ion channels in the membrane of the receptor cell or sensory nerve to open. From the terminals it spreads passively to a low-threshold electrically excitable pacemaker site (Aidley, 1998). In the crayfish stretch receptor, for example, stretch opens mechanosensitive channels in fine terminals of the sensory nerves, and ion-flow through these channels produces the receptor potential (Erxleben, 1989). Sodium ion is the main but not the only one involved (Diamond *et al.*, 1958; Edwards *et al.*, 1981). So the greater the stretch, the more channels open, and so the larger the receptor potential.

In the chemical synapse the action potential leads to an influx of extracellular calcium into the nerve endings due to the presence of voltage-dependent channels. This causes fusion of synaptic vesicles with the presynaptic membrane resulting in exocytosis of neurotransmitter and its diffusion across the synaptic cleft, the neurotransmitters is detected by receptors on the postsynaptic membranes, ultimately leading to the $Na^+$ influx which results in voltage changes in the postsynaptic membrane. In the sensory nerve terminals of muscle spindles it is supposed that $Na^+$ channels themselves undergo conformational changes in response to longitudinal stress in the terminal membrane (Kennedy, Webster and Yoon, 1975; Shepherd, 1983; Quick, 1984). The resulting $Na^+$ current produces a depolarisation recognizable as the receptor potential. (Hunt, Wilkinson and Fukami, 1978).

The mechanism whereby the energy of the stimulus produces excitation of the receptor cell or sensory neuron terminal is known as transduction, although the mechanism underlying its production is not understood. However the basic factor involved is the physical force of the moving muscle fibres, which is transmitted to the nerve endings (Aidley, 1998).

In the nerve terminals the mechanical stimulus probably opens more or less directly mechanosensitive ion channels, which are perhaps attached to cytoskeletal elements on the inner side of the plasma membrane, and this will let cations flow through the membrane. The transduction process acts as an amplification stage, which means that the energy change comprising the receptor potential is much greater than the incident energy which produces it. The system whereby the incident energy alters the ionic permeability of the receptor cell membrane is an ideal system suited to provide the amplification (Aidley, 1998).

The receptor potential mentioned above refers to the immediate response to the stimulus, and generator potential refers to the initiation of action potential. A generator

potential in the nerve terminal produces action potentials in the sensory nerve fibres. There are organs with receptor cells for example in the taste buds, and hair cells, where the receptor potential is quite separate from the generator potential. The receptor potential occurs in the receptor cell while the generator potential occurs in the sensory nerve terminals. In the case of organs with receptor cells there is a synapse between receptor cell and the neuron terminal and a chemical transmission process is involved. The depolarisation forming the receptor potential causes release of neurotransmitter from the receptor cell, the following postsynaptic depolarization of the sensory nerve terminal acts as the generator potential. But in the muscle spindle the generator potential may take place in the sensory nerve terminals. The generator potential carries sensory information in the form of an 'amplitude code' in which the degree of depolarisation is related to the intensity of the stimulus. This amplitude code is converted into the frequency code of action potential in the sensory nerve fibres (Aidley, 1998).

In order for this to take place the sensory nerve terminals may be considered as divided into two functional regions. There is a receptor region, which is particularly sensitive to the stimulus and responds to it by means of a graded receptor/generator potential, and there is a conductile region whose activity consists of all -or-nothing action potentials. The part of the conductile region next to the receptor region is the impulse initiation site. The membrane in the receptor region contains ion channels that are opened by the sensory stimulus so as to allow a non- selective cation current to flow inwards through them. The conductile region is well supplied with voltage-gated sodium and potassium channels so that it can support the propagated action potentials (Aidley, 1998).

The stimulus in this model opens the ion channels in the receptor region so that there is an inward flow of current across the cell membrane; this will produce an outward flow of current at the impulse initiation site assuming that the stimulus is maintained and that the current it produce is constant. (Aidley, 1998)

## 1.7 Physiological properties

In the muscle spindle group Ia (primary ending) and group II (secondary ending) afferents can be distinguished by their different conduction velocities. The two types of ending produce more action potentials at longer length, though only the primary ending gives a high frequency burst of impulses when the muscle is being stretched (Fig 1.2). The primary ending is very sensitive at the start of a movement, and become less sensitive as it proceeds; this nonlinearity means that even quite small movements are readily detected (Cooper, 1961 Bessou and Laporte, 1962).

In the recorded receptor potentials of the primary and secondary endings in isolated cat muscle spindle the receptor potentials of the primary endings showed a marked dynamic component: depolarisation was greater during a stretch than after its completion. This effect was especially evident at the beginning of a stretch, in line with the high sensitivity of the primary endings. In secondary endings the dynamic component of the receptor potential was much smaller (fig. 1.2). So the nervous output of the two types of sensory ending is highly predictable from their receptor potentials (Hunt and Ottoson, 1975).

The difference of the two endings in their dynamic responsiveness might be due to the mechanical properties of the intrafusal muscle fibres. These are more complicated than in extrafusal fibres, the quantities of myofibrils and of elastic material of the intrafusal fibres being known to vary a long their length (Aidley, 1989).

Stretch activation has been evoked to explain some of the after –effects of stretching and fusimotor stimulation (Emonet-Dénand *et al.*, 1985) An alternative view is that these effects can be attributed to the formation of a number of cross- bridges in the resting state (Morgan *et al.*, 1984).

The γ efferent fibres in the cat are of two functionally distinct types, distinguished by their effects on the velocity-sensitive responses of the primary endings during extension. The 'dynamic index' of a response to stretching at a constant velocity was defined as the difference between the frequency of firing of an afferent fibre just before the end of the period of the muscle extending and that occurring at the final length half a second later. The two types of fusimotor fibres are then dynamic fibre, which increase the dynamic index of the primary afferent fibres, and static fibres, which reduce it. In other words, dynamic fibres make the primary endings relatively more sensitive to the velocity of stretching, and the static fibres make them less sensitive. These features are shown in (fig. 1.3) (Matthews, 1962; Crowe and Matthews, 1964; Brown *et al.*, 1965).

It has been found that static γ axons innervate both bag and chain muscle fibres, whereas dynamic γ axons innervate predominantly $bag_1$ fibres. The static γ axons correspond to γ-trail axons and dynamic γ axons correspond to $p_2$-plate axons. In a more simple description it could be said that fusimotor axons innervating $bag_1$ fibres are dynamic and those which innervate $bag_2$ or chain fibres are static. In accordance with this, β axons have dynamic actions if they end on $bag_1$ fibres, static actions if they do not (fig 1.1) (Barker *et al*, 1977; Jami *et al* 1982; Banks *et al.*, 1985).

The work in chapter two of this thesis is to detect the changes in nerve endings of the primary endings in response to flexion and extension in fixed samples which means that the changes are already fixed and in a static form and not in a dynamic form.

Figure 1.2 this diagram shows the receptor potentials from an isolated cat muscle spindle in response to stretching at three different velocities. The upper trace shows the response of the primary ending, the middle trace show that of the secondary ending, and the lower trace shows the length applied to the spindle (reproduce from Hunt & Ottoson, 1975).

Figure1.2 this diagram shows the receptor potentials from an isolated cat muscle spindle in response to stretching at three different velocities from Aidley (1989).

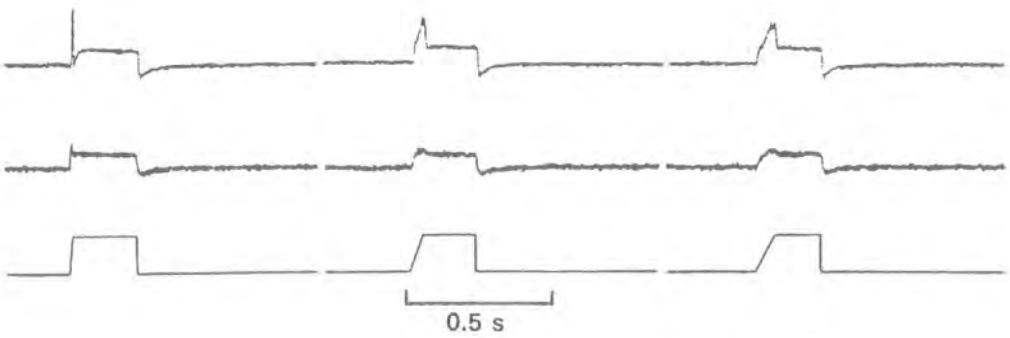

Figure 1.3 Diagram showing the effect of stimulating static and dynamic γ fibres on the response of a single primary ending in a cat soleus muscle to stretching the muscle at different velocities. Each action potential is shown as a dot whose vertical position is proportional to the instantaneous frequency (i.e. the reciprocal of the time since the preceding action potential).

i) Traces *a* to *c* show the response to stretching at three different speeds with no stimulation of the fusimotor fibres (passive phase)

ii) Traces *d* to *f* show corresponding responses during stimulation of a γ-static fibre at 70 s.

iii) Traces *g* to *I* show responses to stimulation of a γ- dynamic fibre at 70 s. (From Crowe & Matthews. 1964.).

Figure.1.3 Diagram showing the effect of stimulating static and dynamic γ fibres on the response of a single primary ending in a cat soleus muscle to stretching the muscle at different velocities from Aidley (1989).

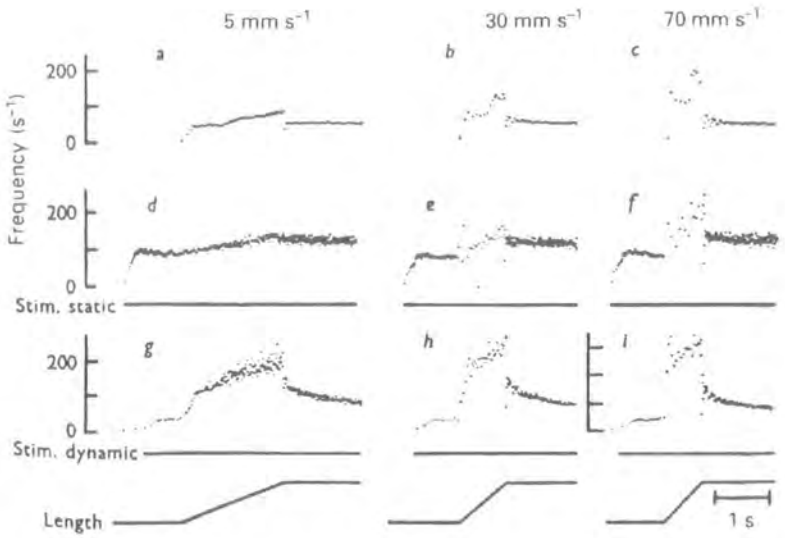

## 1.8 Morphometric changes in sensory nerve endings of the muscle spindle intrafusal fibres

Muscle spindles are stretch-sensitive mechanoreceptors that are found in virtually all-skeletal muscles including, in humans, the extrinsic ocular muscles. They are particularly dense in muscle concerned with fine, manipulative tasks such as the intrinsic muscles of the hand. Their highest density is in dorsal neck muscles, presumably because of the importance of information about head position and movement for maintenance of posture. Muscle spindles are thought to provide the central nervous system with information about length and changes in the length of a muscle. Muscle spindles together with tendon organs that signal muscle tension, therefore provide the afferent limb of a local feedback system (Proske, 1997)

The stretch sensitivity is thought to originate from some kind of shearing stress that is transmitted directly to the terminal membrane at the sensory neuromuscular junction (Kennedy, Webster and Yoon, 1975; Quick, 1984). In a study by (Bridgman, Sweeney and Eldred (1966), on cat muscle spindle it was reported that stretching leads to lengthening of the capsules and both bag and chain fibres and that induced contracture was accompanied by shortening of both bag and chain fibres.

Karlsson *et al.* (1970) made a qualitative and quantitative study of the ultrastructural changes of frog intrafusal fibres in response to passive stretch and concluded that ultrastructural changes occur in the frog muscle spindle with physiological stimulation and that these changes could be utilized as an instrument for a better understanding of the phenomenon of transduction. In another study, the same team (Hooker, Bendeich and Karlsson (1976) investigated intrafusal surface deformation in the sensory region of the frog muscle spindle by two-dimensional and three-dimensional ultrastructural analysis of relaxed and maximally stretched spindles. This study showed that muscle surface deformation occurs in the sensory zone of the intrafusal fibre with maximum

muscle stretch. If it is assumed that the transduction occurs at the nerve muscle interface, the surface deformation demonstrated here is a structural reflection of the forces acting upon the nerve endings during stretching (Hooker, Bendeich and Karlsson, 1976).

In a study by Banks (1986) on the primary sensory endings of the tenuissimus muscle spindle in the cat, it was supposed that an increase in mean sarcomere length on each side of the primary ending of intrafusal muscle fibres correlates with the increasing amount of static stretch during fixation. It was also noted that the terminals are progressively less indented into the bag fibres and that the decreases in indentation correlate to the increasing amount of static stretch. The present study was carried out with all these observations of deformational changes of the muscle spindle in mind. Three cats were chosen because of their suitability for the experiment, with one hind limb used as a control and the other as the experimental preparation. Six samples of tenuissimus muscle were fixed by perfusion. Serial sections of the intrafusal fibre were examined with emphasis on the primary nerve endings. Topographic changes were observed in the muscle spindle and were quite marked with regard to the diameter of the intrafusal fibres, the sarcomeres of both intrafusal and extrafusal fibres, also at the primary nerve endings. The morphometric changes were measured using two computer programs (Image Tool and LaserPix) respectively. The data were analysed and charts for all parameters were plotted: These all indicated real changes in the muscle spindle intrafusal fibre in response to a passive stretch.

## 1.9 Calretinin immunoreactivity in the rat muscle spindle

Nerve cells have the ability to propagate an action potential and to communicate through the nerve synapses, which are specialized contact zones at which information is

transferred from one cell to another by means of neurotransmitters such as acetylcholine, biogenic amins and amino acids or neuromodulators. These are small peptides that act either alone or in combination (Furness *et al,* 1988; Hökfelt, 1992).

Many of the intracellular messengers that mediate the effects of neurotransmitters on intracellular events have been studied: among these are cAMP and intracellular calcium. The targets of these messengers include protein kinases and protein phosphatases, G-proteins, and intracellular calcium-binding proteins (CaBPs) such as calretinin and calmodulin (Cheung, 1980)

Intracellular calcium ions ($Ca^{2+}$) are second messengers that regulate a wide variety of cellular functions such as nucleotide metabolism, muscle contraction, muscle and non-muscle motility, differentiation and signal transduction. However $Ca^{2+}$ does not act alone: many cells contain a variety of cytosolic CaBPs that either modulate or mediate the actions of these ions. Among many of the CaBPs in the nervous system are par-albumin, calbindin-D28k and calretinin. The CaBPs are very specific in their distribution and in their abundance. Calretinin is a CaBP found mainly in the central nervous system (CNS). It is most homologous to the intestinal CaBP, calbindin-D28k. Both calretinin and calbindin are expressed in largely separate sets of neurons in birds and in mammals (Resibois and Rogers, 1992). Although functions of calretinin have not yet been elucidated it is believed to be important in the intracellular transport of calcium and also as a calcium buffer. Antibodies against CaBPs are used for neuroanatomical studies of the vertebrate nervous system, as they give excellent cyto-architectural staining (Resibios and Rogers, 1992; Van Brederode, Hlliesen and Hendrichson, 1991).

Chapter 3 in this thesis describes the calretinin immunoreactivity in the rat soleus muscle sensory endings, intrafusal bag fibres, chain fibres and tendon organs in order to compare any results with those of a previous study (on the cat abductor digiti quinti medius) that had detected calretinin immunoreactivity in cat chain fibres and tendon

organs (El-tarhouni, 1996). In this study, the calretinin distribution in the soleus muscle spindle was mapped on the primary nerve endings of $bag_1$ and $bag_2$ fibres. It was also detected on the primary nerve endings of chain fibres. No secondary endings or tendon organs were seen.

## 1.10 Detection of glutamate in the cat muscle spindle

As glutamate is the major excitatory neurotransmitter in the CNS, glutamate receptors play a vital role in the mediation of excitatory synaptic transmission. This process is the means by which neuronal cells communicate with each other. An electrical impulse in one cell causes an influx of calcium ions and then the release of a chemical neurotransmitter (e.g. glutamate). The transmitter diffuses across a small gap, the synaptic cleft, between the two neuronal cells, and either stimulates (or inhibits) the next cell in line by interacting with receptor proteins. The group of specialised structures that perform this vital function is termed the synapse, and it is in the synapse that the ionotropic glutamate receptors are generally found.

The ionotropic receptors themselves are ligand-gated ion channels. By binding glutamate that has been released from a companion cell, charged ions such as $Na^+$ and $Ca^{2+}$ pass through a channel in the centre of the receptor complex. This flow of ions results in a depolarisation of the plasma membrane and the generation of an electrical current that is propagated down through the processes of the neuron, the dendrites, and the axons and from there to the next in line. The development of antisera that can recognize the amino acids in a fixed tissue section (Storm-Mathisen *et al.*, 1983) was the gateway to many studies revealing the localization of amino acids in specific neuronal pathways that might use them as neurotransmitter (Ottersen and Bramham,

1988). With the antisera that conjugate to glutamate it has become possible to localize glutamate-rich nerve terminals.

In the study reported here, the sensory nerve endings of the cat tenuissimus muscle spindle were examined for glutamate –like immunoreactivity (glutamate-1R). It has been demonstrated that glutamate-1R was greater in the secondary nerve endings and their associated intrafusal fibres in comparison with the primary nerve endings and their associated intrafusal fibres and intrafusal fibre nuclei.

# CHAPTER TWO

## Morphometric Changes of the Primary Sensory Ending of the Cat Tenuissimus Muscle Spindle

### 2.1 Introduction

The intrafusal fibres of muscle spindles lie as bundles in parallel with ordinary extrafusal muscle fibres, their long ends attached to connective tissue, tendon or extrafusal endomysium. The shorter fibres seem to attach to the inner surface and partitions of the capsule pole. The intrafusal fibres receive sensory innervation which responds to active and passive changes in muscle length is protected by a fusiform, fluid-filled capsule and occupies the equatorial region of the intrafusal bundle. The motor innervation is distributed to the polar regions (see Fig 1.1) (Banks and Barker 2004). The sensory nerve terminals vary in their size and location and also in the degree of indentation into the three types of muscle fibre: they are more superficial on $bag_1$ fibres (less indented); rather more indented into $bag_2$ and most deeply indented into chain fibres. Terminals also vary according to their position on the intrafusal muscle fibres (Banks *et al.*, 1986). They are mostly located on the surface of the muscle fibres with their outer surfaces covered by basal lamina continuous with that of the underlying muscle fibres (Merrillees 1960). Each terminal profile is bounded on the outer and inner surfaces by curves forming approximate arc segments of circles as seen on longitudinal section of the nerve terminals (Banks 1986) (Fig 2.1).

It might be thought that since the intrafusal fibres of the muscle spindles lie in parallel with ordinary extrafusal muscle fibres, the spindle will share with the extrafusal fibres any changes in length of the gross muscle, both in extension beyond the resting state of the muscle and in shortening when induced by gross muscle contraction (i.e. the bag and chain intrafusal fibres react in the same manner as the extrafusal tissue). But this is not the case since the differences between the extrafusal fibres and intrafusal fibres in their

myofibril and elastic properties has been established, as well as are the differences between intrafusal fibres themselves and within them in terms of elasticity and viscosity (Poppele *et al*, 1979).

The anatomical and physiological explanation of the spindle mechanism is that the central region of the intrafusal fibres which lack myofilaments and are not contractile, serve as a receptive region for the spindle (primary and secondary endings) which send sensory input to the CNS (Marieb, 2001). Lengthening of the muscle stretches the spindle intrafusal fibres, which in turn stretch the wrappings of the sensory primary endings and, at least in the frog spindle, leads to deformation in the sensory nerve terminals (Karlsson *et al*, 1970). It supposed that some kind of shearing stress is transmitted directly to the terminal membrane at the sensory neuromuscular junction (Kennedy, Webster and Yoon, 1975; Quick, 1984) which would results in $Na^+$ channels opening and starting the first step towards depolarisation. The depolarisation produced by stretch is rapidly decreased by the removal of $Na^+$ and $Ca^{2+}$ but the addition of normal $Ca^{2+}$ can substitute for $Na^+$ and partially restores the response (Hunt, Wilkinson and Fukami, 1978). The resulting depolarisation is assumed to cause an increased sensory discharge (Bridgman *et al.* 1966), which is characterized by a pattern consisting of a dynamic and a static phase (Katz *et al*, 1950).

## 2.2 Methodology

Charles Bridgman (1966) noted that stretching of cat muscle spindles caused lengthening of the capsules and both bag and chain fibres; he also observed that induced contracture was accompanied by shortening of both bag and chain fibres. By using frog (*Rana pipiens*) extensor muscle (extensor digitorium longus IV), Karlsson *et al* (1970) studied ultrastructural changes in the intrafusal fibres due to passive stretch in three

different experimental conditions: in the slackened, maximally joint-flexed position "S", in the physiological relaxation position "PR", and in the physiologically stretched "PS" which is maximal joint extension. He found that, with stretch, the muscle lengthens and becomes thinner and the sarcomeres in the compact zones change their periodicity: however, he did not compare the equatorial to the polar regions nor did he compare the intrafusal to the extrafusal sarcomeres. Karlsson also noted changes in the muscle nuclei in the reticular zone area. The sensory nerve bulbs in the frog, that are apposed to the tops of reticulomeres, changed from relatively round profile in the slackened and physiologically relaxed preparations to an elongated form in the physiologically stretched sample, suggesting that ultrastructural changes occur in the frog muscle spindle with physiological stimulation. Another study of the frog muscle spindle by Hooker *et al*, (1976) demonstrated surface deformation occurring in the sensory zone of the intrafusal fibres on maximum muscle stretch.

Banks observed the degree of terminal deformation in the primary sensory ending of tenuissimus muscle spindle in the cat (Banks, 1986), and noted the following: (a) an increase in the mean sarcomere length on each side of the primary ending of intrafusal muscle fibres suggesting increasing amount of static stretch during fixation;

(b) a progressive decrease of indentation of the nerve terminals into the bag fibres also correlating with increasing mean sarcomere length (Fig 2.1).

Thus, the idea of longitudinal stress in the terminal, when taken into account with other considerations, may demonstrate an anatomical basis for the mechanism that is commonly assumed to cause transduction. To investigate such a possibility in mammals, the problem of stretch differentiation has been approached through obtaining light microscope micrographs of serial sections from pairs of control and experimental tenuissimus muscles of cats fixed by vascular perfusion. Statistical data collected from measurements of the intrafusal fibre diameter at the equatorial region and measurements

of sarcomere length adjacent to the primary endings. Also the measurements of the radii of curvature of the terminal profiles at the equatorial region in $bag_1$, $bag_2$ and chain fibres. The micrographs were also used for visual analysis and comparison to detect the tension differences between control and experimental muscles. In all the study the muscles from the left-hand side of the body in each preparation were extended and served as a control for detection of the effects induced on the right-hand side by fixing the hip and knee angles at various amounts of flexion. See table 2.1 and fig 2.2, and fig 2.3.

## 2.3 Aim of the study

Since the nerve endings are mostly located on the surface of the muscle fibres with their outer surfaces covered by basal lamina continuous with that of the underlying muscle fibres (Merrillees 1960) it is assumed that tension due to passive stretch might be transmitted in part through the basal lamina. The aim of this study was to detect the possibility of any passive tension effects by fixing muscle spindle deformation in response to stretch due to different degrees of extension and flexion of the cat tenuissimus muscle at different lengths; of particular interest was the deformation of primary nerve endings of the bag fibres; their shapes, size and diameter, the rearrangements of equatorial nuclei, changes in sarcomeres length and changes in the nerve endings, and relating these changes with the amount of static stretch. The changes in the nerve endings will be used to test the hypothesis of deformational tension in the basal lamina due to such tension.

Detection of such effects or changes might shed some light on the idea of an anatomical basis of the mechanism that is commonly assumed to cause the transduction in primary nerve endings upon stretching, or shortening during contraction, of the gross muscle.

For this purpose sets of micrographs were taken from the serial longitudinal -section slides for the left-hand side samples (LHS; the control), which were fully extended, and the right-hand side samples (RHS; the experimental side), which were flexed by various amounts. The photos were computer enlarged for comparison

The first trial using micrographs for comparison was set to measure the sarcomere lengths, the fibre diameters, and the nerve endings, of both the control (LHS) and the experimental (RHS) section using Image Tool computer program. For the nerve endings the Image Tool program was set to measure the following:

O (the radius of curvature the outer section of the nerve-ending profile), I (the radius of curvature the inner section of the nerve ending profile), and C (the semicord between the two sections). The program was also set to compute the correlation between them as I/O, O/C and I/C see Fig 2.4)

The nearest previous work to this done in the past was by Karlsson *et al*, (1970) and Hooker *et al.*, (1976) This work was done on the frog spindle which lacks the three distinct types of intrafusal fibres. Mammal spindles are the subject of the present experiment, which is also greater in scope and with greater control of variables than in the previous observations by Banks (1986).

Fig 2.1 show mean sarcomere length of 50 sarcomeres on each side of the primary which is increasing in the spindle fibres going from spindle 4 to 10 then to 5. Also seen is the amount of terminal indentation on the primary sensory ending, (Reproduce from Banks and Barker, review of muscle spindle 2003 with permission from R. Banks).

Figure 2.1 show mean sarcomere length of 50 sarcomeres on each side of the primary which is increasing in the spindle fibres going from spindle 4 to 10 then to 5 from Banks (1986).

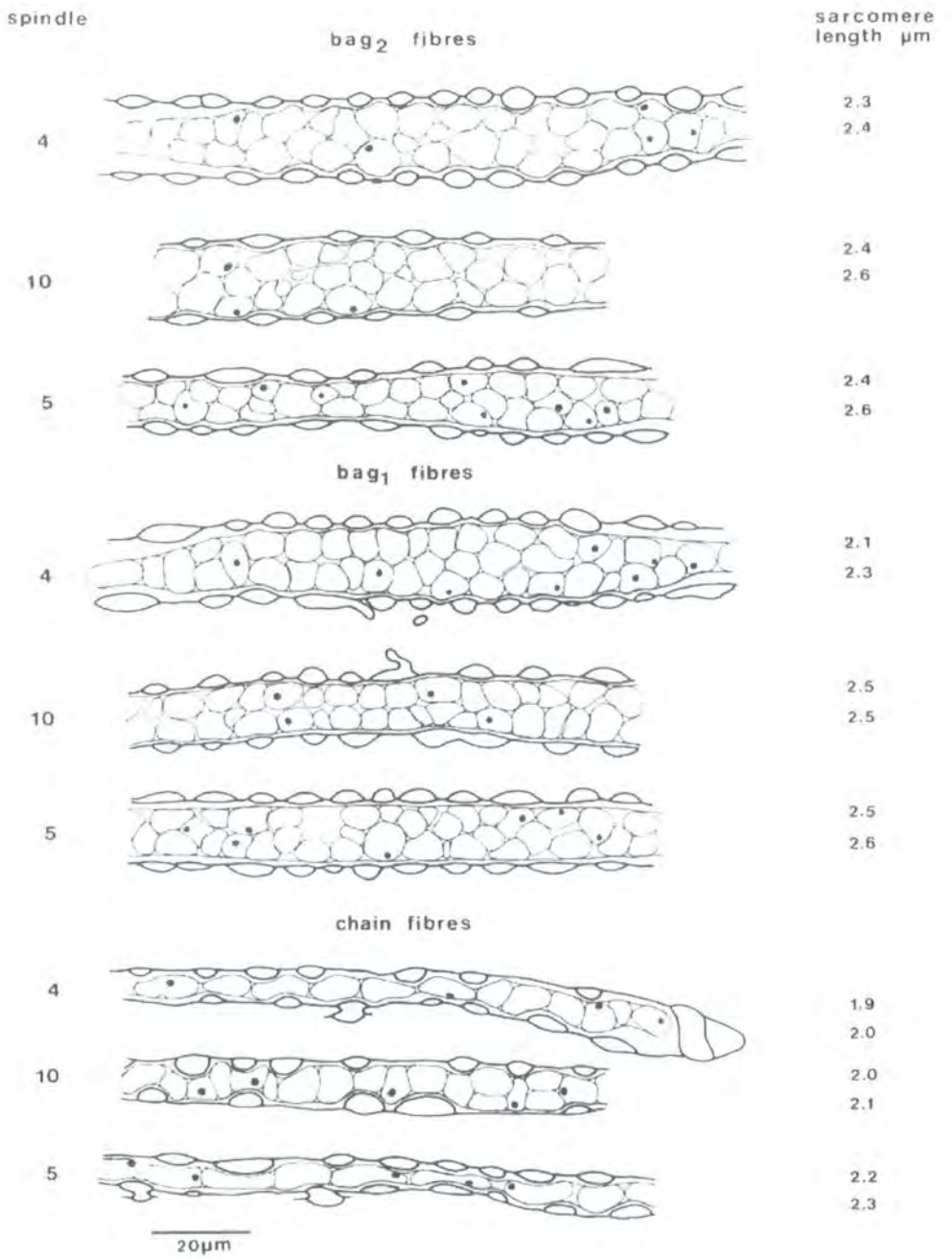

## 2.4 Materials and methods.

Six tenuissimus muscles of different length were dissected out of three adult cats. The tenuissimus muscle originates on the transverse process of the second caudal vertebra and inserts with the biceps femoris (Crouch, 1969). All cats were prepared under deep anaesthesia and were then killed individually by an over dose of sodium pentobarbitone. This was done while their hind limbs were fixed in various positions, as shown in table (2.1) and figures (2.2 and 2.3). The animals were then perfused with heparinized Ringer solution, followed by Karnovsky's fixative; the perfusion method was preferred in order to minimise changes in muscle length.

Table 2.1 Details the animal number and weight, the hip and knee angles of both the control (left) side which is (the extended limb) and the experimental (right) side (the flexed limb). For both sides the length of the tenuissimus muscle is shown in mm. The table also give the percentage of flexion to extension of every muscle.

| Control side (LHS) | | | | | | Experimental side (RHS) | | | |
|---|---|---|---|---|---|---|---|---|---|
| | Weight kg | Hip angle degrees | Knee angle Degrees | Length in (mm) | | Hip angle degrees | Knee angle degrees | Length (mm) | Flex/ext% |
| C-866 | 2.4 | 130 | 155 | 150 | E-866 | 55 | 45 | 102 | 68% |
| C-872 | ? | 130 | 155 | 152 | E-872 | 95 | 87 | 125 | 82% |
| C-869 | 2.9 | 140 | 145 | 148 | E-869 | 75 | 85 | 141 | 95% |

The range of anatomical length changes are shown in the length difference between the flexed and the extended it is also expressed in the flexion/extension percentage.

Fig 2.2 extension of control samples animals C.866.LHS, C.872.LHS, and C.869.LHS, C is for control, 866 is the animal number LHS is referring to the left hand side of the animal been used as control. In this figure the hips angles were extended to 130°, 130° and 140°, respectively. The knees were extended to 155°, 155° and 145°, respectively.

Figure 2.2 Hip and knee extensions of control limps: C.866.LHS, C.872.LHS, and C.869.LHS

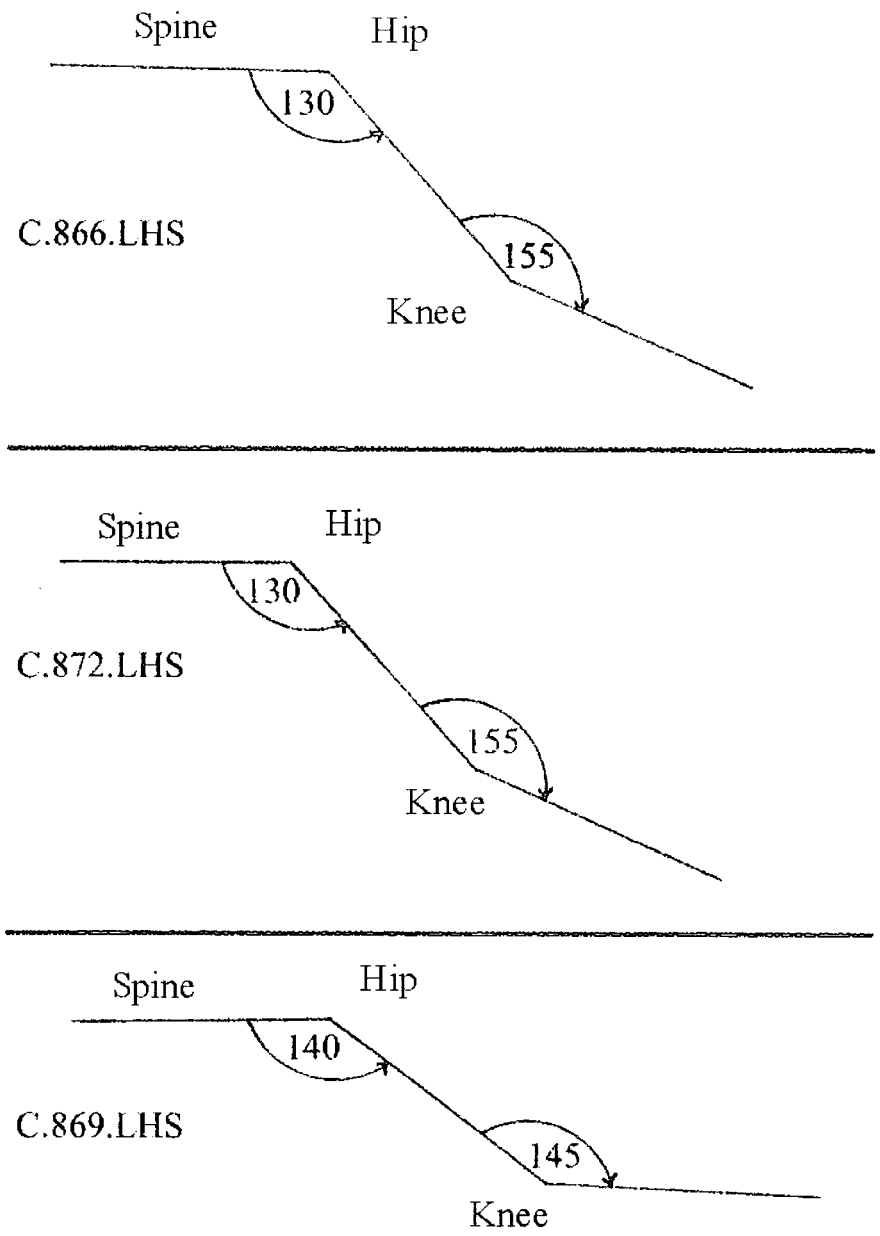

Fig 2.3 flexion, on the experimental side samples E.866.RHS, E.872.RHS and E.869.RHS, E is for experimental, 866 is the animal number, and RHS is right hand side of the animal which been used as experimental and so on for the rest. In this set the hip was flexed to 55°, 95°, and 75°, respectively and the knees to 45°, 87° and 85° respectively.

Figure 2.3 Hip and knee flexion, of the experimental limps: E.866.RHS, E.872.RHS and E.869.RHS

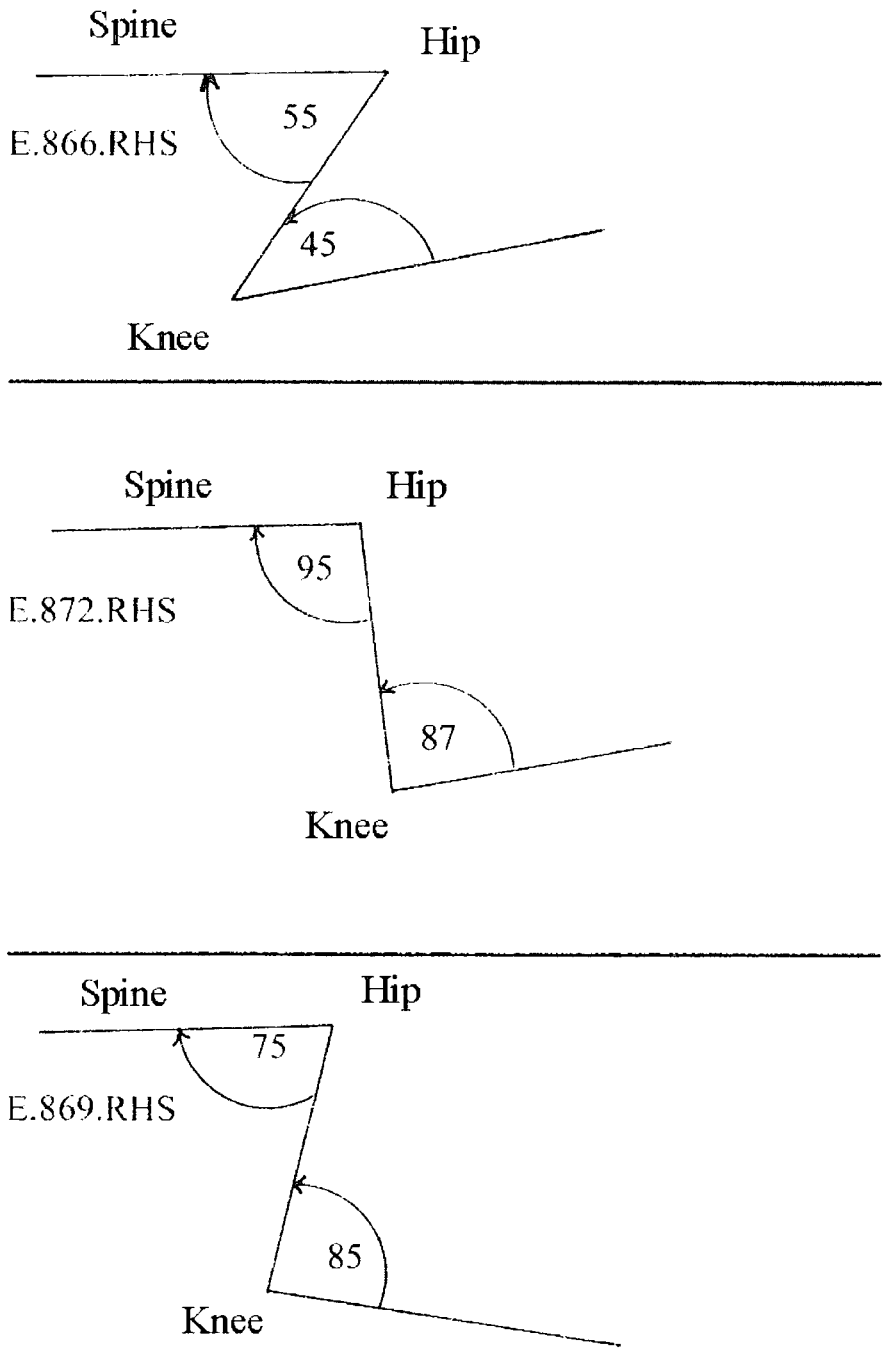

In Fig 2.4, the letter O represents the radius of curvature of the outer free boundaries of the lenticular sensory nerve profiles. The inner neuromuscular boundary of the same profile is represented by the letter I, and the half-length of the cord shared by both circle sections is designated C.

As illustrated in Fig 2.4 (a) if O = I = C, the terminals would appear circular in cross-section, comprising two equal half-circles, with one-half embedded in the intrafusal muscle fibres.

However, if I = O and both exceed the semi cord C as in fig 2.4 (b), the nerve endings would be lenticular or elliptoid, although the endings would be symmetrical with the inner half embedded too.

Furthermore, if O > I the terminals are more deeply embedded in the muscle fibres, as in most chain fibres and some $bag_2$ fibres (Fig 2.4 c).

Finally if I > O (Fig 2.4 d) the nerve endings would be prominent and bulging outwards i.e. less indented into the intrafusal muscle fibres, most noticeably in $bag_1$ and some of the $bag_2$ fibres.

To detect such changes in the radii of nerve endings and other changes in intrafusal fibres in general, the longitudinal section areas of nuclear $bag_1$, $bag_2$, and chain intrafusal fibres were examined. Measurements were taken of the lenticular sensory nerve endings, including radii of curvature of the outer free boundaries (O) and inner neuromuscular boundaries, the internal radii (I) and the half-length of their joint sector cord (C). Comparisons were made of the effects of different angles of flexion /extension (Fig 2.2, 2.3) on the intrafusal muscle status and nerve endings.

In addition measurements were made of intrafusal fibre diameter and the intrafusal and extrafusal fibres sarcomeres.

Fig.2.4 diagram showing the radii of curvature of lenticular sensory nerve endings. The letter O meaning outer curvature radius represents outer free boundaries. For the inner neuromuscular boundary, the same nerve ending is represented by the letter I (the internal radius) and the half-length of the cord shared by both circles is designated C. The diagram depicts the proposed correlation between O, I and C at different situations of passive stretch due to changes of the hind-limb angles by either flexion or extension. The changes in the shape of the nerve endings as depicted in diagrams reflect either the followings cases:

A) No stretch and no tension.

B) Stretch in case of equal tension in "both" side, the basal lamina and the intrafusal fibre.

C) Stretch in case of basal lamina with higher tension than that of the intrafusal fibre.

D) Stretch in case of intrafusal fibre with higher tension than that of the basal lamina.

Figure 2.4 Diagram showing the radii of curvature of lenticular profiles of sections through sensory nerve endings

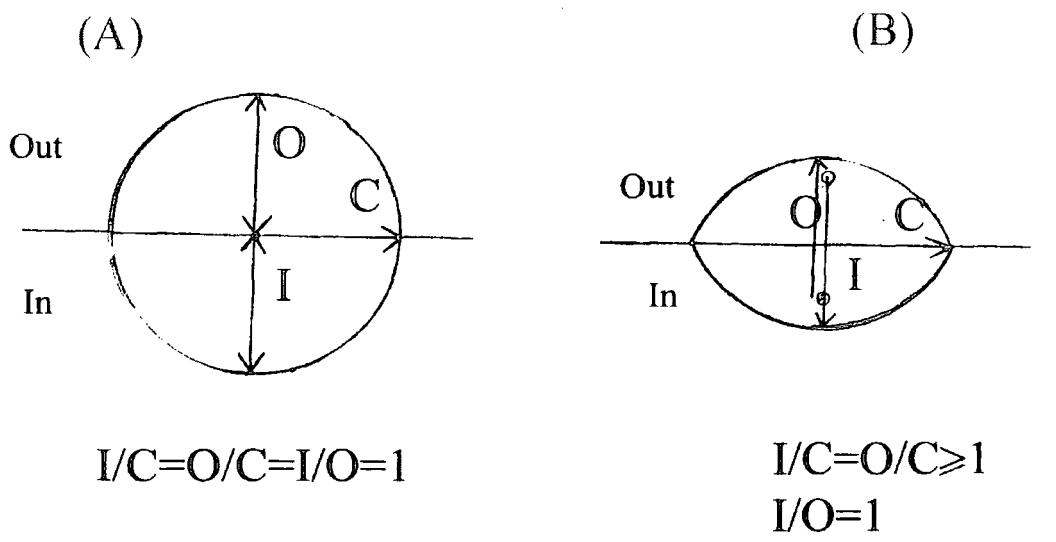


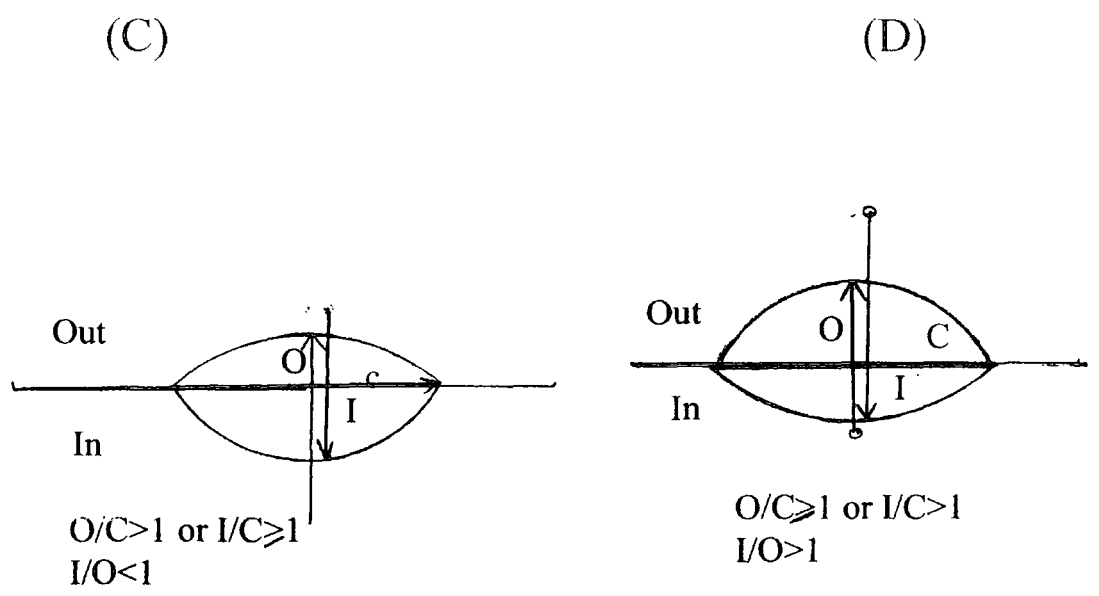

## 2.4.1 Tissue processing

The tenuissimus muscles were immersed in Karnovsky's fixative overnight at 4°C; as these muscles are generally thin, fixative should penetrate evenly. The following procedure was subsequently followed:

1. The muscles were postfixed in 1% buffered osmium tetroxide (2% osmium tetroxide mixed with an equal volume of 0.2M sodium cacodylate (pH 7.3)) for 4 hours at 4°C.

2. They were dehydrated at room temperature in (ethanol)

| | | |
|---|---|---|
| 70% | alcohol: | 3 changes of 5 min each; |
| 95% | alcohol: | 3 changes of 5 min each; |
| 100% | alcohol: | 3 changes of 10 min each; |

3. The samples were then infiltrated with intermediate solution.

| | | | |
|---|---|---|---|
| 50 % | alc/propylene oxide | 3 changes | 10 mins each |
| Pure | propylene oxide | 3 changes | 10 mins each |

4. They were then infiltrated with resin at 45°C, in unstoppered bottles, at ratios of propylene oxide to araldite as follows:

| | |
|---|---|
| 1:1 | 30 min |
| 1:1 | 30 min |
| 1:2 | 30 min |

pure resin over night.

5. The muscles were then cut into serial by approximately 5mm portion, from origin to insertion.

6. Samples were placed in mould in serial order, mould A for muscle region near origin, mould B for the middle portion and mould C for the region near insertion then covered with fresh araldite. The resin moulds were sectioned, maintaining the samples serial order. Each mould yielded at least five portions between 4 and 5mm in length. Samples

were coded C or E (control or experimental, where control is the extended and experimental is the flexed limb); LHS or RHS (indicating the left or right limb); 866, 872 or 869 (the animal number); and A, B, or C (indicating the muscle region as described above: this was essential in order to look for any regional variations of the intrafusal fibres) so the final sample labelling can be read as follows C.LHS.B which means control left hand side region B.

### 2.4.2 Cross-sectioning:

The muscle tissue samples prepared as described above were embedded in a rounded resin block, the first step was to cut the resin impregnated tissue out from the big block, taking care to leave sufficient resin around the tissue in order not to fragment or crack the tissue specimens. The tissue blocks were then numbered accordingly as described above. Cross-sectioning of the muscle tissue was taken every 50μm to find the spindle first and to exclude muscle specimens that might not have a spindle. Once a spindle was found cross sectioning was continued so as to approach the sensory endings of the intrafusal muscle fibres; the tissue was then prepared for longitudinal sectioning.

### 2.4.3 Longitudinal sectioning

Tissue blocks were carefully sectioned longitudinally after examination of the cross sections and measurement of the distance between the spindle and the edge of resin blocks. Muscle spindle blocks were then remounted longitudinally on hard resin blocks and cemented to them with cementing glue; excess resin was then shaved off in order to get closer to the spindle longitudinally. Upon nearing the spindle, 1μm thick sections

were taken every 10μm in order not to miss any part of the spindle. Serial sectioning was started as soon as any spindle capsule tissue first appeared on any 1μm section.

### 2.4.4 Serial sectioning

The serial longitudinal sections were of 1μm thickness and were collected on slide cover slip that had been previously cut by diamond pen to small rectangular slips. Each slip were then laid serially on a microscope slide, the cover-slip fragments were fixed to the slide by tiny drops of DPX mounting medium and a cover slip was added to complete the preparation. The microscope slides bear the code number of the sampled tissue blocks.

### 2.4.5. Section staining

All serial sections were taken at 1μm and stained with a solution made by dissolving 0.1g toluidine blue + 0.05g pyronine + 0.1 borax (sodium tetraborate) in 60 ml distilled water; this solution was usually filtered before use.

### 2.4.6 Microscopic examination of the slides

All the serial sections were examined, using a Nikon light microscope, for the existence of a complete spindle, along the entire extent of the capsule. The intrafusal fibres were then examined and classified as $bag_1$, $bag_2$ or chain, on the basis of the outer curvature of the nerve ending judged to bulge outwards more on $bag_1$ and less on $bag_2$ and least on

chain fibres. Once classified, fibres were counted from their first appearance on the sections until their disappearance (e.g. if one fibre extended over 20 sections, then the three middle sections in this case sections 9, 10, and 11, would usually be selected as the mid most; however, sometimes the best one of the three in term of staining and freedom from folds and other artefacts would be selected to represent the middle of the intrafusal fibre. In this way the less-rounded nerve endings near the beginning or end of the fibres were avoided. The aim was to get the muscle fibres and the nerve endings at their greatest equatorial diameter.

### 2.4.7. Photomicroscope calibration

With Nikon Photomicroscope set at X100 (objective lens) and 0.9 (numerical aperture of condenser) and an exposure of 0.6 seconds, a calibration slide was photographed, using its small division of 10μm to calibrate subsequent measurements of the nerve endings and sarcomeres.

### 2.4.8. Photography

#### 2.4.8.1 Nerve endings

Each intrafusal fibre examined and found to have suitable nerve endings (i.e. without any abnormality such as an unusually large size or fusion with another nerve ending) was photographed, targeting the middle of the primary endings area and using a setting of X100 (objective lens) and a Nikon FX 35 camera. Most of the photos produced of the primary nerve endings area of bag fibres contain an average of 5 to 8 nerve ending profiles.

### 2.4.8.2 Sarcomeres

Once the nerve endings had been photographed the slide was then moved three objective fields from the end of any sensory endings, which is approximately equal to 30μm to the right or to the left and the sarcomeres of the same intrafusal fibre were photographed. The field of view was then moved to the adjacent extrafusal muscle fibres outside the muscle spindle and their sarcomeres were photographed. Three photographs of the primary nerve endings were usually taken (the one before the middle, the middle one and the one after) middle here refer to the most equatorial sections on the slide as explained in section 2.4.6 in order to chose the best one in term of fine staining and freedom from artefacts. This was applied to the nerve endings of both bag and chain fibres; in all, 201 micrographs were taken. The number of photographs includes those of the sarcomeres, the intrafusal fibres, and sarcomeres of the adjacent extrafusal muscle.

### 2.4.8.3 Photographic and Computer Analysis

The negative images were scanned using an Epson GT-700 photo scanner and then transferred into the Adobe Photoshop program. Using this program the photographs were readjusted for brightness and contrast and rearranged in horizontal orientation and then saved before assessment for comparison between the control (LHS) and the experimental (RHS) samples. All photographs showed some similarity between the left and right side in each animal, at least at first glance.

### 2.4.8.4 Computer analysis

The images were then transferred into the Image Tool program for measurement. Image Tool is a mathematical computer program that can be downloaded from the Internet. It was modified to measure the radii of outer curvature of the nerve endings (referred to as O), the radii of the opposite circle segment which is the indented part of the nerve endings (referred to as I) and also one half-length of their common cord (C).The program was also used to measure the mathematical correlation between I/O, O/C, and I/C Fig 2.4.

Measurements including sarcomere length and the diameter of the intrafusal fibres were made on all the micrographs, and tabled results were saved and analysed.

### 2.4.8.5 Sarcomeres

Skeletal muscle is also termed striated muscle because of the regular arrangement of the myofilaments which create repeating pattern of light and dark bands. These repeating units are, in fact, sarcomers, the basic functional units of the muscle. The borders of the sarcomeres (which are the Z lines) are aligned up in adjacent myofibrils and contribute to the striations visible with the light microscope. The thin filaments are attached to the Z lines and project toward the centre of the sarcomeres, while the thick filaments are centred in the sarcomeres. At rest, the thick and thin filaments do not overlap completely and the area near the edge of the sarcomeres where only thin filaments are found is termed I band, and whereas A band is the broad region that corresponds to the length of the thick filaments. The thin filaments do not extend completely across the sarcomeres, so the H zone in the centre of the A band contains only thick filaments and

the connection among these thick filaments form the dark M line within the H zone. This arrangements of thick and thin filaments are the key elements to how the sarcomeres, and hence the whole muscle, contracts.

## i- Measurements of intrafusal sarcomeres.

In this study, where extended control side (LHS) intrafusal sarcomeres are compared with those on the experimental flexed side (RHS), these intrafusal sarcomeres show the same pattern as that described above. The extended side (LHS) sarcomeres, measured from the beginning of one sarcomere unit I line to the end of A line of a fifth sarcomere, are longer than those of the experimental side measured similarly over five sarcomeres. The patterns of difference between control and experimental samples are nearly identical for animals 866 and 872, but not for animals 869 where the intrafusal sarcomeres of $bag_2$ fibres sarcomeres for both control and experimental appear to be of equal length. See detailed of tables (2.2-2.3) and charts (2.1-2.2) of intrafusal sarcomeres and extrafusal sarcomeres on the following sections.

## ii- Measurements of extrafusal sarcomeres.

Every time muscle spindle intrafusal sarcomeres were measured and photographed, the adjacent extrafusal sarcomeres were also measured, in both the control and the experimental samples. Two extrafusal muscle fibres adjacent to each spindle were measured in this way and the values were averaged. The mean extrafusal sarcomere lengths show a pattern similar to the difference found in the intrafusal sarcomeres between control and the experimental samples. This study is probably the only one to include extrafusal sarcomeres for comparison. (See table 2.4 and chart 2.3).

## 2.5.1 Results of the measurements of sarcomeres, diameter and nerve endings using Image Tool program

Using the same photo of the microscopic calibration slide for calibration, a line between the small lines scale on the slide was drawn and set to 10μm, and saved on the computer to be used as a reference standard for calibration for all sarcomeres.

For sarcomere measurement, an area was chosen that was at least three microscopic fields about 30μm away from any sensory ending using an objective lens of X100 in order to be sure that the sarcomeres measured are for the same intrafusal fibres being classified as $bag_1$ or $bag_2$ and to avoid a possible variation in measurements which might result due to different viscoelastic properties along the same fibre. In each case standard five sarcomeres were measured, from the beginning of the I band line until the end of the fifth A band.

Measurements of sarcomeres from all samples of the left hind limb (the control LHS) side were done on the intrafusal sarcomeres of $bag_1$ fibre and then the intrafusal sarcomeres of $bag_2$ fibre.

The results were amalgamated into groups 866, 872 and 869 (corresponding to each animal number). Similar measurements were taken on the right hind limb (the experimental hind limb RHS) see Tables 2.2-2.3 and charts 2.1 and 2.2 for intrafusal sarcomeres. Whenever an intrafusal fibre was measured the adjacent extrafusal fibre was also measured (see table 2.4 and chart 2.3 for extrafusal sarcomeres). The results gave the first indication that tension differences were detectable by numerical data indicating changes in the sarcomere of the experimental, compared with that of the control, side. The measurements of the intrafusal and extrafusal sarcomeres based on Image Tool are shown in tables 2.2, 2.3 and 2.4 (charts 2.1- 2. 3). Also initial measurements (not shown) of only one site of the diameter of primary area indicates some difference between the experimental and control in terms of diameter.

The Image Tool Program measurements of the primary sensory nerve endings used the same calibration and measured all the nerve endings radii in each micrograph. The repetitive trial of such measurements of the sensory primary nerve endings failed to show any difference between the experimental and control side which contrast with the difference noticed in the results of the sarcomere measurements so re-photographing the nerve endings using a new digital camera was considered.

Charts 2.1 Lengths of intrafusal sarcomeres of $bag_1$ fibre which show that all the control are higher than the experimental samples and sample 872 show the biggest tension difference.

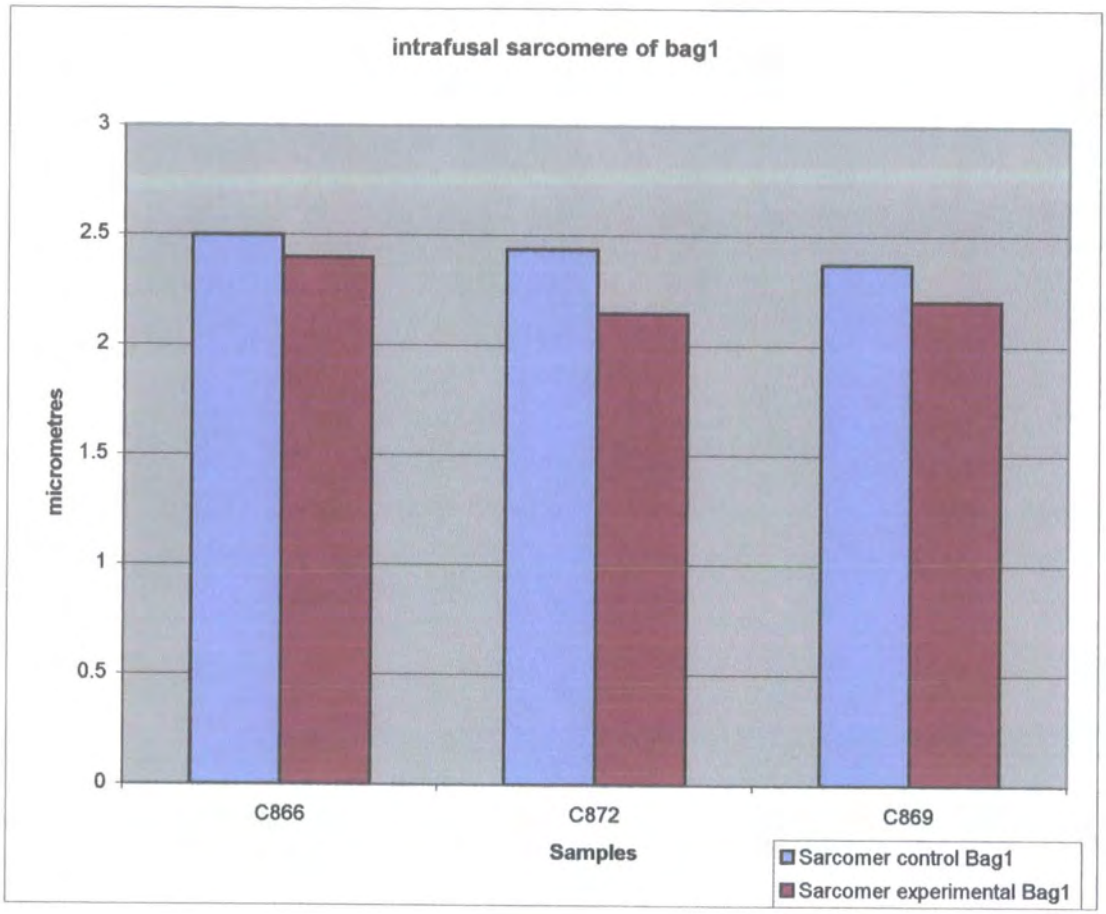

Table2.2 Lengths of intrafusal sarcomeres of bag $_1$ control vs. sarcomeres of bag$_1$ experimental. Sample 872 shows the biggest difference; region C in control sample 872 is not included due to inadequate fixation though it was done in the experimental but was not so clear to be measured.

| Control | | | Experimental | | |
|---|---|---|---|---|---|
| Sample | | Sarcomere length (μm) | Sample | | Sarcomere length (μm) |
| C866 | LHS.A.B1 | No spindle | E866 | RHS.A.B1 | 2.34 |
| | LHS.B.B1 | 2.58 | | RHS.B.B1 | 2.27 |
| | LHS.C.B1 | 2.41 | | RHS.C.B1 | 2.59 |
| | Average | 2.5 | | Average | 2.4 |
| C872 | LHS.A.B1 | 2.32 | E872 | RHS.A.B1 | 1.9 |
| | LHS.B.B1 | 2.56 | | RHS.B.B1 | 2.39 |
| | LHS.C.B1 | No spindle | | RHS.C.B1 | Inadequate fixation |
| | Average | 2.44 | | Average | 2.15 |
| C869 | LHS.A.B1 | 2.46 | E869 | RHS.A.B1 | 2.18 |
| | LHS.B.B1 | 2.23 | | RHS.B.B1 | 2.22 |
| | LHS.C.B1 | 2.41 | | RHS.C.B1 | Inadequate fixation |
| | Average | 2.37 | | Average | 2.2 |

Mean.

| | C866 | C872 | C869 |
|---|---|---|---|
| Sarcomeres of control Bag$_1$ | 2.5 | 2.44 | 2.37 |
| Sarcomeres of experimental Bag$_1$ | 2.4 | 2.15 | 2.2 |

One reading for each sarcomere at its most clear and straight site. All measurements are in μm and done by Image Tool.

Charts 2.2 Lengths of intrafusal sarcomeres of $bag_2$ fibre which show that all the control are higher than the experimental samples and sample 872 shows the biggest difference and sample 869 show the least.

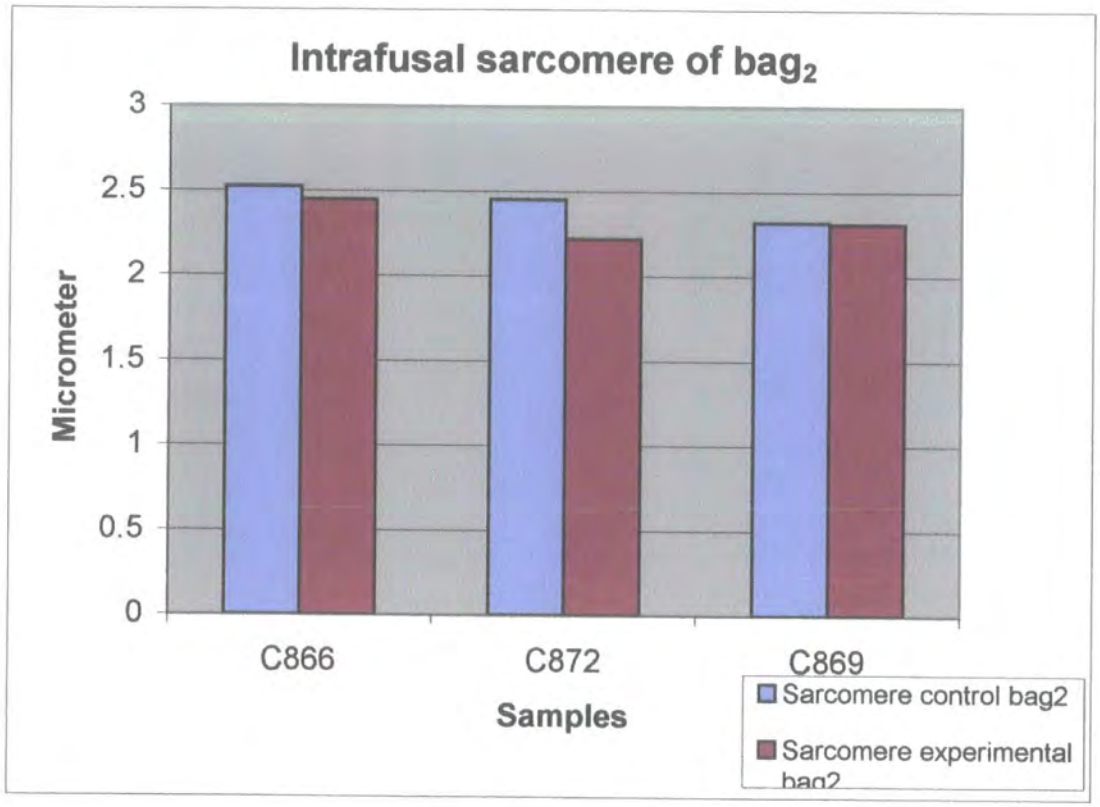

Table 2.3 Lengths of intrafusal sarcomeres of $bag_2$ control vs. sarcomeres of $bag_2$ experimental. Sample 872 shows the biggest difference, region C in control sample 872 is not included due to inadequate fixation, and in the experimental it was done but not so clear to be measured.

| Control | | | Experimental | | |
|---|---|---|---|---|---|
| Sample | | Sarcomere length (μm) | Sample | | Sarcomere length (μm) |
| C866 | LHS.A.B2 | 2.39 | E866 | RHS.A.B2 | 2.51 |
| | LHS.B.B2 | 2.51 | | RHS.B.B2 | 1.78 |
| | LHS.C.B2 | 2.65 | | RHS.C.B2 | 3.05 |
| Average | | 2.52 | Average | | 2.45 |
| C872 | LHS.A.B2 | 2.44 | E872 | RHS.A.B2 | 2.51 |
| | LHS.B.B2 | 2.46 | | RHS.B.B2 | 1.93 |
| | LHS.C.B2 | No spindle | | RHS.C.B2 | Inadequate fixation |
| Average | | 2.45 | Average | | 2.22 |
| C869 | LHS.A.B2 | 2.23 | E869 | RHS.A.B2 | 2.08 |
| | LHS.B.B2 | 2.24 | | RHS.B.B2 | 2.51 |
| | LHS.C.B2 | 2.47 | | RHS.C.B2 | 2.34 |
| Average | | 2.32 | Average | | 2.31 |

Over all mean

| | C866 | C872 | C869 |
|---|---|---|---|
| Sarcomeres of control $Bag_2$ | 2.52 | 2.45 | 2.32 |
| Sarcomeres of experimental $Bag_2$ | 2.45 | 2.22 | 2.31 |

Chart 2.3 Lengths of extrafusal sarcomere adjacent to control spindles vs. sarcomeres adjacent to experimental spindle. In this chart the outcome fitted exactly with what had been expected when the experiment was designed: where the greatest difference is seen in 866 followed by 872 and then 869.

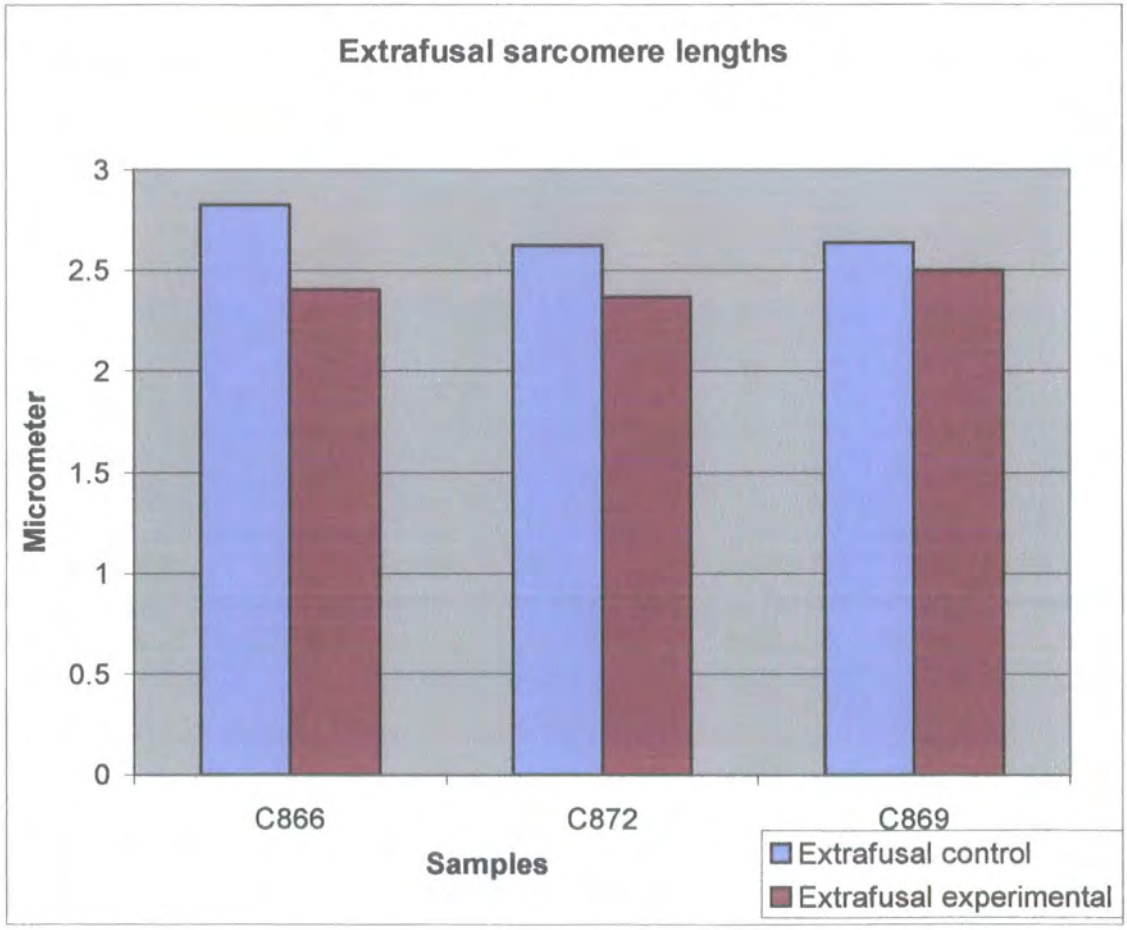

Table 2.4 Lengths of extrafusal sarcomeres adjacent to control spindle vs. sarcomeres adjacent to experimental spindles. Region C in control sample 872 is not included due to inadequate fixation. The measurements reflect the assumed tension difference where 866 is the highest followed by intermediate 872. One reading of each sarcomere at its most clear and straight site. All measurements are in μm and done by Image Tool.

| Control | | | Experimental | | |
|---|---|---|---|---|---|
| Sample | | Sarcomere length (μm) | Sample | | Sarcomere length (μm) |
| C866 | LHS.A.B1 | 3.04 | E866 | RHS.A.B1 | 2.34 |
| | LHS.A.B2 | 2.32 | | RHS.A.B2 | 2.23 |
| | LHS.B.B1 | 2.89 | | RHS.B.B1 | 1.64 |
| | LHS.B.B2 | 2.95 | | RHS.B.B2 | No spindle |
| | LHS.C.B1 | 2.90 | | RHS.C.B1 | 2.94 |
| | LHS.C.B2 | 2.83 | | RHS.C.B2 | 2.88 |
| Average | | 2.82 | Average | | 2.41 |
| C872 | LHS.A.B1 | 2.48 | E872 | RHS.A.B1 | Inadequate fixation |
| | LHS.A.B2 | 2.55 | | RHS.A.B2 | Inadequate fixation |
| | LHS.B.B1 | 2.61 | | RHS.B.B1 | 2.43 |
| | LHS.B.B2 | 2.84 | | RHS.B.B2 | 2.39 |
| | LHS.C.B1 | | | RHS.C.B1 | 2.31 |
| | LHS.C.B2 | | | RHS.C.B2 | 2.31 |
| Average | | 2.62 | Average | | 2.36 |
| C869 | LHS.A.B1 | 2.70 | E869 | RHS.A.B1 | 2.22 |
| | LHS.A.B2 | 2.58 | | RHS.A.B2 | 2.49 |
| | LHS.B.B1 | 2.58 | | RHS.B.B1 | 2.74 |
| | LHS.B.B2 | 2.46 | | RHS.B.B2 | No spindle |
| | LHS.C.B1 | 2.80 | | RHS.C.B1 | No spindle |
| | LHS.C.B2 | 2.68 | | RHS.C.B2 | 2.56 |
| | Average | 2.63 | | Average | 2.5 |

| Summary of the extrafusal as separate. | C866 | C872 | C869 |
|---|---|---|---|
| Extrafusal Sarcomeres of control $Bag_1$ | 2.95 | 2.55 | 2.7 |
| Extrafusal Sarcomeres of experimental $Bag_1$ | 2.3 | 2.38 | 2.48 |
| | C866 | C872 | C869 |
| Extrafusal Sarcomeres of control $Bag_2$ | 2.7 | 2.7 | 2.58 |
| Extrafusal Sarcomeres of experimental $Bag_2$ | 2.55 | 2.36 | 2.52 |
| | | | |
| | As Total since extrafusal are the same | | |
| | C866 | C872 | C869 |
| Extrafusal control | 2.82 | 2.62 | 2.64 |
| Extrafusal experimental | 2.406 | 2.37 | 2.5 |

### 2.5.2 Digital photography.

As mentioned in section 2.4.9.4 the photography was repeated, focusing only on the most central section of the spindle and using a digital camera for a greater speed. The digital camera was used to photograph all the slides again; new digital micrographs were obtained. The Nikon photomicroscope was set at X100 (objective) lens and 0.9 (numerical aperture of the condenser), as before, and a Nikon Coolpix 950 digital camera was used for photography. In total 119 digital micrographs were made.

### 2.5.3 Visual comparison of experimental versus control samples using digital micrographs

After the unsuccessful preliminary trial of measurements of the nerve endings using ordinary micrographs, the digital micrographs were used for visual assessment of the images, in order to clarify the initial results and to measure the nerve endings again. For these new visual assessments of the fibres, the micrographs of the two sides (LHS and RHS) were arranged side by side on screen for ease of comparison; two at a time, one control (LHS) micrograph being compared with one experimental (RHS) micrograph from the same animal, specimen and site.

On first inspection, the corresponding left and right micrographs appeared to be fairly similar; however closer visual examination revealed differences between the two, particularly in fibre diameter which been detected in the initial measurements using Image Tool program. The differences further support the conclusion that changes had occurred as reflected by visible changes in the inner capsule and the fibres diameter. The spindle capsules were not included in any micrographs and the inner capsule diameter is quite irregular in many of them and for this reason their diameter were not

measured for comparison. So a visible difference had been detected in addition to the changes reflected in the numerical data of the measurements of sarcomeres though changes in nerve endings were not very obvious to be detected visually. The visual assessments were not done on the previous micrographs taken by the Nikon FX 35 ordinary camera.

### 2.5.4. New measurements of fibre diameter and nerve endings

The initial visual assessment of the digital micrographs of intrafusal fibres seem to indicate morphological changes that had taken place in the experimental compared with control samples, as reflected by the parameters described in the visual assessments sections, see section (2.5.3) which include fibre diameter and the equatorial nuclei. All these findings, including the previous measurement of the fibre sarcomeres, support the idea of morphometric changes due to tension as originally hypothesised in section (2.3). Because initial visual assessment of the intrafusal fibres suggested a difference in the fibre diameter, the fibre diameter was measured in three different areas of the primary ending (left, middle and right of the primary endings) and the average of that was taken. The results obtained by the use of Image Tool program had shown clearly that there are differences in the measurements of the control and the experimental samples in terms of fibre diameter and sarcomere length. It was much easier to measure the diameter and the sarcomere length of the intrafusal fibre using Image Tool program, by using the image of the calibration slide that was set to a scale of 10μm.

However, similar visual and numerical differences with regard to the nerve endings could not be found, despite two attempts using the Image Tool program to measure morphometric changes in the nerve endings these efforts were time consuming and their results were puzzling.

Measurement of the intrafusal sarcomere lengths also had revealed differences between the control and the experimental samples (see table 2.2 – 2.4 for both intrafusal and adjacent extrafusal sarcomere, with charts 2.1 and 2.2 for intrafusal sarcomers). As previously mentioned, these results are consistent with the observations of Banks (1986). So the difference in measurements of the fibre diameters, discrepancies between sarcomeres and the visually apparent morphological differences between the intrafusal fibres are all indicative of changes that took place in the intrafusal fibres as a result of muscle flexion. However, measurement of the nerve endings using the Image Tool program was more difficult though such measurements would be less variable if the nerve endings were parallel with the outline of the intrafusal fibres and if both outer and inner sector were regular in shape, which is far from being the case when many different fibres are being considered, or even within a specific fibre where the nerve endings would be slanted especially away from the centre of the primary endings. A final attempt to achieve meaningful nerve-ending measurements focused on those endings in which the cord of the outer and inner circle sector were in line with the fibre and were more regular in shape (see figure 2.4.)

Thus the measurements were repeated with that in mind; using Image Tool and no more than three nerve endings were measured in each case. The findings obtained in such a way produced the first meaningful results that could be consistent with results of measurement of the sarcomeres and fibre diameter and the visible changes in the intrafusal fibre.

### 2.5.6 Measurements of fibre diameter and nerve endings using LaserPix

The initial results of the nerve endings obtained in the previous section 2.5.5 make the results with regard to the nerve endings consistent with the results of other tests mainly

the sarcomere lengths and fibre diameters, and gives the first sign that changes in the nerve endings could be detected by numerical data, but these data were not subjected to rigorous statistical testing because of the possible bias due to exclusion of many nerve endings and the selection of only three from between five to eight nerve endings available in every micrograph. In order to have more data regarding nerve endings for statistical analysis, another way of measuring all the nerve endings without any exclusion was sought. Lately, a new computer program has been introduced to accompany the confocal microscope which is more capable and easier to use than the Image Tool program particularly when it comes to measuring the circle sector.

This LaserPix Program can be used to click on any three different points on the circumference of a nerve ending sector and the program will draw a full circle that fully eclipsed the sector as part of the full circle.

Using the stage micrometer slide, the program is set to 10μm calibration. In order to avoid personal bias and to confirm the previous results obtained by the Image Tool the LaserPix was used to repeat all the previous measurements of the fibre diameter and nerve endings in every micrograph, but not that of the sarcomeres.

The program gives values of diameter, radius and area, and was also used to measure the cords of every circle sector; thus using this program the outer and inner radius measurements O, I, and the semi cord C, were repeated. The results are given in table 2.15 and charts in 2.6-2.8 for $bag_1$, and in table 2.20, and charts in 2.9-2.11 for $bag_2$. LaserPix program was not set to measure the ratios of I/O, I/C, O/C, and for that the data of O, I, C, were saved and a calculated I/O, I/C, O/C, were done using Excel program. All results are summarised and listed in tables 2.25 for $bag_1$ followed by their charts in 2.12-2.14 and then their ANOVA and t-test and in table 2.28 for $bag_2$ and followed by their charts in 2.15-2.17 and then their ANOVA and t-test.

## 2.5.7. Length and diameter

The longest intrafusal fibre in most spindles is the $bag_2$ with mean polar lengths of 2947 μm for $bag_2$ fibres, 2760 μm for $bag_1$ fibres and 1382 μm for chain fibres (Kucera 1982). The mean juxta-equatorial diameters (inner region B, are 16.86 ± 2.35μm for $bag_1$ and $bag_2$ fibres and 8.37 ± 1.85μm for chains (Boyd 1962). The three type of fibres become thinner as they pass through the equatorial region.

## 2.5.8. Measurements of $bag_1$ and $bag_2$ intrafusal fibre diameters

Banks, Harker and Stacey (1977) found that in the rabbit $bag_1$ and $bag_2$ are usually about the same length, but $bag_2$ fibres are only of significantly greater diameter than $bag_1$ fibres in the rat. Chain fibres are shorter than both $bag_1$ and $bag_2$ fibres, and have a significantly smaller diameter although, in the polar region, the difference is not that significant at least between $bag_1$ fibres and chain fibres as those intrafusal fibres that extend well into region C tend to become thickest in this region.

In this study, the fibre diameters in both $bag_1$ and $bag_2$ fit exactly with the muscle lengths where the shortest muscle give the thickest diameter, on 866 the experimental (flexed) side are the thickest followed by 872 and 869 reflecting their lengths which as seen in table 2.1 are as follows: 102mm, 125mm and 141mm. All those in the experimental are thicker than those in the control (extended) side in both animal 866 and 872, and are nearly equal in animal 869, for both $bag_1$ and $bag_2$ fibres. This could be due to the fact that the sample E-869 on the experimental side are only 7mm shorter than the control which is the least difference among the three experimental sets compared with 48mm in E-866 and 27mm in E-872. Tables 2.5 to 2.9 list the

measurements and the statistical analysis of fibre diameter for $bag_1$ (see also charts 2.4 for $bag_1$ fibre diameter) like wise tables 2.10 to 2.14 list the measurements and the statistical analysis of fibre diameter for $bag_2$ (see also charts 2.5 for $bag_2$ fibre diameter). For $bag_1$ and $bag_2$ the result fit exactly with what had been expected when the experiment was designed where the greatest difference is seen in 866 followed by 872 and then 869. $Bag_2$ fibres in almost all samples have a greater diameter than $bag_1$ fibres, as shown in tables 2.5-2.10 and on charts (2.4, and 2.5) thus in terms of intrafusal bag fibre thickness, this study confirms that $bag_2$ fibres of the cat tenuissimus muscle are greater in diameter than $bag_1$ fibres.

Chart 2.4 Mean diameters of control (LHS) $bag_1$ fibres in blue and average diameters of experimental (RHS) $bag_1$ fibres in brown. In this chart just as in the extrafusal sarcomeres the result fit exactly with what had been expected when the experiment was designed where the greatest difference is seen in 866 followed by 872 and then 869.

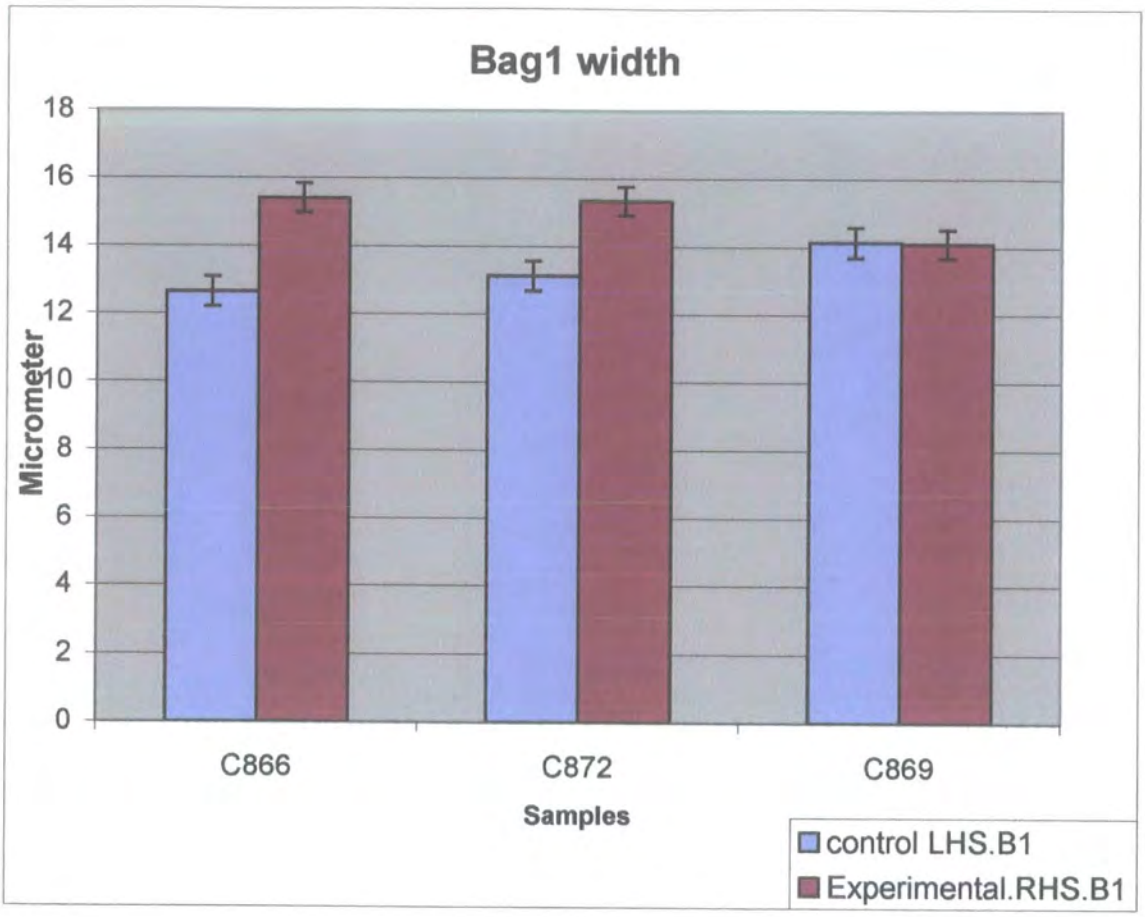

Table 2.5 Mean diameter of $bag_1$ fibre of control and experimental samples all measurements are in μm and done by LaserPix (see appendix 5). The measurements reflect the assumed tension difference where 866 show the greatest difference in diameters followed by 872 and 869.

| Control | | | Experimental | | |
|---|---|---|---|---|---|
| Sample | | Diameter width | Sample | | Diameter width |
| C866 | LHS.A.B1 | 13.4 | E866 | RHS.A.B1 | 12.9 |
| | | 15.5 | | | 16.1 |
| | | 13.5 | | | 13.6 |
| | LHS.B.B1 | 12.9 | | RHS.B.B1 | 16.8 |
| | | 13.5 | | | 17.2 |
| | | 13.4 | | | 14.8 |
| | LHS.C.B1 | 10.1 | | RHS.C.B1 | 16.1 |
| | | 10.4 | | | 16.2 |
| | | 11 | | | 15.0 |
| Average | | 12.6 | Average | | 15.4 |
| C872 | LHS.A.B1 | 14.1 | E872 | RHS.A.B1 | 16.3 |
| | | 13.2 | | | 16.0 |
| | | 12.1 | | | 14.8 |
| | LHS.B.B1 | 12.9 | | RHS.B.B1 | 16.2 |
| | | 13.8 | | | 17.2 |
| | | 12.7 | | | 15.4 |
| | LHS.C.B1 | | | RHS.C.B1 | 14.5 |
| | | | | | 14.8 |
| | | | | | 12.9 |
| Average | | 13.1 | Average | | 15.3 |
| C869 | LHS.A.B1 | 15.9 | E869 | RHS.A.B1 | 14.5 |
| | | 15.1 | | | 14.8 |
| | | 15.1 | | | 13.3 |
| | LHS.B.B1 | 14.9 | | RHS.B.B1 | 14.6 |
| | | 15.5 | | | 15.9 |
| | | 11.9 | | | 14.4 |
| | LHS.C.B1 | 13.5 | | RHS.C.B1 | 12.1 |
| | | 12.3 | | | 13.3 |
| | | 13.1 | | | 14 |
| | Average | 14.1 | | Average | 14.1 |

| Bag 1 Diameter total of all averages | | | |
|---|---|---|---|
| | C866 | C872 | C869 |
| Control of LHS.B1 | 12.6 | 13.1 | 14.1 |
| Experimental.RHS.B1 | 15.4 | 15.3 | 14.1 |
| Standard error | | | |
| Control of LHS.B1 | 0.59 | 0.31 | 0.49 |
| Experimental.RHS.B1 | 0.48 | 0.42 | 0.36 |

Table 2.6 $Bag_1$ fibre diameter; control versus the experimental measured in μm which are used for the analysis of variance.

| Sample | Control | Experimental |
|---|---|---|
| 866A | 13.4 | 12.9 |
| | 15.5 | 16.1 |
| | 13.5 | 13.6 |
| 866B | 12.9 | 16.8 |
| | 13.5 | 17.2 |
| | 13.4 | 14.8 |
| 866C | 10.1 | 16.1 |
| | 10.4 | 16.2 |
| | 11.0 | 15.0 |
| 872A | 14.1 | 16.3 |
| | 13.2 | 16.0 |
| | 12.1 | 14.8 |
| 872B | 12.9 | 16.2 |
| | 13.8 | 17.2 |
| | 12.7 | 15.4 |
| 896A | 15.9 | 14.5 |
| | 15.1 | 14.8 |
| | 15.1 | 13.3 |
| 896B | 14.9 | 14.6 |
| | 15.5 | 15.9 |
| | 11.9 | 14.4 |
| 896C | 13.5 | 12.1 |
| | 12.3 | 13.3 |
| | 13.1 | 14.0 |

Table 2.7 Analysis of variance of $bag_1$ diameter.

| ANOVA: Two-Factor With Replication for $Bag_1$ | | | |
|---|---|---|---|
| SUMMARY | Control | Experimental | Total |
| *866A* | | | |
| Count | 3.0 | 3.0 | 6.0 |
| Sum | 42.4 | 42.6 | 85.0 |
| Average | 14.1 | 14.2 | 14.2 |
| Variance | 1.3 | 2.7 | 1.6 |
| *866B* | | | |
| Count | 3.0 | 3.0 | 6.0 |
| Sum | 39.9 | 48.8 | 88.7 |
| Average | 13.3 | 16.3 | 14.8 |
| Variance | 0.1 | 1.7 | 3.4 |
| *866C* | | | |
| Count | 3.0 | 3.0 | 6.0 |
| Sum | 31.5 | 47.3 | 78.8 |
| Average | 10.5 | 15.8 | 13.1 |
| Variance | 0.2 | 0.4 | 8.6 |
| *872A* | | | |
| Count | 3.0 | 3.0 | 6.0 |
| Sum | 39.4 | 47.1 | 86.5 |
| Average | 13.1 | 15.7 | 14.4 |
| Variance | 1.1 | 0.7 | 2.7 |
| *872B* | | | |
| Count | 3.0 | 3.0 | 6.0 |
| Sum | 39.4 | 48.8 | 88.2 |
| Average | 13.1 | 16.3 | 14.7 |
| Variance | 0.3 | 0.8 | 3.4 |
| *896A* | | | |
| Count | 3.0 | 3.0 | 6.0 |
| Sum | 46.1 | 42.6 | 88.7 |
| Average | 15.4 | 14.2 | 14.8 |
| Variance | 0.2 | 0.6 | 0.7 |
| *896B* | | | |
| Count | 3.0 | 3.0 | 6.0 |
| Sum | 42.3 | 44.9 | 87.1 |
| Average | 14.1 | 15.0 | 14.5 |
| Variance | 3.7 | 0.6 | 2.0 |
| *896C* | | | |
| Count | 3.0 | 3.0 | 6.0 |
| Sum | 38.9 | 39.4 | 78.3 |
| Average | 13.0 | 13.1 | 13.1 |
| Variance | 0.4 | 0.9 | 0.5 |
| *Total* | | | |
| Count | 24.0 | 24.0 | |
| Sum | 319.9 | 361.4 | |
| Average | 13.3 | 15.1 | |
| Variance | 2.4 | 1.9 | |

Table 2.8 Analysis of variance (two –factor with replication) showing very low P-value which indicates a significant difference in diameter between control and experimental $bag_1$ fibre.

| ANOVA | | | | | | |
|---|---|---|---|---|---|---|
| *Source of Variation* | *SS* | *Df* | *MS* | *F* | *P-value*** | *F crit* |
| Sample | 21.2 | 7.0 | 3.0 | 3.0 | 0.014401 | 2.3 |
| Columns | 36.0 | 1.0 | 36.0 | 36.2 | 1.04E-06 | 4.1 |
| Interaction | 46.8 | 7.0 | 6.7 | 6.7 | 6.33E-05 | 2.3 |
| Within | 31.8 | 32.0 | 1.0 | | | |
| | | | | | | |
| Total | 135.7 | 47.0 | | | | |
| | | | | | | |

Table 2.9 t-Test: Paired Two Sample for Means for bag1 diameter. The P (T<=t) one-tail is less than 0.05

| | *Variable 1* | *Variable 2* |
|---|---|---|
| Mean | 13.3 | 15.1 |
| Variance | 2.4 | 1.9 |
| Observations | 24.0 | 24.0 |
| Pearson Correlation | -0.1 | |
| Hypothesized Mean Difference | 0.0 | |
| Df | 23.0 | |
| t Stat | -3.9 | |
| P(T<=t) one-tail | 0.0 | |
| t Critical one-tail | 1.7 | |
| P(T<=t) two-tail | 0.0 | |
| t Critical two-tail | 2.1 | |

Chart 2.5 Means diameters of control (LHS) $bag_2$ fibres in blue and average diameters of experimental (RHS) $bag_2$ fibres in brown. In this chart just as in the extrafusal sarcomeres the result fit exactly with what had been expected when the experiment was designed where the greatest difference is seen in 866 followed by 872 and then 869.

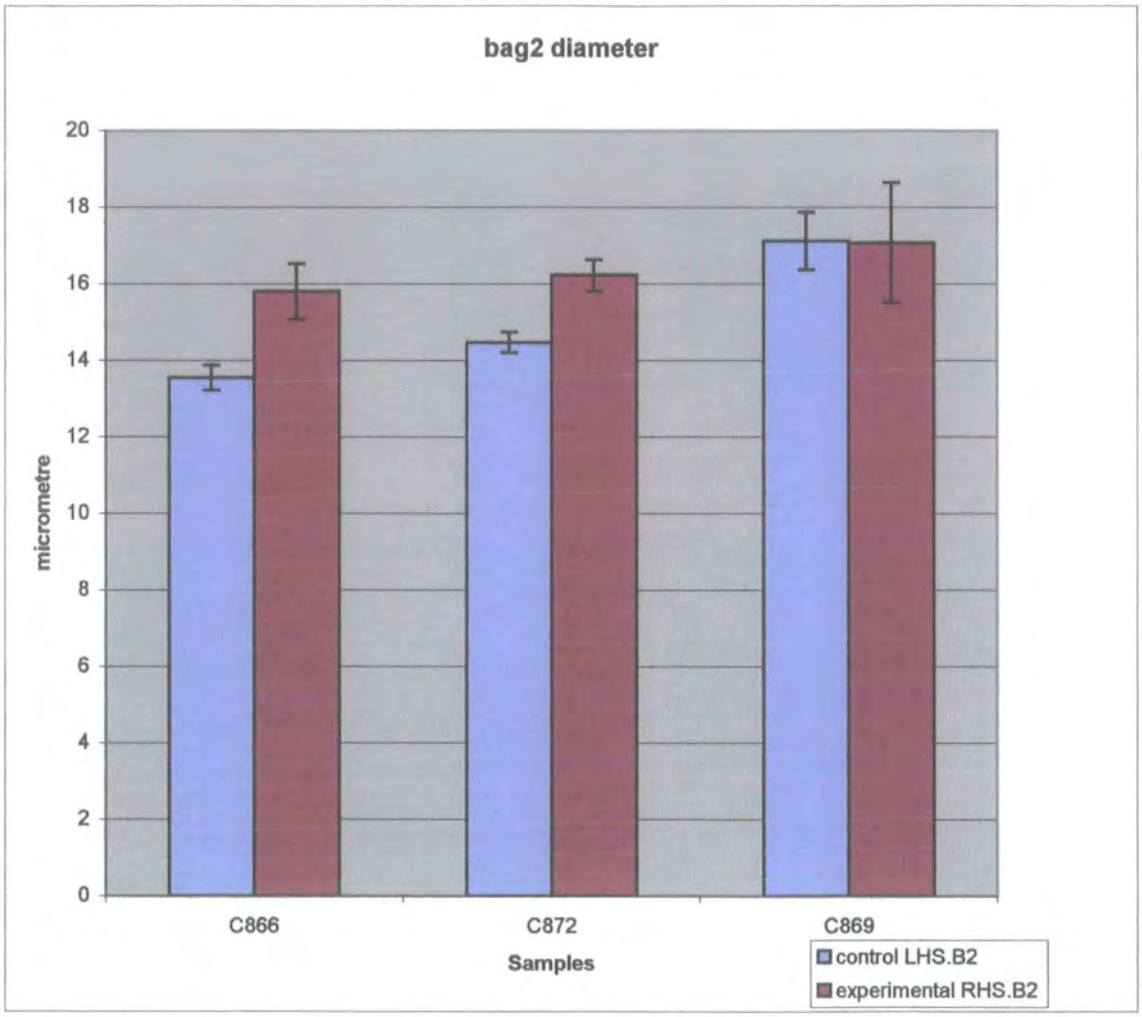

Table 2.10 Mean diameters of $bag_2$ fibres of control and experimental samples measured in μm.

| Control | | | Experimental | | |
|---|---|---|---|---|---|
| Sample | | Diameter width | Sample | | Diameter width |
| C866 | LHS.A.B2 | 16.1 | E866 | RHS.A.B2 | 16.2 |
| | | 17.6 | | | 17.5 |
| | | 14.4 | | | 15.5 |
| | LHS.B.B2 | 11.5 | | RHS.B.B2 | 16.1 |
| | | 11.9 | | | 16.7 |
| | | 11.0 | | | 14.8 |
| | LHS.C.B2 | 13.1 | | RHS.C.B2 | 15.7 |
| | | 13.1 | | | 15.6 |
| | | 13.4 | | | 14.1 |
| Average | | 13.6 | Average | | 15.8 |
| C872 | LHS.A.B2 | 14.2 | E872 | RHS.A.B2 | 17.2 |
| | | 14.3 | | | 16.2 |
| | | 15.4 | | | 16.8 |
| | LHS.B.B2 | 15.9 | | RHS.B.B2 | 15.6 |
| | | 14.1 | | | 15.2 |
| | | 13.1 | | | 16.8 |
| | LHS.C.B2 | | | RHS.C.B2 | 14.9 |
| | | | | | 16.8 |
| | | | | | 16.5 |
| Average | | 14.5 | Average | | 16.2 |
| C869 | LHS.A.B2 | 19.02 | E869 | RHS.A.B2 | 18.2 |
| | | 20.92 | | | 20.4 |
| | | 21.22 | | | 20.6 |
| | LHS.B.B2 | 19.88 | | RHS.B.B2 | 16.2 |
| | | 21.1 | | | 16.2 |
| | | 18.9 | | | 13.9 |
| | LHS.C.B2 | 9.999 | | RHS.C.B2 | 15.4 |
| | | 10.73 | | | 15.9 |
| | | 12.32 | | | 17.0 |
| | Average | 17.1 | | Average | 17.1 |

| $Bag_2$ Diameters | | | |
|---|---|---|---|
| | C866 | C872 | C869 |
| Control of LHS.B2 | 13.6 | 14.5 | 17.1 |
| Experimental of RHS.B2 | 15.8 | 16.2 | 17.1 |
| Standard errors | | | |
| Control.LHS.B2 | 0.72 | 0.41 | 1.56 |
| Experimental.RHS.B2 | 0.33 | 0.27 | 0.75 |

All measurements are in μm and done by LaserPix see appendix 5.

Table 2.11 $Bag_2$ fibre diameters; control versus experimental measured in μm, which are used for the analysis of variance.

| Sample | Control | Experimental |
|---|---|---|
| 866A | 16.1 | 16.2 |
| | 17.6 | 17.5 |
| | 14.4 | 15.5 |
| 866B | 11.5 | 16.1 |
| | 12.0 | 16.7 |
| | 11.0 | 14.8 |
| 866C | 13.1 | 15.7 |
| | 13.1 | 15.6 |
| | 13.4 | 14.2 |
| 872A | 14.2 | 17.2 |
| | 14.3 | 16.2 |
| | 15.4 | 16.8 |
| 872B | 15.9 | 15.6 |
| | 14.2 | 15.2 |
| | 13.1 | 16.8 |
| 869A | 19.0 | 18.2 |
| | 20.9 | 20.4 |
| | 21.2 | 20.6 |
| 869B | 19.9 | 16.2 |
| | 21.1 | 16.2 |
| | 18.9 | 13.9 |
| 869C | 10.0 | 15.4 |
| | 10.7 | 15.9 |
| | 12.3 | 17.0 |

Table 2.12 Analysis of variance for $bag_2$ diameter control versus experimental.

| ANOVA: Two-Factor With Replication | | | |
|---|---|---|---|
| SUMMARY | Control | Experimental | Total |
| *866A* | | | |
| Count | 3.0 | 3.0 | 6.0 |
| Sum | 48.0 | 49.2 | 97.2 |
| Average | 16.0 | 16.4 | 16.2 |
| Variance | 2.5 | 1.0 | 1.4 |
| *866B* | | | |
| Count | 3.0 | 3.0 | 6.0 |
| Sum | 34.4 | 47.6 | 81.9 |
| Average | 11.5 | 15.9 | 13.7 |
| Variance | 0.2 | 1.0 | 6.3 |
| *866C* | | | |
| Count | 3.0 | 3.0 | 6.0 |
| Sum | 39.5 | 45.5 | 85.0 |
| Average | 13.2 | 15.2 | 14.2 |
| Variance | 0.1 | 0.8 | 1.5 |
| *872A* | | | |
| Count | 3.0 | 3.0 | 6.0 |
| Sum | 43.8 | 50.2 | 94.0 |
| Average | 14.6 | 16.7 | 15.7 |
| Variance | 0.4 | 0.3 | 1.6 |
| *872B* | | | |
| Count | 3.0 | 3.0 | 6.0 |
| Sum | 43.1 | 47.7 | 90.8 |
| Average | 14.4 | 15.9 | 15.1 |
| Variance | 2.0 | 0.7 | 1.8 |
| *869A* | | | |
| Count | 3.0 | 3.0 | 6.0 |
| Sum | 61.2 | 59.2 | 120.3 |
| Average | 20.4 | 19.7 | 20.1 |
| Variance | 1.4 | 1.8 | 1.4 |
| *869B* | | | |
| Count | 3.0 | 3.0 | 6.0 |
| Sum | 59.9 | 46.3 | 106.2 |
| Average | 20.0 | 15.4 | 17.7 |
| Variance | 1.2 | 1.8 | 7.3 |
| *869C* | | | |
| Count | 3.0 | 3.0 | 6.0 |
| Sum | 33.1 | 48.2 | 81.2 |
| Average | 11.0 | 16.1 | 13.5 |
| Variance | 1.4 | 0.7 | 8.5 |

Table 2.13 Analysis of variance (two–factor with replication) showing very low P- value which indicates a significant difference between control and experimental $bag_2$ fibre.

| *Total* | | | | | |
|---|---|---|---|---|---|
| Count | 24.0 | 24.0 | | | |
| Sum | 362.9 | 393.8 | | | |
| Average | 15.1 | 16.4 | | | |
| Variance | 12.1 | 2.5 | | | |
| ANOVA | | | | | |
| *Source of Variation* | *SS* | *df* | *MS* | *F* | *P-value* |
| Sample | 208.2 | 7.0 | 29.7 | 27.6 | 7.55E-12 |
| Columns | 19.9 | 1.0 | 19.9 | 18.5 | 0.000149 |
| Interaction | 94.9 | 7.0 | 13.6 | 12.6 | 1.23E-07 |
| Within | 34.4 | 32.0 | 1.1 | | |
| | | | | | |
| Total | 357.5 | 47.0 | | | |

2.14 t-Test: Paired Two Sample for Means for $bag_2$. P (T<=t) one-tail is less than 0.5

| | *Variable 1* | *Variable 2* |
|---|---|---|
| Mean | 15.1 | 16.4 |
| Variance | 12.1 | 2.5 |
| Observations | 24.0 | 24.0 |
| Pearson Correlation | 0.5 | |
| Hypothesized Mean Difference | 0.0 | |
| Df | 23.0 | |
| t Stat | -2.1 | |
| P(T<=t) one-tail | 0.0 | |
| t Critical one-tail | 1.7 | |
| P(T<=t) two-tail | 0.0 | |
| t Critical two-tail | 2.1 | |

## 2.5.9. Sensory innervation and nerve endings.

Most intrafusal muscle fibres are supplied by two types of sensory axons: these are large primary and small secondary afferent axons.

### 2.5.9.1. Sensory endings

Sensory nerve endings usually occupy small channels in the surface of intrafusal muscle fibres and form an annulospiral covering the nucleated region of the equatorial part of the fibres. On the $bag_1$ fibres these terminals may lie parallel to the axis of the intrafusal fibres on either side of the spiral (Banks, Barker and Stacey, 1982)

### 2.5.9.2. Primary endings

The primary nerve endings terminate on the equatorial parts of the intrafusal muscle fibres which are the most densely nucleated parts of the fibres. The terminals are annulspiral in form and occupy a length of about 350$\mu$m.

Within the primary ending the terminals are not symmetrically distributed; their form depends on the location of each one on the complete system. On the bag fibres, pure spirals are confined to those parts of the terminals that happen to overlie the nuclear bag. Ultrastructural studies of primary nerve terminals have shown that they lie in shallow grooves on the surface of the muscle fibres to form smooth myoneural junctions. In contrast to the motor myoneural junctions there is no intervening basal lamina, and the terminals are not covered by Schwann cells but by basal lamina continuous with that of the muscle fibres. In longitudinal sections of spindles, terminals appear as typically

lenticular in profile, with differential indentation into the three types of muscle fibre: most deeply in the chain and least in the $bag_1$ fibres (Fig. 2.1). It is believed that the lenticular profile is consistent with the terminals being deformed from a condition of minimum energy and surface area (circular profile) by longitudinal tension in the muscle fibre as well as in the basal laminae that cover the outer surfaces of both the fibres and the terminals. If it is assumed that the basal laminae associated with the different types of intrafusal fibre have similar mechanical properties, the differential indentation of the fibres by the terminals would be due to the mechanical properties of the fibres. Moreover, increased static stretch of the spindle would be expected to increase standing tension in the basal laminae and muscle fibres, thereby also causing the radii of curvature of the outer and inner surfaces of the lenticular terminal profiles to increase (Banks, 1986).

### 2.5.9.3. Secondary Endings

The secondary sensory nerve endings are more distributed to the chain fibres. Most spindles contain one or more secondary endings, which will terminate on one or both sides of the primary. The most seen by Barker and Banks on one side is five, and on both sides six. Each secondary ending occupies a length of about 350μm and is designated $S_1$, $S_2$, $S_3$, and so on, according to its position relative to the primary. (Banks and Barker 2004)

## 2.5.10. Nerve ending measurements.

Measurements of nerve endings of the outer sector radius (O), inner radius (I) and their cord (C) on the extended control and the flexed experimental sides for both $bag_1$ and $bag_2$ were achieved using the LaserPix program. Measurements of their absolute value are summarised in table 2.15 for $bag_1$ with statistical analysis on tables 2.16 to 2.19. Charts of O, I, C are also shown in charts 2.6 to 2.8 respectively: For $bag_2$ the summary of absolute is given in table 2.20 with statistical analysis in tables 2.21 to 2.24. Charts of O, I, C for $bag_2$ are shown in charts 2.9 to 2.11.

## 2.5.11. Descriptive statistics, ANOVA and t-test.

As mentioned in section 2.5.10 the values of O, I, and C, were subjected to descriptive statistics, analysis of variance, and t–test on all mean data for $bag_1$ (experimental vs. control). These mean values were also used to plot charts for every measured parameter of the nerve endings namely O, I, C, for the experimental vs. the control sample for $bag_1$ and subsequently the experimental vs. the control samples for $bag_2$ fibres. From the analysis of the mean values, the charts, and comparison of the LHS and RHS indicative parameters O, I and C, which were measured in order to detect changes in the nerve endings due to tension on their intrafusal fibre, it appears that the changes did occur in a consistent pattern that reflects changes on the experimental side (RHS) in comparison to the control side (LHS), as seen from the following sections.

## 2.5.12. $Bag_1$

The outer radii O of the control intrafusal $bag_1$ fibres from samples 866, 872 and 869, are all greater than the outer radii O of samples from the $bag_1$ experimental samples (see table 2.15 and chart 2.6). The inner radii (I) of the control intrafusal $bag_1$ fibres from samples 866, 872 and 869 are all greater than the inner radii (I) of samples from the $bag_1$ experimental samples (see table 2.15 and chart 2.7). The length of the semi cords (C) of control samples of $bag_1$ fibres from samples 866, 872 and 869 are all slightly greater than that on the experimental side, the least difference being in 872 (see table 2.15 and chart 2.8). The semicord, C seem to show the least differences between control and experimental spindles in comparison with the radii O and I, which is an indication that the size or volumes of the nerve endings changes little if any. Sample 872 seem to stand out as the one expressing the highest tension difference between control and experimental in both $bag_1$and $bag_2$.

Chart 2.6 Outer radii (O), of control vs. experimental $bag_1$ fibres. In each case the mean value of O in the control is greater than that of the corresponding experimental.

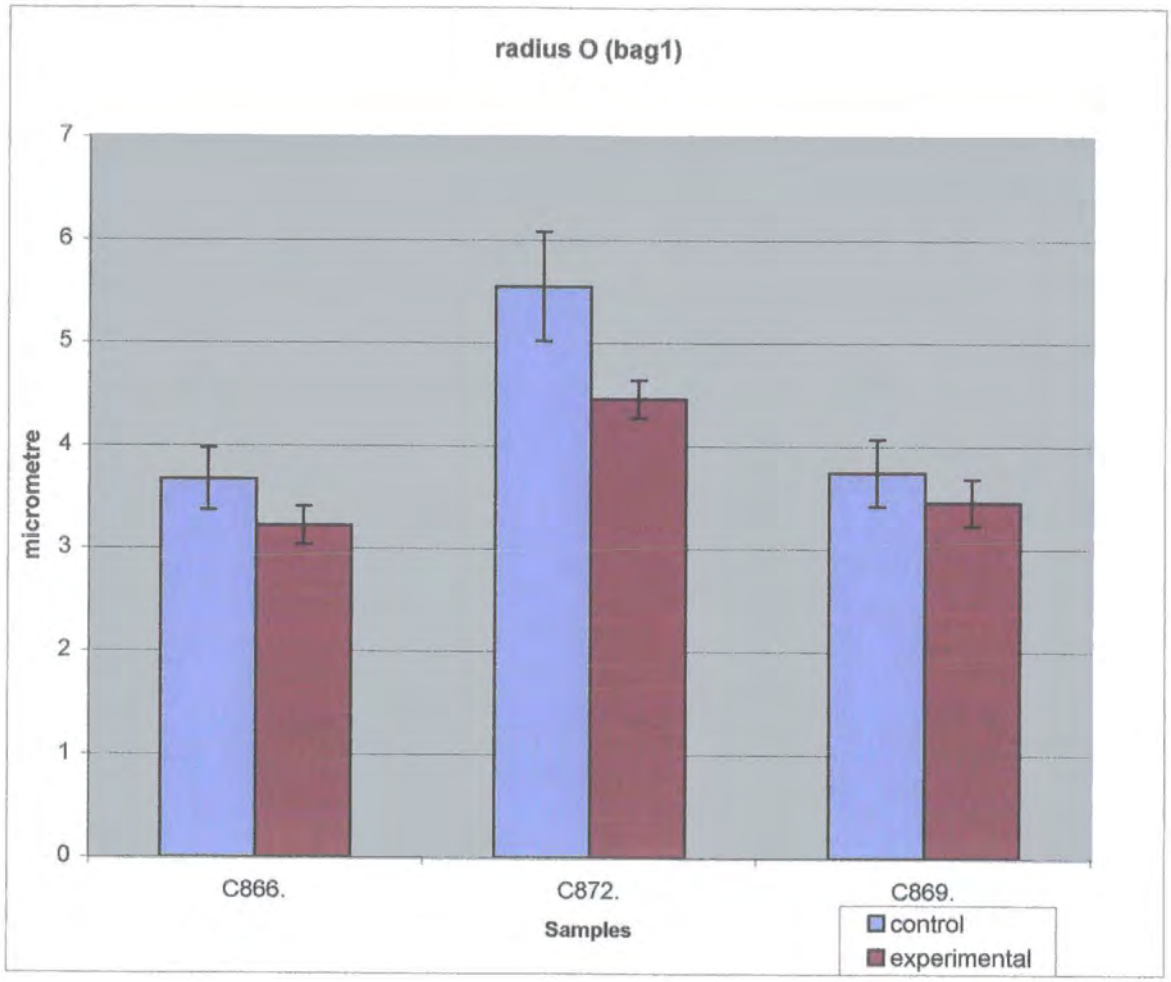

Chart 2.7 Inner radii (I), of control vs. experimental $bag_1$ fibres. In each case the mean value of I in the control is greater than that of the corresponding experimental.

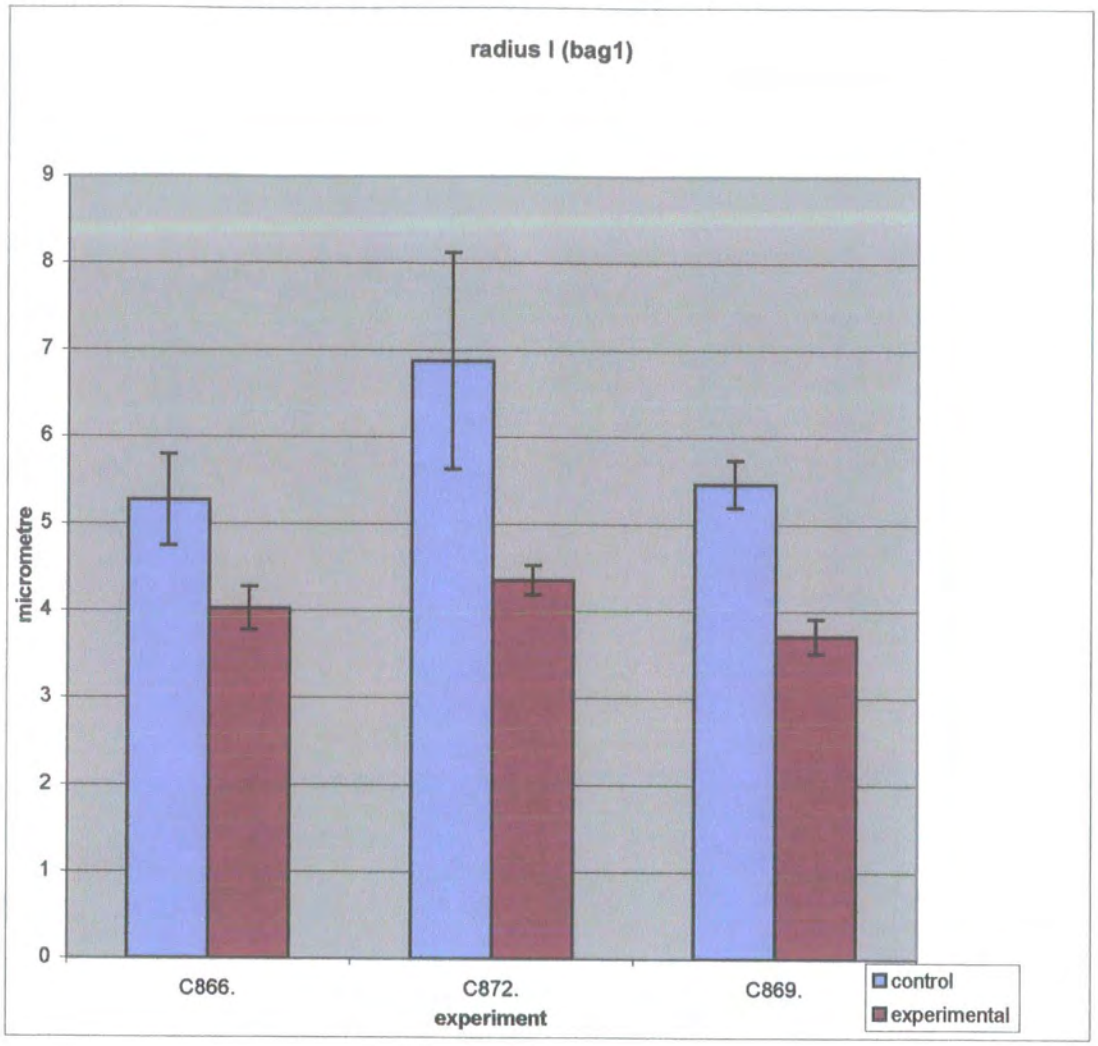

Chart 2.8 Semi cord (C), of control vs. experimental $bag_1$ fibres. In each case the mean value of C in the control is slightly greater than that of the corresponding experimental.

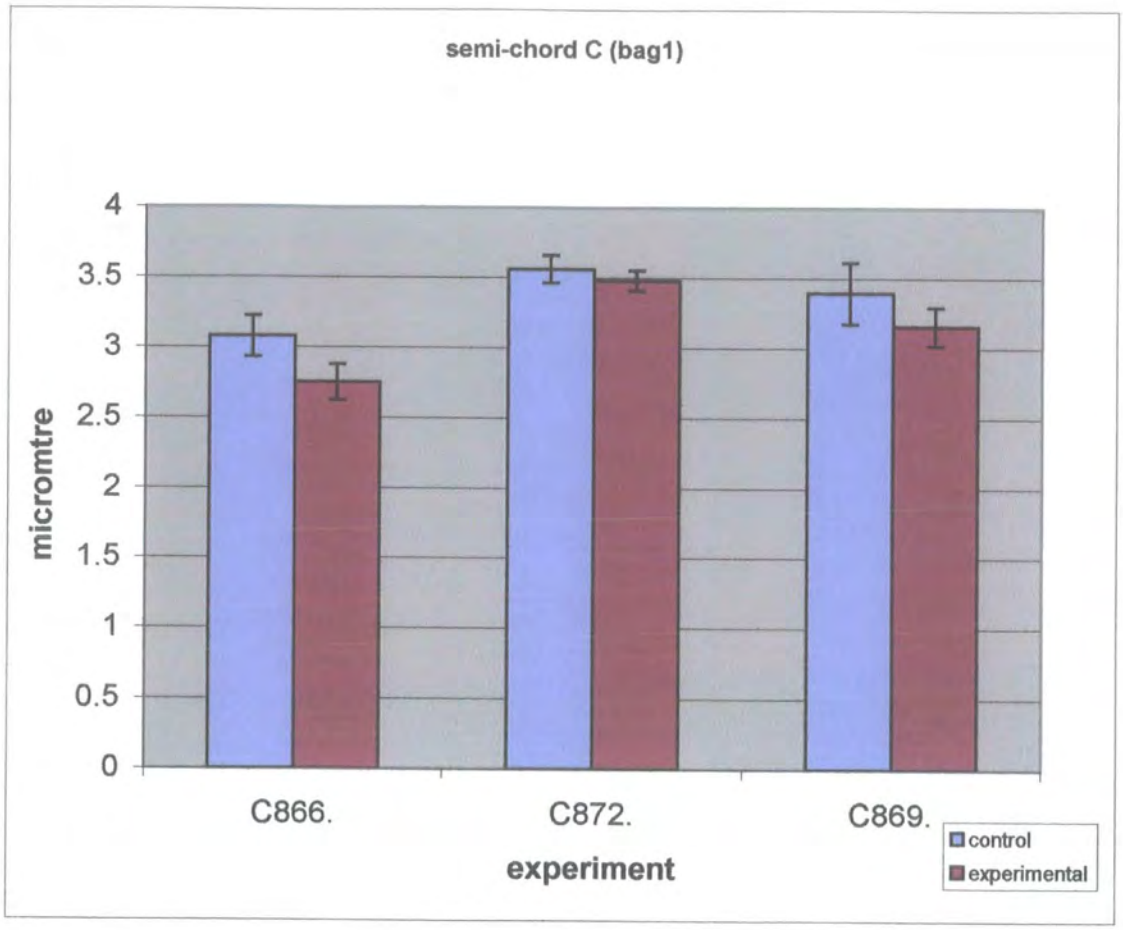

Table 2.15 Summary of mean and standard errors of the values of O, I, C, for the experimental and control samples of $bag_1$ measured in μm. O and I of control spindles are all higher than those of experimental spindles, while semicord C is only slightly different.

| | Outer Radius, O (μm) | | |
|---|---|---|---|
| Sample | 866 | 872 | 869 |
| Control. LHS | 3.7 | 5.5 | 3.7 |
| Experimental. RHS | 3.2 | 4.5 | 3.5 |
| S E of control | 0.3 | 0.5 | 0.3 |
| S E of experimental | 0.2 | 0.2 | 0.2 |
| | Inner Radius I (μm) | | |
| Samples | 866 | 872 | 869 |
| Control. LHS | 5.27 | 6.88 | 5.47 |
| Experimental. RHS | 4.03 | 4.36 | 3.72 |
| S E of control | 0.53 | 1.24 | 0.27 |
| S E of experimental | 0.25 | 0.17 | 0.2 |
| | Samples Semicord C (μm) | | |
| | 866 | 872 | 869 |
| Control. LHS | 3.08 | 3.56 | 3.4 |
| Experimental. RHS | 2.75 | 3.48 | 3.16 |
| S E of control | 0.15 | 0.1 | 0.22 |
| S E of experimental | 0.13 | 0.07 | 0.14 |

All measurements are in μm (see Fig 2.4).

Table 2.16 Values of O, I, and C in (μm) for control versus the experimental $bag_1$ fibres as used for the analysis of variance.

| Samples | Radii | control | Experimental |
|---|---|---|---|
| 866 | O | 3.7 | 3.2 |
| | I | 5.3 | 4.0 |
| | C | 3.1 | 2.8 |
| 872 | O | 5.6 | 4.5 |
| | I | 6.9 | 4.4 |
| | C | 3.6 | 3.5 |
| 869 | O | 3.7 | 3.5 |
| | I | 5.5 | 3.7 |
| | C | 3.4 | 3.2 |

Table 2.17 Analysis of variance of the means of the absolute values of O, I, C of

$bag_1$ control versus experimental.

| *SUMMARY* | *Count* | *Sum* | *Average* | *Variance* |
|---|---|---|---|---|
| O | 2 | 6.9 | 3.45 | 0.1 |
| I | 2 | 9.3 | 4.65 | 0.78 |
| C | 2 | 5.83 | 2.91 | 0.05 |
| O | 2 | 10 | 5 | 0.6 |
| I | 2 | 11.2 | 5.62 | 3.18 |
| C | 2 | 7.04 | 3.52 | 0 |
| O | 2 | 7.2 | 3.6 | 0.04 |
| I | 2 | 9.18 | 4.59 | 1.53 |
| C | 2 | 6.55 | 3.28 | 0.03 |
| Control | 9 | 40.6 | 4.51 | 1.71 |
| Experimental | 9 | 32.6 | 3.63 | 0.32 |

Table 2.18 Analysis of variance (two –factor without) replication of the mean of the absolute values of O, I, C of $bag_1$ control versus experimental. The column *P-value* shows the differences between control and experimental values are significant.

| ANOVA TWO FACTORS WITHOUT REPLICATION | | | | | | |
|---|---|---|---|---|---|---|
| Source of Variation | *SS* | *df* | *MS* | *F* | *P-value* | *F crit* |
| Rows | 13.5 | 8 | 1.69 | 4.88 | 0.02 | 3.44 |
| Columns | 3.55 | 1 | 3.55 | 10.3 | 0.01 | 5.32 |
| Error | 2.76 | 8 | 0.35 | | | |
| Total | 19.8 | 17 | | | | |

Table 2.19 Paired *t*- test on all mean data for $bag_1$- experimental versus control. *P* (*T*<=t) two-tail is less than 0.05

| Sample | 866 | 872 | 869 | 866 | 872 | 869 | 866 | 872 | 869 |
|---|---|---|---|---|---|---|---|---|---|
| Radii | O | O | O | I | I | I | C | C | C |
| Control | 3.67 | 5.55 | 3.74 | 5.27 | 6.88 | 5.47 | 3.08 | 3.56 | 3.4 |
| Expert | 3.22 | 4.46 | 3.46 | 4.03 | 4.36 | 3.72 | 2.75 | 3.48 | 3.16 |

| | *Variable 1* | *Variable 2* |
|---|---|---|
| Mean | 4.51 | 3.63 |
| Variance | 1.71 | 0.32 |
| Observations | 9 | 9 |
| Pearson Correlation | 0.9 | |
| Hypothesized Mean Difference | 0 | |
| Df | 8 | |
| T Stat | 3.21 | |
| P(T<=t) two-tail | 0.01 | |
| T Critical two-tail | 2.31 | |

## 2.5.13. $Bag_2$

As with $bag_1$, the outer radii O of the control intrafusal $bag_2$ fibres from samples 866, 872, are all greater than the outer radii O of samples from the $bag_2$ experimental samples, but in 869 it is the experimental which is bigger than that of the control (see Table 2.20 and chart 2.9).

The inner radii (I) of the control intrafusal $bag_2$ fibres from samples 866, 872, 869 are all greater than the inner radii (I) of samples from the $bag_2$ experimental side (see table 2.20 and chart 2.10).

The lengths of the semicord (C) of control samples of $bag_2$ fibres from samples 866, 872 are all slightly greater than that on the experimental side, but the length of semicord sector C of 869 is slightly greater in the experimental side (see table 2.20 and chart 2.11)

So in general most of the mean values of O, I, C in both $bag_1$ and $bag_2$ on the experimental side are less than those of the corresponding control side.

Sample 872 seems to stand out as the one expressing the highest tension difference between control and experimental in both $bag_1$and $bag_2$.

Chart 2.9 Outer radii (O) of control vs. experimental $bag_2$ fibres. The outer radii O of the control spindles are greater than those of the corresponding experimental spindles except in sample 869.

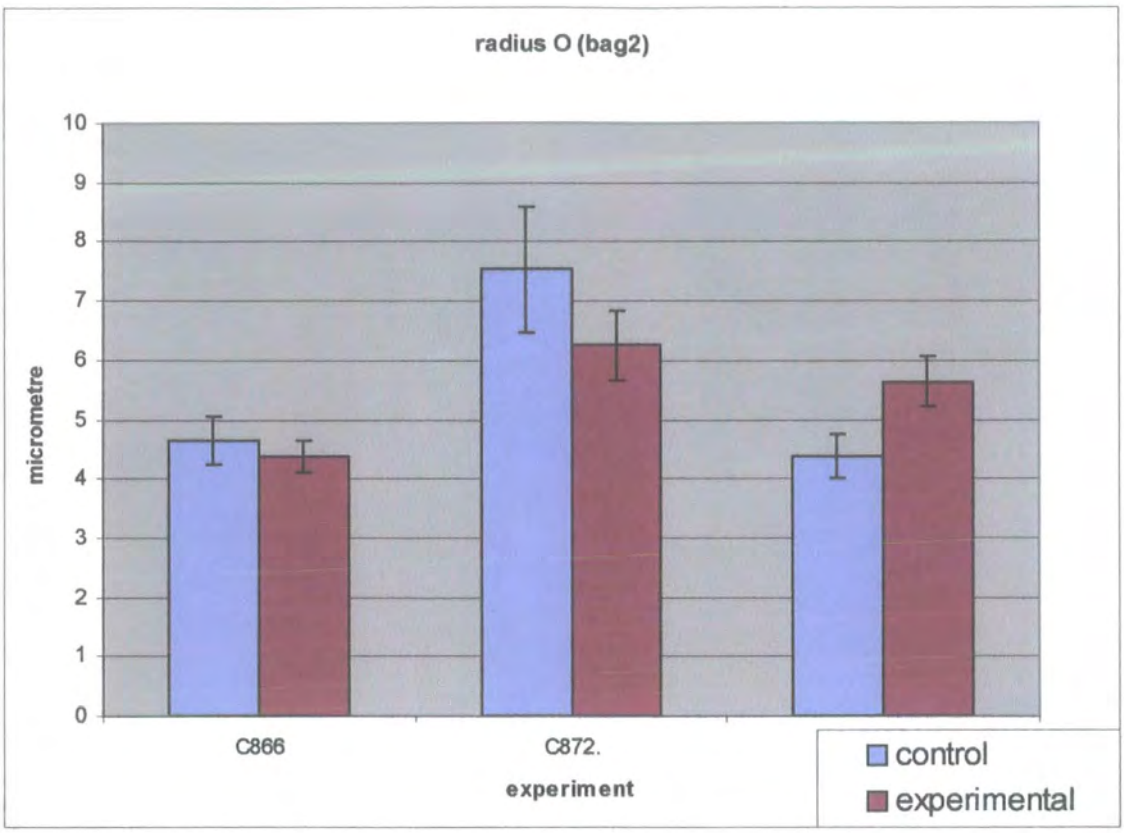

Chart 2.10 Inner radii (I) of control vs. experimental $bag_2$ fibres. The inner radii I of the control spindles am greater than those of the corresponding experimental spindles.

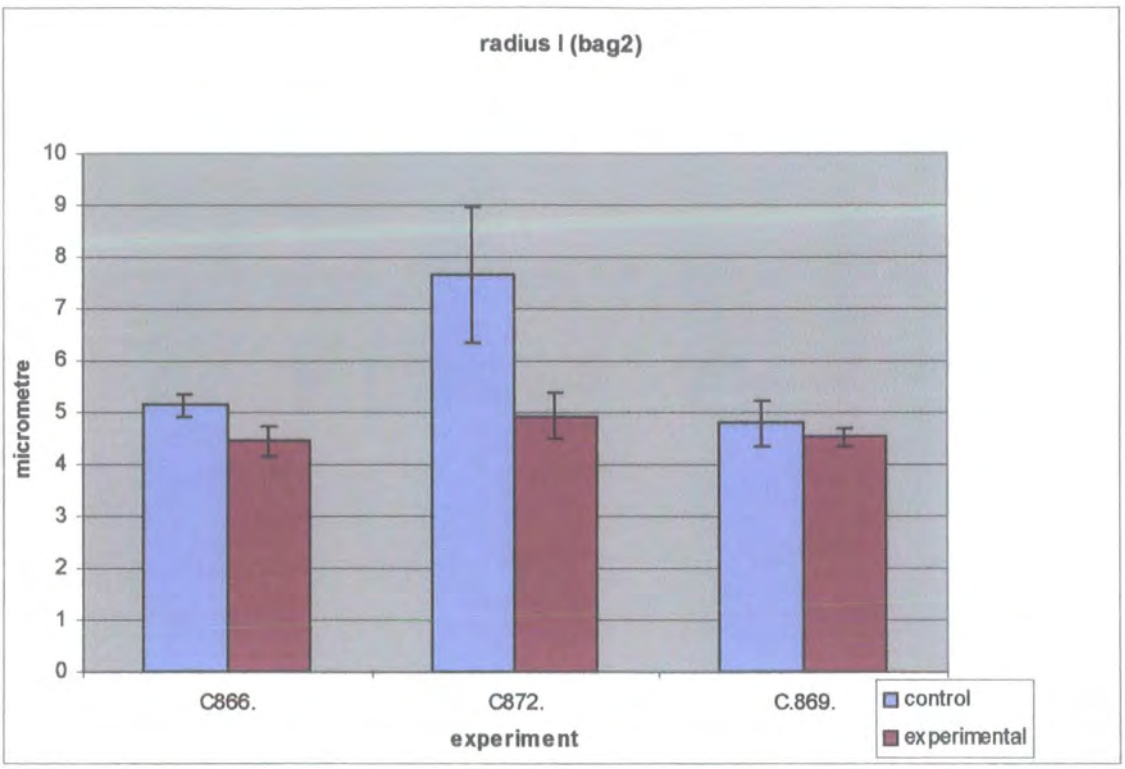

Chart 2.11 Semicored (C) of control vs. experimental $bag_2$ fibres. The semicord C of the control spindles is greater than those of the corresponding experimental spindles except in sample 869.

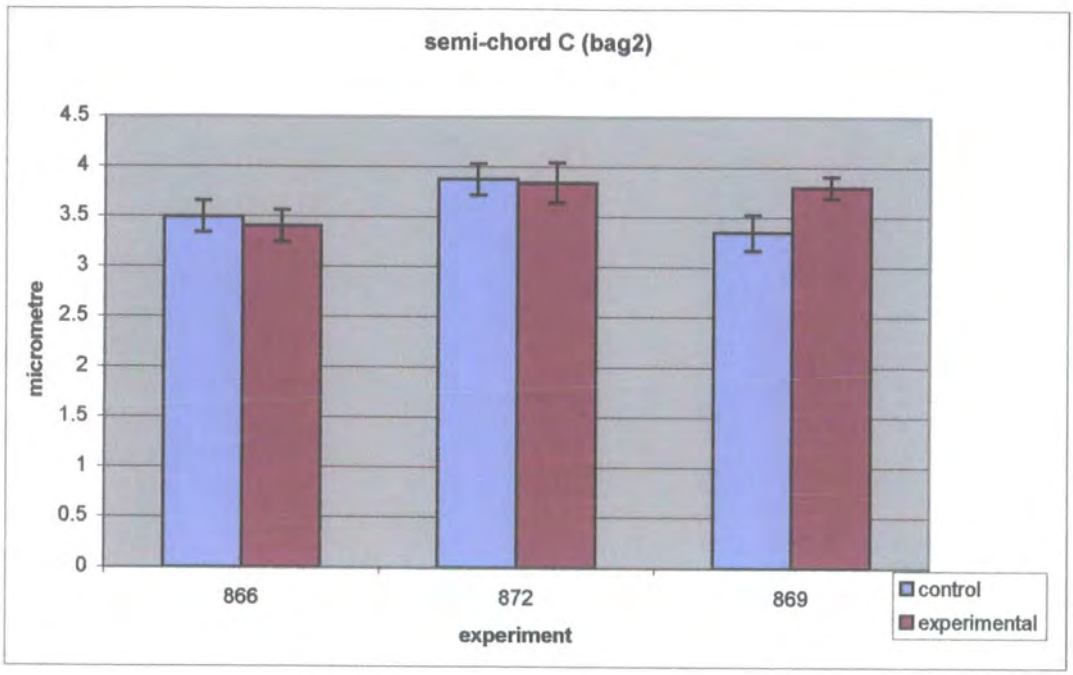

Table 2.20 Summary of mean and standard errors of the values of O, I, C, of the experimental and control samples for $bag_2$. O and I of controls are all greater than those of experimental spindles while semi cord C is only slightly different.

| | Outer Radius, O (μm) | | |
|---|---|---|---|
| | 866 | 872 | 869 |
| Control. LHS | 4.65 | 7.53 | 4.38 |
| Experimental. RHS | 4.37 | 6.25 | 5.63 |
| S E of control | 0.4 | 1.07 | 0.37 |
| S E of experimental | 0.27 | 0.59 | 0.43 |
| | Inner Radius I (μm) | | |
| | 866 | 872 | 869 |
| Control. LHS | 5.15 | 7.66 | 4.8 |
| Experimental. RHS | 4.45 | 4.93 | 4.52 |
| S E of control | 0.21 | 1.3 | 0.44 |
| S E of experimental | 0.3 | 0.45 | 0.18 |
| | Samples Semicord C (μm) | | |
| | 866 | 872 | 869 |
| Control. LHS | 3.5 | 3.88 | 3.35 |
| Experimental. RHS | 3.4 | 3.82 | 3.8 |
| S E of control | 0.16 | 0.16 | 0.18 |
| S E of experimental | 0.16 | 0.2 | 0.11 |

All measurements are in μm.

Table 2.21 Summary of mean values of O, I, and C (μm) for control versus experimental $bag_1$ and $bag_2$ fibres, as used for the analysis of variance.

| | Radii | sample | $bag_2$ | $bag_1$ |
|---|---|---|---|---|
| Control | O | 866 | 4.6 | 3.7 |
| | | 872 | 7.5 | 5.6 |
| | | 869 | 4.4 | 3.7 |
| | I | 866 | 5.1 | 5.3 |
| | | 872 | 7.7 | 6.9 |
| | | 869 | 4.8 | 5.5 |
| | C | 866 | 3.5 | 3.1 |
| | | 872 | 3.9 | 3.6 |
| | | 869 | 3.4 | 3.4 |
| Experimental | O | 866 | 4.4 | 3.2 |
| | | 872 | 6.2 | 4.5 |
| | | 869 | 5.6 | 3.5 |
| | I | 872 | 4.9 | 4.0 |
| | | 872 | 5.3 | 4.4 |
| | | 872 | 4.5 | 3.7 |
| | C | 866 | 3.4 | 2.8 |
| | | 872 | 3.8 | 3.5 |
| | | 869 | 3.8 | 3.2 |

Table 2.22 Analysis of variance of the means of O, I, C of $bag_1$ and $bag_2$ control versus experimental.

| ANOVA: Two-Factor Without Replication | | | | |
|---|---|---|---|---|
| *SUMMARY* | *Count* | *Sum* | *Average* | *Variance* |
| control | 2 | 8.32 | 4.16 | 0.47 |
| | 2 | 13.1 | 6.54 | 1.95 |
| | 2 | 8.13 | 4.06 | 0.2 |
| | 2 | 10.4 | 5.21 | 0.01 |
| | 2 | 14.5 | 7.27 | 0.3 |
| | 2 | 10.3 | 5.13 | 0.22 |
| | 2 | 6.58 | 3.29 | 0.09 |
| | 2 | 7.44 | 3.72 | 0.05 |
| | 2 | 6.75 | 3.37 | 0 |
| experimental | 2 | 7.59 | 3.8 | 0.65 |
| | 2 | 10.8 | 5.39 | 1.73 |
| | 2 | 9.09 | 4.54 | 2.36 |
| | 2 | 8.48 | 4.24 | 0.09 |
| | 2 | 9.61 | 4.81 | 0.41 |
| | 2 | 8.24 | 4.12 | 0.33 |
| | 2 | 6.16 | 3.08 | 0.21 |
| | 2 | 7.32 | 3.66 | 0.07 |
| | 2 | 6.96 | 3.48 | 0.21 |
| $bag_2$ | 18 | 86.5 | 4.8 | 1.65 |
| $bag_1$ | 18 | 73.3 | 4.07 | 1.17 |

Table 2.23 Analysis of variance (two –factor without replication) of the mean values of O, I, and C of $bag_1$ and $bag_2$ control versus experimental. Very low column *P-value* shows that the differences between control and experimental spindles are highly significant.

| ANOVA | | | | | | |
|---|---|---|---|---|---|---|
| Source of Variation | SS | df | MS | F | P-value | F crit |
| Rows | 43.3 | 17 | 2.55 | 9.65 | $10^{-5}$ | 2.27 |
| Columns | 4.87 | 1 | 4.87 | 18.4 | 0.0005 | 4.45 |
| Error | 4.49 | 17 | 0.26 | | | |
| Total | 52.7 | 35 | | | | |

Table 2.24 Paired t- test on all mean data for $bag_1$- $bag_2$ experimental versus control P (T<=t) one-tail is less than 0.5.

| | *Variable 1* | *Variable 2* |
|---|---|---|
| Mean | 5.0 | 4.6 |
| Variance | 2.5 | 0.9 |
| Observations | 9.0 | 9.0 |
| Pearson Correlation | 0.8 | |
| Hypothesized Mean Difference | 0.0 | |
| Df | 8.0 | |
| t Stat | 1.1 | |
| P (T<=t) one-tail | 0.2 | |
| t Critical one-tail | 1.9 | |
| P(T<=t) two-tail | 0.3 | |
| t Critical two-tail | 2.3 | |

## 2.5.14. Discussion

Since samples 866 are the most extended in the control side at length of 150mm and with an obtuse angles at both hip and knee, and the experimental side of the same sample are the most flexed with acute angles for both hip and knee and the shortest muscle length at 120mm, these parameters are assumed to give sample 866 the biggest degree of tension difference, followed by 872 and then 869 in accordance with the different percentage amount of flexion to extension as seen in table 2.1. Though the results with extrafusal sarcomeres and the $bag_1$ and $bag_2$ fibre diameters comply with this assumption, the situation is different when it comes to intrafusal sarcomeres and nerve ending profiles where it seems that sample 872 stands out in all tables as charts and showing the greatest, tension difference. To further scrutinise the statistical data of the nerve endings profiles, the means of all ratios I/O, I/C, O/C were subjected to the same analysis as that of the mean absolute values of O, I, C. See tables 2.25-2.27 and charts 2.12 to 2.14 for $bag_1$ ratios and table 2.28-2.30 and charts 2.15 to 2.17 for $bag_2$, which show results nearly identical to the results seen in the tables and charts of the mean values of O, I, and C. Sample 872 seems also to stand out in the calculation of nerve ending profile ratios as the sample with the greater tension difference between control and experimental spindles in both $bag_1$ and $bag_2$.

Table 2.25 Summary of mean and standard errors of ratios I/O, I/C and O/C of the experimental and control samples of $bag_1$.

| 866- $bag_1$ cont | | | |
|---|---|---|---|
| | Ratio | | |
| | I/O | I/C | O/C |
| Mean | 1.5 | 1.7 | 1.2 |
| Standard Error | 0.1 | 0.1 | 0.1 |
| 866-$bag_1$ experimental | | | |
| | Ratio | | |
| | I/O | I/C | O/C |
| Mean | 1.3 | 1.5 | 1.2 |
| Standard Error | 0.0 | 0.1 | 0.1 |
| 872-$bag_1$ cont | | | |
| | Ratio | | |
| | I/O | I/C | O/C |
| Mean | 1.2 | 1.9 | 1.6 |
| Standard Error | 0.2 | 0.3 | 0.1 |
| 872-$bag_1$ experimental | | | |
| | Ratio | | |
| | I/O | I/C | O/C |
| Mean | 1.0 | 1.3 | 1.3 |
| Standard Error | 0.0 | 0.0 | 0.0 |
| 869-$bag_1$ cont | | | |
| | Ratio | | |
| | I/O | I/C | O/C |
| Mean | 1.5 | 1.6 | 1.1 |
| Standard Error | 0.1 | 0.1 | 0.0 |
| 869-$bag_1$ experimental | | | |
| | Ratio | | |
| | I/O | I/C | O/C |
| Mean | 1.1 | 1.2 | 1.1 |
| Standard Error | 0.0 | 0.0 | 0.0 |

Chart 2.12 Means of ratio (I/O), of control vs. experimental $bag_1$ fibres. In each case the mean values of ratio I/O in the control is greater than that of the corresponding experimental.

| I/O charts of $bag_1$ control vs. experimental. | | | |
|---|---|---|---|
| $Bag_1$ | I/O | I/O | I/O |
| | 866 | 872 | 869 |
| Control | 1.5 | 1.2 | 1.5 |
| Experimental | 1.3 | 1.0 | 1.1 |
| Standard Error | 0.1 | 0.2 | 0.1 |
| Standard Error | 0.0 | 0.0 | 0.0 |

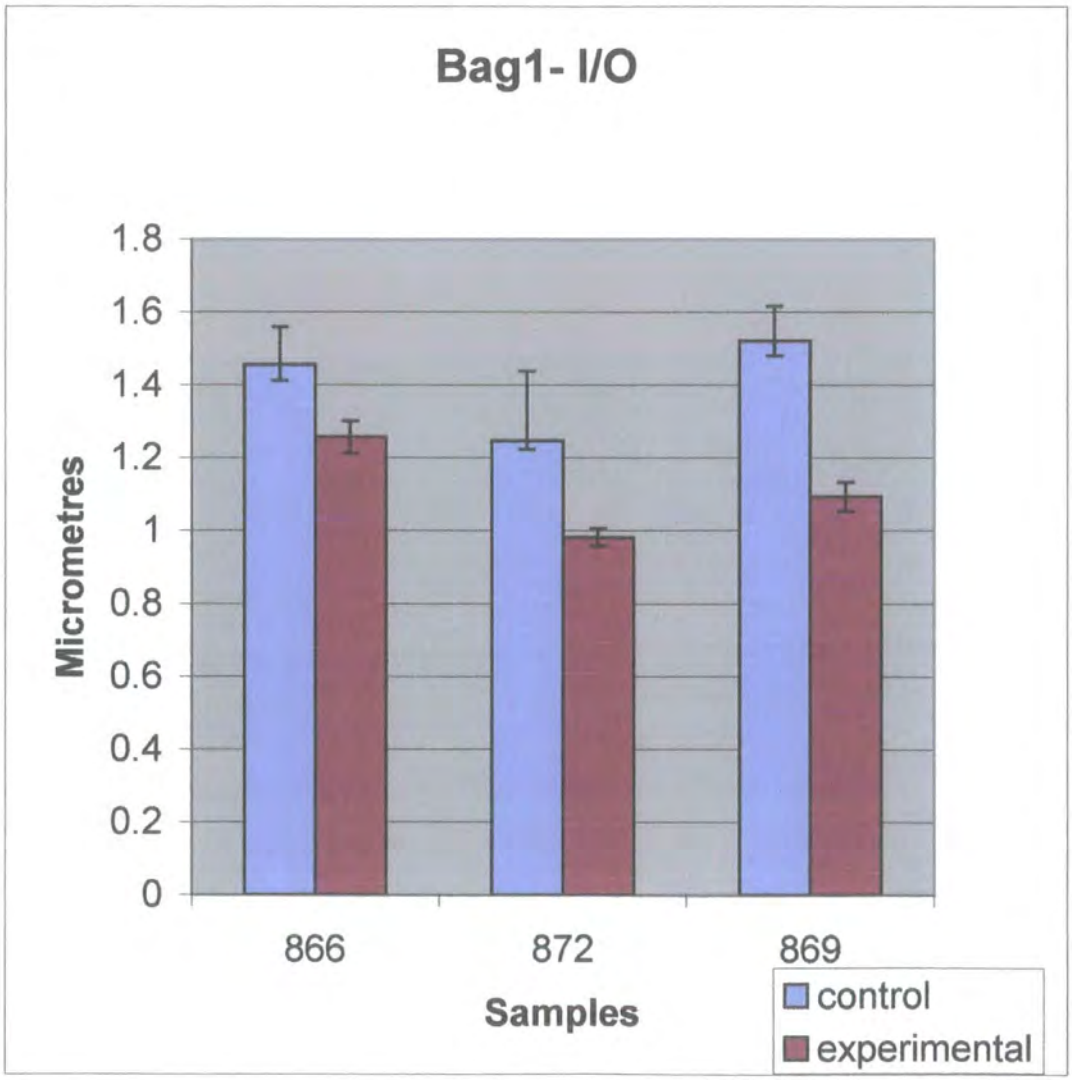

Chart 2.13 Means of ratio (I/C), of control vs. experimental $bag_1$ fibres. In each case the mean values of ratio I/C in the control is greater than that of the corresponding experimental.

| $Bag_1$ | I/C | I/C | I/C |
|---|---|---|---|
| | 866 | 872 | 869 |
| Control | 1.7 | 1.9 | 1.6 |
| Experimental | 1.5 | 1.3 | 1.2 |
| Standard Error | 0.1 | 0.3 | 0.1 |
| Standard Error | 0.1 | 0.0 | 0.0 |

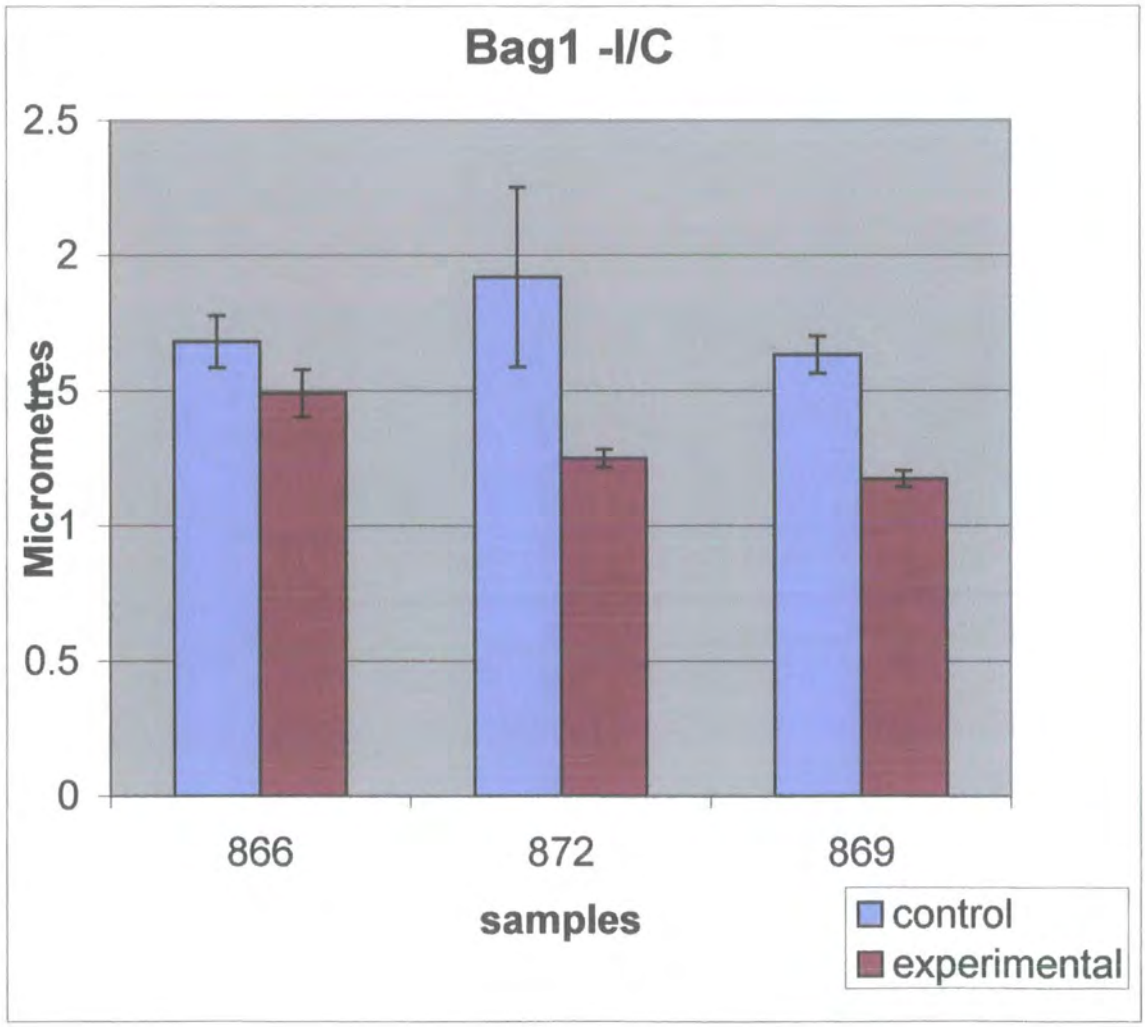

Chart 2.14 Means of ratio (O/C), of control vs. experimental $bag_1$ fibres. In each case the mean values of ratio O/C in the control is greater than that of the corresponding in 872, experimental but nearly equal in sample 869 and 866.

| $Bag_1$ | O/C | O/C | O/C |
|---|---|---|---|
| | 866 | 872 | 869 |
| Control | 1.2 | 1.6 | 1.1 |
| Experimental | 1.2 | 1.3 | 1.1 |
| Standard Error | 0.1 | 0.1 | 0.0 |
| Standard Error | 0.1 | 0.0 | 0.0 |

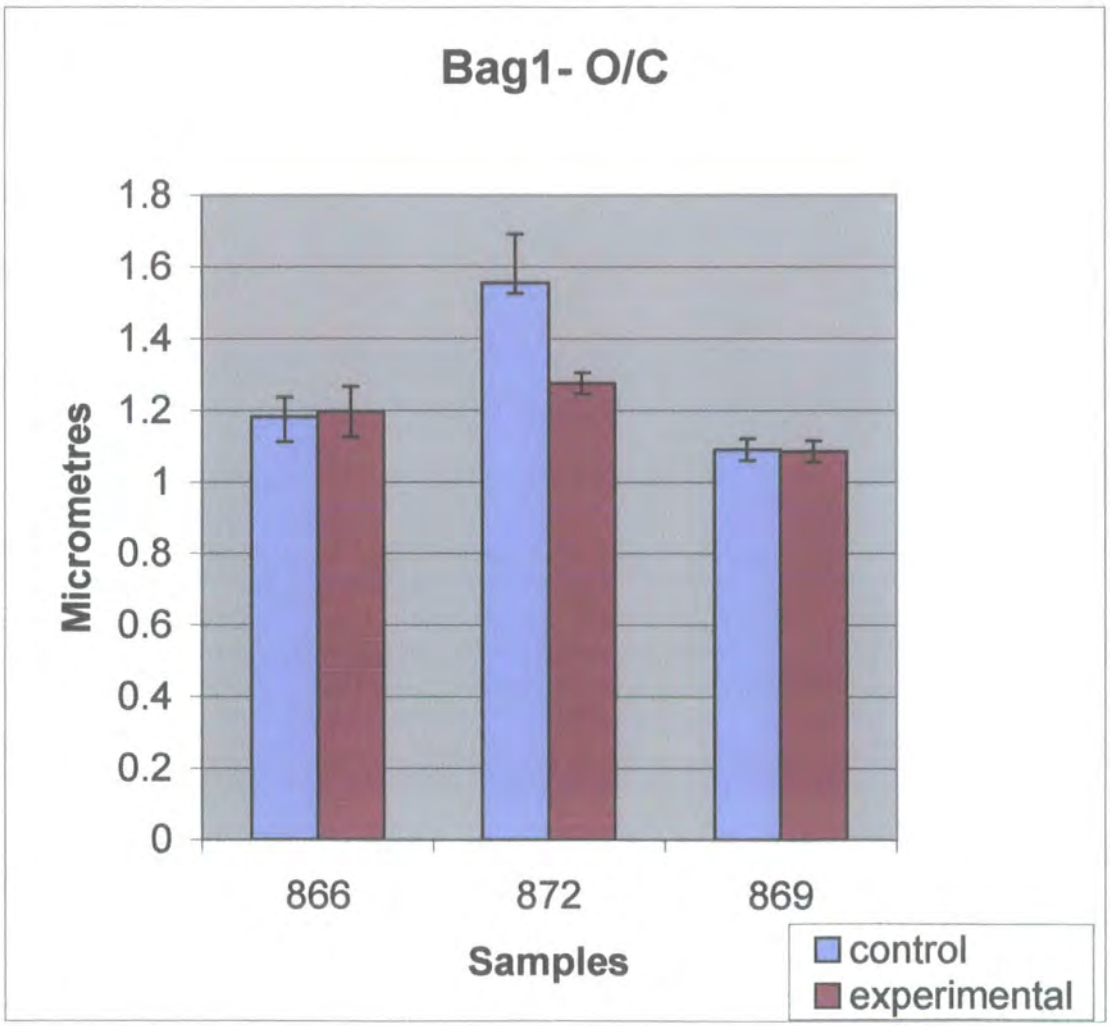

Table 2.26 Mean of ratios I/O, I/C, O/C for control versus experimental $bag_1$ fibres as used for the analysis of variance (Two-Factor Without Replication) column *P-value* indicates significant difference between control and experimental.

ANOVA: Two-Factor without Replication for $bag_1$ radii ratio control vs. experimental.

| $Bag_1$ | Cont | Exp |
|---|---|---|
| I/O-866 | 1.5 | 1.3 |
| I/C | 1.7 | 1.5 |
| O/C | 1.2 | 1.2 |
| I/O-872 | 1.2 | 1.0 |
| I/C | 1.9 | 1.3 |
| O/C | 1.6 | 1.3 |
| I/O-869 | 1.5 | 1.1 |
| I/C | 1.6 | 1.2 |
| O/C | 1.1 | 1.1 |

| ANOVA: Two-Factor Without Replication for $bag_1$ | | | | |
|---|---|---|---|---|
| | | | | |
| *SUMMARY* | *Count* | *Sum* | *Average* | *Variance* |
| Row 1 | 2.00 | 2.71 | 1.36 | 0.02 |
| Row 2 | 2.00 | 3.17 | 1.59 | 0.02 |
| Row 3 | 2.00 | 2.38 | 1.19 | 0.00 |
| Row 4 | 2.00 | 2.23 | 1.12 | 0.04 |
| Row 5 | 2.00 | 3.17 | 1.59 | 0.22 |
| Row 6 | 2.00 | 2.83 | 1.42 | 0.04 |
| Row 7 | 2.00 | 2.61 | 1.31 | 0.09 |
| Row 8 | 2.00 | 2.81 | 1.40 | 0.11 |
| Row 9 | 2.00 | 2.18 | 1.09 | 0.00 |
| | | | | |
| Column 1 | 9.00 | 13.29 | 1.48 | 0.07 |
| Column 2 | 9.00 | 10.81 | 1.20 | 0.02 |

| ANOVA | | | | | | |
|---|---|---|---|---|---|---|
| *Source of Variation* | *SS* | *df* | *MS* | *F* | *P-value* | *F crit* |
| Rows | 0.54 | 8.00 | 0.07 | 2.81 | 0.08 | 3.44 |
| Columns | 0.34 | 1.00 | 0.34 | 14.35 | 0.01 | 5.32 |
| Error | 0.19 | 8.00 | 0.02 | | | |
| Total | 1.07 | 17.00 | | | | |

Table 2.27 t-Test: Paired Two Sample for Means of $bag_1$ radii ratio of control vs. experimental

P (T<=t) one-tail is less than 0.05

| $Bag_1$ | I/O-866 | I/O-872 | I/O-869 | I/C | I/C | I/C | O/C | O/C | O/C |
|---|---|---|---|---|---|---|---|---|---|
| Cont | 1.46 | 1.68 | 1.18 | 1.25 | 1.92 | 1.56 | 1.52 | 1.63 | 1.09 |
| Exprt | 1.26 | 1.49 | 1.20 | 0.98 | 1.25 | 1.28 | 1.09 | 1.17 | 1.09 |

t-Test: Paired Two Sample for Means

| | *Variable 1* | *Variable 2* |
|---|---|---|
| Mean | 1.48 | 1.20 |
| Variance | 0.07 | 0.02 |
| Observations | 9.00 | 9.00 |
| Pearson Correlation | 0.56 | |
| Hypothesized Mean Difference | 0.00 | |
| Df | 8.00 | |
| t Stat | 3.79 | |
| P (T<=t) one-tail | 0.00 | |
| t Critical one-tail | 1.86 | |
| P(T<=t) two-tail | 0.01 | |
| t Critical two-tail | 2.31 | |

Tabl 2.28 Means and standard errors of ratios I/O, I/C and O/C of the experimental and control samples of $bag_2$.

| 866-$bag_2$ control | Ratio | | |
|---|---|---|---|
| | I/O | I/C | O/C |
| Mean | 1.17 | 1.49 | 1.31 |
| Standard Error | 0.09 | 0.06 | 0.06 |
| 866 $bag_2$ expert | Ratio | | |
| | I/O | I/C | O/C |
| Mean | 1.05 | 1.30 | 1.28 |
| Standard Error | 0.07 | 0.06 | 0.05 |
| | | | |
| 872-$bag_2$ control | Ratio | | |
| | I/O | I/C | O/C |
| Mean | 1.05 | 1.94 | 1.90 |
| Standard Error | 0.14 | 0.30 | 0.21 |
| 872 $bag_2$ exprt | Ratio | | |
| | I/O | I/C | O/C |
| | 0.88 | 1.37 | 1.62 |
| | 0.09 | 0.09 | 0.09 |
| 869- $bag_2$ control | Ratio | | |
| | I/O | I/C | O/C |
| Mean | 1.12 | 1.41 | 1.29 |
| Standard Error | 0.07 | 0.08 | 0.07 |
| 869 $bag_2$ exp | Ratio | | |
| | I/O | I/C | O/C |
| Mean | 0.84 | 1.19 | 1.47 |
| Standard Error | 0.06 | 0.04 | 0.08 |

Chart 2.15 Means of ratio (I/O), of control vs. experimental $bag_2$ fibres. In each case the mean values of ratio I/O in the control is greater than that of the corresponding experimental.

| I/O charts of $bag_2$control vs. experimental. | | | |
|---|---|---|---|
| $Bag_2$ | I/O | I/O | I/O |
| | 866 | 872 | 869 |
| Control | 1.17 | 1.05 | 1.12 |
| Experimental | 1.05 | 0.84 | 0.88 |
| Standard Error | 0.09 | 0.14 | 0.07 |
| Standard Error | 0.07 | 0.06 | 0.09 |

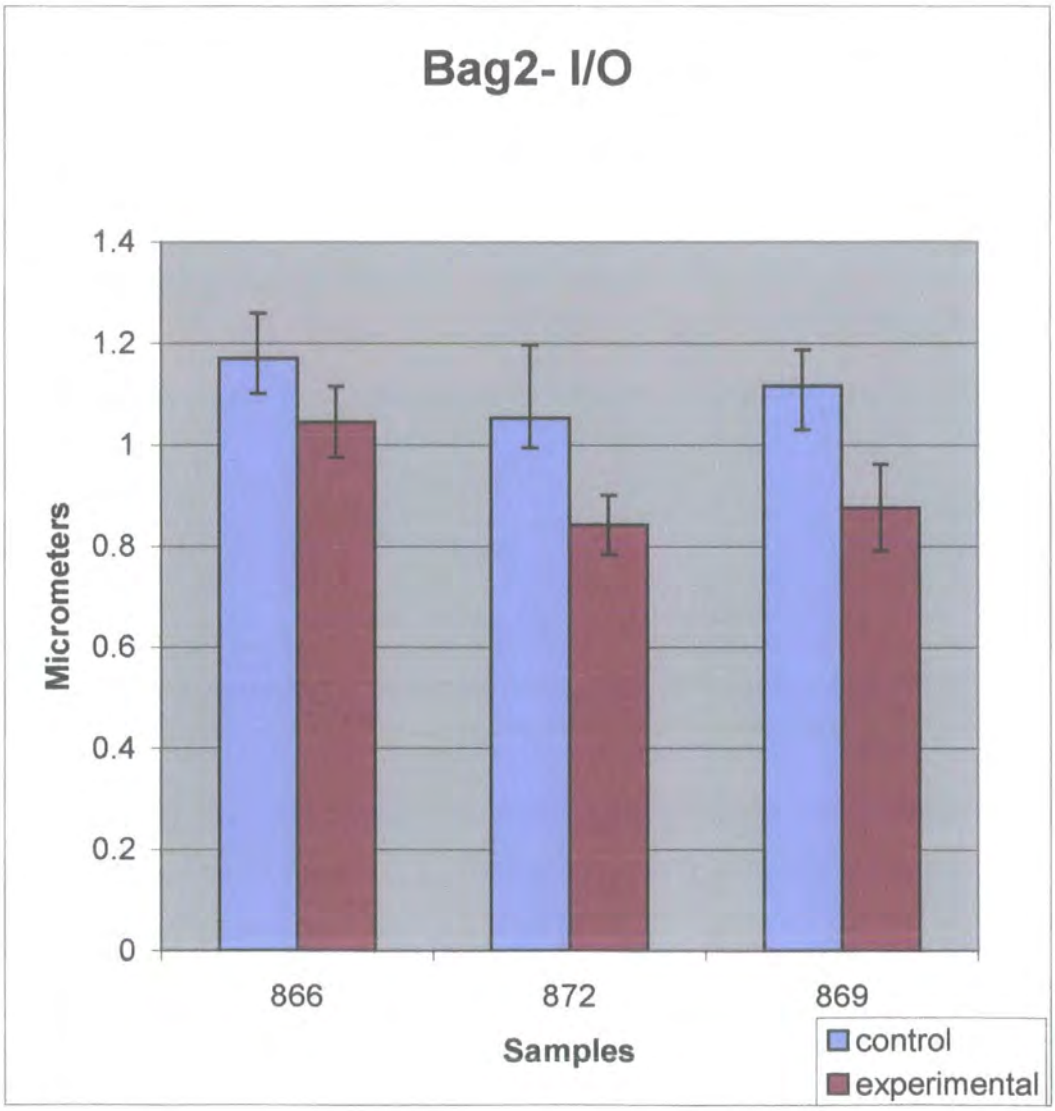

Chart 2.16 Means of ratio (I/C), of control vs. experimental $bag_2$ fibres. In each case the mean values of ratio I/C in the control is greater than that of the corresponding experimental.

| I/C chart of $bag_2$ control vs. experimental. | | | |
|---|---|---|---|
| $Bag_2$ | I/C | I/C | I/C |
| | 866 | 872 | 869 |
| Control | 1.49 | 1.94 | 1.41 |
| Experimental | 1.30 | 1.19 | 1.37 |
| Standard Error | 0.06 | 0.30 | 0.08 |
| Standard Error | 0.06 | 0.04 | 0.09 |

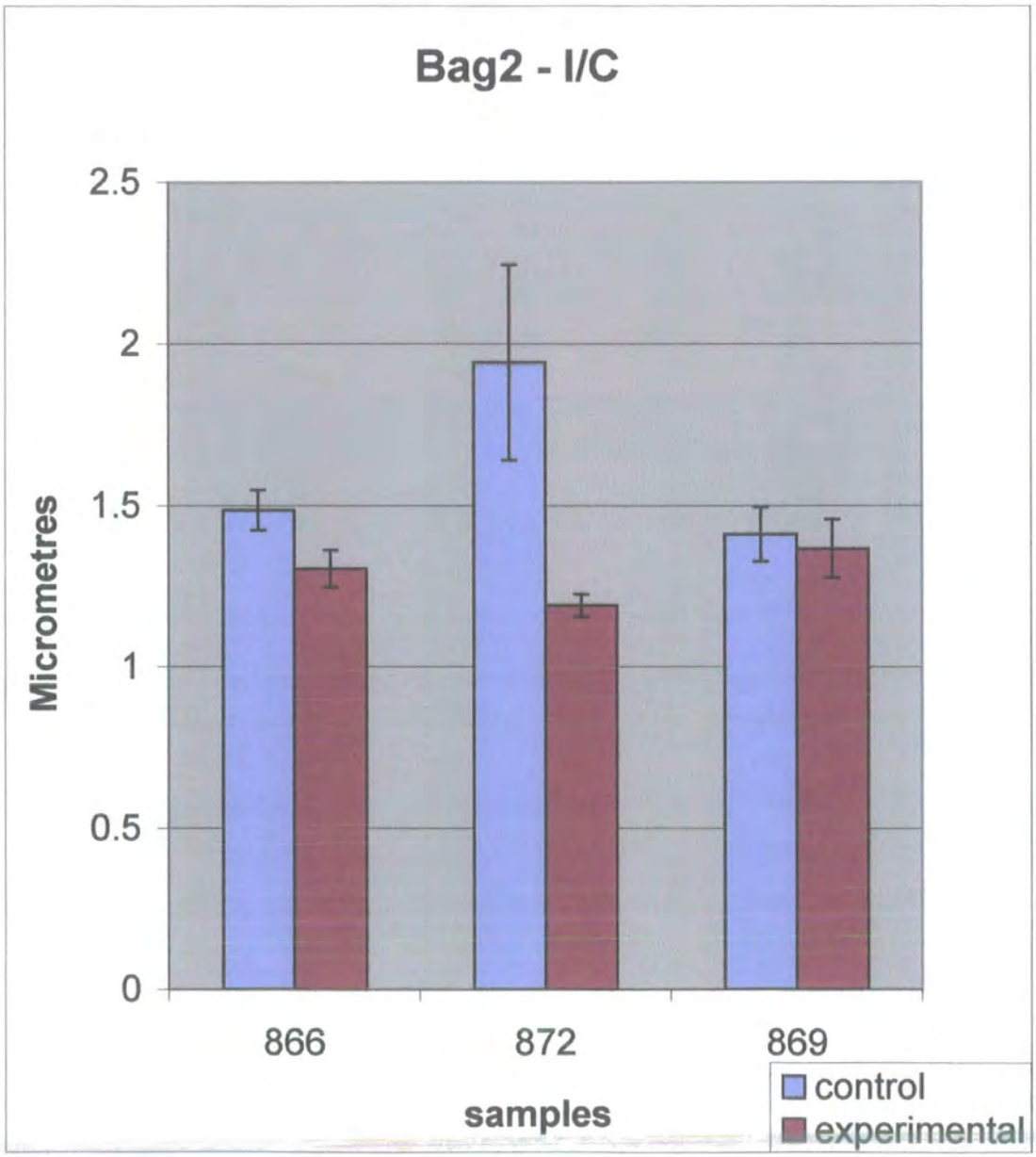

Chart 2.17 Means of ratio (O/C), of control vs. experimental $bag_2$ fibres. The mean values of ratio O/C in the control is greater than that of the corresponding in 872, about the same in 866, and less in 869.

| O/C charts of $bag_2$ control vs. experimental. | | | |
|---|---|---|---|
| $Bag_2$ | O/C | O/C | O/C |
| | 866 | 872 | 869 |
| Control | 1.31 | 1.90 | 1.29 |
| Experimental | 1.28 | 1.47 | 1.62 |
| Standard Error | 0.06 | 0.21 | 0.07 |
| Standard Error | 0.05 | 0.08 | 0.09 |

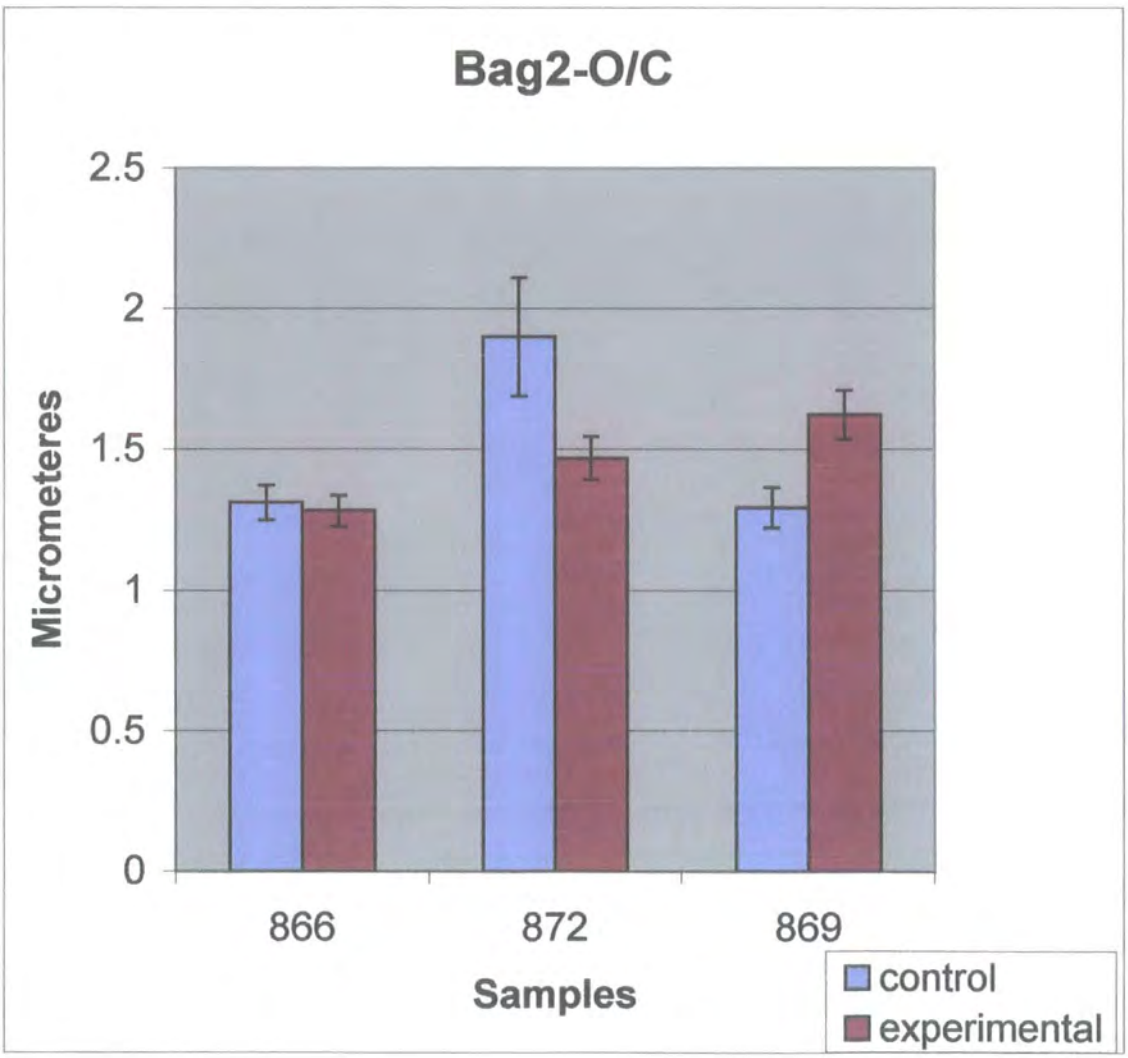

Table 2.29 Means of ratios I/O, I/C, O/C of control versus the experimental $bag_2$ fibres as used for the analysis of variance (Two-Factor Without Replication ). Column *P-value* is greater than 0.05 in this case.

| $Bag_2$ | Cont | Exprt |
|---|---|---|
| I/O-866 | 1.17 | 1.05 |
| I/C | 1.94 | 1.19 |
| O/C | 1.31 | 1.28 |
| I/O-872 | 1.05 | 0.84 |
| I/C | 1.94 | 1.19 |
| O/C | 1.90 | 1.47 |
| I/O-869 | 1.12 | 0.88 |
| I/C | 1.41 | 1.37 |
| O/C | 1.29 | 1.62 |

| ANOVA: Two-Factor Without Replication | | | | |
|---|---|---|---|---|
| *SUMMARY* | *Count* | *Sum* | *Average* | *Variance* |
| Row 1 | 2.00 | 2.22 | 1.11 | 0.01 |
| Row 2 | 2.00 | 3.13 | 1.57 | 0.28 |
| Row 3 | 2.00 | 2.59 | 1.30 | 0.00 |
| Row 4 | 2.00 | 1.90 | 0.95 | 0.02 |
| Row 5 | 2.00 | 3.13 | 1.57 | 0.28 |
| Row 6 | 2.00 | 3.37 | 1.68 | 0.09 |
| Row 7 | 2.00 | 1.99 | 1.00 | 0.03 |
| Row 8 | 2.00 | 2.78 | 1.39 | 0.00 |
| Row 9 | 2.00 | 2.92 | 1.46 | 0.05 |
| Column 1 | 9.00 | 13.14 | 1.46 | 0.13 |
| Column 2 | 9.00 | 10.89 | 1.21 | 0.07 |

| ANOVA | | | | | | |
|---|---|---|---|---|---|---|
| *Source of Variation* | *SS* | *df* | *MS* | *F* | *P-value* | *F crit* |
| Rows | 1.13 | 8.00 | 0.14 | 2.30 | 0.13 | 3.44 |
| Columns | 0.28 | 1.00 | 0.28 | 4.60 | 0.06 | 5.32 |
| Error | 0.49 | 8.00 | 0.06 | | | |
| Total | 1.90 | 17.00 | | | | |

Table 2.30 t-Test: Paired Two Sample for Means of $bag_2$ radii ratio of control vs. experimental. P (T<=t) one-tail is less than 0.5.

| $Bag_2$ | I/O-866 | I/O-872 | I/O-869 | I/C | I/C | I/C | O/C | O/C | O/C |
|---|---|---|---|---|---|---|---|---|---|
| Cont | 1.17 | 1.05 | 1.12 | 1.94 | 1.94 | 1.41 | 1.31 | 1.90 | 1.29 |
| Exprt | 1.05 | 0.84 | 0.88 | 1.19 | 1.19 | 1.37 | 1.28 | 1.47 | 1.62 |

t-Test: Paired Two Sample for Means

| | *Variable 1* | *Variable 2* |
|---|---|---|
| Mean | 1.46 | 1.21 |
| Variance | 0.13 | 0.07 |
| Observations | 9.00 | 9.00 |
| Pearson Correlation | 0.42 | |
| Hypothesized Mean Difference | 0.00 | |
| Df | 8.00 | |
| t Stat | 2.14 | |
| P(T<=t) one-tail | 0.03 | |
| t Critical one-tail | 1.86 | |
| P(T<=t) two-tail | 0.06 | |
| t Critical two-tail | 2.31 | |

## 2.5.15. $Bag_2$ compared with $bag_1$

The classification of $bag_1$ and $bag_2$ in this chapter was based on the prominence of sensory terminals on $bag_1$ as compared to $bag_2$. Other criterion of classification such as the pattern of motor innervation and the pattern of elastic distribution around the bag fibres were, not possible in this study which was mostly restricted to the equatorial region.

In comparing $bag_2$ with $bag_1$ fibres, based on the means of absolute values of all the measurements for O, I and C the values for $bag_2$ are generally greater than the corresponding values for $bag_1$, as seen on table 2.31. Analysis of I/O and O/C for each sample of $bag_1$ control versus $bag_2$ control and $bag_1$ experimental versus $bag_2$ experimental, see charts (2.18-2.21) confirmed the visual classification in that the ratio I/O is higher for fibres identified as $bag_1$ and that the ratio of O/C is higher for fibres identified as $bag_2$ (see figure 2.4 d and c). In the few cases where the individual values Show some anomalies for example in chart (2.21) for sample E.866.RHS, the classification was reiewed by rexamining the slides and the anomaly was attributed to the positioning of $bag_1$ in that specific spindle. Some of the tables contain no more than three variables so the ANOVA and t- test were not performed.

Table 2.31 Comparison of O, I, and C for $bag_1$ and $bag_2$ fibres from both control and experimental samples based on mean values. Nearly all the measurements for $bag_2$ appear to be greater than the corresponding $bag_1$ measurements.

| | Sample of Control side LHS | | | | Sample of Experimental side RHS | | |
|---|---|---|---|---|---|---|---|
| | C-866 | C-872 | C-869 | | E-866 | E-872 | E-869 |
| Length | 150mm | 152mm | 148mm | | 102mm | 125mm | 141mm |
| $Bag_1$ Radii | | | | | | | |
| O | Smaller | Smaller | Smaller | | Smaller | Smaller | Smaller |
| I | Bigger | Smaller | Bigger | | Smaller | Smaller | Smaller |
| C | Smaller | Smaller | Equal | | Smaller | Smaller | Smaller |
| $Bag_2$ Radii | | | | | | | |
| O | Bigger | Bigger | Bigger | | Bigger | Bigger | Bigger |
| | | | | | | | |
| I | Smaller | Bigger | Smaller | | Bigger | Bigger | Bigger |
| | | | | | | | |
| C | Bigger | Bigger | Equal | | Bigger | Bigger | Bigger |

Table 2.32 All ratios of $bag_1$ control samples notice the absence of region C from sample 872-$bag_1$ control due to inadequate fixation.

| Bag 1 control | | |
|---|---|---|
| | I/O | O/C |
| C866.LHS.A.B1 | 1.86 | 1.02 |
| | 1.72 | 1.03 |
| | 1.34 | 1.00 |
| | 1.50 | 1.11 |
| | 2.33 | 1.03 |
| Mean | 1.75 | 1.04 |
| C866.LHS.B.B1 | 1.01 | 1.34 |
| | 0.98 | 1.54 |
| | 1.48 | 1.56 |
| | 1.04 | 1.36 |
| Mean | 1.13 | 1.45 |
| C866.LHS.C.B1 | 1.50 | 1.11 |
| | 1.26 | 1.05 |
| | 1.53 | 1.13 |
| | 1.37 | 1.09 |
| Mean | 1.42 | 1.09 |
| | | |
| C872.LHS.A.B1 | 2.22 | 1.70 |
| | 1.59 | 1.37 |
| | 0.76 | 2.29 |
| Mean | 1.52 | 1.79 |
| C872.LHS.B.B1 | 1.04 | 1.36 |
| | 1.26 | 1.37 |
| | 0.92 | 1.57 |
| | 0.95 | 1.22 |
| Mean | 1.39 | 1.84 |
| | | |
| C869.LHS.A.B1 | 2.11 | 0.99 |
| | 1.57 | 1.05 |
| | 1.32 | 1.20 |
| | 1.94 | 0.97 |
| | 1.46 | 1.10 |
| Mean | 1.68 | 1.06 |
| C869.LHS.B.B1 | 1.92 | 1.03 |
| | 1.11 | 1.22 |
| | 1.41 | 1.05 |
| Mean | 1.48 | 1.10 |
| C896.LHS.C.B1 | 1.47 | 0.99 |
| | 1.63 | 0.99 |
| | 1.11 | 1.24 |
| | 1.21 | 1.25 |
| Mean | 1.36 | 1.12 |

Table 2.33 all ratios of $bag_2$ control samples notice the absence of region C from sample 872 due to inadequate fixation.

| Bag 2 control | I/O | O/C |
|---|---|---|
| C866.LHS.A.B2 | 1.68 | 1.12 |
| | 0.97 | 1.46 |
| | 1.28 | 1.17 |
| | 1.52 | 1.03 |
| | 0.86 | 1.56 |
| Mean | 1.26 | 1.27 |
| C866.LHS.B.B2 | 0.92 | 1.46 |
| | 0.67 | 1.71 |
| | 1.32 | 1.18 |
| Mean | 0.97 | 1.45 |
| C866.LHS.C.B2 | 0.93 | 1.30 |
| | 1.27 | 1.26 |
| | 1.15 | 1.31 |
| | 1.24 | 1.34 |
| Mean | 1.15 | 1.30 |
| | | |
| C872.LHS.A.B2 | 1.38 | 1.97 |
| | 1.39 | 2.21 |
| | 1.64 | 1.69 |
| | 1.09 | 2.13 |
| Mean | 1.37 | 2.00 |
| C872.LHS.B.B2 | 0.88 | 1.37 |
| | 0.38 | 3.10 |
| | 0.83 | 1.44 |
| | 0.83 | 1.29 |
| Mean | 0.73 | 1.80 |
| | | |
| C.869.LHS.A.B2 | 1.09 | 1.31 |
| | 1.60 | 1.18 |
| | 1.52 | 1.33 |
| | 1.25 | 1.34 |
| | 1.13 | 1.34 |
| Mean | 1.32 | 1.30 |
| C869.LHS.B.B2 | 0.88 | 1.45 |
| | 1.03 | 1.25 |
| | 0.80 | 1.74 |
| | 0.69 | 1.76 |
| Mean | 0.85 | 1.55 |
| C896.LHS.C.B2 | 1.05 | 0.96 |
| | 1.16 | 1.00 |
| | 1.08 | 0.99 |
| | 1.22 | 1.15 |
| Mean | 1.13 | 1.03 |

Table 2.34 All ratios of $bag_1$ experimental sample.

| $Bag_1$ experimental | I/O | O/C |
|---|---|---|
| E866.RHS.A.B1 | 1.14 | 1.75 |
| | 1.22 | 1.65 |
| | 1.18 | 1.70 |
| | 1.34 | 1.50 |
| | 1.24 | 1.62 |
| Mean | 1.22 | 1.64 |
| E866.RHS.B.B1 | 1.50 | 1.00 |
| | 1.11 | 1.00 |
| | 1.54 | 0.94 |
| | 1.51 | 0.98 |
| | 1.34 | 0.93 |
| | 1.47 | 1.04 |
| | 1.16 | 0.96 |
| | 1.50 | 1.03 |
| Mean | 1.39 | 0.98 |
| E866.RHS.C.B1 | 1.09 | 1.05 |
| | 1.06 | 1.07 |
| | 1.06 | 0.91 |
| | 0.91 | 1.23 |
| Mean | 1.03 | 1.06 |
| E872.RHS.A.B1 | 0.91 | 1.23 |
| | 1.11 | 1.13 |
| | 0.93 | 1.17 |
| | 0.86 | 1.33 |
| Mean | 0.96 | 1.22 |
| E872.RHS.B.B1 | 1.15 | 1.26 |
| | 0.94 | 1.21 |
| | 0.91 | 1.33 |
| | 0.94 | 1.20 |
| | 0.97 | 1.20 |
| Mean | 0.98 | 1.24 |

[continued

Table 2.34 continued

| | | |
|---|---|---|
| E872.RHS.C.B1 | 1.02 | 1.41 |
| | 1.13 | 1.22 |
| | 1.00 | 1.36 |
| | 0.89 | 1.55 |
| Mean | 1.01 | 1.39 |
| E869.RHS.A.B1 | 1.41 | 1.05 |
| | 1.23 | 1.02 |
| | 1.15 | 1.09 |
| | 1.21 | 0.96 |
| | 1.24 | 1.03 |
| Mean | 1.25 | 1.03 |
| E869.RHS.B.B1 | 0.83 | 1.37 |
| | 0.84 | 1.27 |
| | 0.98 | 1.11 |
| | 1.08 | 1.14 |
| Mean | 0.93 | 1.22 |
| E869.RHS.C.B1 | 1.04 | 1.07 |
| | 1.18 | 0.98 |
| | 1.00 | 1.17 |
| | 1.14 | 0.97 |
| | 1.00 | 0.98 |
| Mean | 1.07 | 1.03 |

Table 2.35 All ratios of $bag_2$ experimental samples.

| $Bag_2$ Experimental | | |
|---|---|---|
| | I/O | O/C |
| E866.RHS.A.B2 | 1.20 | 1.19 |
| | 1.52 | 1.13 |
| | 1.21 | 1.21 |
| | 1.19 | 1.27 |
| | 0.96 | 1.41 |
| Mean | 1.22 | 1.24 |
| E866.RHS.B.B2 | 1.02 | 1.26 |
| | 1.01 | 1.34 |
| | 1.24 | 1.09 |
| | 1.21 | 1.09 |
| Mean | 1.12 | 1.19 |
| E866.RHS.C.B2 | 0.73 | 1.49 |
| | 0.94 | 1.04 |
| | 0.61 | 1.71 |
| | 0.77 | 1.47 |
| Mean | 0.76 | 1.43 |
| | | |
| E872RHS.A.B2 | 0.71 | 1.89 |
| | 0.67 | 1.62 |
| | 0.54 | 1.99 |
| | 0.70 | 1.57 |
| Mean | 0.66 | 1.77 |
| E872.RHS.B.B2 | 0.86 | 1.26 |
| | 0.98 | 1.34 |
| | 1.08 | 1.41 |
| | 0.82 | 1.49 |
| | 1.15 | 1.28 |
| Mean | 0.98 | 1.35 |
| E872.RHS.C.B2 | 0.86 | 2.05 |
| | 0.75 | 1.65 |
| | 0.59 | 1.81 |
| Mean | 0.73 | 1.84 |

[continued

Table 2.35 continued

| | | |
|---|---|---|
| E869.RHS.A.B2 | 0.88 | 1.33 |
| | 1.12 | 1.12 |
| | 0.86 | 1.49 |
| | 0.79 | 1.53 |
| | 0.48 | 2.21 |
| Mean | 0.83 | 1.53 |
| E869.RHS.B.B2 | 0.72 | 1.51 |
| | 1.20 | 1.24 |
| | 1.02 | 1.27 |
| | 0.72 | 1.47 |
| Mean | 0.92 | 1.37 |
| E869.RHS.C.B2 | 0.68 | 1.57 |
| | 0.71 | 1.56 |
| | 0.67 | 1.62 |
| | 1.09 | 1.18 |
| Mean | 0.79 | 1.48 |

Chart 2.18 Ratio of I/O $bag_1$ control vs. radii ratio I/O $bag_2$ control using the mean of ratios of each sample. All I/O ratio of $bag_1$ control are greater than these of $bag_2$ control.

| Control $Bag_1$-I/O vs. $Bag_2$-I/O | | |
|---|---|---|
| Samples | Means $Bag_1$-I/O | Means $Bag_2$-I/O |
| C866.LHS.A. | 1.75 | 1.26 |
| C866.LHS.B. | 1.13 | 0.97 |
| C866.LHS.C. | 1.42 | 1.15 |
| C872.LHS.A. | 1.52 | 1.37 |
| C872.LHS.B. | 1.39 | 0.73 |
| C869.LHS.A. | 1.68 | 1.32 |
| C869.LHS.B. | 1.48 | 0.85 |
| C896.LHS.C. | 1.36 | 1.13 |

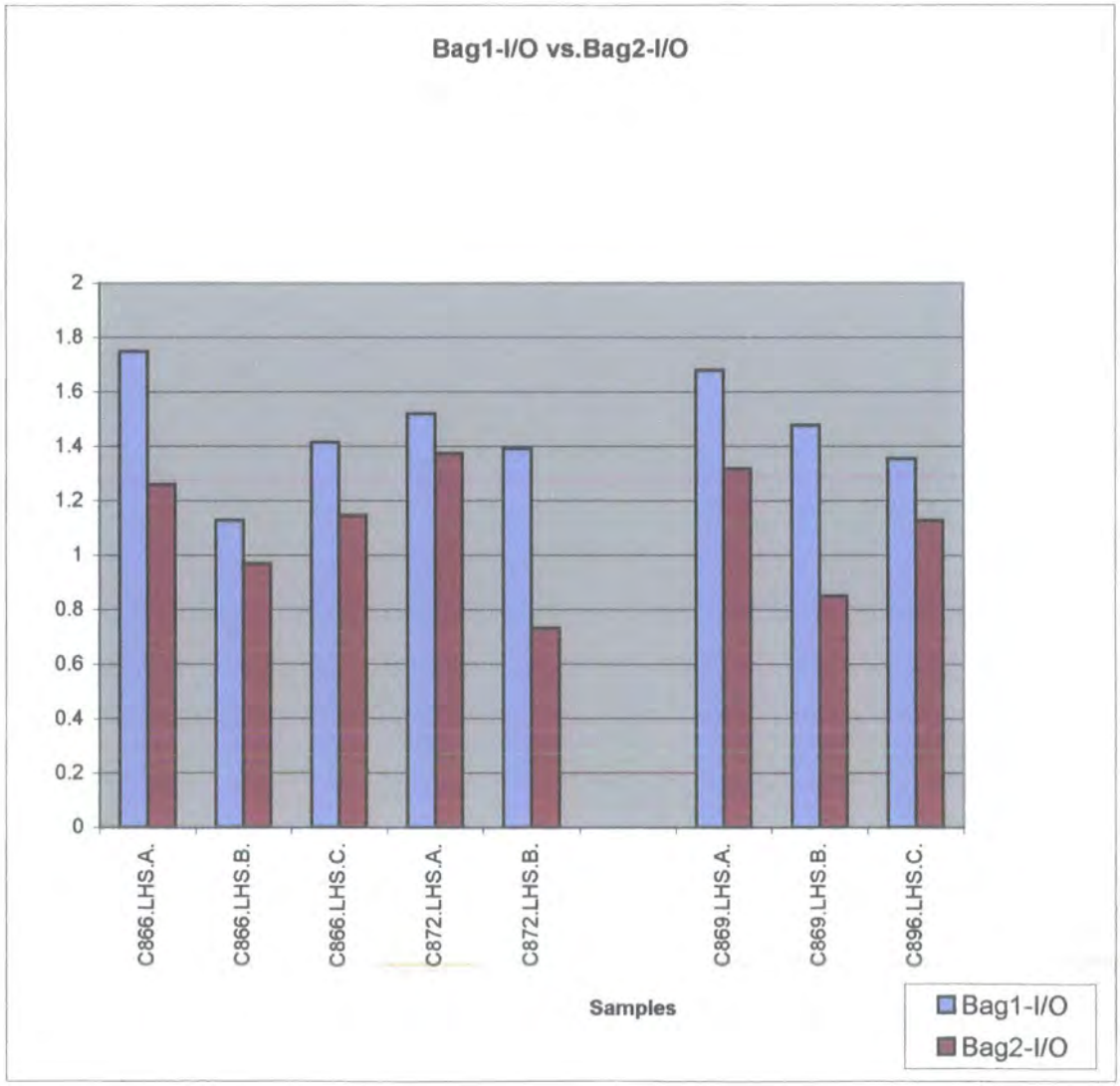

Charts 2.19 Ratio O/C $bag_1$ control vs. radii ratio O/C of $bag_2$ control using the means of ratio of each sample five out of eight paired samples show that O/C of $bag_2$ are greater than $bag_1$ and three are nearly equal.

| Control $Bag_1$-O/C vs. $Bag_2$-O/C | | |
|---|---|---|
| Samples | Means | Means |
| | $Bag_1$-O/C | $Bag_2$-O/C |
| C866.LHS.A. | 1.04 | 1.27 |
| C866.LHS.B. | 1.45 | 1.45 |
| C866.LHS.C. | 1.09 | 1.74 |
| C872.LHS.A. | 1.79 | 2.00 |
| C872.LHS.B. | 1.84 | 1.80 |
| C869.LHS.A. | 1.06 | 1.30 |
| C869.LHS.B. | 1.10 | 1.55 |
| C896.LHS.C. | 1.12 | 1.03 |

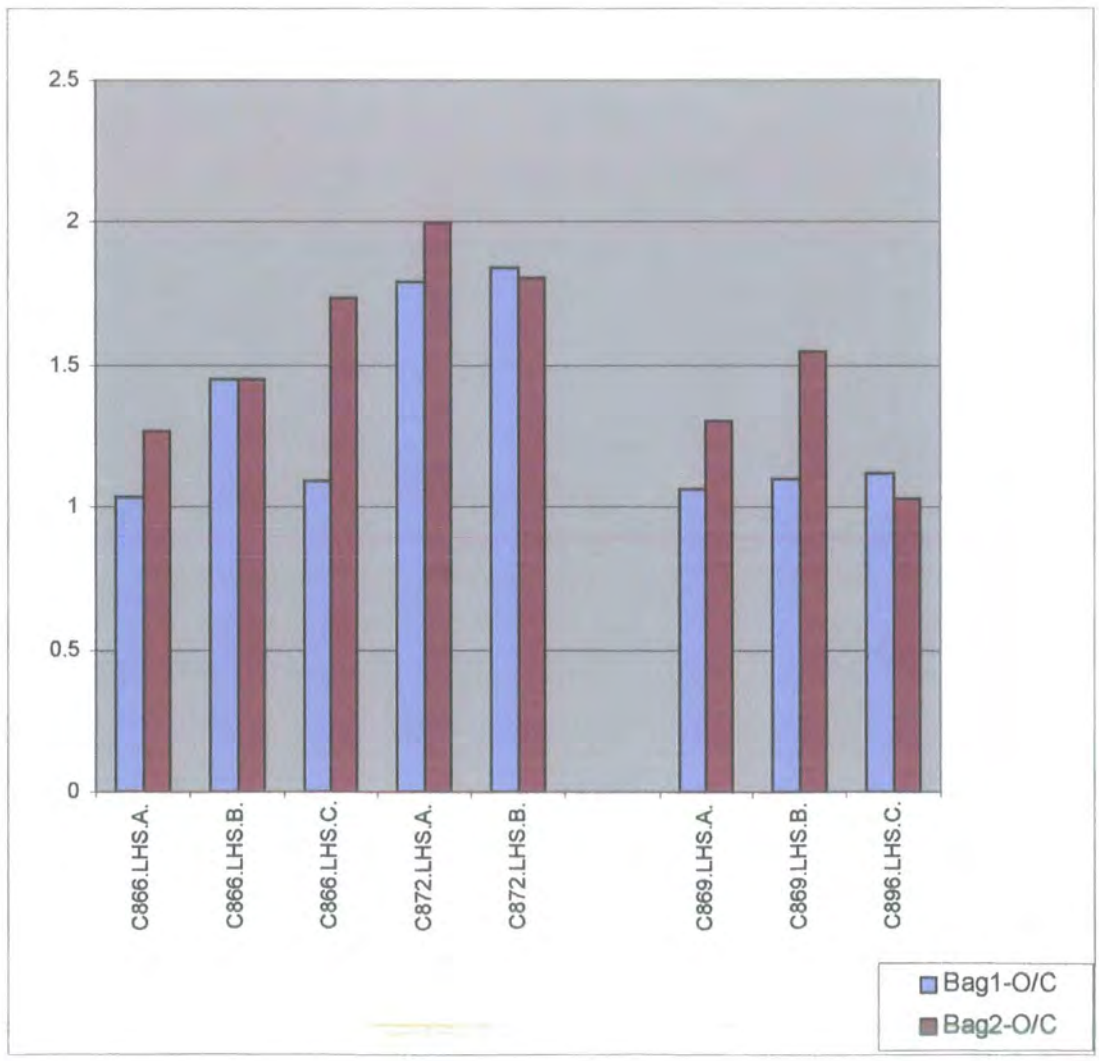

Charts 2.20 Ratio I/O $bag_1$ experimental vs. radii ratio I/O of $bag_2$ experimental by using the mean of ratios of each sample eight out of nine paired samples show that I/O of $bag_1$ is greater than these of $bag_2$.

| Experimental $Bag_1$-I/O vs. $Bag_2$-I/O | | |
|---|---|---|
| Samples | Means | Means |
| | $Bag_1$-I/O | $Bag_2$-I/O |
| E866.RHS.A. | 1.22 | 1.22 |
| E866.RHS.B. | 1.39 | 1.12 |
| E866.RHS.C. | 1.03 | 0.76 |
| E872.RHS.A. | 0.96 | 0.66 |
| E872.RHS.B. | 0.98 | 0.98 |
| E872.RHS.C. | 1.01 | 0.73 |
| E869.RHS.A. | 1.25 | 0.83 |
| E869.RHS.B. | 0.93 | 0.34 |
| E869.RHS.C. | 1.07 | 0.79 |

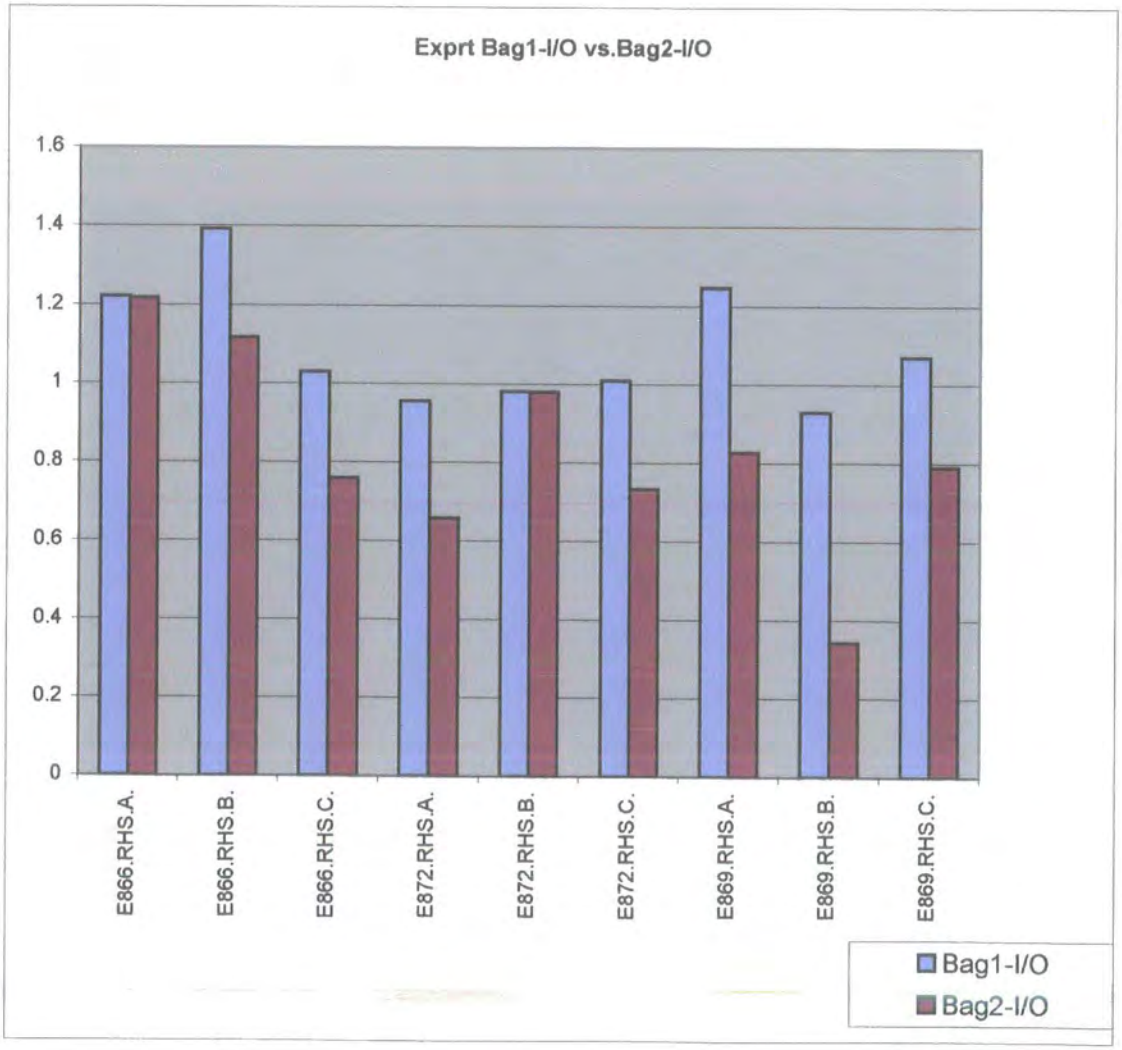

Chart 2.21 Ratio O/C $bag_1$ experimental vs. ratio O/C of $bag_2$ experimental by using the mean of ratios of each sample eight out of nine paired samples show that O/C ratio is greater for $bag_2$ compared to these of $bag_1$, the anomaly seen in experimental sample E866.RHS.A in this chart and in chart 2.20 was due to the position of $bag_2$ in that specific sample spindle.

| Experimental $Bag_1$-O/C vs. $Bag_2$-O/C | | |
|---|---|---|
| Simples | Means | Means |
| | $Bag_1$-O/C | $Bag_2$-O/C |
| E866.RHS.A. | 1.64 | 1.24 |
| E866.RHS.B. | 0.98 | 1.19 |
| E866.RHS.C. | 1.06 | 1.43 |
| E872.RHS.A. | 1.22 | 1.77 |
| E872.RHS.B. | 1.24 | 1.35 |
| E872.RHS.C. | 1.39 | 1.84 |
| E869.RHS.A. | 1.03 | 1.53 |
| E869.RHS.B. | 1.22 | 1.37 |
| E869.RHS.C. | 1.03 | 1.48 |

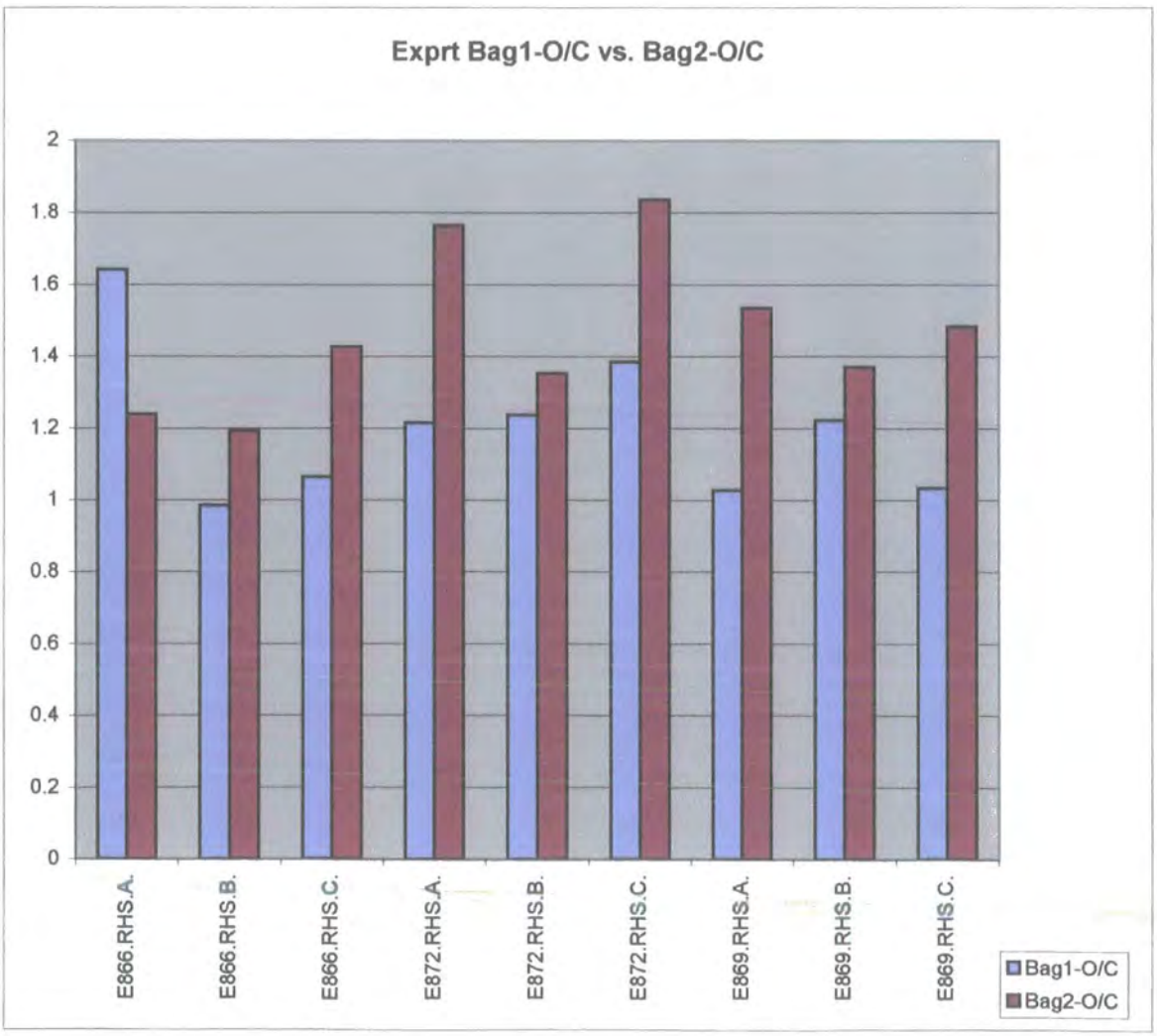

## 2.5.16. Diagrammatic representation of nerve ending changes

In figure 2.4 a diagrammatic representation was given of the changes in the nerve-ending profile radii in relation mostly to the outer radii O and the inner radii I in different situation A, B, C, D determined by differential tension. The following diagrammatic figures represent the average results of nerve ending shapes after they had been subjected to stretched and flexed positions as seen in table 2.1 and diagrams 2.2 and 2.3. The measured means of the nerve endings radii, the outer curvature radii O and the inner curvature I were represented diagrammatically in order to reflect the amount of changes in the nerve endings due to tension difference as a result of the passive stretch of the muscle spindles in samples 866, 872 and 869. Comparing figure 2.5, which represents the nerve endings of bag1 control side (extended) with the next figure (2.6), which represents the nerve endings of $bag_1$ of the experimental side (flexed), the experimental side outer curvature seems to be more prominent and the inner curvature seems to be more indented in the muscle fibre as compared the control side. The same observation can be said about $bag_2$ control vs. $bag_2$ experimental in figures 2.7and 2.8. The length of the muscle fibre and the length of internal and external sarcomere are listed next to each diagram which indicates that the prominence of the nerve endings profiles seem to correlate with the length of sarcomeres, so the shorter length of sarcomere the more prominent the nerve ending profile as seen in most of the experimental side.

Figure 2.5 this figure represent the mean radii I, O of the nerve ending of $bag_1$ control side (stretched side) to the left of each diagram is the intrafusal muscle fibre length in mm represented by the letters Mus.L and sarcomeres length in μm represented by the letters Sarc.In, and the external sarcomere length represented by the letters Sarc.Ex

Figure 2.5 Average profiles of nerve terminals based on mean values of I, O, and C. $Bag_1$ control side. Sarc.In is the length of internal sarcomere and Sarc.Ex is the length of external sarcomere in $\mu$m.

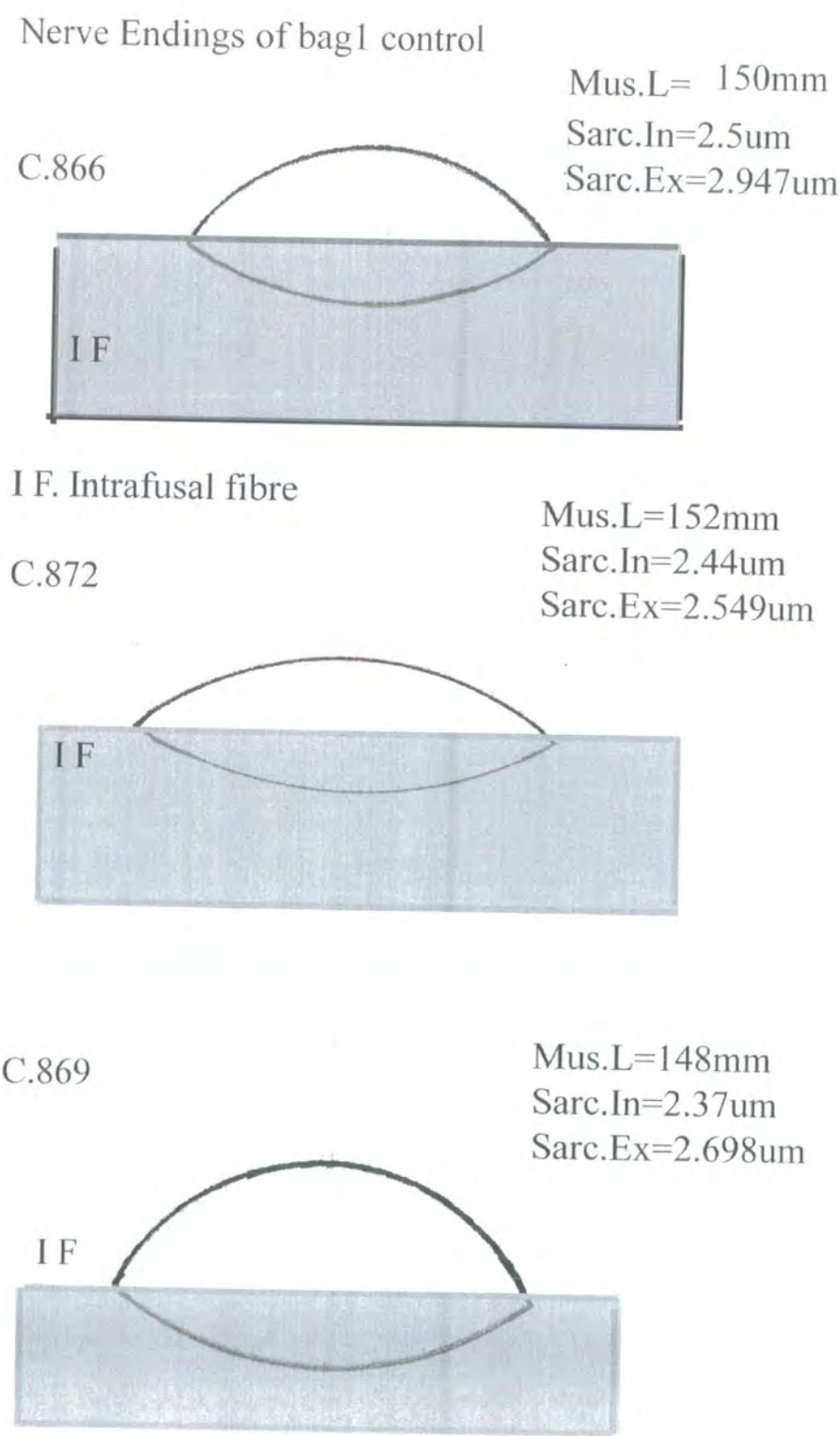

Figure.2.6. Diagrammatic representation of the absolute measurements of the nerve endings radii, the inner curvature I, outer curvature radii O of $bag_1$ experimental side.

Figure 2.6 Average profiles of nerve terminals based on mean values of I, O, and C. $Bag_1$ experimental side. Sarc.In is the length of internal sarcomere and Sarc.Ex is the length of external sarcomere in $\mu$m.

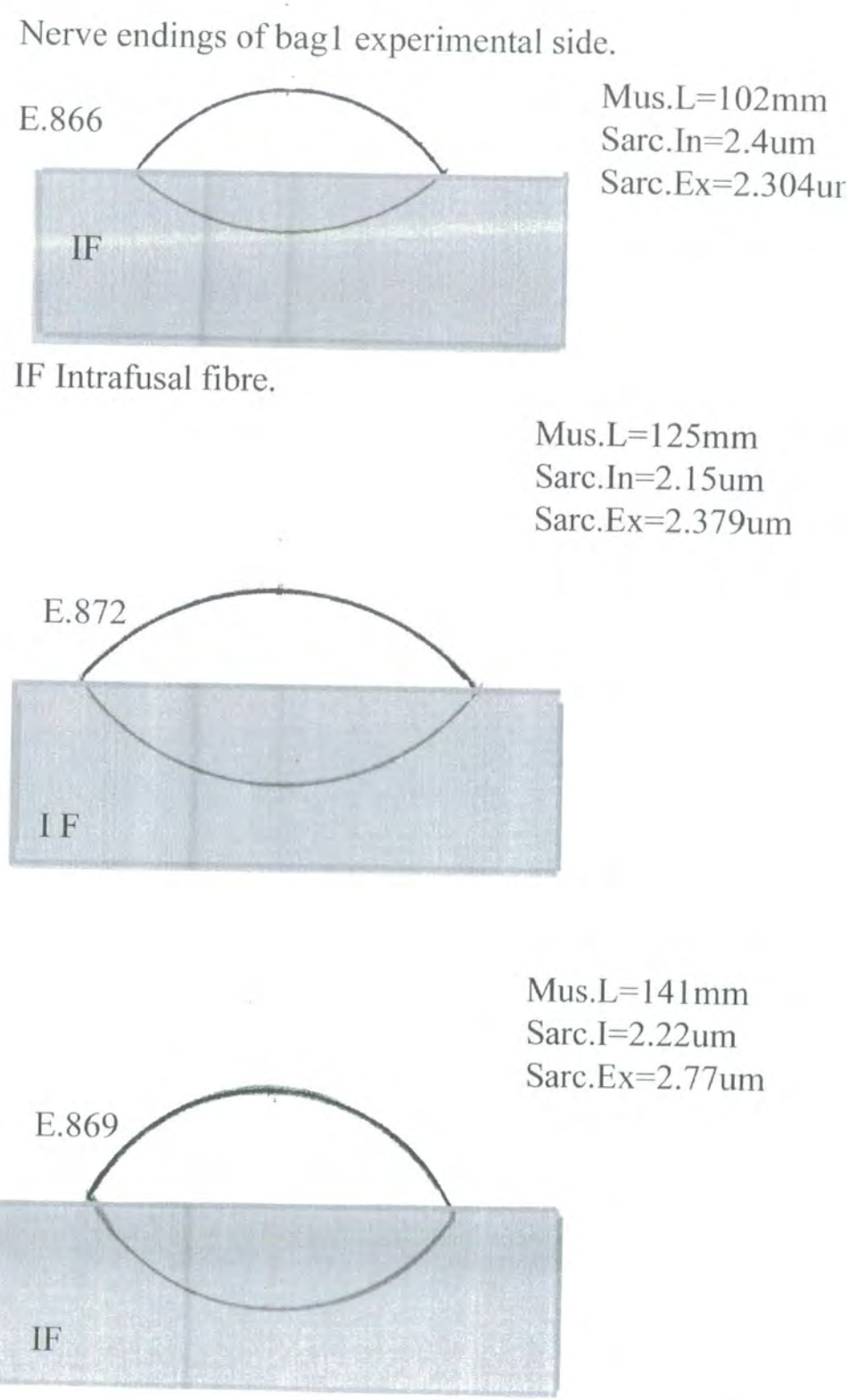

Figure.2.7 Diagrammatic representation of the mean of the nerve endings radii, the outer curvature radii O and the inner curvature I, of $bag_2$ the control side (stretched) in comparing this figure with the next figure (2.8) which represent the nerve ending of bag2 of the experimental side (flexed), the feature looks similar to that seen in $bag_1$ where the experimental side outer curvature seem to be more bulgy and the inner curvature seem to be more indented in compare with that of the control side.

Figure 2.7 Average profiles of nerve terminals based on mean values of I, O, and C. $Bag_2$ the control side. Sarc.In is the length of internal sarcomere and Sarc.Ex is the length of external sarcomere in $\mu$m.

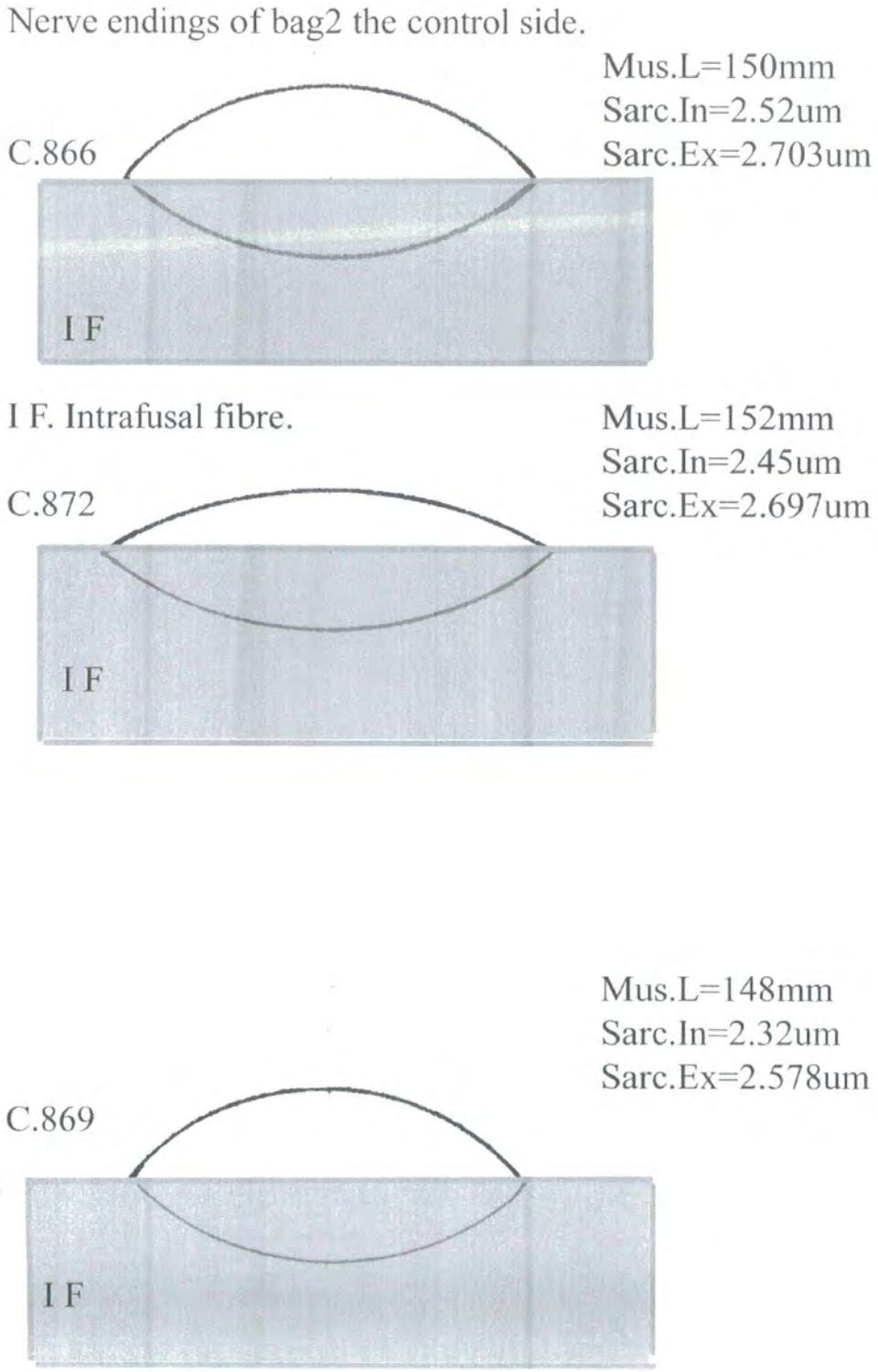

Figure.2.8. Diagrammatic representation of the mean of the nerve endings radii, the outer curvature radii O and the inner curvature I, of $bag_2$ experimental side

Figure 2.8 Average profiles of nerve terminals based on mean values of I, O, and C. $Bag_2$ experimental side. Sarc.In is the length of internal sarcomere and Sarc.Ex is the length of external sarcomere in $\mu$m.

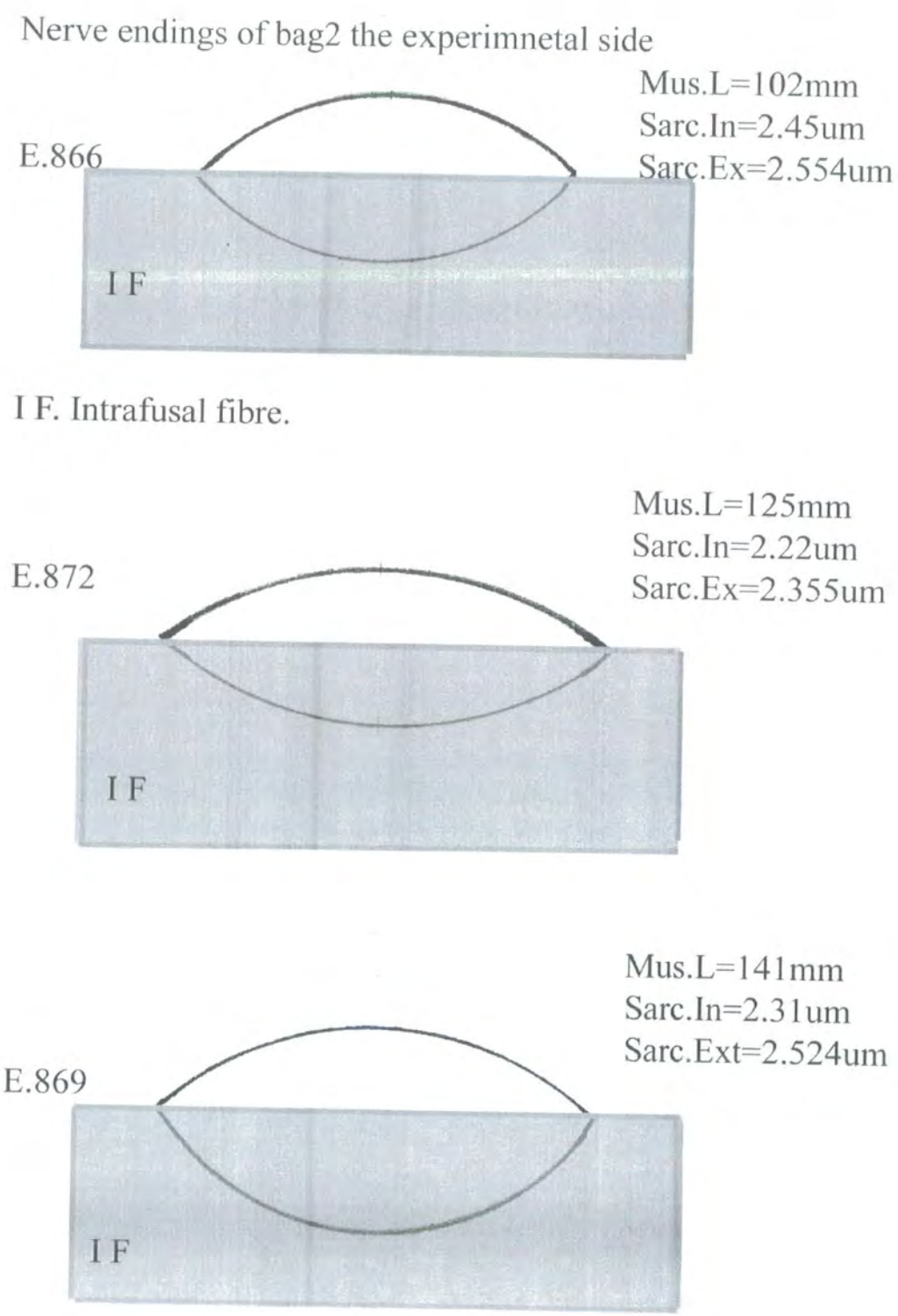

### 2.5.17 Regional variations in the values of O, I, C in regions A, B, and C.

The regional variations were analysed based on the numerical data of the values of the nerve profiles O, I, C, so the equatorial regions of intrafusal fibres from A, the proximal region; B, the middle region; and C, the distal region or the insertion region of the tenuissimus muscle were compared. List of values and their analysis of variance "ANOVA" of these regions in the different samples 866, 872, and 869 are shown in tables 2.36-2.47 and summarised in table 2.48 where all the sample *P-values* of ANOVA show higher values and hence a lack of significant regional variations.

Table 2.36 Values of the outside radii O, inside radii I, and semicords C, of the nerve profiles of $bag_1$ of the control side (LHS).

| $Bag_1$ Control | O | I | C |
|---|---|---|---|
| C866.LHS.A.B1 | 3.20 | 5.96 | 3.14 |
| | 2.20 | 3.78 | 2.14 |
| | 3.76 | 8.79 | 3.67 |
| C866.LHS.B.B1 | 4.98 | 4.89 | 3.23 |
| | 6.48 | 9.59 | 4.15 |
| | 3.82 | 3.96 | 2.81 |
| C866.LHS.C.B1 | 2.68 | 3.38 | 2.56 |
| | 3.10 | 4.76 | 2.74 |
| | 2.85 | 3.90 | 2.62 |
| C872.LHS.A.B1 | O | I | C |
| | 6.13 | 13.57 | 3.60 |
| | 5.45 | 8.64 | 3.96 |
| | 8.26 | 6.28 | 3.61 |
| C872.LHS.B.B1 | 4.52 | 4.71 | 3.32 |
| | 4.36 | 5.49 | 3.17 |
| | 5.84 | 5.36 | 3.72 |
| C869.LHS.A.B1 | O | I | C |
| | 2.85 | 6.03 | 2.87 |
| | 4.24 | 5.59 | 3.54 |
| | 3.28 | 4.79 | 2.99 |
| C869.LHS.B.B1 | 3.47 | 6.66 | 3.36 |
| | 6.84 | 7.57 | 5.61 |
| | 3.76 | 5.30 | 3.60 |
| C896.LHS.C.B1 | 3.09 | 4.53 | 3.11 |
| | 2.77 | 4.51 | 2.81 |
| | 3.87 | 4.31 | 3.11 |

Table 2.37 $Bag_1$ control sampling for regional variations different samples, same region of A, B, and C in all control sample 866 LHS, 869 LHS 6 rows per sample, 872 sample were not included because of the lack of region C data due to inadequate fixation.

| Sample | O | I | C | Site |
|---|---|---|---|---|
| C866.LHS.A.B1 | 3.20 | 5.96 | 3.14 | A |
| | 2.20 | 3.78 | 2.14 | A |
| | 3.76 | 8.79 | 3.67 | A |
| C869.LHS.A.B1 | 2.85 | 6.03 | 2.87 | A |
| | 4.24 | 5.59 | 3.54 | A |
| | 3.28 | 4.79 | 2.99 | A |
| C866.LHS.B.B1 | 4.98 | 4.89 | 3.23 | B |
| | 6.48 | 9.59 | 4.15 | B |
| | 3.82 | 3.96 | 2.81 | B |
| C869.LHS.B.B1 | 3.47 | 6.66 | 3.36 | B |
| | 6.84 | 7.57 | 5.61 | B |
| | 3.76 | 5.30 | 3.60 | B |
| C866.LHS.C.B1 | 2.68 | 3.38 | 2.56 | C |
| | 3.10 | 4.76 | 2.74 | C |
| | 2.85 | 3.90 | 2.62 | C |
| C896.LHS.C.B1 | 3.09 | 4.53 | 3.11 | C |
| | 2.77 | 4.51 | 2.81 | C |
| | 3.87 | 4.31 | 3.11 | C |

Table 2.38 ANOVA: Two-Factor With Replication for regional variations different samples, same region of A, B, and C in all $bag_1$ of control sample 866 LHS, 869 LHS 6 rows per sample, sample *P-value* is not high indicating no significant difference between the samples. This is the only one all the rest show higher *P-value*.

ANOVA: Two-Factor With Replication

| ANOVA: Two-Factor With Replication | | | | | |
|---|---|---|---|---|---|
| Sample | SUMMARY | O | I | C | Total |
| | Count | 6.00 | 6.00 | 6.00 | 18.00 |
| | Sum | 19.54 | 34.94 | 18.34 | 72.82 |
| | Average | 3.26 | 5.82 | 3.06 | 4.05 |
| | Variance | 0.50 | 2.83 | 0.30 | 2.75 |
| *C866 C869 LHS B.B 1* | | | | | |
| | Count | 6.00 | 6.00 | 6.00 | 18.00 |
| | Sum | 29.36 | 37.98 | 22.75 | 90.10 |
| | Average | 4.89 | 6.33 | 3.79 | 5.01 |
| | Variance | 2.15 | 4.20 | 0.99 | 3.30 |
| *C866 C869 LHS. B.B1* | | | | | |
| | Count | 6.00 | 6.00 | 6.00 | 18.00 |
| | Sum | 18.37 | 25.40 | 16.96 | 60.73 |
| | Average | 3.06 | 4.23 | 2.83 | 3.37 |
| | Variance | 0.19 | 0.26 | 0.06 | 0.55 |
| | | | | | |
| | *Total* | | | | |
| | Count | 18.00 | 18.00 | 18.00 | |
| | Sum | 67.27 | 98.32 | 58.05 | |
| | Average | 3.74 | 5.46 | 3.23 | |
| | Variance | 1.55 | 2.99 | 0.58 | |

| ANOVA | | | | | | |
|---|---|---|---|---|---|---|
| *Source of Variation* | *SS* | *df* | *MS* | *F* | *P-value* | *F crit* |
| Sample | 24.21 | 2.00 | 12.10 | 9.50 | 0.0004 | 3.20 |
| Columns | 49.46 | 2.00 | 24.73 | 19.41 | 0.00 | 3.20 |
| Interaction | 5.36 | 4.00 | 1.34 | 1.05 | 0.39 | 2.58 |
| Within | 57.33 | 45.00 | 1.27 | | | |
| | | | | | | |
| Total | 136.35 | 53.00 | | | | |

Table 2.39 Values of the outside radii O, inside radii I, and semicords C, of the nerve endings of $bag_1$ of the experimental side (RHS).

| Bag1-Experimental | O | I | C |
|---|---|---|---|
| E866.RHS.A.B1 | 2.89 | 3.51 | 1.76 |
| | 3.19 | 3.75 | 1.88 |
| | 3.91 | 4.83 | 2.42 |
| E866.RHS.B.B1 | 2.98 | 4.39 | 2.88 |
| | 2.63 | 3.04 | 2.74 |
| | 3.59 | 5.40 | 3.48 |
| E866.RHS.C.B1 | 3.09 | 3.37 | 2.93 |
| | 3.31 | 3.51 | 3.11 |
| | 4.37 | 3.99 | 3.55 |
| E872.RHS.A.B1 | 4.16 | 4.63 | 3.67 |
| | 3.93 | 3.67 | 3.36 |
| | 4.79 | 4.12 | 3.61 |
| E872.RHS.B.B1 | 4.15 | 3.92 | 3.43 |
| | 4.37 | 3.99 | 3.30 |
| | 3.95 | 3.70 | 3.29 |
| E872.RHS.C.B1 | 5.17 | 5.29 | 3.67 |
| | 5.32 | 5.30 | 3.90 |
| | 5.94 | 5.27 | 3.84 |
| E869.RHS.A.B1 | 3.54 | 4.34 | 3.48 |
| | 2.94 | 3.38 | 2.71 |
| | 3.27 | 3.94 | 3.41 |
| E869.RHS.B.B1 | 5.33 | 4.40 | 3.89 |
| | 4.44 | 3.70 | 3.49 |
| | 2.71 | 2.66 | 2.44 |
| E869.RHS.C.B1 | 2.88 | 3.40 | 2.95 |
| | 3.80 | 3.78 | 3.23 |
| | 2.63 | 2.62 | 2.69 |

Table 2.40 $Bag_1$ experimental sampling trial for regional variations of A, B, and C in samples 866 LHS, 872 LHS, 869 LHS 9 rows per sample.

| Sample | O | I | C | Site |
|---|---|---|---|---|
| E866.RHS.A.B1 | 2.89 | 3.51 | 1.76 | A |
| | 3.19 | 3.75 | 1.88 | A |
| | 3.91 | 4.83 | 2.42 | A |
| E872.RHS.A.B1 | 4.16 | 4.63 | 3.67 | A |
| | 3.93 | 3.67 | 3.36 | A |
| | 4.79 | 4.12 | 3.61 | A |
| E869.RHS.A.B1 | 3.54 | 4.34 | 3.48 | A |
| | 2.94 | 3.38 | 2.71 | A |
| | 3.27 | 3.94 | 3.41 | A |
| E866.RHS.B.B1 | 2.98 | 4.39 | 2.88 | B |
| | 2.63 | 3.04 | 2.74 | B |
| | 3.59 | 5.40 | 3.48 | B |
| E872.RHS.B.B1 | 4.15 | 3.92 | 3.43 | B |
| | 4.37 | 3.99 | 3.30 | B |
| | 3.95 | 3.70 | 3.29 | B |
| E869.RHS.B.B1 | 5.33 | 4.40 | 3.89 | B |
| | 4.44 | 3.70 | 3.49 | B |
| | 2.71 | 2.66 | 2.44 | B |
| E866.RHS.C.B1 | 3.09 | 3.37 | 2.93 | C |
| | 3.31 | 3.51 | 3.11 | C |
| | 4.37 | 3.99 | 3.55 | C |
| E872.RHS.C.B1 | 5.17 | 5.29 | 3.67 | C |
| | 5.32 | 5.30 | 3.90 | C |
| | 5.94 | 5.27 | 3.84 | C |
| E869.RHS.C.B1 | 2.88 | 3.40 | 2.95 | C |
| | 3.80 | 3.78 | 3.23 | C |
| | 2.63 | 2.62 | 2.69 | C |

Table 2.41 $Bag_1$ trial of ANOVA two-Factor With Replication for regional variations different samples, same region of A, B, and C in all experimental sample RHS866, RHS869, RHS872, 9 rows per sample, sample *P-value* is high indicating no significant difference between the samples.

| ANOVA two-Factor With Replication | | | | | |
|---|---|---|---|---|---|
| Sample | SUMMARY | O | I | C | Total |
| E866.E872.E869.RHS.A.B1 | Count | 9.00 | 9.00 | 9.00 | 27.00 |
| | Sum | 32.62 | 36.19 | 26.28 | 95.08 |
| | Average | 3.62 | 4.02 | 2.92 | 3.52 |
| | Variance | 0.39 | 0.25 | 0.57 | 0.59 |
| E866.E872.E869RHS.B.B1 | Count | 9.00 | 9.00 | 9.00 | 27.00 |
| | Sum | 34.14 | 35.19 | 28.94 | 98.27 |
| | Average | 3.79 | 3.91 | 3.22 | 3.64 |
| | Variance | 0.81 | 0.64 | 0.20 | 0.60 |
| E866.E872.E869.RHS.C.B1 | Count | 9.00 | 9.00 | 9.00 | 27.00 |
| | Sum | 36.51 | 36.53 | 29.87 | 102.91 |
| | Average | 4.06 | 4.06 | 3.32 | 3.81 |
| | Variance | 1.44 | 0.99 | 0.19 | 0.93 |
| | Total | | | | |
| | Count | 27.00 | 27.00 | 27.00 | |
| | Sum | 103.27 | 107.90 | 85.09 | |
| | Average | 3.82 | 4.00 | 3.15 | |
| | Variance | 0.85 | 0.58 | 0.32 | |

| ANOVA | | | | | | |
|---|---|---|---|---|---|---|
| Source of Variation | SS | df | MS | F | P-value | F crit |
| Sample | 1.15 | 2.00 | 0.57 | 0.94 | 0.39 | 3.12 |
| Columns | 10.77 | 2.00 | 5.38 | 8.84 | 0.00 | 3.12 |
| Interaction | 0.59 | 4.00 | 0.15 | 0.24 | 0.91 | 2.50 |
| Within | 43.83 | 72.00 | 0.61 | | | |
| Total | 56.33 | 80.00 | | | | |

Table 2.42 All Values of the outside radii O inside radii I, and the semicord C of $bag_2$ control side (LHS).

| $Bag_2$ control side | O | I | C |
|---|---|---|---|
| C866.LHS.A.B2 | 3.47 | 5.83 | 3.11 |
| | 5.60 | 5.46 | 3.84 |
| | 4.04 | 5.15 | 3.45 |
| C866.LHS.B.B2 | 5.72 | 5.24 | 3.91 |
| | 7.10 | 4.77 | 4.16 |
| | 4.33 | 5.72 | 3.66 |
| C866.LHS.C.B2 | 3.96 | 3.67 | 3.05 |
| | 3.85 | 4.41 | 2.93 |
| | 3.99 | 4.95 | 2.99 |
| C872.LHS.A.B2 | O | I | C |
| | 7.09 | 9.75 | 3.60 |
| | 7.00 | 11.48 | 4.15 |
| | 9.21 | 10.05 | 4.33 |
| C872.LHS.B.B2 | 5.39 | 4.74 | 3.92 |
| | 13.46 | 5.16 | 4.34 |
| | 5.10 | 4.25 | 3.54 |
| C.869.LHS.A.B2 | O | I | C |
| | 4.97 | 7.57 | 3.72 |
| | 5.06 | 6.33 | 3.78 |
| | 5.91 | 6.68 | 4.42 |
| C869.LHS.B.B2 | 5.76 | 5.06 | 3.97 |
| | 4.34 | 4.47 | 3.48 |
| | 6.26 | 5.02 | 3.60 |
| C896.LHS.C.B2 | 2.82 | 2.96 | 2.94 |
| | 2.59 | 3.02 | 2.58 |
| | 2.46 | 2.99 | 2.13 |

Table2.43 $Bag_2$ control sampling for trial of ANOVA of regional variations of A, B, and C in all control sample 866 LHS, 872 LHS, 869 LHS 9 rows per sample, region C were omitted from all samples due to inadequate fixation in sample 872.

| Sample | O | I | C | Site |
|---|---|---|---|---|
| C866.LHS.A.B2 | 3.47 | 5.83 | 3.11 | A |
| | 5.60 | 5.46 | 3.84 | A |
| | 4.04 | 5.15 | 3.45 | A |
| C872.LHS.A.B2 | 7.09 | 9.75 | 3.60 | A |
| | 7.00 | 11.48 | 4.15 | A |
| | 9.21 | 10.05 | 4.33 | A |
| C.869.LHS.A.B2 | 4.97 | 7.57 | 3.72 | A |
| | 5.06 | 6.33 | 3.78 | A |
| | 5.91 | 6.68 | 4.42 | A |
| C866.LHS.B.B2 | 5.72 | 5.24 | 3.91 | B |
| | 7.10 | 4.77 | 4.16 | B |
| | 4.33 | 5.72 | 3.66 | B |
| C872.LHS.B.B2 | 5.39 | 4.74 | 3.92 | B |
| | 13.46 | 5.16 | 4.34 | B |
| | 5.10 | 4.25 | 3.54 | B |
| C869.LHS.B.B2 | 5.76 | 5.06 | 3.97 | B |
| | 4.34 | 4.47 | 3.48 | B |
| | 6.26 | 5.02 | 3.60 | B |

Table 2.44 $Bag_2$ trial of ANOVA two-Factor With Replication for regional variations, different samples, same region of A, B, and C in all control sample 866 LHS, 869 LHS 9 rows per sample, *P-value* is high indicating no significant difference between the samples.

| ANOVA: Two-Factor With Replication | | | | | |
|---|---|---|---|---|---|
| Sample | SUMMARY | O | I | C | Total |
| *C866.C872. C869.LHS. A.B2* | | | | | |
| | Count | 9.00 | 9.00 | 9.00 | 27.00 |
| | Sum | 52.34 | 68.30 | 34.40 | 155.04 |
| | Average | 5.82 | 7.59 | 3.82 | 5.74 |
| | Variance | 3.06 | 5.24 | 0.18 | 5.07 |
| *C866.C872 C869.LHS. B.B2* | | | | | |
| | Count | 9.00 | 9.00 | 9.00 | 27.00 |
| | Sum | 57.46 | 44.44 | 34.56 | 136.45 |
| | Average | 6.38 | 4.94 | 3.84 | 5.05 |
| | Variance | 7.80 | 0.19 | 0.09 | 3.61 |
| | | | | | |
| | *Total* | | | | |
| | Count | 18.00 | 18.00 | 18.00 | |
| | Sum | 109.80 | 112.74 | 68.96 | |
| | Average | 6.10 | 6.26 | 3.83 | |
| | Variance | 5.20 | 4.42 | 0.12 | |

| ANOVA | | | | | | |
|---|---|---|---|---|---|---|
| *Source of Variation* | *SS* | *df* | *MS* | *F* | *P-value* | *F crit* |
| Sample | 6.40 | 1.00 | 6.40 | 2.32 | 0.13 | 4.04 |
| Columns | 66.54 | 2.00 | 33.27 | 12.05 | 0.00 | 3.19 |
| Interaction | 26.71 | 2.00 | 13.35 | 4.84 | 0.01 | 3.19 |
| Within | 132.50 | 48.00 | 2.76 | | | |
| | | | | | | |
| Total | 232.14 | 53.00 | | | | |

Table 2.45 Values of the outside radii O, inside radii I, semicord C, of the nerve endings profile of $bag_2$ of the experimental side (LHS).

| $Bag_2$ experimental | O | I | C |
|---|---|---|---|
| E866.RHS.A.B2 | 3.76 | 4.52 | 3.17 |
| | 4.21 | 6.41 | 3.73 |
| | 3.89 | 4.71 | 3.23 |
| E866.RHS.B.B2 | 5.21 | 5.30 | 4.15 |
| | 3.84 | 3.86 | 2.87 |
| | 2.93 | 3.54 | 2.68 |
| E866.RHS.C.B2 | 3.86 | 3.61 | 3.72 |
| | 5.52 | 3.35 | 3.23 |
| | 4.22 | 3.23 | 2.87 |
| E872RHS.A.B2 | 7.64 | 5.43 | 4.05 |
| | 5.14 | 3.45 | 3.18 |
| | 4.70 | 3.31 | 2.99 |
| E872.RHS.B.B2 | 4.37 | 5.38 | 3.54 |
| | 4.31 | 5.86 | 2.99 |
| | 5.00 | 6.04 | 3.97 |
| E872.RHS.C.B2 | 10.14 | 8.73 | 4.94 |
| | 7.25 | 5.46 | 4.39 |
| | 8.53 | 5.01 | 4.72 |
| E869.RHS.A.B2 | 5.73 | 4.94 | 3.85 |
| | 6.81 | 5.39 | 4.45 |
| | 10.06 | 4.88 | 4.56 |
| E869.RHS.B.B2 | 4.69 | 5.62 | 3.79 |
| | 4.63 | 4.74 | 3.66 |
| | 5.35 | 3.84 | 3.63 |
| E869.RHS.C.B2 | 6.54 | 4.47 | 4.15 |
| | 5.62 | 3.99 | 3.60 |
| | 5.22 | 3.51 | 3.23 |

Table 2.46 $Bag_2$ experimental samples for trial of ANOVA of regional variations of A, B, and C in all experimental samples 866 LHS, 872 LHS, and 869 LHS 9 rows per sample.

| Sample | O | I | C | Site |
|---|---|---|---|---|
| E866.RHS.A.B2 | 3.76 | 4.52 | 3.17 | A |
| | 4.21 | 6.41 | 3.73 | A |
| | 3.89 | 4.71 | 3.23 | A |
| E872RHS.A.B2 | 7.64 | 5.43 | 4.05 | A |
| | 5.14 | 3.45 | 3.18 | A |
| | 4.70 | 3.31 | 2.99 | A |
| E869.RHS.A.B2 | 5.73 | 4.94 | 3.85 | A |
| | 6.81 | 5.39 | 4.45 | A |
| | 10.06 | 4.88 | 4.56 | A |
| E866.RHS.B.B2 | 5.21 | 5.30 | 4.15 | B |
| | 3.84 | 3.86 | 2.87 | B |
| | 2.93 | 3.54 | 2.68 | B |
| E872.RHS.B.B2 | 4.37 | 5.38 | 3.54 | B |
| | 4.31 | 5.86 | 2.99 | B |
| | 5.00 | 6.04 | 3.97 | B |
| E869.RHS.B.B2 | 4.69 | 5.62 | 3.79 | B |
| | 4.63 | 4.74 | 3.66 | B |
| | 5.35 | 3.84 | 3.63 | B |
| E866.RHS.C.B2 | 3.86 | 3.61 | 3.72 | C |
| | 5.52 | 3.35 | 3.23 | C |
| | 4.22 | 3.23 | 2.87 | C |
| E872.RHS.C.B2 | 10.14 | 8.73 | 4.94 | C |
| | 7.25 | 5.46 | 4.39 | C |
| | 8.53 | 5.01 | 4.72 | C |
| E869.RHS.C.B2 | 6.54 | 4.47 | 4.15 | C |
| | 5.62 | 3.99 | 3.60 | C |
| | 5.22 | 3.51 | 3.23 | C |

Table2.47 Trial of ANOVA of regional variations in A, B, and C in each $bag_2$ experimental sample 866 RHS, 869 RHS and 872 RHS. Sample *P-value* is high indicating no significant difference between the samples.

| ANOVA: Two-Factor With Replication | | | | | |
|---|---|---|---|---|---|
| Sample | SUMMARY | O | I | C | Total |
| *E866. E872. E869. RHS. A.B2* | | | | | |
| | Count | 9.00 | 9.00 | 9.00 | 27.00 |
| | Sum | 51.93 | 43.03 | 33.21 | 128.17 |
| | Average | 5.77 | 4.78 | 3.69 | 4.75 |
| | Variance | 4.32 | 0.93 | 0.34 | 2.47 |
| *E866. E872. E869. RHS.B. B2* | | | | | |
| | Count | 9.00 | 9.00 | 9.00 | 27.00 |
| | Sum | 40.34 | 44.20 | 31.28 | 115.82 |
| | Average | 4.48 | 4.91 | 3.48 | 4.29 |
| | Variance | 0.56 | 0.90 | 0.26 | 0.91 |
| *E866. E872. E869. RHS. C.B2* | | | | | |
| | Count | 9.00 | 9.00 | 9.00 | 27.00 |
| | Sum | 56.90 | 41.36 | 34.85 | 133.11 |
| | Average | 6.32 | 4.60 | 3.87 | 4.93 |
| | Variance | 4.15 | 2.99 | 0.52 | 3.45 |
| | | | | | |
| | *Total* | | | | |
| | Count | 27.00 | 27.00 | 27.00 | |
| | Sum | 149.17 | 128.59 | 99.34 | |
| | Average | 5.52 | 4.76 | 3.68 | |
| | Variance | 3.39 | 1.50 | 0.37 | |

| ANOVA | | | | | | |
|---|---|---|---|---|---|---|
| *Source of Variation* | *SS* | *df* | *MS* | *F* | *P-value* | *F crit* |
| Sample | 5.9 | 2.0 | 2.9 | 1.8 | 0.178199 | 3.12 |
| Columns | 46.4 | 2.0 | 23.2 | 14.0 | 7.49E-06 | 3.12 |
| Interaction | 11.3 | 4.0 | 2.8 | 1.7 | 0.158438 | 2.50 |
| Within | 119.7 | 72.0 | 1.7 | | | |
| | | | | | | |
| Total | 183.4 | 80.0 | | | | |

Table 2.48 Summary comparison of the P- value of regional variations. Different samples, same region.

| Set | Sample | Bag | *P-value* |
|---|---|---|---|
| Control | E.866.E872.E869. | $Bag_1$ | 0.000361 |
| Experimental | R.866.R872.R869. | $Bag_1$ | 0.39 |
| Control | E.866.E872.E869. | $Bag_2$ | 0.13 |
| Experimental | R.866.R872.R869. | $Bag_2$ | 0.18 |

### 2.5.18 Chain fibres

Like the bag fibres, the chain fibres have been measured using Image Tool Program, focusing on the nerve endings and measuring them in each micrograph (as was done in initial trials on the bag fibres). Diameters were also measured. Their sarcomeres were difficult to follow and to identify for each fibre because the chain fibres become more kinked convoluted especially with increasing distance from the equatorial. None of these trials has given any consistent evidences of difference between control and experimental sides.

The measurements of chain -fibre nerve endings were repeated, using LaserPix program measuring the selected nerve endings and fibre diameter.

The diameter of chain fibres were measured three times in three different locations the left, middle and the right sides of the equatorial region just as was done with bag fibres.

Summary of the measurements and their descriptive statistics are listed in the tables, Charts, ANOVA and t-tests as seen in the following pages.

### 2.5.18.1 Chain fibres results

Chart no 2.22 shows the diameter of the control verses the experimental (LHS vs. RHS) based on the mean values derived from diameter readings in table 2.49. There is a negligible of difference between the control and the experimental, which is further proven by the t- test in table 2.51 and the analysis of variance in table 2.53. The absolute values of O, I and C, together with ratios I/O, I/C and O/C for nerve ending profiles on chain fibres in samples 866, 872 and 869 are summarised in tables 2.54-2.56. Charts for O, I and C are plotted in 2.23-2.25 followed by ANOVA and t-test, in tables 2.57-2.58, where the data seem to reflect some features similar to that of $bag_1$ and $bag_2$ except for sample 866 where the balance of tension seem to be reversed. A further analysis of ratios I/O, I/C, O/C in charts 2.26-2.28 reflects mixed features, though the greater ratios O/C and I/C in sample 872 do show the usual outcome as the samples with the greatest apparent tension difference. The charts are followed by ANOVA and t-test in tables 2.59-2.60.

Tables 2.61-2.62 combine the analysis of variance carried out on all the absolute values of ratios O, I, C (not the mean) of chain nerve-endings profiles (which show significant difference between the control and experimental.

Tables (2.63-2.64) is the analysis of variance carried out on all the values (not the mean) of chain nerve endings ratios I/O, O/C, I/C (where *p–values* for columns are very low showing significant difference between the control and experimental.

Table 2.49 Diameters of control and experimental chain fibres measured in $\mu$m.

| Sample | Diameter (μm) | Sample | Diameter μm) |
|---|---|---|---|
| C866.LHS.A.CH1 | 4.42 | E866.RHS.A.CH1 | 4.9 |
| | 5.06 | | 6.6 |
| | 4.23 | | 5.1 |
| C866.LHS.C.CH1 | 6.86 | E866.RHS.C.CH1 | 5.69 |
| | 8.43 | | 6.67 |
| | 8.04 | | 6.47 |
| 866.LHS.C.CH2 | 8.56 | E866.RHS.B.CH1 | 9.22 |
| | 9.41 | | 11.77 |
| | 6.27 | | 10.4 |
| C872.LHS.A.CH1 | 5.88 | E866.RHS.C.CH2 | 7.45 |
| | 9.21 | | 7.65 |
| | 6.27 | | 6.28 |
| C872.LHS.A.CH2 | 7.46 | E872.RHS.B.CH1 | 6.67 |
| | 7.49 | | 8.23 |
| | 6.08 | | 6.08 |
| C872.LHS.B.CH1 | 5.88 | E872.RHS.C.CH1 | 6.67 |
| | 6.67 | | 9.02 |
| | 7.06 | | 6.71 |
| C869.LHS.B.CH1 | 7.06 | E869.RHS.B.CH1 | 5.69 |
| | 7.26 | | 6.09 |
| | 7.65 | | 7.45 |
| C869.LHS.B.CH2 | 6.47 | E869.RHS.C.CH1 | 5.69 |
| | 6.08 | | 6.09 |
| | 7.69 | | 5.49 |
| C869.LHS.C.CH1 | 6.67 | | |
| | 8.04 | | |
| | 8.43 | | |
| C869.LHS.C.CH2 | 6.47 | | |
| | 7.06 | | |
| | 6.67 | | |

Table 2.50 Chain fibre diameter descriptive statistics.

| Control ( LHS) *Column1* | | Experimental ( RHS) *Column1* | |
|---|---|---|---|
| Mean | 6.96 | Mean | 7.00 |
| Standard Error | 0.23 | Standard Error | 0.34 |
| Median | 6.96 | Median | 6.64 |
| Mode | 6.67 | Mode | 5.69 |
| Standard Deviation | 1.25 | Standard Deviation | 1.68 |
| Sample Variance | 1.55 | Sample Variance | 2.83 |
| Kurtosis | 0.11 | Kurtosis | 1.81 |
| Skewness | -0.16 | Skewness | 1.39 |
| Range | 5.18 | Range | 6.87 |
| Minimum | 4.23 | Minimum | 4.90 |
| Maximum | 9.41 | Maximum | 11.77 |
| Sum | 208.83 | Sum | 168.08 |
| Count | 30.00 | Count | 24.00 |

| | LHS | RHS |
|---|---|---|
| Mean | 6.961 | 7.003333 |
| Standard Error | 0.227506 | 0.343107 |

Chart 2.22 Diameters of control and experimental chain fibres.

| | LHS | RHS |
|---|---|---|
| Mean | 6.96 | 7.00 |
| Standard Error | 0.23 | 0.34 |

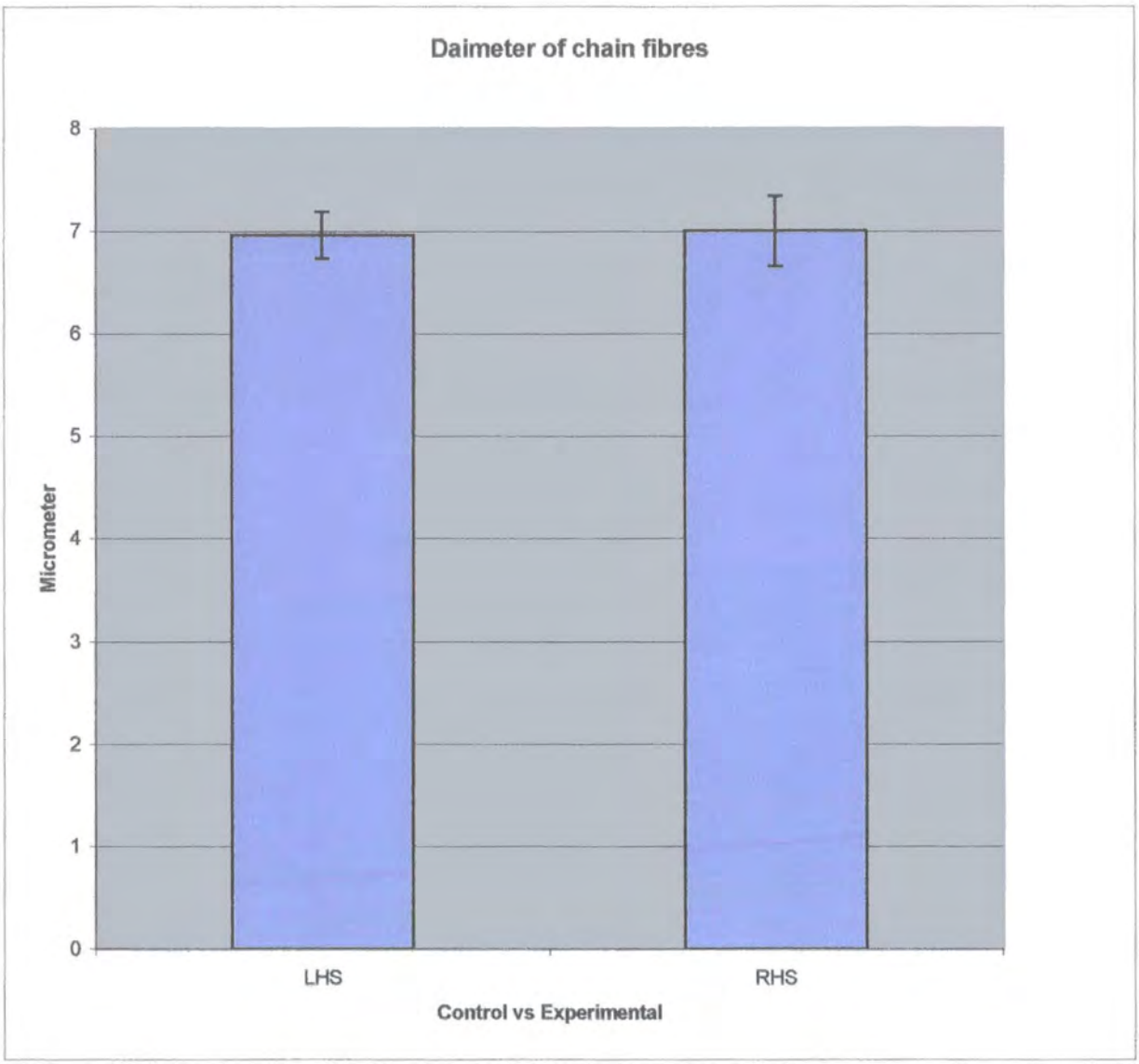

Table 2.51 t-Test: paired two sample for means of chain fibres control vs. experimental.

| Control | Expert |
|---|---|
| 4.42 | 4.9 |
| 5.06 | 6.6 |
| 4.23 | 5.1 |
| 6.86 | 5.69 |
| 8.43 | 6.67 |
| 8.04 | 6.47 |
| 8.56 | 9.22 |
| 9.41 | 11.77 |
| 6.27 | 10.4 |
| 5.88 | 7.45 |
| 9.21 | 7.65 |
| 6.27 | 6.28 |
| 7.46 | 6.67 |
| 7.49 | 8.23 |
| 6.08 | 6.08 |
| 5.88 | 6.67 |
| 6.67 | 9.02 |
| 7.06 | 6.71 |
| 7.06 | 5.69 |
| 7.26 | 6.09 |
| 7.65 | 7.45 |
| 6.47 | 5.69 |
| 6.08 | 6.09 |
| 7.69 | 5.49 |
| 6.67 | |
| 8.04 | |
| 8.43 | |
| 6.47 | |
| 7.06 | |
| 6.67 | |

| t-Test: Paired Two Sample for Means | | |
|---|---|---|
| | *Variable 1* | *Variable 2* |
| Mean | 6.90 | 7.00 |
| Variance | 1.79 | 2.83 |
| Observations | 24.00 | 24.00 |
| Pearson Correlation | 0.50 | |
| Hypothesized Mean Difference | 0.00 | |
| Df | 23.00 | |
| t Stat | -0.34 | |
| P (T<=t) one-tail | 0.37 | |
| t Critical one-tail | 1.71 | |
| P(T<=t) two-tail | 0.73 | |
| t Critical two-tail | 2.07 | |

Table 2.52 Selected samples from chain diameter for ANOVA.

| Sample | Cont | Exprt |
|---|---|---|
| C866.LHS.A.CH1 | 4.42 | 4.9 |
| | 5.06 | 6.6 |
| | 4.23 | 5.1 |
| C866.LHS.C.CH1 | 6.86 | 5.69 |
| | 8.43 | 6.67 |
| | 8.04 | 6.47 |
| 866.LHS.C.CH2 | 8.56 | 9.22 |
| | 9.41 | 11.77 |
| | 6.27 | 10.4 |
| C872.LHS.A.CH2 | 7.46 | 6.67 |
| | 7.49 | 8.23 |
| | 6.08 | 6.08 |
| C872.LHS.B.CH1 | 5.88 | 6.67 |
| | 6.67 | 9.02 |
| | 7.06 | 6.71 |
| C869.LHS.B.CH1 | 7.06 | 5.69 |
| | 7.26 | 6.09 |
| | 7.65 | 7.45 |
| C869.LHS.B.CH2 | 6.47 | 5.69 |
| | 6.08 | 6.09 |
| | 7.69 | 5.49 |

Table 2.53 ANOVA of chain diameter (two-Factor with Replication). Columns *P-value* is greater than 0.5 indicating no significant difference between the control and experimental.

| ANOVA: Two-Factor With Replication | | | | |
|---|---|---|---|---|
| | SUMMARY | Cont | Exprt | Total |
| *C866.LHS.A.CH1* | | | | |
| | Count | 3 | 3 | 6 |
| | Sum | 13.71 | 16.6 | 30.31 |
| | Average | 4.57 | 5.53 | 5.05 |
| | Variance | 0.19 | 0.86 | 0.7 |
| *C866.LHS.C.CH1* | | | | |
| | Count | 3 | 3 | 6 |
| | Sum | 23.33 | 18.83 | 42.16 |
| | Average | 7.78 | 6.28 | 7.03 |
| | Variance | 0.67 | 0.27 | 1.05 |
| *866.LHS.C.CH2* | | | | |
| | Count | 3 | 3 | 6 |
| | Sum | 24.24 | 31.39 | 55.63 |
| | Average | 8.08 | 10.46 | 9.27 |
| | Variance | 2.64 | 1.63 | 3.41 |
| *C872.LHS.A.CH2* | | | | |
| | Count | 3 | 3 | 6 |
| | Sum | 21.03 | 20.98 | 42.01 |
| | Average | 7.01 | 6.99 | 7 |
| | Variance | 0.65 | 1.23 | 0.75 |
| *C872.LHS.B.CH1* | | | | |
| | Count | 3 | 3 | 6 |
| | Sum | 19.61 | 22.4 | 42.01 |
| | Average | 6.54 | 7.47 | 7 |
| | Variance | 0.36 | 1.81 | 1.13 |
| *C869.LHS.B.CH1* | | | | |
| | Count | 3 | 3 | 6 |
| | Sum | 21.97 | 19.23 | 41.2 |
| | Average | 7.32 | 6.41 | 6.87 |
| | Variance | 0.09 | 0.85 | 0.63 |
| *C869.LHS.B.CH2* | | | | |
| | Count | 3 | 3 | 6 |
| | Sum | 20.24 | 17.27 | 37.51 |
| | Average | 6.75 | 5.76 | 6.25 |
| | Variance | 0.71 | 0.09 | 0.61 |
| | *Total* | | | |
| | Count | 21 | 21 | |
| | Sum | 144.13 | 146.7 | |
| | Average | 6.86 | 6.99 | |
| | Variance | 1.72 | 3.19 | |

| ANOVA | | | | | | |
|---|---|---|---|---|---|---|
| *Source of Variation* | *SS* | *Df* | *MS* | *F* | *P-value* | *F crit* |
| Sample | 56.97 | 6.00 | 9.50 | 11.03 | 2.64E-06 | 2.45 |
| Columns | 0.16 | 1.00 | 0.16 | 0.18 | 0.67232 | 4.20 |
| Interaction | 17.15 | 6.00 | 2.86 | 3.32 | 0.013481 | 2.45 |
| Within | 24.10 | 28.00 | 0.86 | | | |
| | | | | | | |
| Total | 98.38 | 41.00 | | | | |

Table 2.54 Summary of the mean values of radii O, I, C of chain nerve endings profiles and the means of their ratios I/O, O/C and I/C.

| Sample | Radii and ratio in (μm) | | | | | | |
|---|---|---|---|---|---|---|---|
| 866 | | O | I | C | I/O | O/C | I/C |
| | cont | 2.44 | 1.83 | 1.63 | 0.89 | 1.35 | 1.13 |
| | exprt | 6.07 | 4.39 | 3.27 | 0.82 | 1.82 | 1.35 |
| | Standard Error | 1.03 | 0.47 | 0.44 | 0.10 | 0.20 | 0.03 |
| | | 0.84 | 0.20 | 0.14 | 0.08 | 0.21 | 0.05 |
| | | Radii and ratio in (μm) | | | | | |
| 872 | | O | I | C | I/O | O/C | I/C |
| | Cont | 18.06 | 6.59 | 4.66 | 0.58 | 3.98 | 1.37 |
| | Exprt | 4.50 | 3.15 | 2.57 | 0.74 | 1.74 | 1.21 |
| | Standard Error | 6.95 | 1.44 | 0.87 | 0.13 | 1.47 | 0.08 |
| | | 0.69 | 0.37 | 0.22 | 0.09 | 0.19 | 0.06 |
| | | Radii and ratio in (μm) | | | | | |
| 869 | | O | I | C | I/O | O/C | I/C |
| | Cont | 8.58 | 4.91 | 3.27 | 0.77 | 2.43 | 1.47 |
| | Exprt | 7.36 | 4.32 | 2.58 | 0.95 | 2.84 | 1.66 |
| | Standard Error | 2.24 | 0.55 | 0.23 | 0.12 | 0.49 | 0.10 |
| | | 3.18 | 0.50 | 0.12 | 0.20 | 1.22 | 0.13 |

Table 2.55 Regrouping of the means of chain O, I, C.

| Mean of absolute value | | | |
|---|---|---|---|
| Sample | 866 | 872 | 869 |
| Outer Radius | O | O | O |
| Cont | 2.44 | 18.06 | 8.58 |
| Exprt | 6.07 | 4.50 | 7.36 |
| Standard Error | 1.03 | 6.95 | 2.24 |
| | 0.84 | 0.69 | 3.18 |
| Sample | 866 | 872 | 869 |
| Inner Radius | I | I | I |
| Cont | 1.83 | 6.59 | 4.91 |
| Exprt | 4.39 | 3.15 | 4.32 |
| Standard Error | 0.47 | 1.44 | 0.55 |
| | 0.20 | 0.37 | 0.50 |
| Sample | 866 | 872 | 869 |
| Semicord | C | C | C |
| Cont | 1.63 | 4.66 | 3.27 |
| Exprt | 3.27 | 2.57 | 2.58 |
| Standard Error | 0.44 | 0.87 | 0.23 |
| | 0.14 | 0.22 | 0.12 |

Table 2.56 Regrouping of the means of radii ratio I/O, O/C, I/C.

| Ratio of the mean of the absolute value | | | |
|---|---|---|---|
| Sample | 866 | 872 | 869 |
| Ratio | I/O | I/O | I/O |
| Cont | 0.89 | 0.58 | 0.77 |
| Exprt | 0.82 | 0.74 | 0.95 |
| Standard Error | 0.10 | 0.13 | 0.12 |
| | 0.08 | 0.09 | 0.20 |
| Sample | 866 | 872 | 869 |
| Ratio | O/C | O/C | O/C |
| Cont | 1.35 | 3.98 | 1.35 |
| Exprt | 1.82 | 1.74 | 1.82 |
| Standard Error | 0.20 | 1.47 | 0.20 |
| | 0.21 | 0.19 | 0.21 |
| Sample | 866 | 872 | 869 |
| Ratio | I/C | I/C | I/C |
| Cont | 1.13 | 1.37 | 1.47 |
| Exprt | 1.35 | 1.21 | 1.66 |
| Standard Error | 0.03 | 0.08 | 0.10 |
| | 0.05 | 0.06 | 0.13 |

Chart 2.23 Radii O for chain fibres control vs. experimental. Sample 872 stands out as the one with biggest tension difference between control and experimental.

| Chain fibres | O | O | O |
|---|---|---|---|
| | C866 | 872 | C869 |
| Cont | 2.44 | 18.06 | 8.58 |
| Exprt | 6.07 | 4.50 | 7.36 |
| Standard Error | 1.03 | 6.95 | 2.24 |
| | 0.84 | 0.69 | 3.18 |

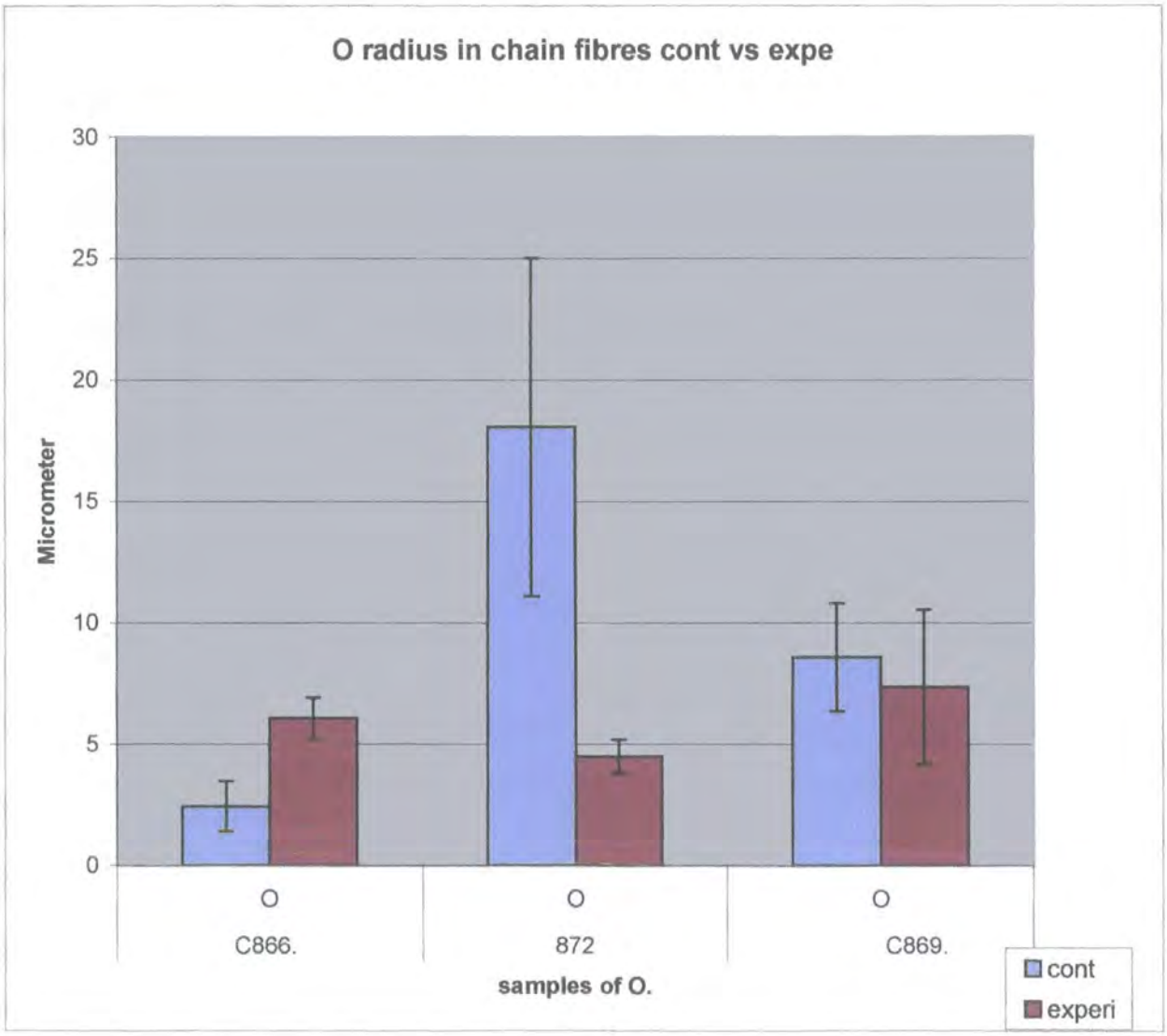

Chart 2.24 Radii I for chain fibres control vs. experimental. Sample 872 stands out as the one with biggest tension difference between control and experimental.

| Chain fibres | I | I | I |
|---|---|---|---|
| | C866 | 872 | C869 |
| Cont | 1.83 | 6.59 | 4.91 |
| Exprt | 4.39 | 3.15 | 4.32 |
| Standard Error | 0.47 | 1.44 | 0.55 |
| | 0.20 | 0.37 | 0.50 |

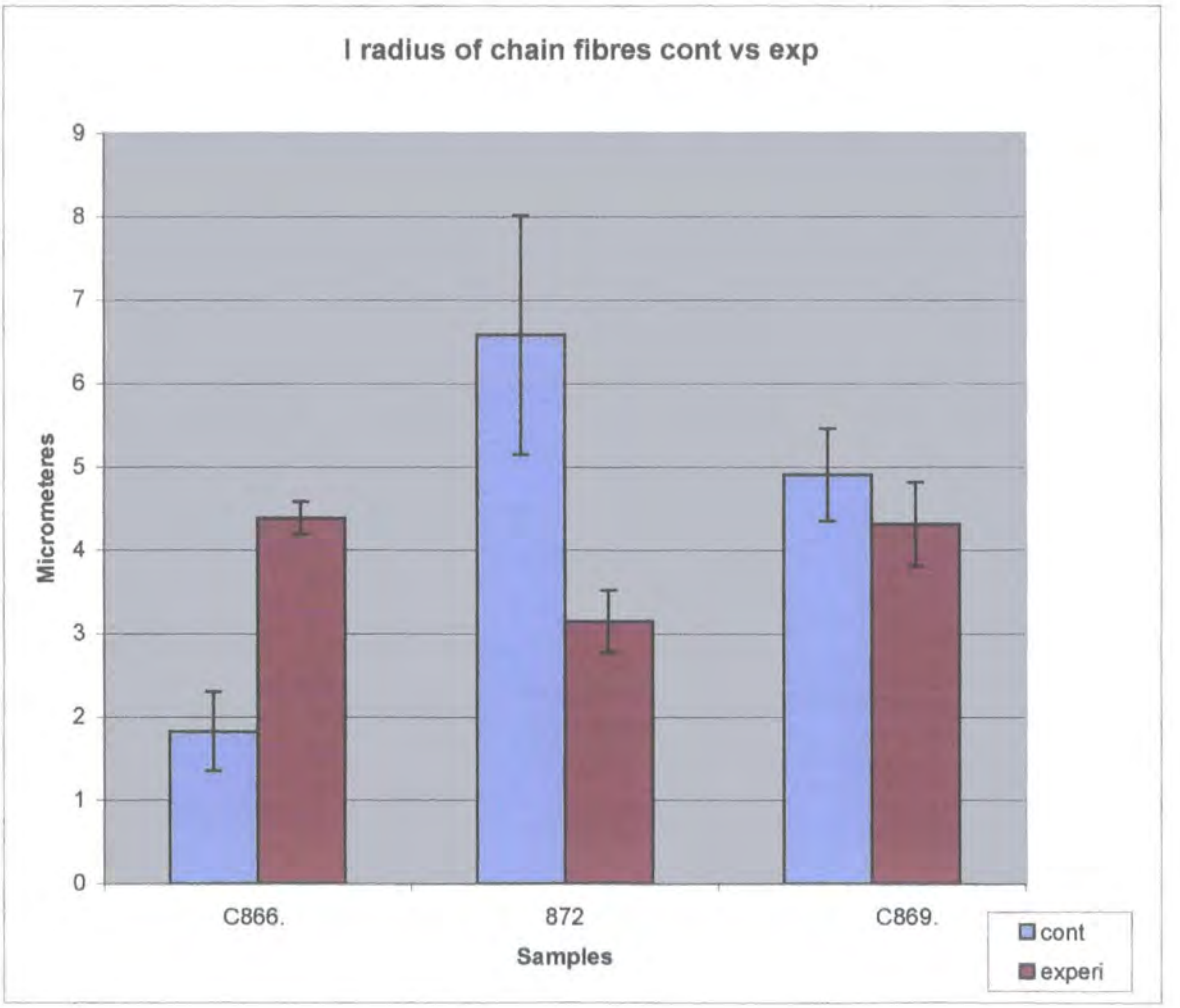

Chart 2.25 Semicord C for chain fibres control vs. experimental. Sample 872 stands out as the one with biggest tension difference between control and experimental.

| Chain fibres | C | C | C |
|---|---|---|---|
| | C866. | 872.00 | C869. |
| Cont | 1.63 | 4.66 | 3.27 |
| Exprt | 3.27 | 2.57 | 2.58 |
| Standard Error | 0.44 | 0.87 | 0.23 |
| | 0.14 | 0.22 | 0.12 |

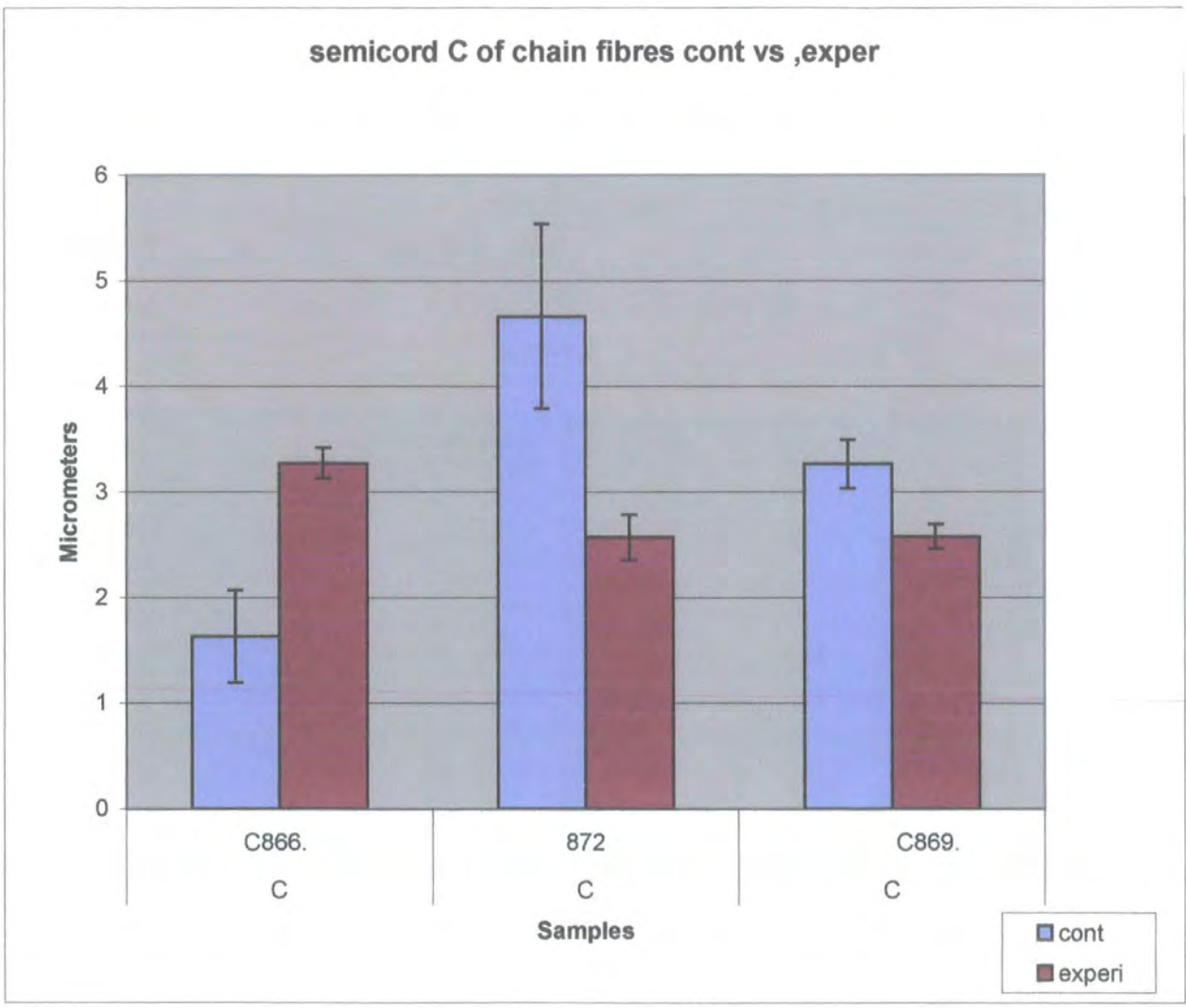

Table 2.57 ANOVA for the means of radii and semi-cord, for chain fibres control vs. experimental.

| ANOVA for chain fibres cont vs. exprt. | | | |
|---|---|---|---|
| C866 | Radii | Cont | Exprt |
| | O | 2.44 | 6.07 |
| | I | 1.83 | 4.39 |
| | C | 1.63 | 3.27 |
| C872 | O | 18.06 | 4.50 |
| | I | 6.59 | 3.15 |
| | C | 4.66 | 2.57 |
| C869 | O | 8.58 | 7.36 |
| | I | 4.91 | 4.32 |
| | C | 3.27 | 2.58 |

| ANOVA: Two-Factor Without Replication | | | | |
|---|---|---|---|---|
| | | | | |
| *SUMMARY* | *Count* | *Sum* | *Average* | *Variance* |
| Row 1 | 2.00 | 8.51 | 4.25 | 6.57 |
| Row 2 | 2.00 | 6.22 | 3.11 | 3.28 |
| Row 3 | 2.00 | 4.91 | 2.45 | 1.35 |
| Row 4 | 2.00 | 22.56 | 11.28 | 92.04 |
| Row 5 | 2.00 | 9.74 | 4.87 | 5.91 |
| Row 6 | 2.00 | 7.24 | 3.62 | 2.19 |
| Row 7 | 2.00 | 15.94 | 7.97 | 0.74 |
| Row 8 | 2.00 | 9.23 | 4.61 | 0.18 |
| Row 9 | 2.00 | 5.85 | 2.92 | 0.24 |
| | | | | |
| Column 1 | 9.00 | 51.97 | 5.77 | 26.46 |
| Column 2 | 9.00 | 38.21 | 4.25 | 2.60 |

| ANOVA | | | | | | |
|---|---|---|---|---|---|---|
| *Source of Variation* | *SS* | *df* | *MS* | *F* | *P-value* | *F crit* |
| Rows | 130.53 | 8.00 | 16.32 | 1.28 | 0.37 | 3.44 |
| Columns | 10.53 | 1.00 | 10.53 | 0.83 | 0.39 | 5.32 |
| Error | 101.96 | 8.00 | 12.75 | | | |
| | | | | | | |
| Total | 243.02 | 17.00 | | | | |
| | | | | | | |

Table 2.58 t-Test: Paired Two Sample for Means of chain radii and semicord the control vs. experimental.

P (T<=t) one-tail is less than 0.5.

| Sample | 866 | 872 | 869 | 866 | 872 | 869 | 866 | 872 | 869 |
|---|---|---|---|---|---|---|---|---|---|
| Radii | O | O | O | I | I | I | C | C | C |
| Cont | 2.44 | 18.06 | 8.58 | 1.83 | 6.59 | 4.91 | 1.63 | 4.66 | 3.27 |
| Exprt | 6.07 | 4.50 | 7.36 | 4.39 | 3.15 | 4.32 | 3.27 | 2.57 | 2.58 |

| t-Test: Paired Two Sample for Means | | |
|---|---|---|
| | *Variable 1* | *Variable2* |
| Mean | 5.77 | 4.25 |
| Variance | 26.46 | 2.60 |
| Observations | 9.00 | 9.00 |
| Pearson Correlation | 0.22 | |
| Hypothesized Mean Difference | 0.00 | |
| Df | 8.00 | |
| t Stat | 0.91 | |
| P (T<=t) one-tail | 0.19 | |
| t Critical one-tail | 1.86 | |
| P(T<=t) two-tail | 0.39 | |
| t Critical two-tail | 2.31 | |

Chart 2.26 Ratio I/O for chain fibres control vs. experimental

| Chain fibres | I/O | I/O | I/O |
|---|---|---|---|
| | C866. | C872. | C869. |
| Cont | 0.89 | 0.58 | 0.77 |
| Exprt | 0.82 | 0.74 | 0.95 |
| Standard Error | 0.10 | 0.13 | 0.12 |
| | 0.08 | 0.09 | 0.20 |

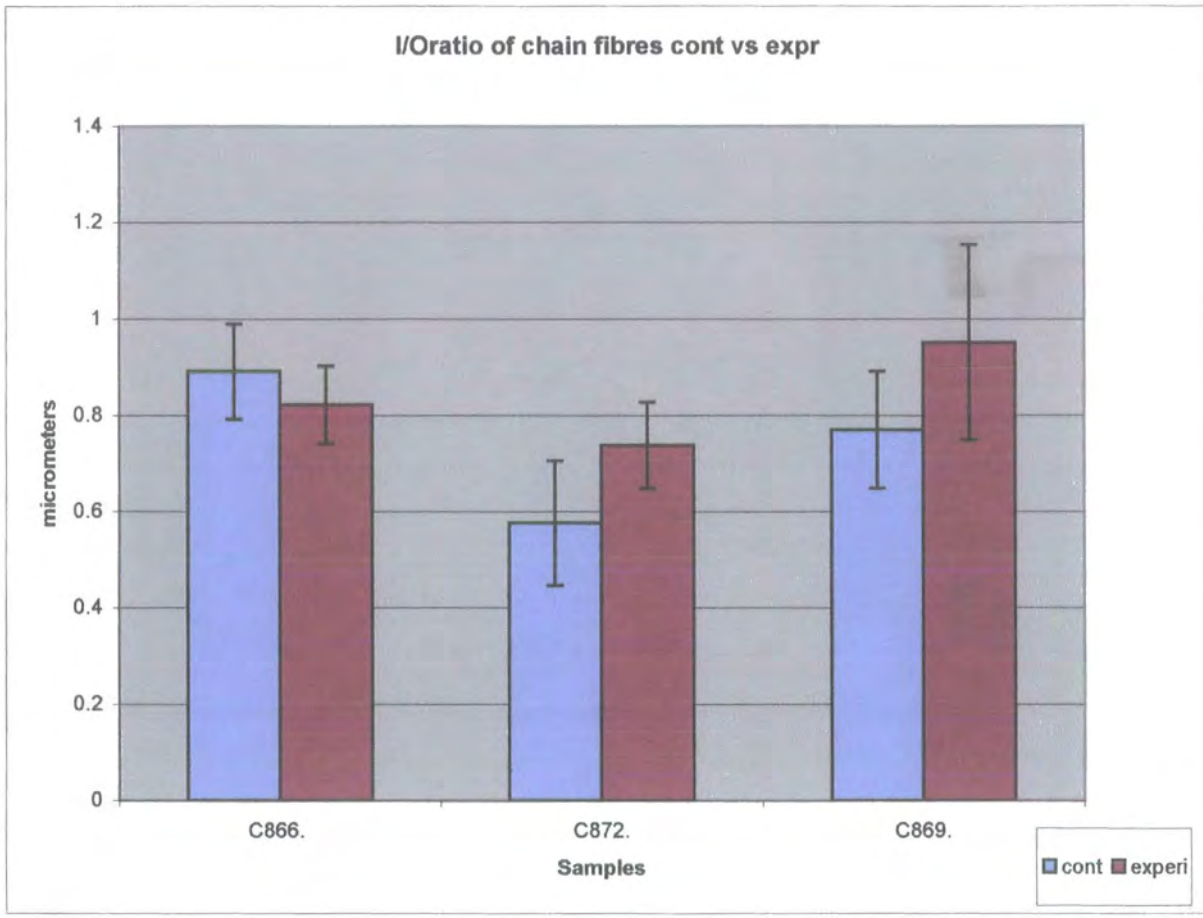

Chart 2.27 Ratio O/C for chain fibres control vs. experimental.

| Chain fibres | O/C C866. | O/C C872. | O/C C869. |
|---|---|---|---|
| Cont | 1.35 | 3.98 | 2.43 |
| Exprt | 1.82 | 1.74 | 2.84 |
| Standard Error | 0.20 | 1.47 | 0.49 |
| | 0.21 | 0.19 | 1.22 |

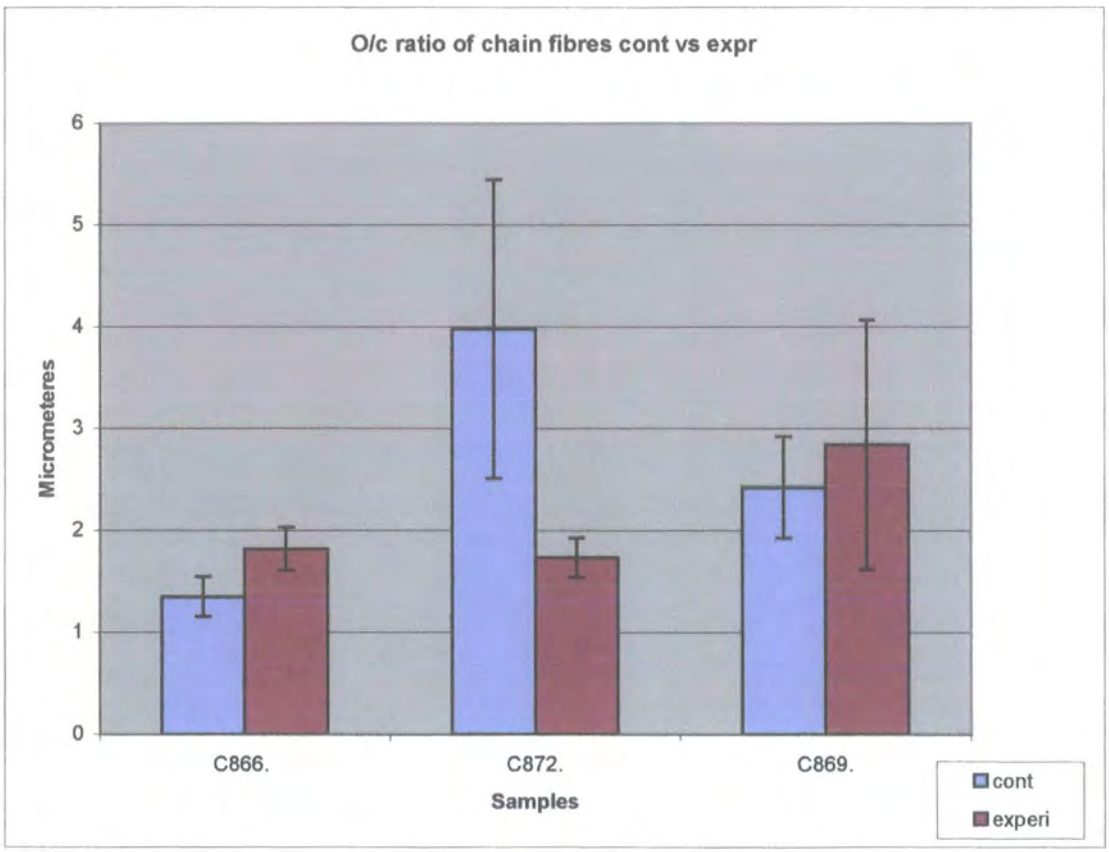

Chart 2.28 Ratio I/C for chain fibres control vs. experimental

| Chain fibres | I/C | I/C | I/C |
|---|---|---|---|
| | C866. | C872. | C869. |
| Cont | 1.13 | 1.37 | 1.47 |
| Exprt | 1.35 | 1.21 | 1.66 |
| Standard Error | 0.03 | 0.08 | 0.10 |
| | 0.05 | 0.06 | 0.13 |

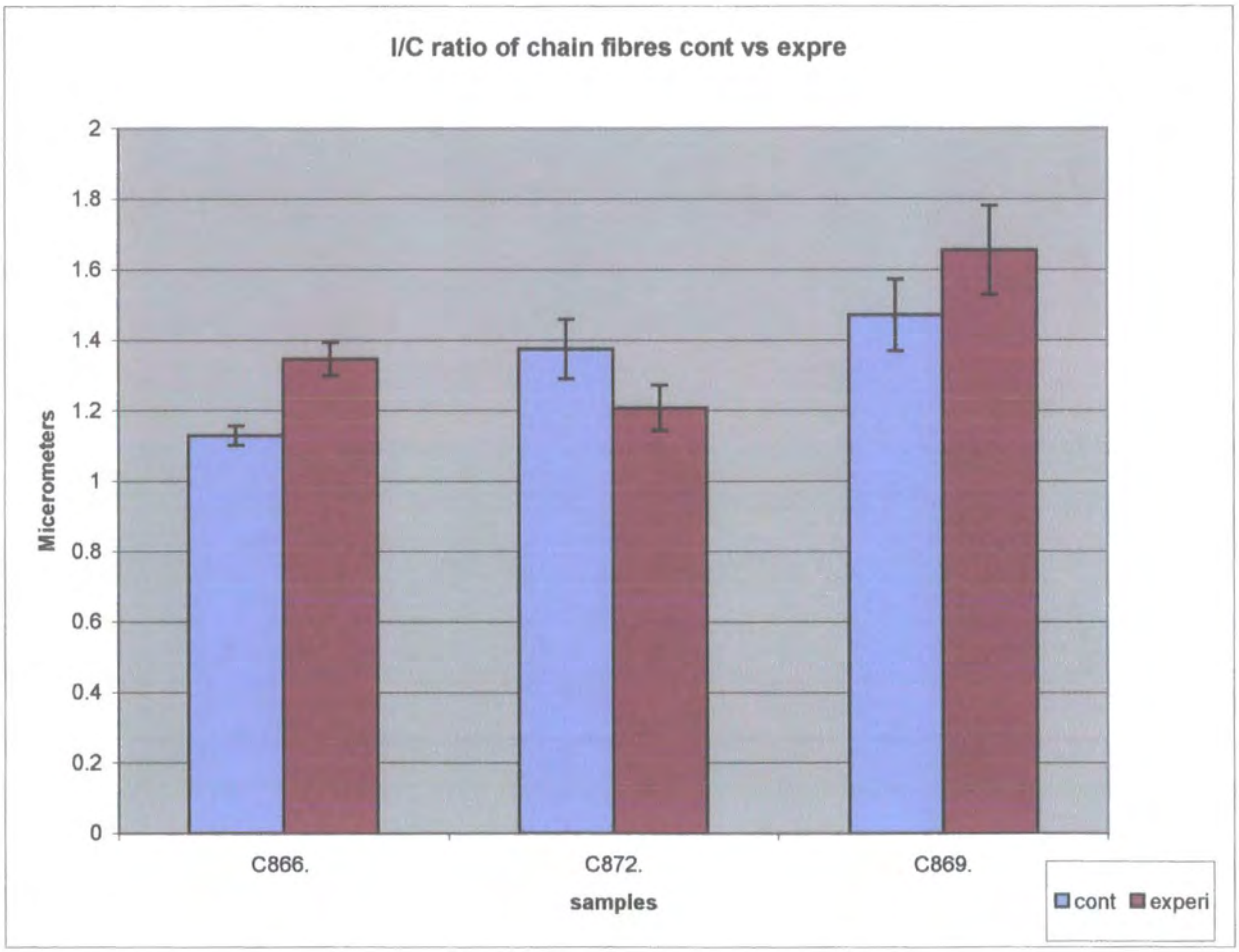

Table 2.59 ANOVA: Two-Factor without Replication for sample of mean ratios for chain fibres the control vs. experimental.

| ANOVA for chain fibres cont vs. exprt | | | |
|---|---|---|---|
| Sample | Ratio | cont | exprt |
| 866. | | | |
| | I/O | 0.89 | 0.82 |
| | O/C | 1.35 | 1.82 |
| | I/C | 1.13 | 1.35 |
| 872. | I/O | 0.58 | 0.74 |
| | O/C | 3.98 | 1.74 |
| | I/C | 1.37 | 1.21 |
| 869. | I/O | 0.77 | 0.95 |
| | O/C | 2.43 | 2.84 |
| | I/C | 1.47 | 1.66 |

| ANOVA: Two-Factor Without Replication | | | | |
|---|---|---|---|---|
| *SUMMARY* | *Count* | *Sum* | *Average* | *Variance* |
| Row 1 | 2.00 | 1.71 | 0.86 | 0.00 |
| Row 2 | 2.00 | 3.17 | 1.59 | 0.11 |
| Row 3 | 2.00 | 2.48 | 1.24 | 0.02 |
| Row 4 | 2.00 | 1.31 | 0.66 | 0.01 |
| Row 5 | 2.00 | 5.71 | 2.86 | 2.50 |
| Row 6 | 2.00 | 2.58 | 1.29 | 0.01 |
| Row 7 | 2.00 | 1.72 | 0.86 | 0.02 |
| Row 8 | 2.00 | 5.27 | 2.63 | 0.09 |
| Row 9 | 2.00 | 3.13 | 1.56 | 0.02 |
| | | | | |
| Column 1 | 9.00 | 13.97 | 1.55 | 1.11 |
| Column 2 | 9.00 | 13.12 | 1.46 | 0.43 |
| | | | | |

| ANOVA | | | | | | |
|---|---|---|---|---|---|---|
| *Source of Variation* | *SS* | *Df* | *MS* | *F* | *P-value* | *F crit* |
| Rows | 9.57 | 8.00 | 1.20 | 3.49 | 0.05 | 3.44 |
| Columns | 0.04 | 1.00 | 0.04 | 0.12 | 0.74 | 5.32 |
| Error | 2.75 | 8.00 | 0.34 | | | |
| | | | | | | |
| Total | 12.36 | 17.00 | | | | |

Table 2.60 t-Test: Paired Two Sample for Means of chain ratios the control vs. experimental.

| t-Test: Paired Two Sample for Means of chain ratios the control vs. experimental. | | | | | | | | | |
|---|---|---|---|---|---|---|---|---|---|
| Sample | 866 | 872 | 869 | 866 | 872 | 869 | 866 | 872 | 869 |
| Ratio | I/O | I/O | I/O | O/C | O/C | O/C | I/C | I/C | I/C |
| Cont | 0.89 | 0.58 | 0.77 | 1.35 | 3.98 | 2.43 | 1.13 | 1.37 | 1.47 |
| Exprt | 0.82 | 0.74 | 0.95 | 1.82 | 1.74 | 2.84 | 1.35 | 1.21 | 1.66 |

| t-Test: Paired Two Sample for Means | | |
|---|---|---|
| | *Variable 1* | *Variable 2* |
| Mean | 1.55 | 1.46 |
| Variance | 1.11 | 0.43 |
| Observations | 9.00 | 9.00 |
| Pearson Correlation | 0.62 | |
| Hypothesized Mean Difference | 0.00 | |
| Df | 8.00 | |
| t Stat | 0.34 | |
| P(T<=t) one-tail | 0.37 | |
| t Critical one-tail | 1.86 | |
| P(T<=t) two-tail | 0.74 | |
| t Critical two-tail | 2.31 | |

Table 2.61 Values of radii O, I, and semi-cord C for chain fibres control and experimental sampled together for ANOVA.

| | Radii | | |
|---|---|---|---|
| | O ($\mu$m) | I ($\mu$m) | C ($\mu$m) |
| C866.LHS.A.CH1 | 1.09 | 1.05 | 0.87 |
| | 1.06 | 0.90 | 0.84 |
| | 1.27 | 1.38 | 1.18 |
| | 2.33 | 2.40 | 2.24 |
| | 6.46 | 3.40 | 3.06 |
| C872.LHS.A.CH1 | 16.97 | 5.48 | 3.63 |
| | 6.25 | 3.57 | 2.65 |
| | 3.74 | 1.95 | 1.76 |
| | 19.97 | 14.52 | 9.43 |
| | 8.29 | 10.35 | 6.64 |
| C869.LHS.B.CH1 | 22.85 | 6.19 | 4.17 |
| | 16.08 | 5.93 | 3.77 |
| | 2.40 | 2.94 | 2.30 |
| | 2.94 | 2.39 | 2.21 |
| | 9.24 | 4.98 | 3.68 |
| C866.RHS.A.CH1 | 5.20 | 3.27 | 2.68 |
| | 13.07 | 3.93 | 3.53 |
| | 7.99 | 5.17 | 4.21 |
| | 7.52 | 5.38 | 3.63 |
| | 4.27 | 4.27 | 3.14 |
| C872.RHS.B.CH1 | 2.70 | 1.97 | 1.96 |
| | 3.65 | 3.01 | 2.45 |
| | 4.19 | 2.24 | 1.96 |
| | 7.65 | 3.49 | 3.04 |
| | 4.77 | 3.92 | 3.14 |
| C869.RHS.B.CH1 | 23.04 | 3.79 | 2.60 |
| | 5.20 | 6.67 | 3.09 |
| | 6.13 | 4.33 | 2.45 |
| | 4.06 | 3.14 | 2.55 |
| | 2.87 | 4.33 | 2.60 |

Table 2.62 ANOVA: Two-Factor with Replication of all the mean value of O, I, C for chain fibres. Column *P-value* is very low indicating a significant difference between control and experimental.

| SUMMARY | O ($\mu$m) | I ($\mu$m) | C ($\mu$m) | Total |
|---|---|---|---|---|
| *C866.LHS.A.CH1* | | | | |
| Count | 5.00 | 5.00 | 5.00 | 15.00 |
| Sum | 12.21 | 9.13 | 8.17 | 29.51 |
| Average | 2.44 | 1.83 | 1.63 | 1.97 |
| Variance | 5.31 | 1.12 | 0.95 | 2.24 |
| | | | | |
| *C872.LHS.A.CH1* | | | | |
| Count | 5.00 | 5.00 | 5.00 | 15.00 |
| Sum | 55.21 | 35.86 | 24.11 | 115.19 |
| Average | 11.04 | 7.17 | 4.82 | 7.68 |
| Variance | 49.70 | 26.82 | 10.01 | 31.77 |
| | | | | |
| *C869.LHS.B.CH1* | | | | |
| Count | 5.00 | 5.00 | 5.00 | 15.00 |
| Sum | 53.51 | 22.43 | 16.12 | 92.06 |
| Average | 10.70 | 4.49 | 3.22 | 6.14 |
| Variance | 76.92 | 3.00 | 0.82 | 34.52 |
| | | | | |
| *C866.RHS.A.CH1* | | | | |
| Count | 5.00 | 5.00 | 5.00 | 15.00 |
| Sum | 38.04 | 22.01 | 17.19 | 77.23 |
| Average | 7.61 | 4.40 | 3.44 | 5.15 |
| Variance | 11.73 | 0.77 | 0.33 | 7.07 |
| | | | | |
| *C872.RHS.B.CH1* | | | | |
| Count | 5.00 | 5.00 | 5.00 | 15.00 |
| Sum | 22.95 | 14.63 | 12.55 | 50.13 |
| Average | 4.59 | 2.93 | 2.51 | 3.34 |
| Variance | 3.50 | 0.68 | 0.32 | 2.15 |
| | | | | |
| *C869.RHS.B.CH1* | | | | |
| Count | 5.00 | 5.00 | 5.00 | 15.00 |
| Sum | 41.30 | 22.26 | 13.28 | 76.85 |
| Average | 8.26 | 4.45 | 2.66 | 5.12 |
| Variance | 69.74 | 1.77 | 0.06 | 26.30 |
| | | | | |
| *Total* | | | | |
| Count | 30.00 | 30.00 | 30.00 | |
| Sum | 223.23 | 126.32 | 91.42 | |
| Average | 7.44 | 4.21 | 3.05 | |
| Variance | 39.82 | 7.52 | 2.72 | |

| ANOVA | | | | | | |
|---|---|---|---|---|---|---|
| *Source of Variation* | *SS* | *df* | *MS* | *F* | *P-value* | *F crit* |
| Sample | 305.91 | 5.00 | 61.18 | 4.18 | 0.002172 | 2.34 |
| Columns | 310.91 | 2.00 | 155.45 | 10.62 | 9.11E-05 | 3.12 |
| Interaction | 91.46 | 10.00 | 9.15 | 0.62 | 0.788018 | 1.96 |
| Within | 1054.25 | 72.00 | 14.64 | | | |
| | | | | | | |
| Total | 1762.53 | 89.00 | | | | |

Table 2.63 Ratio values sampled for ANOVA: Two-Factor with Replication of all ratios for chain fibres.

| Sample | ANOVA: Two-Factor With Replication of the ratio | | |
|---|---|---|---|
| | I/O | O/C | I/C |
| C866.LHS.A.CH1 | 0.96 | 1.26 | 1.21 |
| | 0.85 | 1.27 | 1.08 |
| | 1.08 | 1.08 | 1.17 |
| | 1.03 | 1.04 | 1.07 |
| | 0.53 | 2.11 | 1.11 |
| C872.LHS.A.CH1 | 0.32 | 4.68 | 1.51 |
| | 0.57 | 2.36 | 1.35 |
| | 0.52 | 2.12 | 1.11 |
| | 0.73 | 2.12 | 1.54 |
| | 1.25 | 1.25 | 1.56 |
| C869.LHS.B.CH1 | 0.27 | 5.49 | 1.49 |
| | 0.37 | 4.26 | 1.57 |
| | 1.22 | 1.04 | 1.28 |
| | 0.81 | 1.33 | 1.08 |
| | 0.54 | 2.51 | 1.35 |
| E866.RHS.A.CH1 | 0.63 | 1.94 | 1.22 |
| | 0.30 | 3.70 | 1.11 |
| | 0.65 | 1.90 | 1.23 |
| | 0.72 | 2.07 | 1.48 |
| | 1.00 | 1.36 | 1.36 |
| E872.RHS.B.CH1 | 0.73 | 1.38 | 1.00 |
| | 0.82 | 1.49 | 1.23 |
| | 0.54 | 2.14 | 1.14 |
| | 0.46 | 2.52 | 1.15 |
| | 0.82 | 1.52 | 1.25 |
| E869.RHS.B.CH1 | 0.16 | 8.87 | 1.46 |
| | 1.28 | 1.68 | 2.16 |
| | 0.71 | 2.50 | 1.77 |
| | 0.77 | 1.59 | 1.23 |
| | 1.51 | 1.11 | 1.67 |

Table 2.64 ANOVA: Two-Factor with Replication of all the chain mean of radii ratio. Column *P-value* is very low indicating a significant difference between control and experimental.

| SUMMARY | I/O | O/C | I/C | Total |
|---|---|---|---|---|
| *C866.LHS.A.CH1* | | | | |
| Count | 5.00 | 5.00 | 5.00 | 15.00 |
| Sum | 4.45 | 6.76 | 5.65 | 16.86 |
| Average | 0.89 | 1.35 | 1.13 | 1.12 |
| Variance | 0.05 | 0.19 | 0.00 | 0.11 |
| | | | | |
| *C872.LHS.A.CH1* | | | | |
| Count | 5.00 | 5.00 | 5.00 | 15.00 |
| Sum | 3.39 | 12.52 | 7.06 | 22.98 |
| Average | 0.68 | 2.50 | 1.41 | 1.53 |
| Variance | 0.12 | 1.66 | 0.04 | 1.12 |
| | | | | |
| *C869.LHS.B.CH1* | | | | |
| Count | 5.00 | 5.00 | 5.00 | 15.00 |
| Sum | 3.21 | 14.64 | 6.77 | 24.62 |
| Average | 0.64 | 2.93 | 1.35 | 1.64 |
| Variance | 0.15 | 3.64 | 0.04 | 2.07 |
| | | | | |
| *C866.RHS.A.CH1* | | | | |
| Count | 5.00 | 5.00 | 5.00 | 15.00 |
| Sum | 3.29 | 10.97 | 6.40 | 20.66 |
| Average | 0.66 | 2.19 | 1.28 | 1.38 |
| Variance | 0.06 | 0.79 | 0.02 | 0.67 |
| | | | | |
| *C872.RHS.B.CH1* | | | | |
| Count | 5.00 | 5.00 | 5.00 | 15.00 |
| Sum | 3.37 | 9.04 | 5.77 | 18.18 |
| Average | 0.67 | 1.81 | 1.15 | 1.21 |
| Variance | 0.03 | 0.24 | 0.01 | 0.31 |
| | | | | |
| *C869.RHS.B.CH1* | | | | |
| Count | 5.00 | 5.00 | 5.00 | 15.00 |
| Sum | 4.43 | 15.75 | 8.29 | 28.47 |
| Average | 0.89 | 3.15 | 1.66 | 1.90 |
| Variance | 0.28 | 10.47 | 0.12 | 4.05 |
| | | | | |
| *Total* | | | | |
| Count | 30.00 | 30.00 | 30.00 | |
| Sum | 22.15 | 69.69 | 39.94 | |
| Average | 0.74 | 2.32 | 1.33 | |
| Variance | 0.11 | 2.74 | 0.06 | |

| ANOVA | | | | | | |
|---|---|---|---|---|---|---|
| *Source of Variation* | *SS* | *do* | *MS* | *F* | *P-value* | *F crypt* |
| Sample | 6.17 | 5.00 | 1.23 | 1.24 | 0.30 | 2.34 |
| Columns | 38.46 | 2.00 | 19.23 | 19.33 | 0.00 | 3.12 |
| Interaction | 6.65 | 10.00 | 0.67 | 0.67 | 0.75 | 1.96 |
| Within | 71.63 | 72.00 | 0.99 | | | |
| | | | | | | |
| Total | 122.90 | 89.00 | | | | |

### 2.5.19 Analysis of the micrographs of control and experimental samples

The visual assessments of some micrographs of the control and the experimental samples are given in the next section, Starting with those from animal 866, followed by those from animals 872 and 869, control versus the experimental in their order. The intrafusal muscle fibres of the control side (LHS) of the animals appear to be slim, elongated and with a straighter, more streamlined fibre outline than the experimental counterparts; furthermore, the distance separating nerve endings in some of the control fibres seemed to be greater than those in the experimental samples. See fig 2.9 for the control C866.LHS.C.B1 and compare it with Fig 2.10 for the experimental sample E866.RHS.C.B1.

Fig. 2.9; Control C866.LHS.C.B1. Note: the lenticular less, indented nerve endings (arrowheads), the thin stretched fibre; smooth outline of the fibre (double-head arrows); and rearranged equatorial nuclei without visible internuclear spaces (The nerve endings seem to be big as is the case in most $bag_1$ fibres). Compare this image with the image of the experimental sample from the opposite site Fig 2.10.

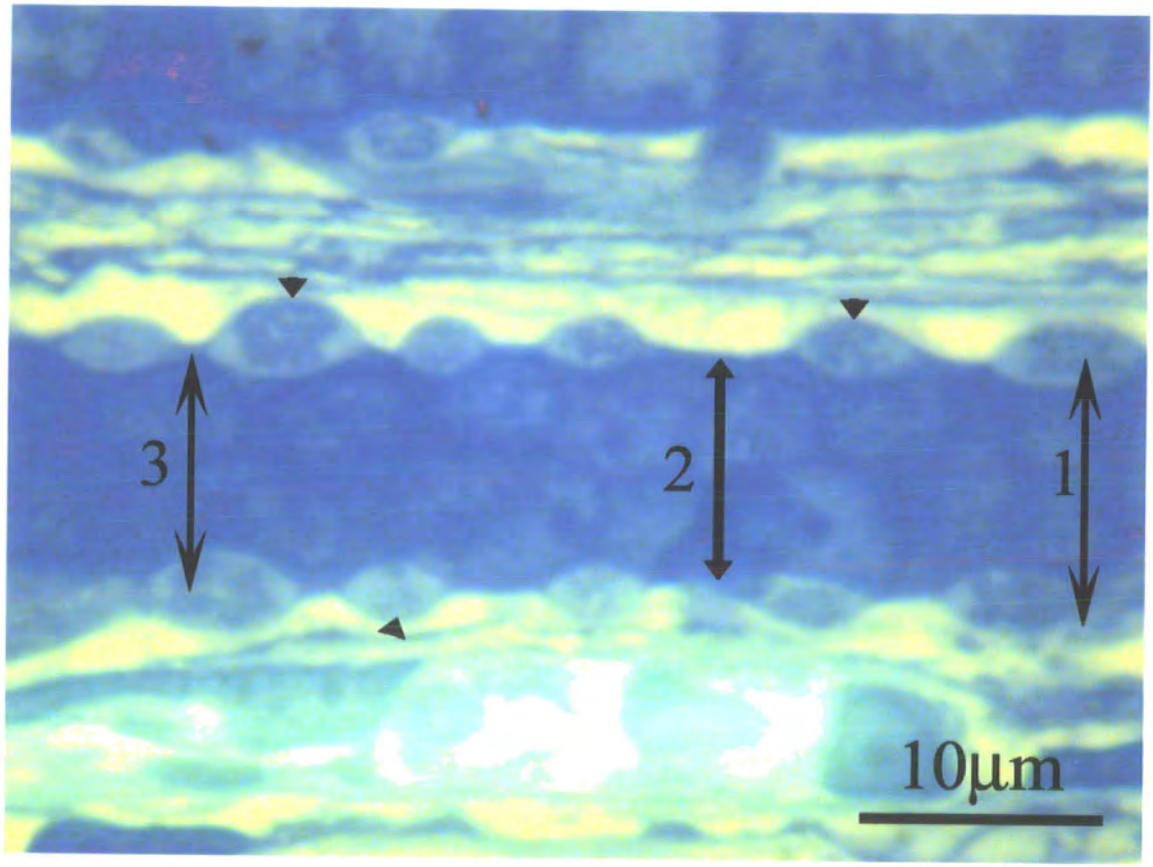


Fig 2.9

Fig.2.10 Experimental E866.RHS.C.B1.Compared to Fig 2.9, on the opposite side of the animal the experimental sample show a thicker fibre without a smooth outline (double-head arrows), prominent but deeply indented nerve endings (arrow heads) and no rearrangement of equatorial nuclei. The single arrows indicates an uneven fibre surface in compare to that of fig 2.9.

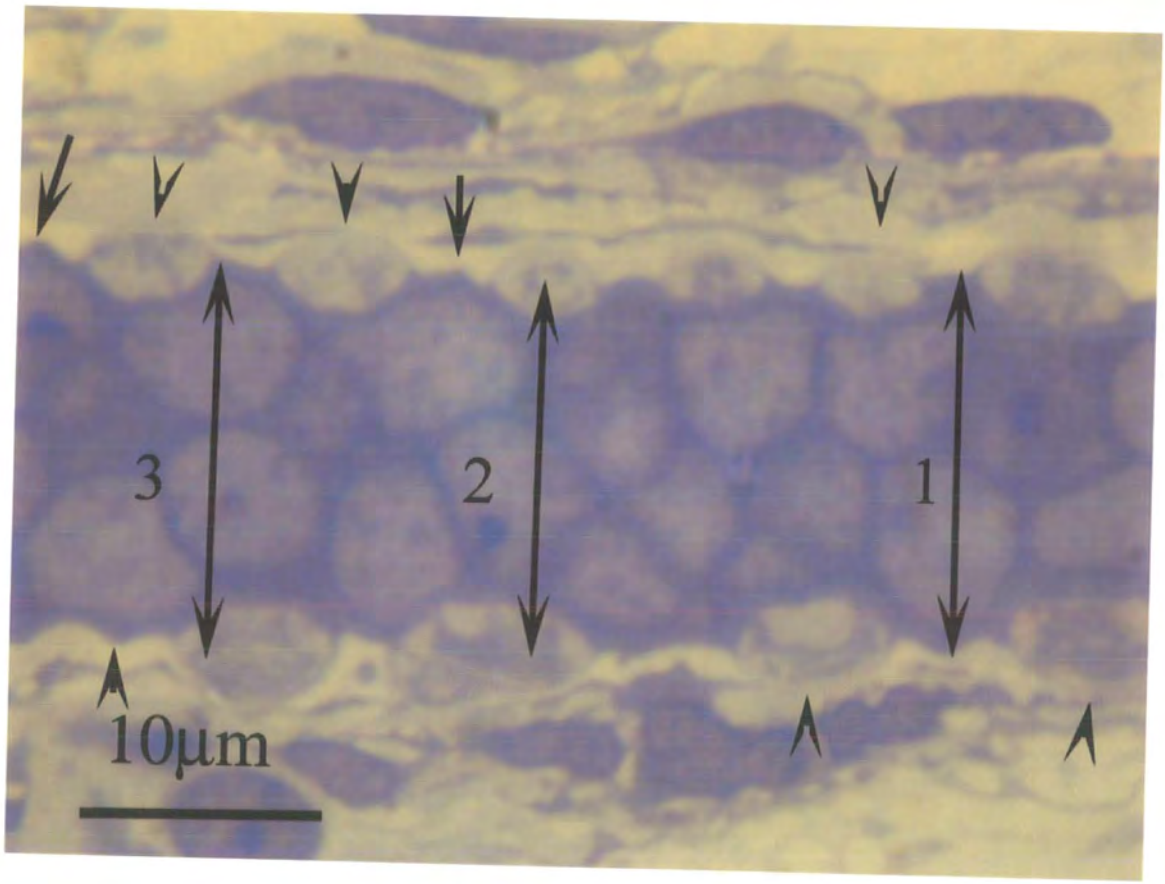


Fig 2.10

Fig 2.11 Control C 872.LHS.A.B1; Here again the fibre is thin with fine outline and the nerve endings are elliptical in appearance and less indented; the equatorial nuclear rearranged into two lines in nearly longitudinal orientation: all these in comparison with the next figure 2.12. Of the experimental E872.RHS.A.B1.

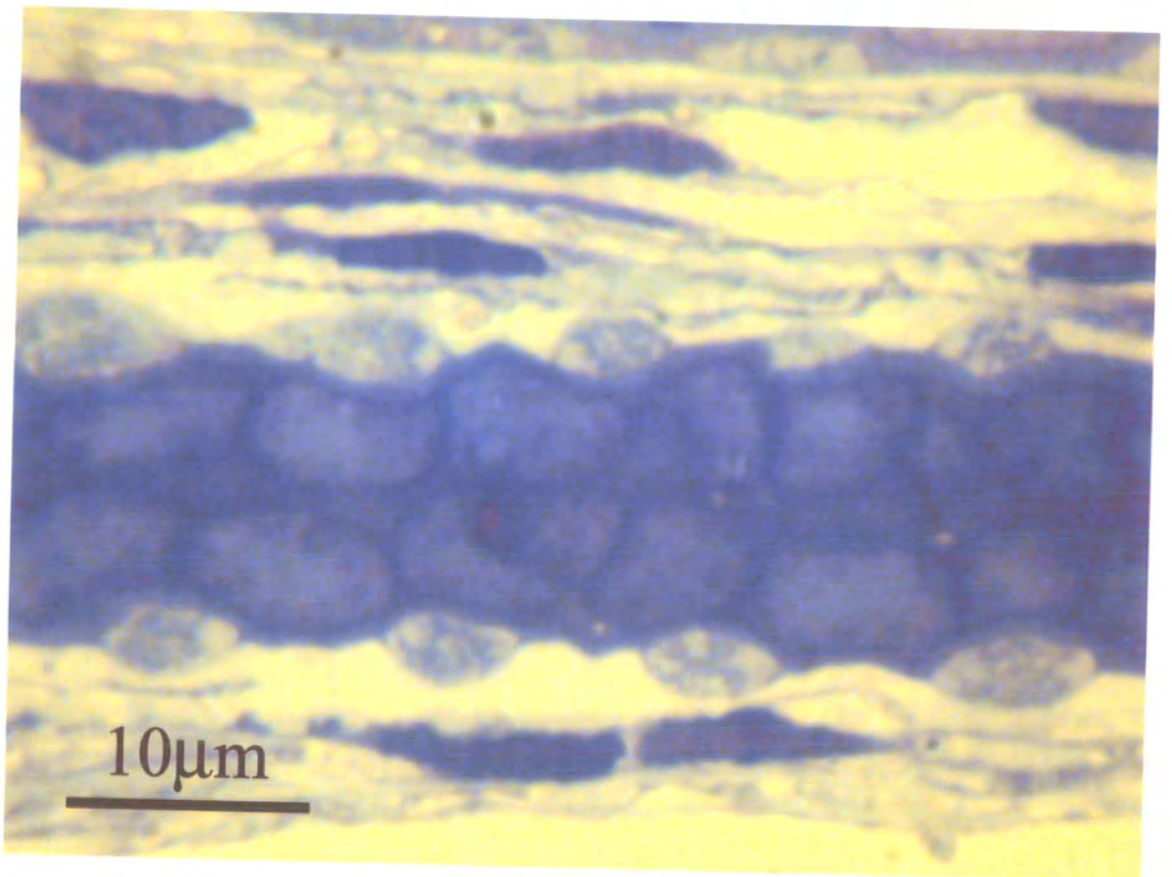


Fig.2.11

Fig. 2.12 Experimental E872.RHS.A.B1. The opposite site to that shown in Figure 2.11 shows contrasting features: The thicker fibre (long double-head arrow); and the deeply indented nerve endings, which are less elliptical (arrow heads). There is also no obvious rearrangement of the equatorial nuclei, which seem to be less compressed.

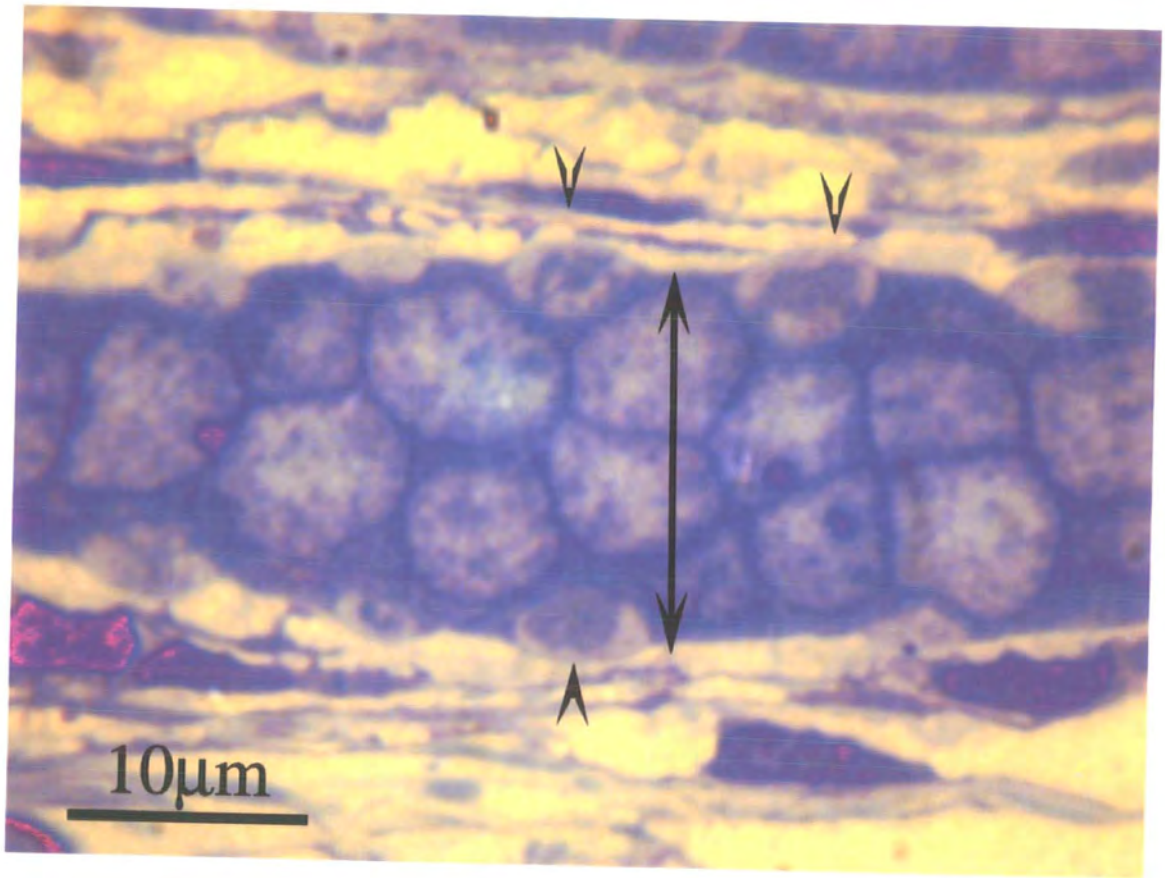


Fig.2.12

Fig.2.13 Control C.869.LHS.A.B1. This is a good example of stretched and thinner fibre with smooth outline (small arrow) and typical feature of $bag_1$ with prominent and less-indented nerve endings (arrow heads) this indicates the amount of extension in the control compared with flexion in the experimental. The stretched fibre and equatorial nuclei rearrangement may have reduced the nerve endings indentation. In this control LHS $bag_1$ fibre the equatorial nuclear are two lines compare this with figure 2.14 from the corresponding experimental side where equatorial nuclei form three horizontal lines.

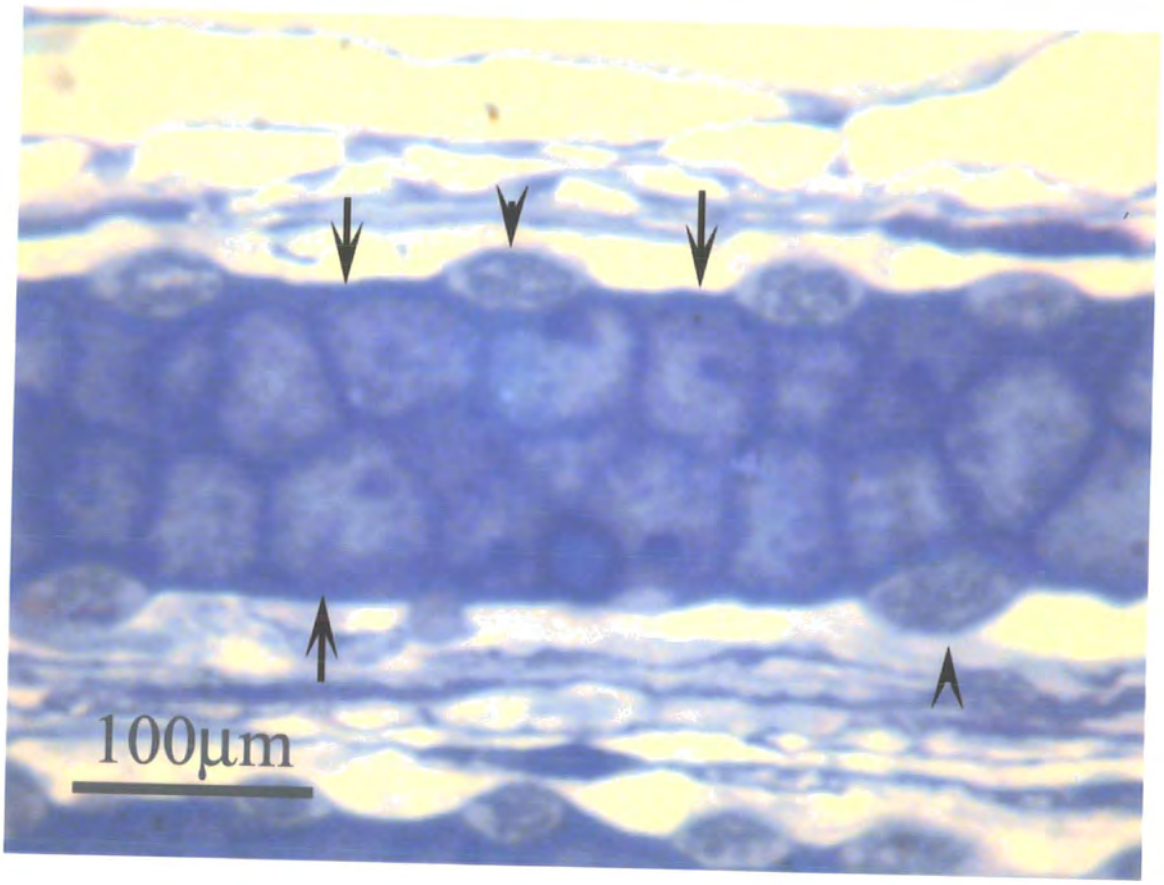


Fig.2.13

Fig. 2.14 Experimental sample E869.RHS.A.B1. This shows typical features of a flexed experimental fibre: the nerve endings seem to be prominent features of $bag_1$ some are relatively more indented than those in Fig 2.13 and the equatorial nuclei form three horizontal lines (double head arrow); in all the figures of the experimental the equatorial nuclei seem not to show sign of compression or longitudinal orientation as in figures 2.11 and 2.13.

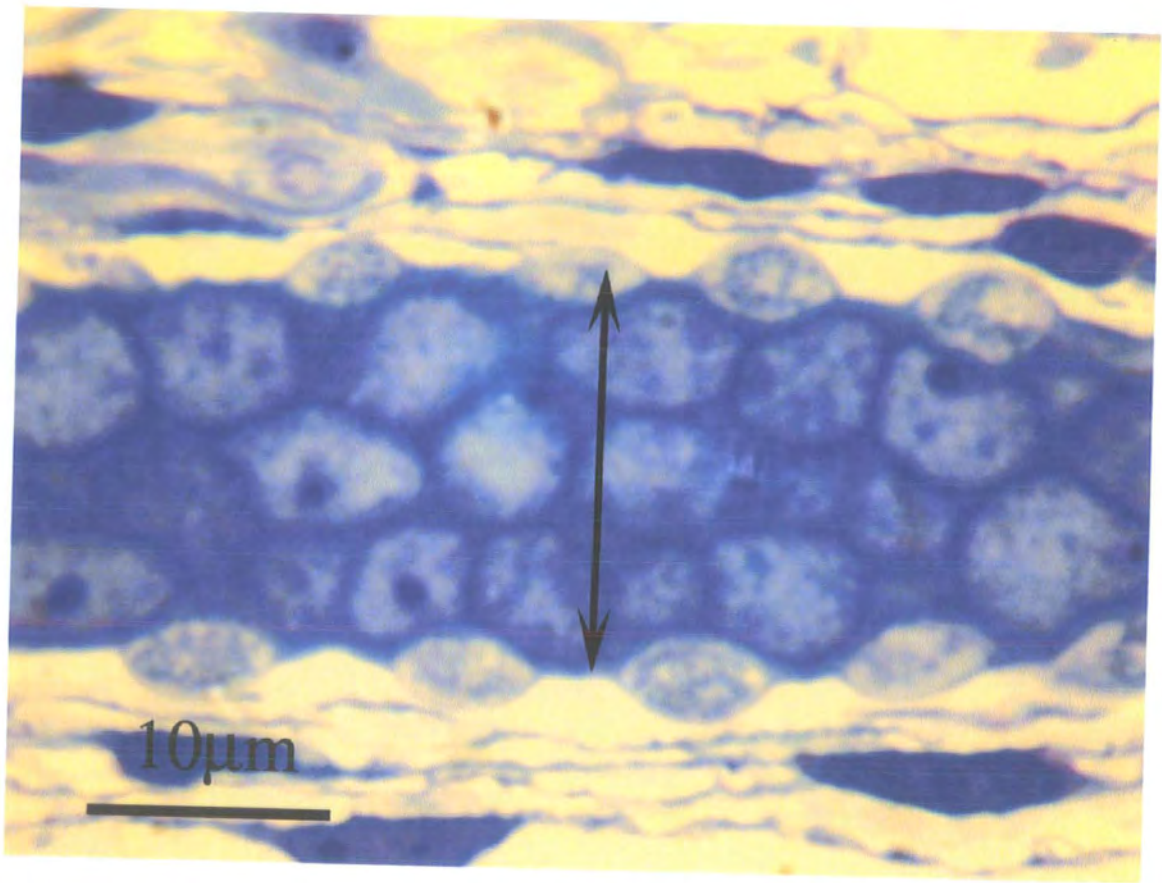


Fig.2.14

## 2.5.20. Some observations on the control samples

To sum up, the visual assessment of LHS samples shows the following:

1. The intrafusal muscle fibres of the control (LHS) of the animals seem to be thinner in appearance, and the distance separating nerve endings in some of these fibres seems to be greater than in the RHS (experimental) sample.

2. $Bag_1$ fibres are thinner than $bag_2$ but both seem to be thinner than those in the experimental RHS samples.

3. The fibres in LHS samples appear more elongated, straighter, and with a more streamlined appearance of the fibres outline surface (less undulating) than those in the RHS samples.

4. The nerve endings seem to be more elliptical.

5. The nerve endings on $bag_1$ fibres are more prominent and less indented.

6. The nerve endings on $bag_2$ fibres, though big sometimes are less prominent and more indented into the fibre.

7. The equatorial nuclei are squashed and may take on a horizontal orientation with little or no visible space between them.

8. In most cases the LHS samples show clear sarcomeres.

It seems, in the control (LHS) side, that the intrafusal fibre outline is stretched; this naturally would affect the nerve endings basal lamina, which is continuous with that of the muscle fibre, and the plasmalemma of the muscle fibre, which in turn may cause the radii of curvature of the outer and inner surfaces of the lenticular profiles to increase. Furthermore, it seems in the control group that the stretch might pull the nerve endings into the muscle fibre, presumably increasing the imbedded part of nerve ending; however, this might not be the case when considering the pressure from within the

nerve terminals, the adjacent equatorial nuclei and the fibre itself which keep the inner radius greater than the outer one.

### 2.5.21 Some observations on the experimental sample

1. In the experimental samples, $bag_1$ fibres are thinner than $bag_2$ fibres but both appear to be thicker than those of the corresponding control LHS samples.

2. The fibres do not have streamlined outlines but undulate between the nerve endings.

3. $Bag_1$ nerve endings are more prominent than those of $bag_2$ fibres and also less indented.

4. $Bag_2$ nerve endings are occasionally large but less prominent and more deeply embedded in the fibres.

5. Nerve endings of both $bag_1$ and $bag_2$ fibres from experimental samples appear to be more deeply embedded in the fibre than do those from the control (left) samples: they also display deformed boundaries.

6. The equatorial nuclei do not exhibit any rearrangement and appear not to be in squashed state and with some spaces between them.

7. Experimental samples display less distinct sarcomeres than the control samples in at least three samples of internal sarcomeres and another three samples of external sarcomeres.

## 2.5.22 Analysis of experimental side

On the experimental side, the intrafusal muscle fibre is thicker than on the control side and the nerve endings show some irregularity or a less circular and less lenticular circumference, especially in the embedded half of the nerve endings compared with those in the LHS sample. This may be due to different morphological changes of the boundaries of the nerve endings in the experimental RHS where some nerve endings appear to be quite deeply embedded in the muscle fibres in comparison with those changes in the stretched sensory terminals the control LHS.

In the flexed samples, the equatorial nuclei of the intrafusal fibres cluster together and their outline looks more deformed as seen for example in Fig 2.14 flexed sample (E869.RHS.A.B1), in comparison with stretched samples as in Fig 2.13 (C869.LHS.A.B1) and fig 2.11 (C872.LHS.A.B1).

## 2.6 Discussion.

Previous studies of the morphometric changes of the muscle spindle had shown a pattern of consistent deformation of various parts of the spindle. In a study of the quantitative changes in the frog muscle spindle with passive stretch using the toe extensor muscle (musculus extensor digitorum longus IV) of the frog (*Rana pipiens*), Karlsson *et al.,* (1970) had observed ultrastructural changes due to stretch in the followings: sarcomeres, muscle nuclei, reticulomeres, extracellular material, leptomeres and internal capsule, and also in sensory nerve terminals. Karlsson's team also found that the sensory nerve endings of the frog (which are longitudinally linked along the sensory region had changed from a relatively round profile in the slackened, physiologically relaxed position groups to an elongated or elliptoid form in the physiologically stretched specimen (Karlsson *et al.,* 1970). In a second study on the same muscle Hooker *et al,* (1976) examined the sensory nerve terminals which, in frog, are apposed to the tops of the reticulomeres, and found them to change from a relatively round profile in the slackened muscle to an elongated form in the physiologically stretched muscles. In a study of the primary sensory endings three muscle spindles, of the tenuissimus muscle of the cat, Banks (1986) observed that, with increased static stretch there was an increase in the mean sarcomere lengths on each side of the primary ending of the intrafusal muscle fibres, combined with progressively less indentation of the terminals into the intrafusal fibres. Karlsson *et al,* (1970) found that the equatorial nuclei of the frog muscle spindle were closely apposed to each other in the slackened and physiologically relaxed fibres, whereas in the physiologically stretched groups they appeared to form a single chain. This also can be observed in the cat tenuissimus muscle see figure 2.1 Banks (1986). Although Karlsson *et al,* (1970) first drew attention to the

morphological changes in the frog muscle spindle, at least in the frog but the study of the quantitative changes occurring in the nerve bulb chains and their topography at various degrees of stretch have not been determined. And apart from the initial observation by Banks (1986), to detect the quantitative changes occurring in the terminal nerve endings of the mammalian muscle spindle, these changes have not systematically been studied in relation to intrafusal muscle fibre length or contractile activity, in a reasonable sample size.

In this study my experimental was aim to detect such changes in the muscle spindle by measuring the sarcomere changes in the extrafusal fibres adjacent to them and by also detecting changes in the intrafusal fibres by measuring their diameter, sarcomere length, and most importantly measuring the changes in the nerve endings. Changes of the nerve- endings were detected by measuring the radii of the outer and inner circle sectors of the nerve ending profile in longitudinal sections. (See Fig.2.4). If the intrafusal muscle fibres are inspected at their widest diameter, the outer half radius of the nerve ending can be represented by the letter O, and the inner half by the letter I; half the line joining them has been represented by C. It is assumed that if O = I = C, the terminals would appear circular in cross-section with two half circles with one-half being embedded in the intrafusal muscle fibres see figure 2.4.

When I = O and both exceed the semicord C, the nerve endings would be lenticular or elliptoid, although the endings would be nearly equal halves and the inner one would be half embedded. If O > I the terminals are deeply embedded in the muscle fibres; the inner portion would be greater than the outer one, and this is the case from most chain fibres and some $bag_2$ fibres. When I > O and both exceed C, the nerve endings would be prominent and protrude outwards; they would be less embedded in the intrafusal muscle fibres, most noticeably in $bag_1$ fibres and some $bag_2$ fibres see Fig 4.2.

These parameters of O, I, C were measured, as were the diameters of fibres at three locations and the sarcomeres lengths. The ratios O/C, I/C and I/O were calculated, a paired t-test was applied to all mean data for $bag_1$ and $bag_2$ fibres of the experimental versus the control samples, as seen in the details of tables and charts.

The experiment did produce detectable differences between control and the experimental in the muscle spindle intrafusal fibres which were expressed by morphometric changes in the fibre diameter, sacomere length and nerve endings, and which could be attributed to differences in static tension. According to the experiment layout the tension difference was suppose to be at its greatest in sample 866 followed by intermediate 872 and the least tension difference would be in sample 869. The results for extrafusal sarcomere length in section (2.5.1) and table 2.4 and chart 2.3, and also the result for the fibre diameter for $bag_1$ and $bag_2$ as seen in section 2.5.8 table 2.5 and chart 2.4 for $bag_1$ and table 2.10 and chart 2.5 for bag2 comply with the expected assumption of tension difference between the control and experimental in the three sample sets. However results of the nerve endings based on the tables of the mean value of O, I, C, for $bag_1$ on table 2.15 charts 2.6 to 2.8 results show sample 872 standing out as the one with the greatest amount of tension difference rather than 866. Nevertheless sample 869 does show the least amount of tension difference; as estimated from these results.

$Bag_2$ as seen in table 2.20 and in charts 2.9-2.11 shows nearly identical features of tension difference as $bag_1$. The calculated mean of ratios I/O, I/C and O/C for all the three samples were done for a further investigation and results for $bag_1$ fibres as seen on tables 2.25-2.27 and on charts 2.12-2.14 were very similar to those seen for the absolute values O, I, C. For $bag_2$ the result ratios I/O, I/C, and O/C as seen in table 2.28-2.30 and charts 2.15-2.17 were almost identical to those of absolute values of O, I, C for $bag_2$, where in all the cases sample 872 stands out as the one with the greatest apparent

tension difference followed by 866 then 869. The similarity of the ratio analysis to the analysis of absolute values indicates the consistency of the results, which were drawn from several muscle spindles in both control and experimental side in each animal.

Diagrammatic representation of the mean nerve-terminal profiles in all the samples of $bag_1$ and $bag_2$ were drawn, and when comparisons of control and experimental sides were carried out based on these diagrams the tension difference was obvious and visually noticeable. In the control side the nerve endings were more lenticular in profile and less indented into the fibre in all sample especially on sample 872 in comparison with the more rounded and more embedded into the intrafusal fibres in the experimental side; see figures 2.5-2.8.

The photo micrographic analysis of figures 2.9-2.14 also shows the tension difference between control and experimental as reflected by the difference in diameter (fibre diameter) and the equatorial nuclei regrouping and also as seen in many nerve endings.

The regional variations were analysed based on the numerical data of the mean values of O, I, C, of spindles from the proximo-distal sequence of regions A, B, and C in samples 866, 872, 869 were compared. "ANOVA" for all are shown in tables 2.48-2.59 and summarised in table 2.6 where all the sample P- values of ANOVA indicate a lack of significant regional variations. As mentioned before in the initial visual analysis the most prominent nerve endings were classified as those of $bag_1$ fibres, but I also used the criteria of crowdedness as a measure (how crowed the nerve endings are as an ndication for $bag_1$) but since I have the control which is extended some $bag_1$ seem to be less crowded though still prominent, in the other hand in the flexed experimental side the nerve endings seem to be crowded in both $bag_1$ and $bag_2$ so the nerve endings prominence was favoured as a criterion for the classification of $bag_1$ and $bag_2$. As in section 2.5.15 and table 2.31 the initial analysis of $bag_1$ and $bag_2$ based on the mean

values of O, I, C indicated that bag2 nerve endings have a greater mean values compared with those of the corresponding $bag_1$. But an additional analysis using the ratios I/O, I/C, and O/C, as seen in tables 2.25-2.27 and charts 2.12-2.14 for $bag_1$ and in tables 2.28-2.30 and charts 2.15-2.17 for $bag_2$ also analysis of all the ratios as seen in tables 2.32 –2.47 and their charts 2.18-2.21, indicated that the most prominent nerve endings are on $bag_1$. $Bag_1$ and $bag_2$ classification could have involved many features, including the pattern of motor innervations, and the pattern of elastic fibres around the bag fibre, but these features were beyond the scope of this study which was limited to the equatorial region. With regards to tension differences between control and experimental in chain fibres, their diameters showed no significant differences as seen in tables 2.49-2.53 and charts 2.22. But the analysis based on the chain nerve- endings profiles (O, I, C) indicated that the tension differences in these fibres are similar if not identical to those in $bag_1$ and $bag_2$, fibres at least in two samples 872 and 869 where again 872 stand out as the one with the greatest tension difference (see tables 2.57-2.58 and charts 2.23-2.25). In these charts experimental sample 866 showed a reverse of tension difference compared to the other samples. However the negligible difference in chain diameters, which might not reflect a real difference of chain tensions as much as the difficulty of tackling chain fibres for measurement and collecting their numerical data. A further analysis of ratios I/O, I, C, O/C gave a mixed outcome, but at least in two charts (2.27-28) sample 872 fell into its familiar outcome as the one with the greatest amount of tension difference. Changes of tension and its difference between control and experimental had taken place in the chain fibres as expected; however these changes were more difficult to detect in chains, owing to some basic differences between the bag and chain fibres. For example:

(a) Chain fibres are smaller and less regular in shape than bag fibres

(b) Chain fibres tend to bend or to be kinked more often

(c) The nerve endings on the chain fibres are deeply indented and are more variable in shape.

## 2.7 Conclusion

Morphometric consequences of the tension difference between the control and experimental muscles have been detected in all samples 866, 872 and 869.They were expressed in all muscle spindles by the difference of the followings; the adjacent extrafusal sarcomeres to the intrafusal fibre (see section 2.5.1 and chart 2.3), the intrafusal fibre diameter (section 2.5.8 and chart 2.4-2.5), in which the tension complies with the layout of the experiments seen in table 2.1 and figures 2.2 and 2.3 where the biggest tension difference between control and experimental is in sample 866, and an intermediate tension difference in sample 872, while the least is in sample 869. Tension difference was also expressed in the difference of the intrafusal sarcomere lengths between the control and the experimental as explained in section 2.5.1 and charts 2.1-2.2. Additionally in the nerve endings morphometric differences have been detected by the nerve-endings profiles ( O, I, C ) as explained in section 2.5.10 and the calculated ratios I/O, I/C, and O/C seen in section 2.5.14 though in the last two (intrafusal sarcomeres and the nerve endings) the tension difference seems to stand out in sample 872 as the greatest instead of falling in the assumed patterns of the experiment set and the outcome results of the extrafusal sarcomeres and fibre diameter of all samples. This feature of sample 872 might be attributed to the delayed fixation of the lower part of the animal, specially its extremities this might have given enough time for cross bridge reformation and so led to the big tension difference in sample 872. In the chain fibres the tension difference was not detected by the measurements of their fibre diameter but by measuring their nerve endings radii they seem to express similar features to that of $bag_1$ and $bag_2$ intrafusal fibres.The regional comparison of region A, B, C at their equatorial parts in each samples showed no regional variations. Analysis of the means values of O, I, C show that the nerve endings of the intrafusal $bag_1$ fibres have a more prominent nerve terminals compared with $bag_2$, a result which complies with previous

findings by Banks (1977). Tension differences were expressed by morphological changes to the followings: extrafusal sarcomeres, fibre diameters, intrafusal sarcomeres, nerve endings, and by the equatorial nuclei. All these morphological changes except for the equatorial nuclei were measured numerically and recorded for analysis. Though the fixation of the hind limbs of animal 872 was inadequate most of the sample had given many results which show the difference in tension between the control (stretched) and the experimental (flexed) and they seem most of the time to comply with experiment lay out in reflecting the tension difference. Any future similar study might draw some guidelines from this study and for a further improvements and accuracy many other factors may have to be considered such as the followings.

1. Animal weight animal weight must be as close to each other to exclude any large variation may be introduced by animal size difference.

2. Age animal ages should be as close for the same above reason.

3. Fixation quick and fast fixation in order to capture changes induced by passive stretch before any further changes or adaptation.

4. Time can be recorded and standardised treatment for each sample to avoid any undesirable effect and to take notice of it if it happened.

5. Fibre activation might be considered in order to remove any slackness in the fibre polar region.

# CHAPTER THREE

## The Distribution of Calretinin in Rat Muscle Spindles

## 3.1 Introduction

Calcium ions $Ca^{2+}$ are important signalling factors that are involved in a variety of cellular functions: they mediate transmission of nerve impulses and muscle contraction; they are essential catalysts in activating clotting factors; they strengthen capillary membranes and take part in many other fundamental physiological processes. In the nervous system they act in (second messenger) role to control functions such as transduction, neurotransmission, rapid adaptation and regulation of intracellular energy metabolism. However calcium ions do not act alone; the cells usually contain proteins named calcium-binding proteins (CaBPs) and the central role of calcium is indicated by the presence of CaBPs in the spindle. Those detected in mammalian spindles are calbindin (Hietanen-Peltola *et al.*, 1992; Duc *et al.*, 1994), calretinin (Duc, Barakat-Walter and Droz, 1994; El-tarhouni and Banks, 1995) and neurocalcin (Iino, 1998); recently frequenin, has been detected in the frog spindle (Werle *et al.*, 2000)

## 3.2 Calcium-binding proteins

### 3.2.1 Definition and localization

CaBPs are a group of homologous proteins that contain a characteristic structure, in the form of pouches for the acceptance of $Ca^{2+}$. This structure, which been termed an EF-hand, is an amino acid sequence with a characteristic three-dimensional structure. The EF-hand that is the high affinity calcium-binding site, and was first described for parvalbumin (Moews and Kretzinger, 1975).

The EF-hand superfamily can be subdivided into two families of proteins with either six EF-hands (calbindin D-28k, calretinin) thought to act as $Ca^{2+}$ buffers (Ikura 1996), or four EF-hands (neurocalcin, frequenin) that function as $Ca^{2+}$-activated switches (Ikura, 1996; Burgoyne and Weiss, 2001). The distribution of these various proteins differs: all have been found in primary sensory endings; calbindin D-28k also occurs in the intrafusal fibres of rat spindles (Duc *et al,* 1994), and calretinin also occurs in the chain fibres of cat spindles (El-Tarhouni and Banks 1995).

The EF-hand binds $Ca^{2+}$ at the physiological concentrations of the intracellular compartments, but mutation in the EF-hand loop results in some domains losing their ability to bind $Ca^{2+}$ (Heizman and Hunziker, 1991).

Calmodulin (CM) was identified in 1967 and is the best-known representative of the CaBPs group. Calbindin (CB) was first identified in the chicken intestine by Wasserman and Taylor (1966) and was found to be the main molecular response to vitamin D derived hormones (Christakos *et al*, 1979). Later, it was described in other locations, including the brain, kidney and pancreatic islets. Parvalbumin (PV) has been found widely distributed in the central nervous system, but was first found in muscular tissue (Lehky *et al*, 1974) and also in the brain (Celio & Heizman, 1981).

Calretinin (CR) was first identified by gene cloning cDNA of the chick retina; it is 60% homologous to that of chick calbindin. The genomic calretinin gene has also been partially sequenced. Calretinin is a protein of 29-30 kilodaltons that has been identified mainly in the central nervous system.

Calbindin (CB) immunoreactivity in the dorsal root ganglia of chickens is expressed by subsets of large and small neurons (Philippe and Droz, 1988). Frequenin, which also is an EF-hand calcium-binding protein, has been recognized in the neurons that innervate the muscle spindle apparatus of the frog (Werle *et al*, 2000).

### 3.2.2 Role and function

There are at least 150 representatives of the so-called EF hand calcium binding proteins. The best-known representative of this family is calmodulin (Cheung 1980), which can change its conformation after binding $Ca^{2+}$ and triggers the activity of neighbouring enzymes. $Ca^{2+}$-CM complexes regulate the activities of more than 20 enzymes. Other CaBPs are less versatile in their function and may simply bind incoming $Ca^{2+}$: three CaBP, namely calbindin D-28k (CB), calretinin (CR) and parvalbumin (PV) can be included in this category. These are particularly interesting from a morphological point of view since they occur only in certain subpopulations of nerve cells in the central and peripheral nervous system (Baimbrige, *et al*, 1982; Braun, 1990; Celio and Heizmann, 1981; Garcia-Segura *et al*, 1984; Roger, Khan and Ellis, 1990). Thus they have been used selectively to visualize cells, neuronal pathways and brain nuclei in a way unknown before.

It is believed that an abnormal increase in intracellular $Ca^{2+}$ concentration is the final common pathway towards irreversible cell injury (Clarke, 1989; Schanne *et al*,1979) Because of the CaBPs potential buffering role, they were thought to protect nerve cells, by reducing their intracellular $Ca^{2+}$ (Chard, Beakman and Miller, 1991; Kohr and Mody 1991; Kohr, Lambert and Mody 1991). Furthermore, Scharfmann and Schwartzkroin (1989) hypothesized that the intracellular concentration of $Ca^{2+}$ buffers is directly proportional to the resistance of neurons to degeneration during prolonged excitation. However, PV and CB can be found in high concentrations in ischemia-vulnerable Purkinje cells and not in ischemia-resistant CA3 pyramidal cells or in the giant cholinergic interneurons of the striatum; the assumption that the CaBPs play a role in protecting neurons against ischemic injuries is therefore difficult to accept.

Although several different calcium-binding proteins are known to be present in the brain, (including PV, CB- and CR) it is not yet known whether they act simply as

calcium buffers, (in which role they could passively modulate several aspects of neuronal activity) or whether they play a more active role in calcium-mediated signal transduction (Taylor, 1974, Jande, Meler and Lawson, 1981; Rogers, 1987, 1991; Rogers, Khan and Ellis, 1990). The spindle nerve terminals contain a population of membrane-bound vesicles that are small and clear micro-vesicles with a mean diameter of 50 nm (Adal, 1969; D. Barker and Saito, unpublished). These 'synaptic-like' vesicles carry an apparent similarity to the synaptic vesicles of presynaptic terminals, including motor neuromuscular junctions.

The activity-dependent recycling of these synaptic-like vesicles implies a control mechanism; the central role of $Ca^{2+}$ is indicated by immunocytochemical evidence for the presence of these various $Ca^{2+}$- binding proteins in the spindle.

### 3.2.3 Detection of CaBPs

Antibodies against CaBPs are increasingly used for neuroanatomical studies of the vertebrate nervous system. They give excellent cytoarchitectonic staining, and visualize a Golgi-like cellular morphology (Blumcke *et al*, 1990; DeFelipe et al, 1990; Gerfen, Baimbridge and Miller, 1985; Jones and Hendry, 1989; Ohm *et al*, 1990, 1991; Resibois and Roger, 1992; Roger, 1992a, b; Stichel *et al*, 1987; Van Brederode, Helliesen and Hendrickson, 1991). They even label whole pathways and sometime entire functional systems (Celio *et al*, 1990) There are three available antisera against CR and they do not cross-react with CB at the dilutions used for Immunohistochemistry, in spite of more than 60% homology between the two proteins (Rogers, 1989).

By using primarily immunohistochemical techniques, interesting distribution patterns of CaBPs have been described in the central nervous system. CB- and PV are largely

present in different groups of neurons in the cerebral cortex (Van Brederode, Helliesen and Hendrickson, 1991), in the hippocampus (Sloviter, 1989), in superior colliculus (Mize et al. 1992) and the spinal cord (Ren, Ruda and Jacobwitz, 1993 and Antal, Freund and Polgar, 1990).

### 3.2.4 Calretinin

CR is mainly found in the central nervous system and was originally detected in the retina in neurons associated with sensory pathways (hence its name); its functions have not been elucidated. It is believed to be important in the intracellular transport of $Ca^{2+}$ and also to act as a calcium buffer (Rogers, 1987).

The neurons in which calretinin (CR) is found differ from those in which CB- and PV is present, although the three CaBPs do overlap to some extent (Resibois and Roger, 1992). Duc, Barakat-Walter and Droz, (1994) studied the distribution of the neurons expressing CB and CR in the rat, as well as their peripheral projections: in their investigation of CB and CR immunoreactivities they concluded that afferent axons of slowly adapting mechanoreceptors, such as secondary afferents of muscle spindles, do not exhibit any CB or CR immunoreactivity, furthermore CB and CR were co-expressed by subpopulations of large and small-primary sensory neurons and co-localised in the majority of large ones. As most of these afferents are considered to be rapidly adapting mechanoreceptors, Duc *et al*, (1994) concluded that CB- or CR-expressing neurons innervate particular mechanoreceptors that display physiological characteristics of rapid adaptation to stimuli. Nevertheless that conclusion could be challenged on the following bases. The responses of the muscle mechanosensory receptor are not readily or easily classifiable as either rapidly or slowly adapting, since under suitable conditions of stimulation they will exhibit both types of behaviour (Matthews, 1972) (Fig 3.15).

Rapid adaptation is attributable not solely to the intrinsic nature of the afferent axon but also to the mechanical properties of the intrafusal fibres.

The reinnervation studies of Banks and Barker (1989) indicate that the adaptation properties of muscle also depend on the non-neural components (such as intrafusal muscle fibres or tendon bundles) with which the sensory endings are in contact.

Some secondary afferent axons would exhibit similar behaviour to that of primary afferent axons when replaced into primary area, and can produce rapid adaptation.

Tendon organs if subjected to cutaneous stimulation can produce rapid adaptation and have shown CR staining. In a previous study to localise CR immunoreactivity in the abductor digiti quuinti medius muscle of the cat (El-tarhouni, 1996), different degrees of CR immunoreactivity were detected in the subsets of nuclear bag and chain fibres according to their type: thus, chain fibres were intensely positive; $bag_1$ fibres and extrafusal muscles were virtually negative, and $bag_2$ fibres showed intermediate staining see (Fig. 3.1).

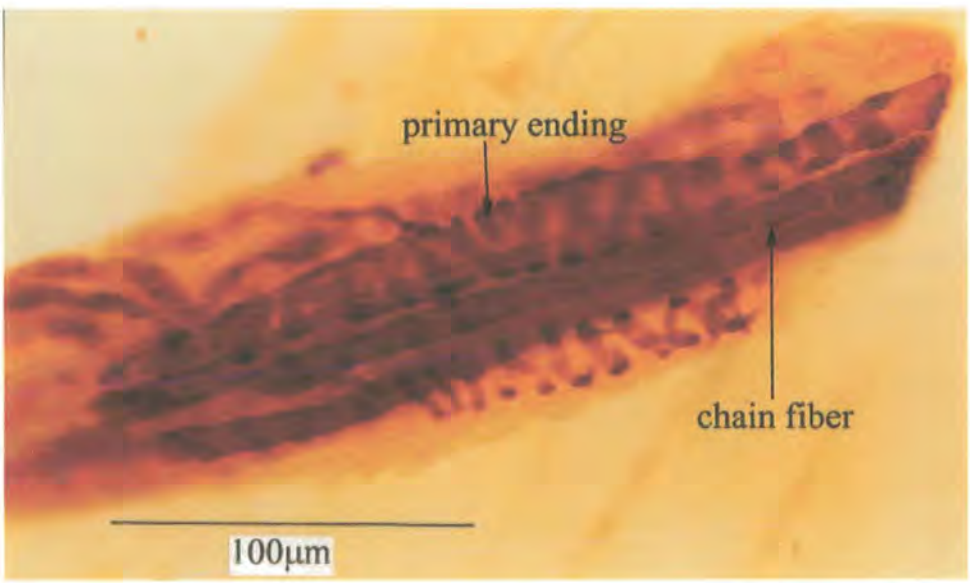


Fig. 3.1 The chain fibres of the cat muscle spindle are intensely positive to calretinin.

Immunoreactivity was also detected in the tendon organs (El-tarhoun, 1996) which Duc, *et al*, (1994) stated do not contain CR (See Fig.3.2); they assume that secondary endings

are slowly adapting, whereas primary endings and paciniform corpuscles are rapidly adapting and concluded that calretinin was somehow associated with rapid adaptation

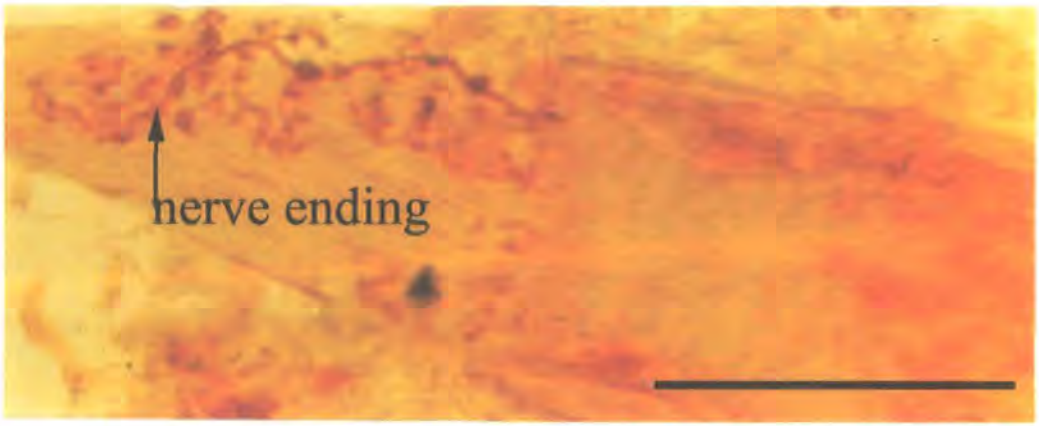


Fig 3.2 Tendon organs show immunoreactivity to calretinin magnification scale is 100μm (El-tarhouni, 1996).

## 3.3. Aim of this study

Following the same technique and methods used by Duc *et al,* (1994) and by El-tarhouni (1996) in their studies of CR in both rat and cat, I intended my study to test the hypothesis that calretinin exists not only in what have been described as rapidly adapting nerve endings of the muscle spindle but also in the slowly adapting nerve endings such as the secondary nerve endings, and to highlight some of the differences in CR distribution in the muscle spindle nerve endings of the rat compared with that of the cat by looking for secondary nerve endings, tendon organs with their nerve endings, or for any intrafusal fibre of the rat that might express CR,

## 3.4 Materials and method

In order to achieve immunohistochemical staining of the nerves and nerve endings of the muscle spindle of the rat, the gastrocnemius and the soleus muscle were selected. Two rats were killed by carbon dioxide and their hind limbs were dissected to yield

four soleus muscles and four gastrocnemius muscles (Table 3.1). The muscles were stretched on a piece of thin card to straighten them and then they were fixed overnight in a mixture of 1 volume 0.075 M L-lysine monohydrochloride, 3 volumes of phosphate-buffered saline, 4% paraformaldehyde, and 0.23% periodate. The next morning the muscles were placed in a solution of 30% sucrose which acts as a cryoprotectant and prevents the formation of ice crystals during rapid freezing (Duc, *et al*, 1994).

Table 3.1 Number of rat muscles used for initial cry sectioning of both soleus and gastrocnemius.

| | Number and type of muscle used | Type of embedding | Method of sectioning | Spindle number | Results |
|---|---|---|---|---|---|
| Number | | | | | |
| 2 Rats | 4 soleus | None | Cryosectioning | 1 | Faint staining |
| | 4 Gastrocnemius | None | Cryosectioning | 0 | 0 |

## 3.4.1 Freezing technique

All these muscles were treated equally by leaving them for overnight after the fixation in a 30% sucrose solution (as described in the previous section). The muscles were then fast-frozen with isopentane in a liquid-nitrogen bath. Subsequently they were wrapped in aluminium foil, placed in a tightly sealed bag, all this took place in the cryostat and at temperature of -15C°, and then they were stored in a deep freezer.

### 3.4.2 Cryostat sectioning

All muscles received the same treatment. Sections of soleus muscles were handled with pre-cooled forceps and then glued to the cold cryostat chuck with a small amount of the cryomatrix agar, care being taken to fit the muscle to the chuck in a proper longitudinal orientation, after which the muscle was further cemented to the chuck with more agar. Care was taken to avoid thawing of the muscle, by carrying out the procedure inside the cryostat and applying cryofreeze spray when necessary. The cryostat temperature was maintained below -15C° for optimal sectioning; at higher temperatures the sections might fold up or become too soft to be handled by forceps. Sections were done longitudinally at a thickness of 15-20μm in order to slice through the capsule and retain the whole spindle. Five or six serial sections were placed on each microscope slide which had been treated with TESPA in order to help the tissue adhere to the slide. Trays of slides were left inside the cryostat ready for immunostaining.

### 3.4.3. Immunohistochemistry

CR immunoreactivity was detected in the spindle structure using the peroxidase - antiperoxidase method (Dako universal PAP kit). The primary antibody used was the Swant 7676, which had been reconstituted with 200μl double-distilled water and stored frozen in micro-centrifuge tubes (1.7μl at -80°C°) For continuous use the antiserum was kept at 4 C° to avoid repeated freezing and thawing.

The second antibody (or link antibody) was included in the Dako universal PAP kit; the PAP method is the most commonly used immunoperoxidase staining method because of its great sensitivity, and ready availability.

### 3.4.4. Principle of the method

The method used is an indirect method that utilizes a pre-formed, cyclic enzyme-anti-enzyme immune complex composed of three enzyme molecules and two antibody molecules. The methods are named after the particular enzyme-antibody complex that is used in the technique. The peroxidase-anti-peroxidase (PAP) technique utilizes a peroxidase-anti-peroxidase immune complex (Beesley, 1995).

This method involves preliminary treatment of the tissue with a hydrogen peroxide solution to suppress endogenous peroxidase activity, if necessary. This is followed by incubation with normal serum to quench non-specific protein binding to certain tissue elements. Antibody to the target antigen (primary antibody), antibody to the primary antibody (link antibody), and PAP reagent are then applied sequentially, with interposed washing steps.

### 3.4.5. Immunostaining procedure.

For the two sets of slides (the experimental and the control) the following technique was used

1. The tissue sections were treated for 20 min with $H_2O_2$ to inhibit endogenous peroxidase.
2. Rinsed in Tris-buffer three times for 10 min each rinse.

3. Normal rabbit serum (blocking serum) was applied for 30 min. As this step may be omitted where non-specific protein binding does not interfere with specific staining this option was subsequently taken without apparently affecting the final results.

4. The slides were incubated overnight with the rabbit antiserum (primary antibody) at a dilution of 1/1000 to 1/2000 in Tris-buffer pH 7.3 with 10% horse serum and 0.4% Triton X 100 at 4 C°.

5. They were rinsed in Tris-buffer twice for 10 min.

6. They were then transferred into immunoglobulin anti-rabbit serum (link antibody) and incubated at room temperature for 4 hours.

7. They were rinsed in Tris-buffer (2x 10 min).

8. The peroxidase complex (PAP) from the red bottle was applied for 2 hours at room temperature.

9. Rinsed again in Tris-buffer (2 x 10 min).

10. A substrate mixture was prepared by transferring sufficient buffer into the graduated test tube (all supplied with the PAP kits) for the number of slides to be stained (each 2 ml is sufficient for 5-8 slides). For each 2 ml of buffer, one drop of anti-enzyme complex (AEC) was added, mixed immediately; then one drop of hydrogen peroxide was added and mixed again. If a precipitate formed, it was removed by filtering it out. Any precipitate that may form on the slides during staining was not removed, as it did not interfere with the staining process. Sections were incubated from 20-30 minutes and then rinsed gently with distilled water.

11. Sections were not allowed to dry and cover slips were mounted on them, slides were ready for light microscope examination.

### 3.4.5.1 The control

The control samples were treated with the same steps except step number four, the primary antibody was not applied.

## 3.5 Interim results (batch 1)

Cryosectioning of the large gastrocnemius muscles was difficult because of incomplete freezing, particularly the centre of the muscles.

The thin soleus muscles freeze quite well, but it was difficult to retain them on the slides on their serial sectioning order: although the slides were treated with TESPA, many sections became detached during the many stages of staining.

The results were not very good because only five sections showed some staining of primary nerve endings and this was quite faint as in (Fig.3.3)

Fig 3.3 Initial result of staining which shows very faint staining of a nerve ending magnification scale at 100μm.

In order to overcome this problem a new rabbit anti-calretinin sample (SWANT 7696) was obtained and it was reconstituted with 200μl doubled-distilled water, as before

stored in small aliquots of 1μl and kept at temperature of -80C°. Additionally, some modifications to the fixation methods, slide coating, and immunostaining procedure were introduced. Hot and cold paraffin sectioning was also carried out

## 3.6. Interim results (batch 2)

Because of the lack of initial success, other sets of muscles were used in this batch. Three rats were killed by lethal injection and the muscles were then fixed by perfusion (instead of being immersed in the fixative solution, as previously).

The fixative solution comprised 1 volume 0.075 M L-lysine monohydrochloride, 3 volumes of phosphate-buffered saline, 4% paraformaldehyde, and 0.23% periodate. The hind limbs of the three rats were dissected, yielding six soleus muscles; 19 other muscles were obtained to test various methods of paraffin wax embedding. All muscles were then left in the same fixative overnight.

Table 3.2 shows the number of muscles, type of embedding, and method of sectioning (Compare with table 3.1). Cold paraffin embedding was set at 45C° and the hot method at 60C° since a higher temperature would have destroyed the antigens.

| Number of Rats | Number and type of Muscles used | Type of Embedding | Method of Sectioning | Slide no | Result |
|---|---|---|---|---|---|
| 3 | 6 Soleus | None | Cryo | Numb.160 | Stained |
| | 2 small Muscles | Hot Paraffin 60C° | Rotary | No good sections | |
| | 2 small Muscles | Cold paraffin 45C° | Rotary | No good sections | |
| | 4 gastrocnemius | None | Cryo | No good sections | |
| | 11 various | None | None | None | |

## 3.6.1 Paraffin embedding and sectioning

Four of the small muscles were dehydrated in a series of increasing concentrations of alcohol, cleared with Histoclear, and impregnated with wax. Subsequently then two muscles were embedded in cold paraffin and another two were embedded in hot paraffin (Table 3.2). The blocks were then sectioned; however, the hot paraffin sections were brittle and fragmented easily while the cold one were soft and easily folded on the knife-edges no good sections were produced thus no slides or staining for hot and cold paraffin embedding. Cryosectioning was therefore preferred because such sections were better than the paraffin sections.

## 3.6.2 Cryosectioning

Six soleus muscles were sectioned as previously described (section 3.4.2) including the controls (Table 3.2); however the cutting thickness was increased from 20μm to 25μm

in order to obtain sections that were easier to handle, since the thinner ones were easily torn and fragmented. The slides were not coated with TESPA as this had not prevented the sections from falling off; instead, the slides were modified by dipping their edges on a hot paraffin bath thus enabling a pool of immunostaining solution to be formed on which the sections could float, thus remaining in their serial order. The duration of each immunohistochemical stage was reduced, especially the number and duration of washes in buffer, in order to reduce the amount of wear and tear on the tissue.

### 3.6.3. Photography

The experiment slides were photographed using a Nikon light microscope with an objective lens of x 20 or x40 and a Nikon FX 35 camera. The control slides produced no staining and so were not photographed.

## 3.7 Results

Six rat soleus muscles produced 135 experimental slides and a batch of 25 slides for the control, which showed no sign of immunoreactivity. In the experimental batches of slides seven spindles were seen; in which the calcium-binding protein CR was immunohistochemically investigated using the peroxidase- antiperoxidase method. In those sectioned muscle spindles, the CR immunoreactivity was detected on the Ia axon, on the preterminal branches, and on the annulospiral nerve terminals of the primary sensory nerve endings. On those slides examined and photographed the nerve endings

were immunoreactive, as seen on the bag fibres and chain fibres which made it easier to identify them. Figs 3.4 -3.11 show some variation in their CR intensity.

### 3.7.1 Controls

In the control slides (lacking the first antibody) no significant immunoreactivity that could be detected.

## 3.7.2 The muscle spindle arrangement

The spindles were examined in longitudinal sections at 25μm thickness. According to the structural features of the intrafusal fibres and detail of the primary endings usually each spindle contains up to two $bag_1$ fibres, one or two $bag_2$ fibres, and between one and seven chain fibres. In the slides examined only $bag_1$ and $bag_2$ fibres were seen and none of them were duplicates either bag $bag_1$ or $bag_2$. No tandem linked spindles or tendon organs were seen.

## 3.7.3. Innervation of muscle spindles

### 3.7.3.1 Nerve supply to the spindle

Each spindle receives one large afferent nerve fibre, which supplies the primary endings on all the intrafusal fibres (Fig.3.12), and usually one or more smaller afferents that supply the secondary endings, especially on the chain fibres that were detected in this study.

Fig.3.4 A long Ia axon stained intensely red — a sign of high CR immunoreactivity; part of the bag fibres are shown in this photograph. Note that, unusually, the Ia axon is here stained intensely all the way to the fibre (see also Fig 3.5). It's possible that this axon was parallel to the plane of sectioning and without many missing sections.


Fig.3.4

Fig.3.5 Higher power view of the previous slide showing a spindle unit receiving a large afferent Ia nerve which stained intensely. The nerve endings of the $bag_1$ and $bag_2$ fibres are also indicated.


Fig.3.5

Fig.3.6 A muscle spindle unit showing two bag fibres with their primary nerve endings. The axon and the terminal branches are not seen. The nerve endings of one bag fibre appear to be close to each other, which is typical of $bag_1$ fibres, whereas the one next to it is much smaller (nearly half the size) and shows primary nerve endings that are further apart and less transversal (typical of a chain fibre). The primary nerve endings of $bag_1$ fibre are more transversely oriented.

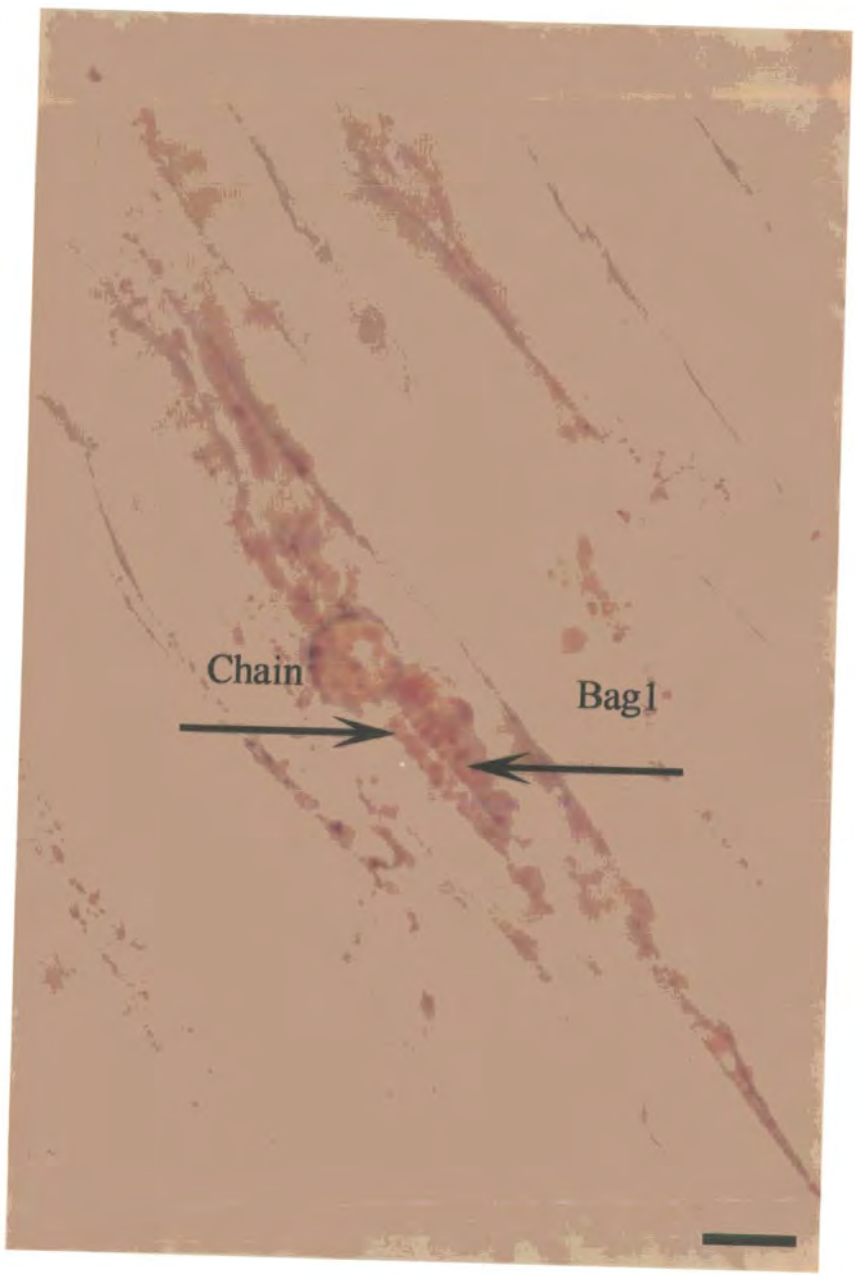


Fig.3.6

Fig .3.7 Another muscle spindle showing two bag fibres. $Bag_2$ is in the background and out of focus behind $bag_1$ which is clearly stained showing the primary nerve endings annulospiral formation. Note the intrafusal fibre increase in size just after passing through the primary nerve endings annulospiral. The primary sensory region appears to be thinner, compare that with the fibre width just outside the primary region, where the fibre seems to be thicker. The fibre both left of $bag_1$ fibre shows loose and widely spaced spiral, which is a sign of another, stained chain fibre. To the right is a Ia afferent axon (faintly stained).

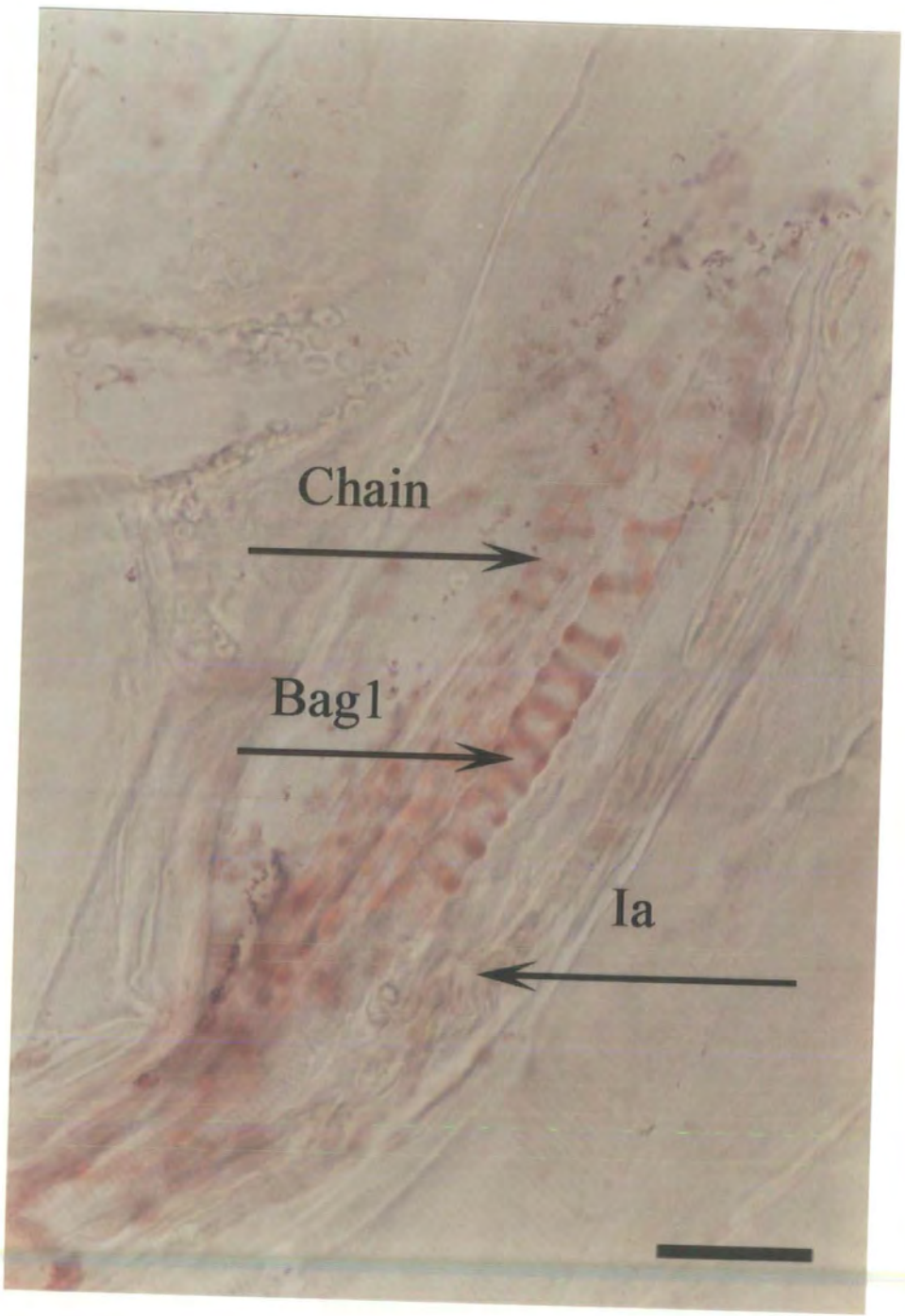


Fig.3.7

Fig. 3.8 A spindle unit with bag fibres; a precipitate has formed as a by-product of immunohistochemical staining and appears to have accumulated at the spindle capsule giving patchy definition of the capsule wall.

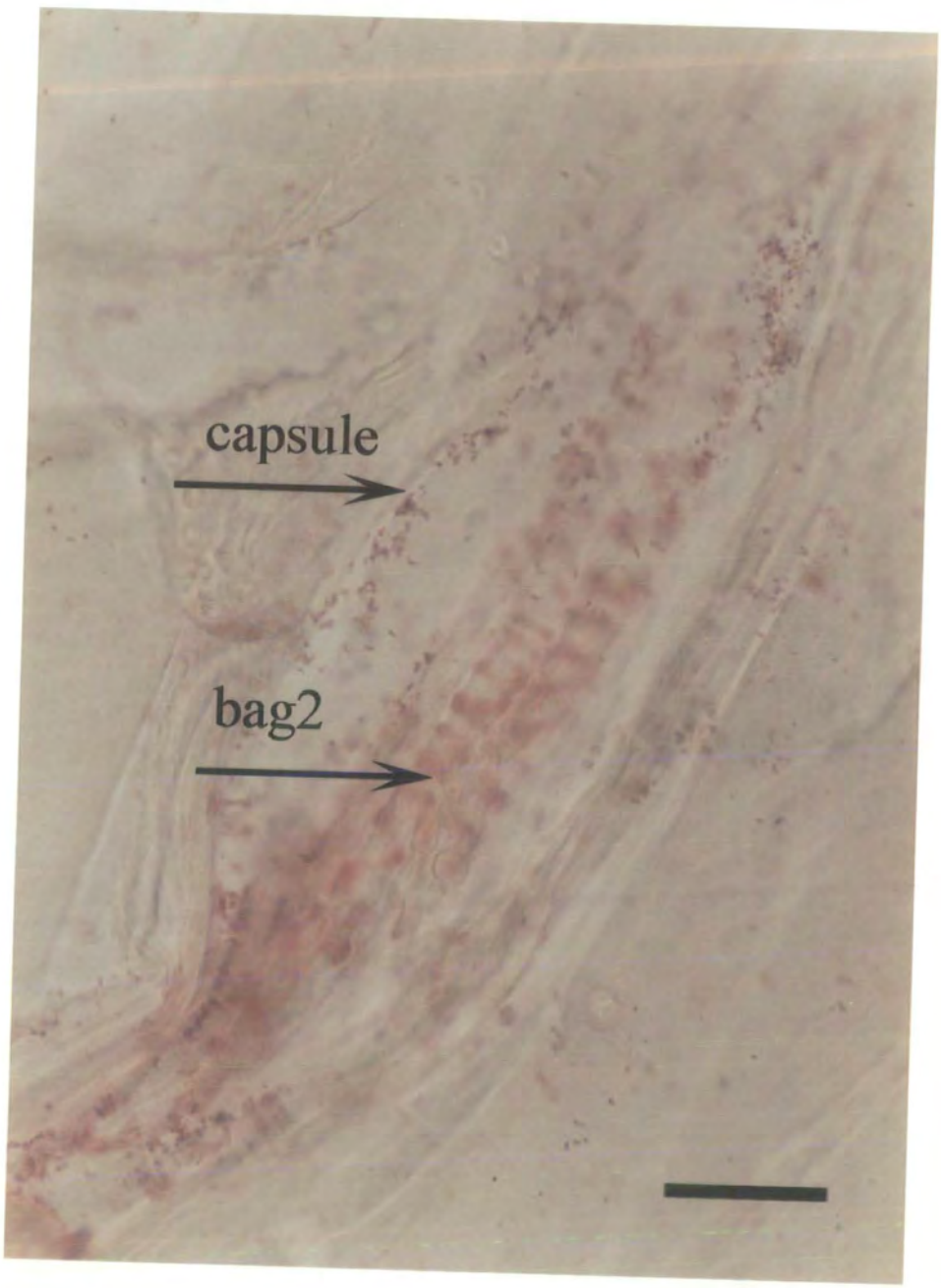


Fig.3.8

Fig.3.9. A muscle spindle with a single bag fibre, probably $bag_2$, visible in this section.

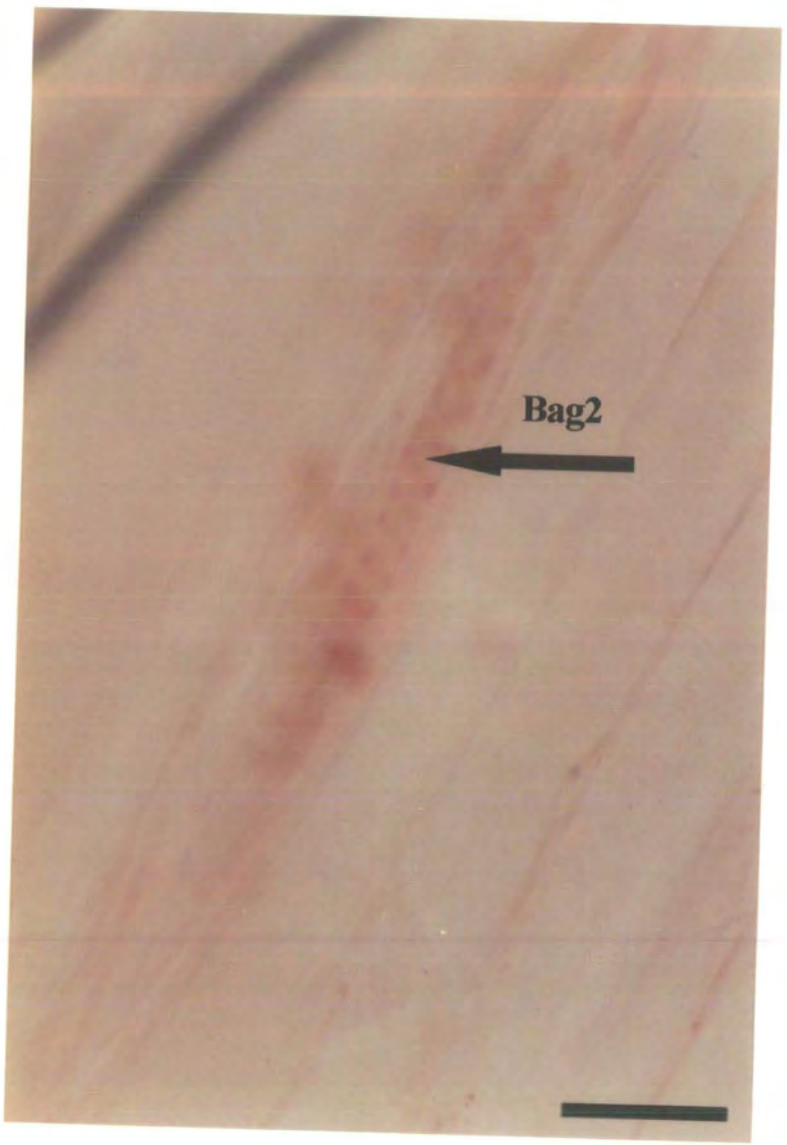


**Fig 3.9**

Fig.3.10. A muscle spindle showing an unidentified bag fibre.

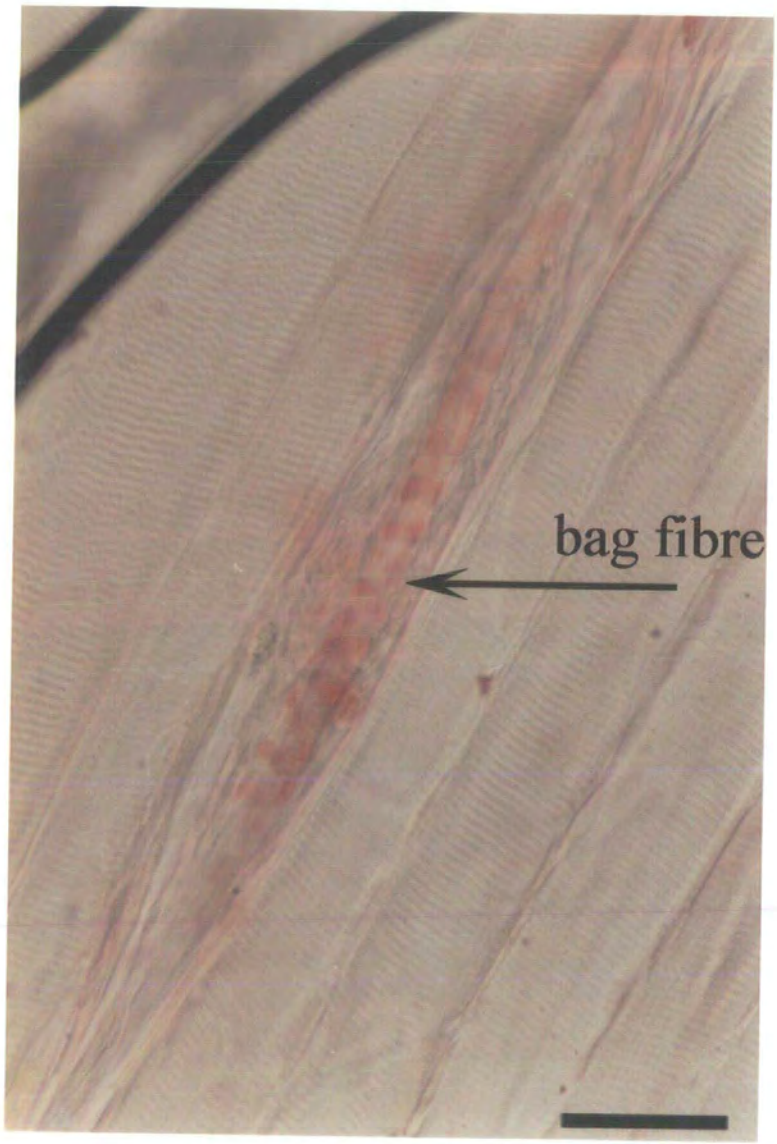


Fig.3.10

Fig 3.11. A muscle spindle showing the Ia afferent, two bag fibres and a blood vessel packed with red blood cells. At the top right-hand corner is a faintly stained afferent Ia axon.

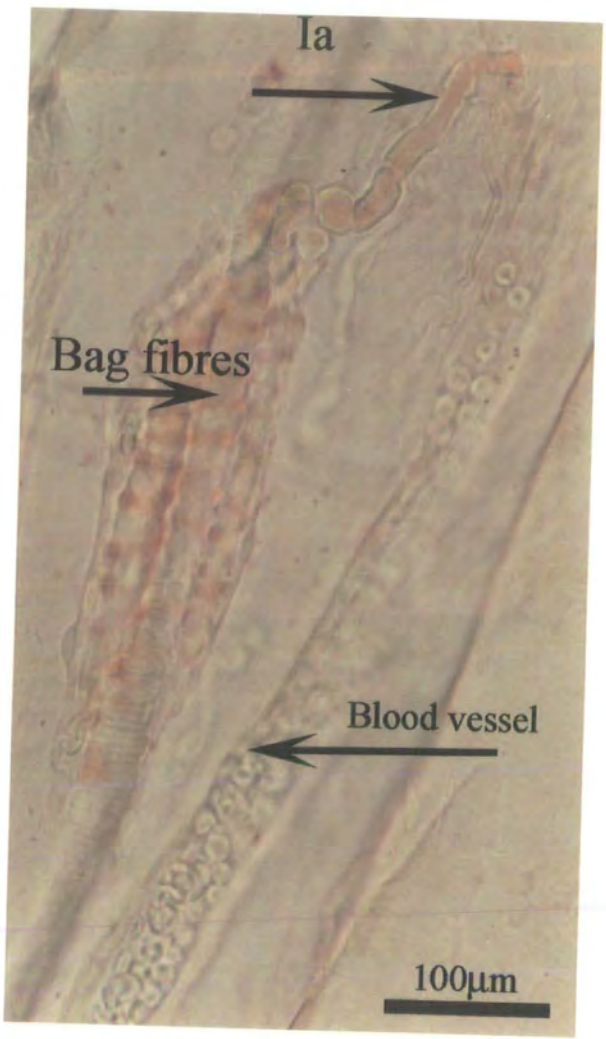


Fig.3.11

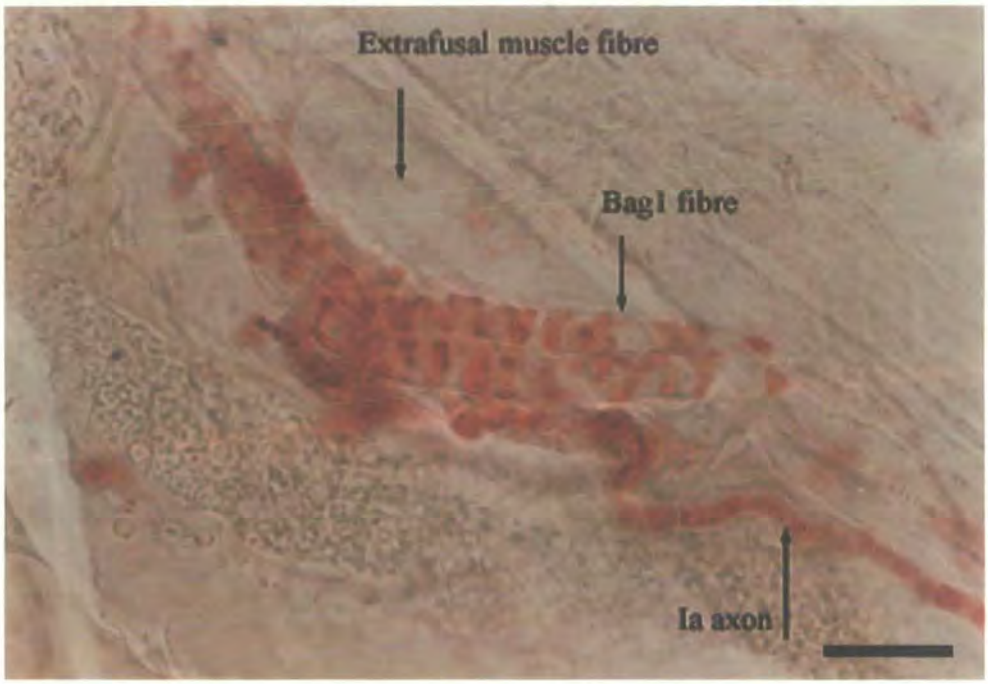


Fig.3.12 Typical muscle spindle unit showing the stained large afferent Ia axon, preterminal branching, $bag_1$ and $bag_2$ fibre and the annulospiral formation of their primary nerve endings all intensely stained magnification scale at 100μm.

### 3.7.3.2 Sensory endings

In the middle of the nuclear bag and nuclear chain fibres, the sensory endings overlay these intrafusal fibres and occupied small channels that were partially indented into the intrafusal fibre and ran transversely to the fibre (Figures .3.10. 3.7). On the bag fibres observed in this study the nerve ending terminations on either side of the spiral are less transverse and become more oblique, especially in $bag_1$ fibres but no terminations were seen in parallel to the axis of the intrafusal fibre (Fig 3.14)

### 3.7.3.3 Primary nerve endings and axon

The primary sensory nerve ending is derived from a myelinated large-diameter nerve fibre that innervates the intrafusal muscle fibres and forms an annulospiral around the equatorial regions of the fibres.

Generally, each muscle spindle is supplied by one, thick, sensory-fibre Ia axon afferent that enters the spindle near the equator of the capsule. Inside the periaxial space the Ia axon will divide into several terminal branches to form the sensory endings, which will overlay the three types of intrafusal muscle fibres ($bag_1$, $bag_2$, and chains) at their most dense equatorial area. (see Figs.3. 4 and Fig.3.5).

Some spindles may be supplied by more than one axon to form two separately innervated primary nerve endings, lying side by side or end to end, referred to as a double primary by Banks, Barker and Stacey (1982).

### 3.7.3.4 Secondary endings

The secondary afferent terminals are supplied by an afferent II axon to form secondary endings, which terminate on one or both sides of the primary. In cat spindles the average number of secondary endings is five to six, the most that could be situated on one side is five and on both of the primary endings the highest number seen is six. (Banks and Barker, 2004) However in the rat soleus muscle, secondary afferent terminals could occur less frequently.

### 3.7.3.5 Terminals on $bag_1$ and $bag_2$

The terminals appear to consist of annulospirals which are more common around chain fibres than bag fibres. Their ring formation arises from blind-ended terminals that wind once around an intrafusal fibre before abutting against themselves. The total number of spirals is greater in the middle of $bag_1$ primary terminals, where they are arranged and wrapped closely together; $bag_1$ fibres also display more extensive irregular portions at each end than do $bag_2$ fibres. Conversely $bag_2$ fibres are more widely spaced and with minimal irregularity at each end, (Barker and Banks, 1994).

Fig.3.13. The terminals appear to have structural differences in the two types of bag fibres. In $bag_1$ the fibres the terminals are transversely oriented, regularly arranged and wrapped closely together around the bag.

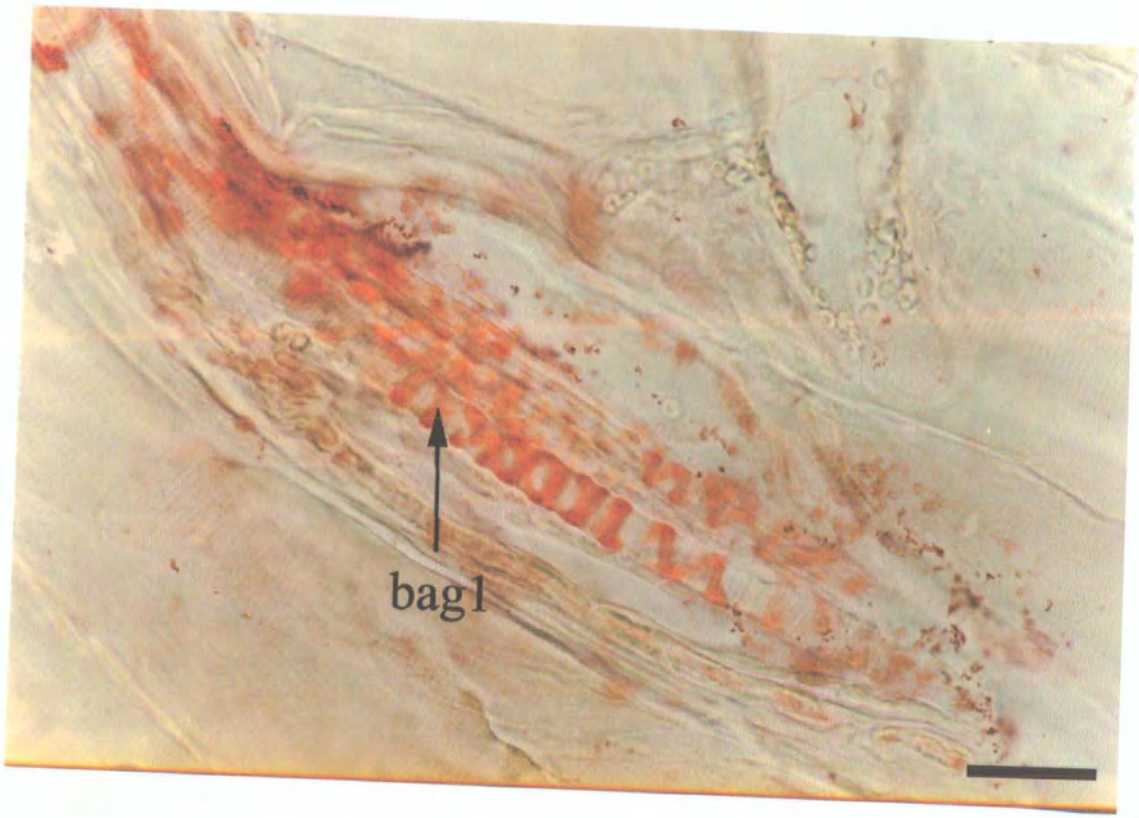


Fig .3.13 magnification scale at 100μm.

Fig.3.14. In $bag_2$ fibres the terminals are more widely spaced and more transversely oriented. Secondary endings which are more developed on the chain fibres were not detected by immunoreaction in any of the spindles.

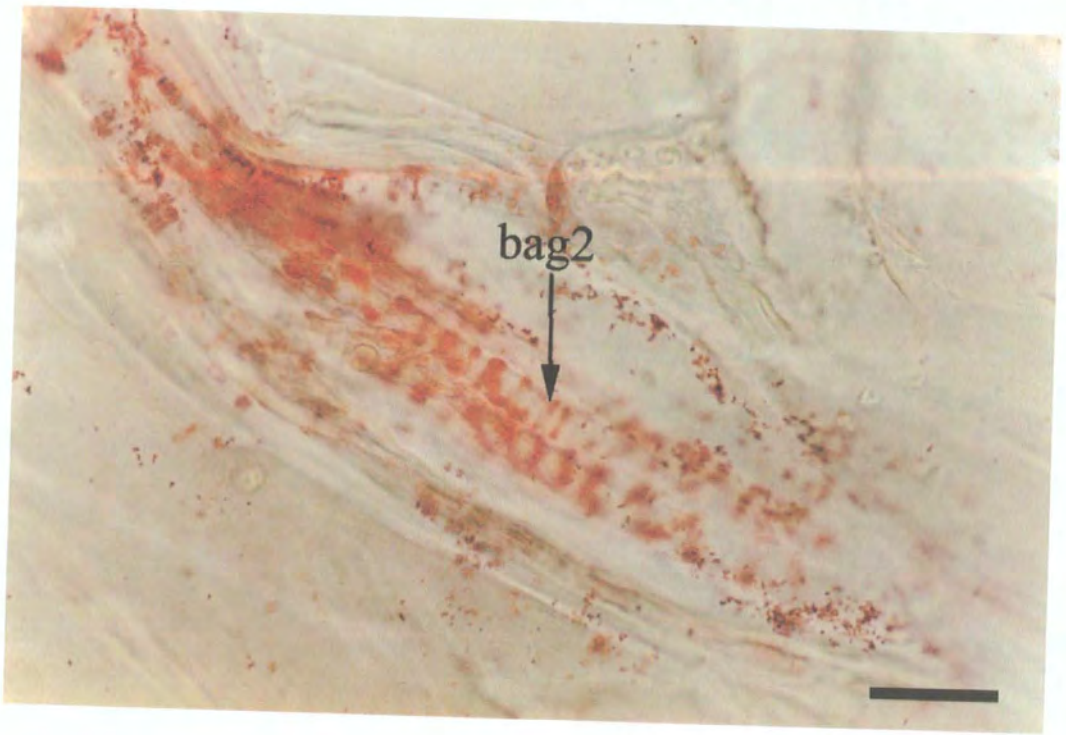


Fig.3.14 magnification scale at 100μm.

Fig.4.1.This image shows part of the nerve ending. In the upper section of the micrograph the primary nerve ending show many mitochondria and immunogold labelled glutamate all over the micrograph (see small arrow).

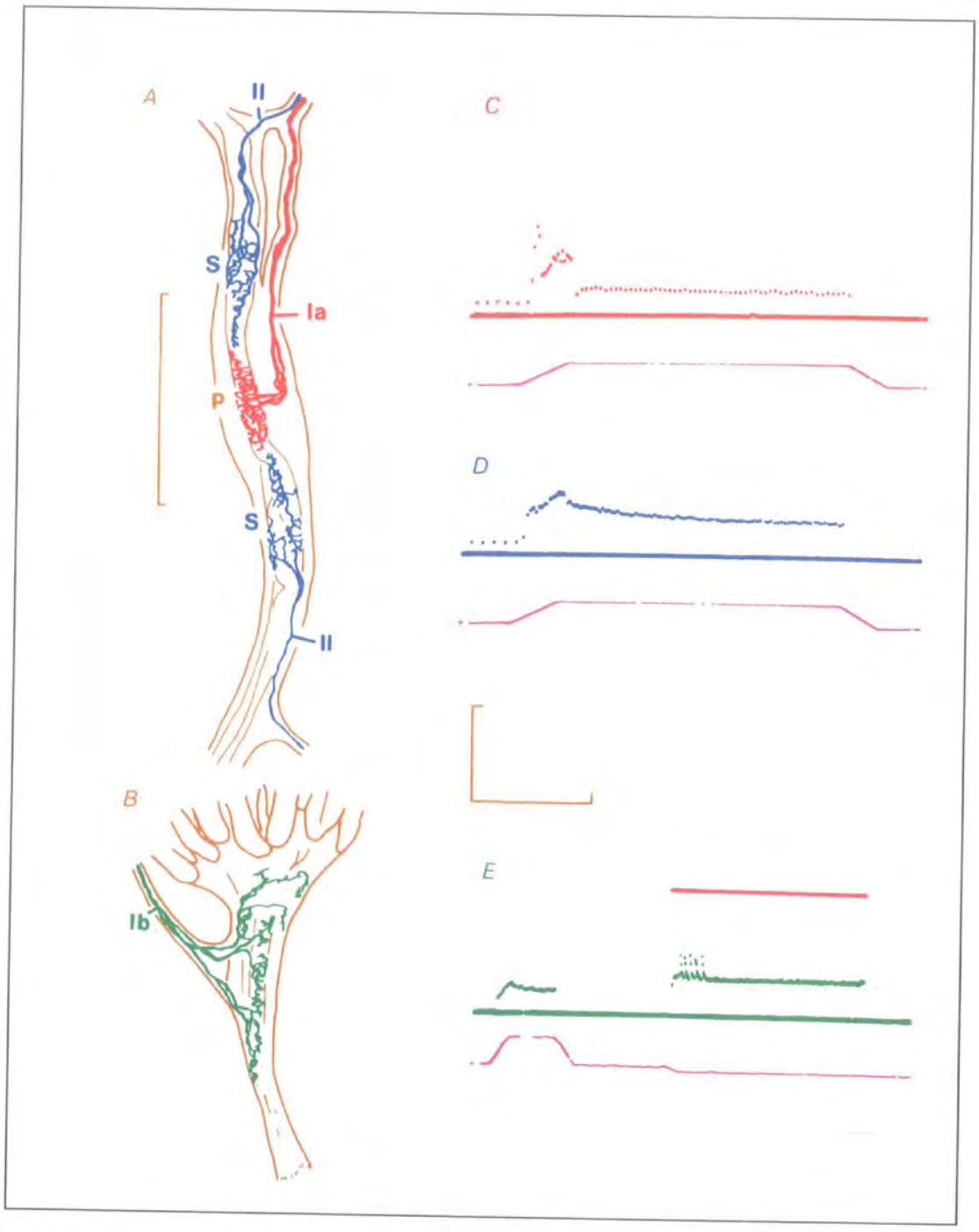


Fig.3.15 Primary axon (red), secondary in (blue), and tendon organ (green) all three structures show rapidly and slowly adapting aspects of their responses. (Robert W. Banks).

### 3.8.1. Comparison of results

Duc, Barakat-Walter and Droz (1994) localised calretinin immunohistochemically in rat muscle, using the same antibody as that used here.

Calretinin is a highly conserved calcium-binding protein (Parmentier, 1990). It is expressed in specific subsets of neurons, although its role therein is unknown. In this study calretinin immunoreactivity was detected only on the Ia axon and the sensory terminals of the primary nerve endings and not in the subsets of the nuclear bag or nuclear chain fibres or in any of the intrafusal fibres. Thus the results of this study do not differ materially from those of Duc, Barakat-Walter and Droz (1994). Few chain fibres were detected and no secondary endings were detected the rat soleus muscle; however, secondary afferent terminals may occur less frequently than in the cat.

In an unpublished study by Banks and Stacey, (personal communications) of 24 rat soleus muscles only 10 had secondary afferents. Four of those were found in two rats and, overall, of the 50 afferents found in the entire sample, only 12 are secondary afferents. This may explain the difficulty in tracing any secondary endings in this sample described here. Chain fibres are innervated mainly by secondary endings, but few secondaries are restricted to chain fibres only: most are distributed to all three fibre types and the restriction of terminals to one or two fibre types is more prevalent among secondaries terminating in the more polar positions.

### 3.8.2. Intrafusal muscle fibres

Two types of fibres are known to exist in muscle spindle and were named at an early stage bag and chain fibres. This terminology has now been modified to three types of fibres, known as $bag_1$, $bag_2$, and chain fibres (Barker and Banks, 1994). The number of intrafusal fibres in the rat soleus muscle varies from five to nine. On the basis of the

different sizes of the intrafusal fibres and on the primary sensory endings, I was able confidently to identify $bag_1$ and $bag_2$ fibres with their annulospiral nerve endings in the immunohistochemically stained sections; chain fibres were also stained.

### 3.8.3. Distribution of terminals

The terminals seen in this study were those of the primary nerve endings that appear in slightly different form in the two bag fibres. The terminals on the $bag_2$ fibres were more widely spaced, with minimal irregularity at each end, whereas on the $bag_1$ fibres the terminals were regularly arranged, wrapped closely together around the nuclear bag. Chain fibres' primary sensory endings were seen in their distinct spiral form.

### 3.8.4. The capsule

The capsule is composed of layers of thin, flat cells arranged in concentric tubular fashion alternating with collagenous and elastic fibrils. The capsular sheet cells are continuous with the cells that form the perineurium of the spindle nerve and act as a diffusion barrier (Merrillees, 1960). In some sections the capsule wall was faintly defined by precipitate of the immunostaining by product see (Fig 3.8).

### 3.8.5. Capillary vessels

The muscle spindle is known to be highly vascular and the rat muscle spindle is no exception. The function of capillaries within the spindles may be related to the myglobin content of the intrafusal fibres, where myglobin either acts as an oxygen store or accelerates the diffusion of oxygen in response to high demand.

In this study a large blood vessel was seen, packed with red blood cells and running the whole length of the spindle in the periaxial space see (Figs 3.11).

### 3.8.6. Tendon organ

The tendon organ in birds and mammals was described more than a hundred years ago by Golgi (1880). The structure and function of tendon organs has been reviewed by Barker (1974) and Jami (1992). Tendon organs are spindle–shaped mechanoreceptors protected by a multilayered capsule. Their bodies are formed by branching and fusing collagen bundles, which are innervated by Ib myelinated axon terminals. At the muscular end, each tendon organ body is attached individually to a group of extrafusal muscle fibres. In this study it was hoped to find a tendon organ in the rat soleus muscle; unfortunately, no such organ was seen, stained or unstained.

## 3.9. Discussion

In the neuronal communication, synaptic transmission is a fundamental process. A highly regulated process, triggered by a rise in cytosolic calcium concentration releases the neurotransmitter (Werle, Roder and Jeromin, 2000).

Many proteins that are essential for regulated exocytosis have been identified recently. The molecular identity of these calcium sensors is controversial and distinct molecular calcium sensors probably regulate the different stages of exocytosis. Moreover in the multiple stages of neurosecretion, both vesicle fusion and recycling are likely to be regulated by calcium. Among these calcium sensors is the EF-hand calcium-binding (CBP) protein CR, which is similar to other calcium binding proteins including calmodulin, calbindin D-28k and parvalbumin (Kretsinger *et al*, 1988). Those calcium-binding proteins, which are all expressed in neurons, exhibit four functional calcium binding domains and N-terminal myristoylation. No direct evidence has been obtained to link this calcium-binding protein to specific electrophysiological characteristics; Nevertheless, the highly specific distribution, especially that within the spindle primary endings, clearly indicates a particular physiological role that has yet to be elucidated. The coexistence of calretinin and gamma-aminobutyric acid (GABA) in the majority of calretinin-immunoreactive neurons has been demonstrated (Miettinen *et al*, 1992), as has the coexistence of calretinin and probably glutamate. Calretinin is believed to be important in the intracellular transport of $Ca^{2+}$; it is not known whether it simply acts as a calcium buffer (Braun, 1990), in which role it could passively modulate several aspects of neuronal activity, or whether it plays a more active role in calcium-mediated signal transduction (also thought to participate in phosphorylation). The precise function of most CaBPS IS still largely unknown.

Li, Decavel and Hatton (1995) revealed that calbindin D-28k acts as an endogenous $Ca^{2+}$ buffer, playing an important role in determining the firing patterns of hypothalamic neuroendocrine neurons. Oxytocin-releasing cells are normally tonically active whereas

vasopressin-releasing cells fire in phasic bursts due to the balance between $Ca^{+}$ dependent depolarising and hypopolarizing processes. Introduction of anti-calbindin antibody into oxytocin cells caused them to fire phasically, whereas introduction of calbindin into vasopressin cells caused them to fire continuously. From studies which show that calretinin is closely related to calbindin D-28k, (60% of their amino acids being identical), and from evidence presented here on the distribution of calretinin in muscle receptors, it seems likely that calretinin is involved in modulating the responses of the muscle receptors. Immunohistochemical studies of the CaBPs are still in progress, and this information, together with other studies of cells expressing calretinin in different species or under different physiological conditions, may lead some day to the identification of functional specialization, which may help to elucidate the role of calretinin.

This study of calretinin in the spindle of the rat soleus muscle localised its immunoreactivity by the use of anti calretinin-antisera (SWANT 7696). The immunoreactivity appears to be most abundant on the Ia afferent axon and its branches to form the primary nerve endings. (Resibios *et al,* 1990) suggested that anti-calretinin antisera may cross-react with calbindin D-28k because of the great degree of homology between calretinin and calbindin D-28k however this was not the case in this study because anti-calretinin anti-serum detects only calretinin but not calbindin D-28k on a protein blot of the muscle receptors (Schwaller *et al*, 1993)

## 3.10. Conclusions

The results of this study on the distribution of calretinin in rat spindles may be compared with those from a previous study on the cat.

Calretinin is present in primary endings of both rat and cat (Fig.3.1).

As in the cat, calretinin is present in the chain primary sensory-nerve endings but no secondary was seen from rat chain fibres. (Fig3.6, 3.7).

In contrast to the cat, no rat chain fibres were stained for calretinin.

These results on the distribution of calretinin in rat spindles confirm those of Duc, Barakat-Walter and Droz (1994). However, their conclusion that calretinin is associated specifically with rapidly adapting receptors cannot be supported for the following reasons:

The calretinin-positive spindle primary ending, identified by Duc and colleagues as rapidly adapting, in fact shows both rapid and slow adaptation characteristics (Fig. 3.15c).

Calretinin is present in the tendon organ, but absent from the spindle secondary endings, (at least those of the cat), yet both receptors show somewhat similar stretch responses, identified by Duc and colleagues as slowly adapting (Fig. 3.15, d, e).

# CHAPTER FOUR

## Detection of Glutamate in the Tenuissimus Muscle Spindle of The cat

### 4.1.1 Introduction

Excitatory amino acid transmitters account for most of the synaptic transmission that occurs in the mammalian central nervous system. To date five common amino acids have been considered as possibly serving a neurotransmitter function. Glutamate and aspartate are two of the major excitatory amino acid neurotransmitters; several related amino acids (e.g., homocysteic acid and *N*-acetylaspartylglutamate) also may have neurotransmitter roles (Zigmond, 1999).

GABA and glycine have been shown to function as inhibitory transmitters in vertebrate and invertebrate nervous systems. The major difference between amino acid neurotransmitter and other types of neurotransmitter are their high concentration in neural tissue and their ever-present and multiple involvements in mainstream biochemical processes, such as protein biosynthesis and intermediary metabolism (Bradford, 1989). Thus they share with GABA the problem of dissociating neurotransmitter from metabolic roles. The roles of amino acids both as transmitters and in intermediary metabolism make it difficult to describe them fully as neurotransmitters (Zigmond, 1999).

### 4.1.2. Synthesis of glutamate.

The amino acids glutamate and aspartate both carry a net negative charge and are close homologues in the dicarboxylic amino acid series. Although glutamic acid is found in very high concentrations in the CNS, the brain glutamate and aspartate levels are

derived solely by local synthesis from glucose, because neither amino acid crosses the blood- brain barrier.

Two processes contribute to synthesis of glutamate in the nerve terminal: (a) the glutamate may be formed from glucose through the Krebs cycle and transamination of α-ketoglutarate; (b) and in addition, glutamate can be formed directly from glutamine. There is a degree of interaction between glia and neurons in the regulation of availability of the transmitter pool of glutamate because the glutamine that is formed in glia is transported into nerve terminals and then locally converted by glutaminase into glutamate. The enzyme glutaminase is localized to mitochondria (Zigmond, 1999).

### 4.1.3. Storage of glutamate

In glutamate-containing nerve terminals, the amino acid is stored in synaptic vesicles which occur commonly in the central synaptic terminals of mechanosensory neurones from which the transmitter is released in a calcium-dependent manner upon depolarisation of the nerve terminal. However, the process by which glutamate is exported to allow vesicular storage of the transmitter remains poorly understood.

The vesicular storage of glutamate has been demonstrated but the vesicular transporters for these amino acids have not been cloned, although a vesicular glutamate transporter has been characterized biochemically and purified (Zigmond, 1999).

### 4.1.4. Regulation of glutamate release

#### 4.1.4.1 Glutamate and receptors

Chemical synaptic transmission is the functional process for neuron-to-neuron and neuron-to-muscle communication. A two-step process can explain the simplest form of

chemical transmission. First, transmitter is released from the presynaptic terminal; next transmitter diffuses across the synaptic cleft and binds to specific receptors embedded in the presynaptic and postsynaptic cell membranes. The type of receptor (or receptors) present in the plasma membrane determines the neuronal response to a neurotransmitter. This can either be the direct opening of an ion channel (ionotropic receptors) or the modulation of the concentration of intracellular metabolites (metabotropic receptors). The final stage of the response can be inhibitory or excitatory (Bradford, 1989).

Glutamate receptors are widespread in the nervous system. They are responsible for mediating most of excitatory synaptic transmission in the brain and spinal cord. Studies have suggested that glutamate receptors are not homogenous. Distinguishing the difference between glutamate receptor subtypes was significantly advanced by the development of agonists that could open and activate the receptors (Watkins, 1980).

The receptors of glutamate and other neurotransmitters that mediate the responses to transmitters are classified into two structurally distinct types as follows.

### 4.1.4.2 Ionotropic receptors

The ionotropic glutamate receptors are multimeric assemblies of four or five subunits that combine to form an ion channel through the plasma membrane and are subdivided into three groups (AMPA, NMDA and kainate receptors) based on their pharmacology and structural similarities. All ionotropic glutamate receptor subunits share a common basic structure. The subunits are designated $\alpha$, $\beta$, $\gamma$ and $\delta$, and each receptor complex contains two copies of the $\alpha$-subunit. The subunits are homologous membrane-bound proteins that congregate in the bilayer as a ring, forming a central pore. Each subunit consists of four transmembrane-spanning segments, or domains, referred to as TM1–TM4. Each segment is composed mainly of hydrophobic amino acids that stabilize the

domain within the hydrophobic environment of the lipid membrane. The ion channels of these receptors are largely impermeable to ions in the absence of neurotransmitter. Neurotransmitter binding to an ionotropic receptor induces a series of very rapid conformational changes that are translated into an increase in the diameter of the pore, permitting ion influx down their electrochemical gradients. Cation or anion selectivity is obtained through the coordination of specific negatively or positively charged amino acids at strategic locations in the receptor pore. The ion flow ceases when transmitter dissociates from the receptor or when the receptor becomes desensitised (Zigmond, 1999).

### 4.1.4.3 Metabotropic glutamate (mMGlu) receptors

MGlu receptors are G-protein coupled receptors (GPCRs) and have been subdivided into three groups, based on sequence similarity and on biochemical and intracellular signalling mechanisms. The mGluR are similar in general structure (in having seven transmembrane-spanning segments) to other metabotropic receptors. In contrast to ionotropic receptors, each metabotropic receptor is composed of a single polypeptide and exerts its effects through a mechanism differing from that of the ionotropic receptors. The term (metabotropic) describes the fact that intracellular metabolites are produced when these receptors bind ligand. Metabotropic receptors produce their effects by interacting with the family of trimeric G proteins that, when activated, exchange GDP for GTP and activate other intracellular enzymes. These enzymes produce diffusible second messengers (metabolites) that stimulate secondary biochemical processes, including the activation of protein kinases. Transmitters that activate metabotropic receptors typically produce responses of slower onset and longer duration than do ionotropic receptors owing to the series of enzymatic steps necessary to produce

a response. Most small neurotransmitters, such as ACh, glutamate, serotonin, and GABA, can bind to both ionotropic and metabotropic receptors and activate them. Thus, each of these transmitters can induce both fast responses (milliseconds), such as typical excitatory or inhibitory postsynaptic potentials, and slow-onset and longer-duration responses (from tenths of seconds to, potentially, hours (Zigmond, 1999).

### 4.1.4.4 Action of glutamate

A wide range of neurons in different brain regions are excited, particularly by glutamate, though their sensitivities to this amino acid vary and neurons in some regions are quite insensitive (Davidson, 1976; Krnjevic, 1974). Glutamate receptors are very widely distributed and occur on neurons receiving inputs from many other transmitter systems. The glutamate is stored in vesicles in the presynaptic nerve endings; when these presynaptic nerve endings are electrically depolarised, the synaptic vesicles release the glutamate which then diffuses into the synaptic cleft. The glutamate will then bind to the glutamate channel which lies in the postsynaptic membrane; the channel will open, allowing the ions to flow through it and thus depolarise the postsynaptic membrane and excite the postsynaptic nerve. Ultimately, the glutamate dissociates from the binding sites on the channel, the channel closes and the postsynaptic membrane repolarizes (Bradford, 1989).

## 4.1.5. Glutamate in muscle spindles.

### 4.1.5.1 Synaptic vesicles:

As described in previous sections, the primary sensory ending of the mammalian muscle spindle is supplied by a large-diameter (Ia) axon of a dorsal-root ganglion cell. Through a system of preterminal branches, the axon distributes expanded sensory terminals to a small bundle of highly specialised muscle fibres–intrafusal fibres (Banks, 1986; Banks, Barker and Stacey, 1982). Large numbers of vesicles most of which are small and clear vesicles with a mean diameter of 50 nm have been known to exist in these sensory terminals (Adal, 1969). These synaptic like vesicle (SLV) populations have been noted in all types of vertebrate mechanosensory terminal ultrastructure examined (including frog skin, rat atrioventricular junction and human knee-joint capsule) which implies a widespread and important functional role for SLVs in mechanosensory endings. (Halata and Schultze, 1985; Moravec and Moravec 1982; Whitear, 1974). Among these functions could be the storage of amino acid neurotransmitter such as glutamate.

### 4.1.5.2 The evidence of glutamate

Given the similarity of SLV to synaptic vesicles they might be expected to contain a classical neurotransmitter. From Dale's Principle, this should be glutamate — the transmitter at the central synaptic terminals of the Ia afferent (Engberg *et al.*, 1993; Walmsley and Bolton, 1994). In an examination of rat muscle spindles for evidence of elevated intracellular glutamate levels, post-embedding immunocytochemistry was used to examine the rat extensor digitorum brevis primary endings: these were found to contain much greater levels of glutamate (7.65 ± 0.15, 22 gold particles/$\mu m^2$; mean ±

SE, *n*) than adjacent intrafusal (2.08 ± 0.22, *22*) or more distant extrafusal (1.21 ± 0.16, *9*) muscle fibres (Student's t-test; $P<0.001$ in each case). These data, therefore, indicate that SLVs, like synaptic vesicles, contain neuroactive chemicals (Banks *et al.* 2002). In a test to ascertain whether exogenous glutamate affected stretch-evoked spindle discharge the application of 0.1–1mM glutamate to a rat lumbrical muscle reversibly increased spindle discharge frequency 75% above non-treated control levels. This suggests that recycling SLVs may release their contents during exocytosis. Similar findings have been reported for postsynaptic primary afferent terminals of epithelial mechanoreceptors, which contain SLVs and are also immunopositive for glutamate (Banks *et al,* 2002).

### 4.1.6 Detection of glutamate

Selective immunocytochemical visualization of the putative transmitters glutamate (Glu) and γ-aminobutyrate (GABA) by the use of antibodies raised against the amino acids coupled to bovine serum albumin (BSA) with glutaraldehyde (GA) was first reported by Storm-Mathisen and colleagues in 1983.

They found that the tissue localization of Glu-like and GABA-like immmunoreactivities (Glu-LI and GABA-LI) matched those of specific uptake sites for Glu and GABA, and, in the case of GABA-LI, also that of the specific marker enzyme glutamic acid decarboxylase (GAD). Thus GABA-LI was located in what are believed to be GABAergic inhibitory neurons, whereas Glu-LI was concentrated in excitatory, possibly glutamatergic neurones. Electron microscopic observations suggest that the transmitter amino acids are significantly concentrated in synaptic vesicles (Storm-Mathisen *et al*, 1983)

## 4.2 Aim of this study

In a recent study of the rat extensor digitorum brevis, Banks and colleagues found glutamate at the primary nerve endings (Banks *et al*, 2002). This study using cat tenuissimus muscle goes a bit further and detects the density of glutamate-LI in the primary nerve endings together with their adjacent intrafusal fibres and its nuclei, all to be compared with that of the secondary nerve endings and its surrounding intrafusal fibres and its nuclei

## 4.3 Materials and methods

### 4.3.1 Initial preparation

From a cat that had been killed by an overdose of sodium pentobarbitone the tenuissimus muscles were removed after they had been perfused with heparinized Ringer solution, followed by Karnovsky's fixative.

The muscles were then immersed in the same fixative overnight. The tenuissimus muscle is thin so fixative would penetrate evenly; then the following procedure was done.

The muscle was post-fixed in 1% buffered osmium tetroxide (prepared from 2% of osmium tetroxide with an equal volume of 0.2 M sodium cacodylate, pH 7.3) for 4 hours at 4 C°.

The muscles were then dehydrated in a series of alcohols and propylene oxide; finally, the tissue was embedded in araldite.

### 4.3.2 Cross-sectioning

Cross-sections of one muscle to locate one spindle were taken at 1μm semi thin sections to locate the spindle, after which the specimen was sectioned to locate the secondary endings marked by the widening of the periaxial space. When these secondary endings had been reached the specimen was trimmed for ultra-thin sectioning. Sections of secondary endings were then placed on formvar-coated nickel grids.

The same procedure was followed to locate and section the primary endings at the widest periaxial space; again, ultra-thin sections were taken on the same kind of grids as above. Eight grids were taken from the secondary endings as well as the primary; another four were destined to be used as controls.

### 4.3.3 Post embedding immunogold labelling

The post embedding immunogold labelling technique (De Mey, 1983) is very well suited for quantitative studies at the electron-microscopic level. The gold particles are easily identified and counted and, since this labelling is restricted to antigens exposed at the surface of the section (Bendayan, 1993). (Bendayan, Nanci and Kan, 1987), problems related to uneven penetration of the immunoreagents into the different tissue compartments are eliminated. The post-embedding immunogold technique has been utilized in semi-quantitative studies of several neuroactive amino acids (de Jong, Romijn and Buijs, 1987, Ottersen and Bramhan, 1988, Somogyi *et al.*, 1986). The use of a quantitative approach seems particularly important in immunocytochemical studies of glutamate.

### 4.3.4 Immunogold labelling of araldite blocks

#### 4.3.4.1 Immunostaining solutions

The Tris buffer was prepared as follows:

0.242g TRIS (20mM) (MW121.1g)

0.9g NaCl

0.1g BSA

This was made up to 100 ml with milliq water pH 8.2

The above solution was used to fill a 50 ml bottle; the pH was adjusted to 7.2 with 0.1 N HCl. Also added to the 50ml bottle was 0.5 ml of Tween surfactant 20 for each 50ml.

#### 4.3.4.2 Sodium Periodate

Asaturated solution of sodium periodatee was prepared by dissolving some sodium periodate in water, remove lid, as it is an oxidizing agent, store in the dark. This was done on the day before use.

#### 4.3.4.3 Normal Goat Serum 10%

This was inactivated at 56C° for 30 minutes to destroy complement. The solution contained 0.5ml serum + 4.5ml TRIS pH7.4 = 5ml 10%

### 4.3.5 Immunostaining procedure for araldite blocks

The following procedure was used:

1. Sections were collected on formvar-coated grids.

2. The osmicated material was etched for 5min with a saturated solution of sodium periodate. All sections were given exactly the same amount of etching by staggering incubation times.

3. Wash thoroughly with deionised water 5 X 5 mins.

4. Incubated in goat serum in TRIS/BSA pH 7.4 for 30min.

5. Incubated in primary ab rabbit antiglutamate kindly donated by Dr J. B. Leitch 1:2000 in TRIS/BSA ph 7.4 for overnight at 4°C. The Control grids omitted this stage.

6. Washed thoroughly in TRIS/BSA pH 7.4 5 x 5 min.

7. Washed again in TRIS/ BSA pH 8.2, 1 x 5 min.

8. Incubated in secondary ab goat antirabbit IgG 10nm diluted 1:20 in TRIS/BSA pH 8.4 for 1 hour at room temperature.

9. Washed in milliq water.

10. Stained in uranyl acetate and lead citrate for electron microscopy.

#### 4.3.5.1 The control

The control samples were treated with the same steps except step number five, the primary antibody was not applied.

### 4.3.6 Electron Microscopy

All grids were examined using a Philips electron microscope and the gold particles were assessed. On all the grids the gold particles were seen on the primary and secondary nerve endings, the intrafusal and extrafusal fibres, at different concentrations. The control grids showed few particles.

### 4.3.7 Photography

Photographs were taken at magnification of 10,000 from the primary, secondary and control grids a total of 24 photographs were taken.

Care was taken to ensure that photographs covered the entire intrafusal fibre, including the nerve endings, the intrafusal myofibres and their nuclei, and some of the adjacent extrafusal muscle fibres. Representative images are shown Figs 4.1.to 4.4.

### 4.3.8 Computer analysis

All electron micrographs were computer scanned and saved into the Scion program to be enlarged further; then the whole area of the intrafusal muscle fibre primary nerve endings (which included the nerve ending itself, the enclosed intrafusal fibre with its nuclei and the adjacent extrafusal fibres) were measured using Scion program and the data was saved as Excel files.

Fig.4.1.This image shows part of the nerve ending. In the upper section of the micrograph the primary nerve ending show many mitochondria and immunogold labelled glutamate all over the micrograph (see small arrow).

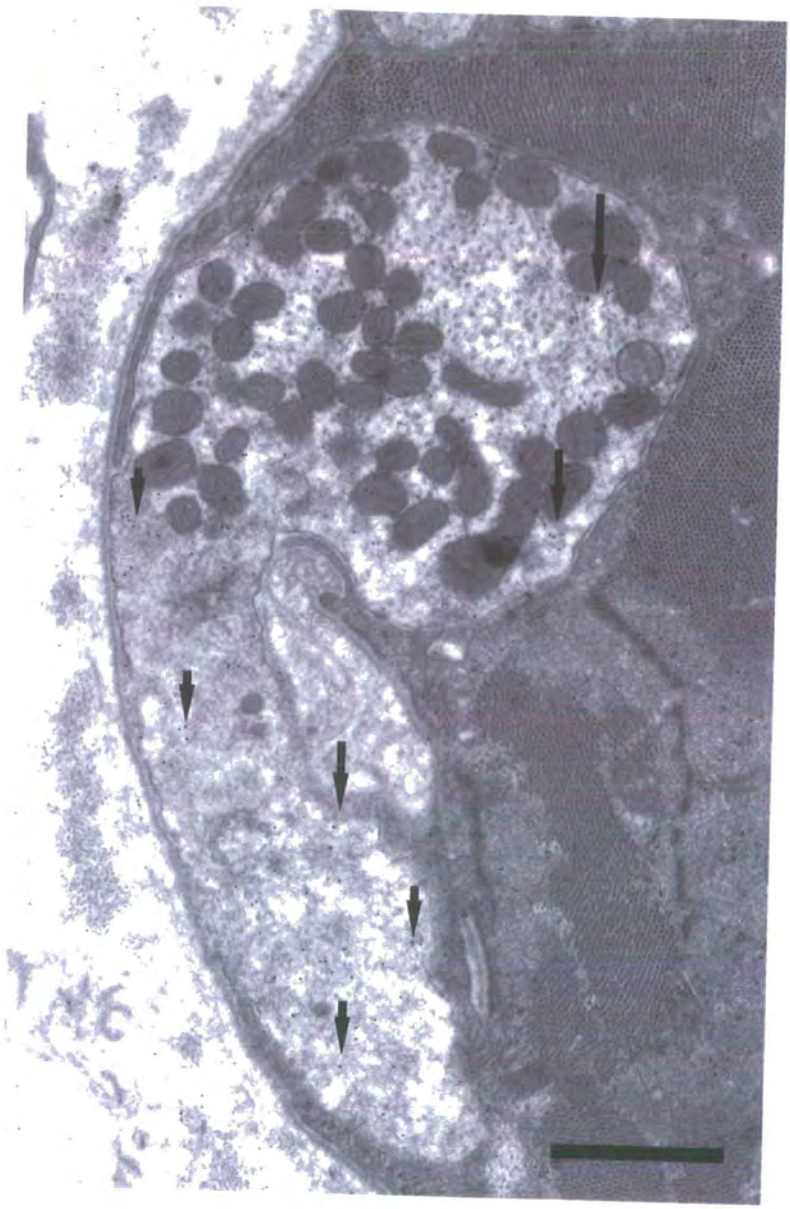

1μ

Fig 4.1

Fig.4.2. Cropped micrograph shows the primary nerve ending with some mitochondria and immunogold labelled glutamate. Fewer immunogold particles are seen outside the nerve ending and in the adjacent intrafusal fibre (see small arrow).

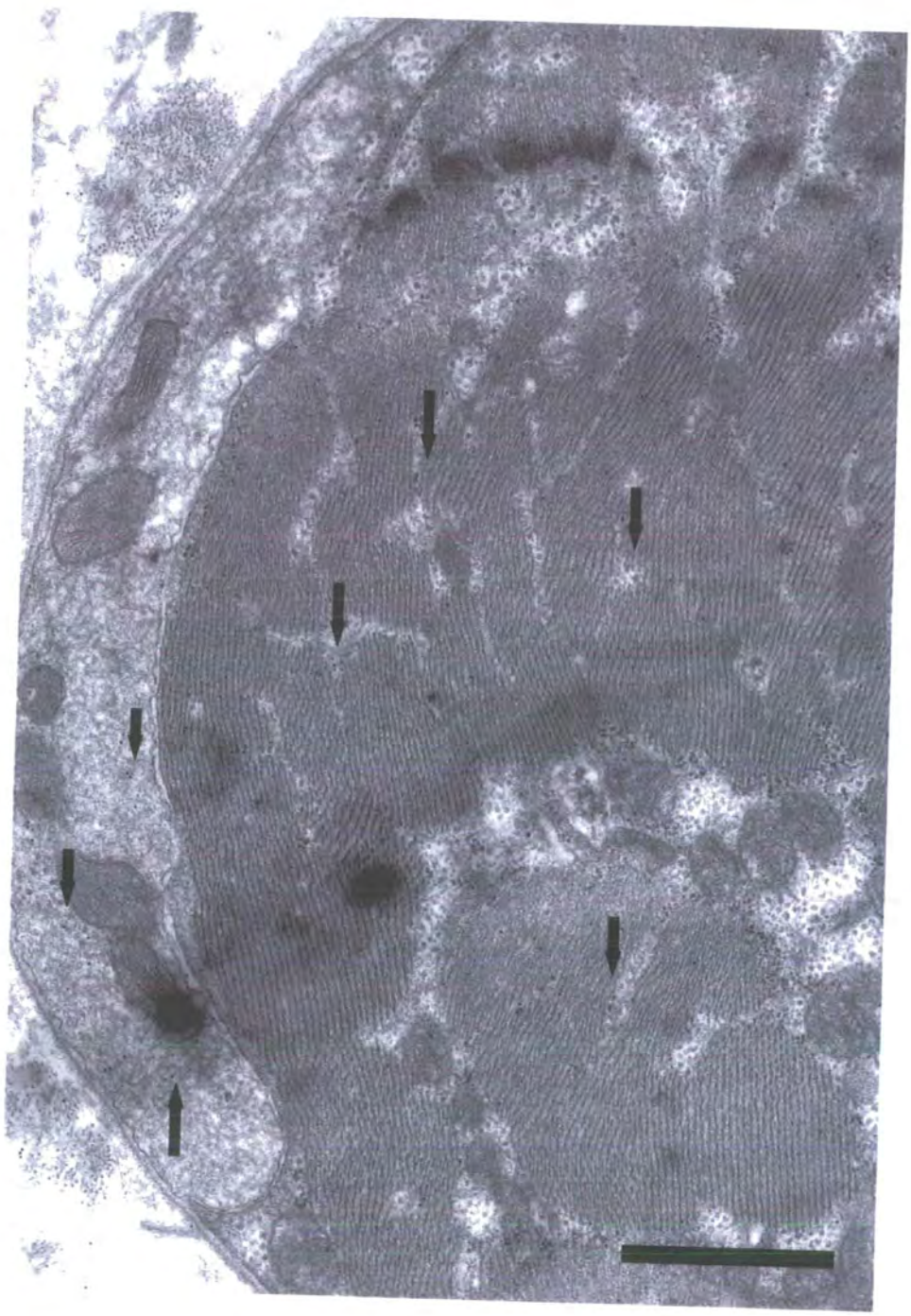

1μ

Fig 4.2

The images were then reopened using Image Tool and the latter was used to count the gold particles in each of the measured areas the counts were then saved in Excel with its corresponding areas.

## 4.4 Results of photographic analysis

### 4.4.1 The controls

The control sections, for which stage 5 of the immunogold labelling (incubation in the primary ab rabbit antiglutamate) had been omitted, showed negligible reactivity.

### 4.4.2 Primary nerve endings

The intrafusal fibre as a whole takes on a circular appearance, and the nerve endings are confined to a crescent shaped area extending around at least one-third of the circumference of the intrafusal fibre.

Glutamate particles are detectable in the nerve endings, showing the same patterns of distribution in and around the mitochondria as in the secondary endings, although less concentrated (see Fig 4.1).

#### 4.4.2.1 Primary intrafusal fibres

Glutamate particles are present across the intrafusal fibre adjacent to the primary nerve endings but to a lesser extent than those seen in the intrafusal fibres adjacent to the secondary nerve endings (see Figs 4.2)

#### 4.4.2.2 Primary intrafusal nuclei.

These contain less glutamate than the area of the primary nerve endings and the intrafusal fibre.

### 4.4.3 Secondary nerve endings

The glutamate particles are more abundant on the secondary nerve endings in comparison with that of the primary nerve endings and particularly in and around the mitochondria and in the body of the nerve ending itself. (See Figs 4.3)

#### 4.4.3.1 Secondary intrafusal

The section of secondary intrafusal fibre (see Fig 4.3, 4.4) shows a greater concentration of glutamate labelling, in comparison with that of the primary intrafusal fibre (see Fig 4.1, 4.2). Glutamate labelling is distributed throughout the fibre but the majority can be seen in the area adjacent to the nerve ending.

#### 4.4.3.2 Secondary intrafusal nuclei.

As in the primary fibres the secondary intrafusal fibre nuclei contain less glutamate labelling than any other area in the secondary nerve endings.

Fig.4.3.This micrograph shows a secondary nerve ending with clusters of mitochondria where most of the immunogold labelling can be seen. Fewer gold particles are seen outside the nerve ending and in the adjacent intrafusal fibre. The secondary nerve ending shows much more labelling density than the primary nerve ending.

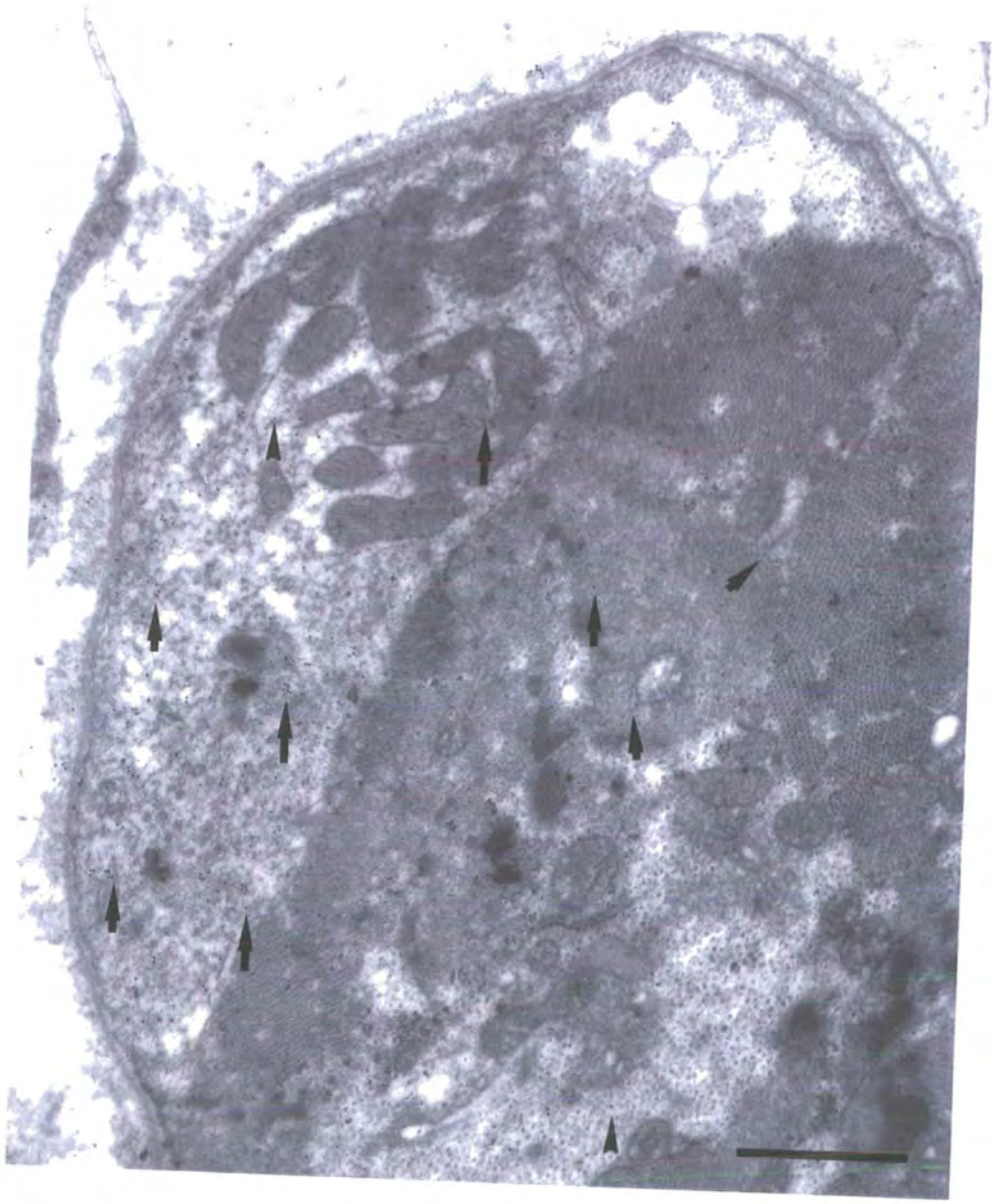

Fig 4.3

iμ

Fig.4.4. This micrograph shows a secondary nerve ending a with greater amount of immunogold labelled glutamate in the nerve ending, adjacent intrafusal fibre and the intrafusal fibre nuclei, where the secondary nerve endings and its surroundings seem to show a greater particle density than in the primary nerve endings and its surroundings.

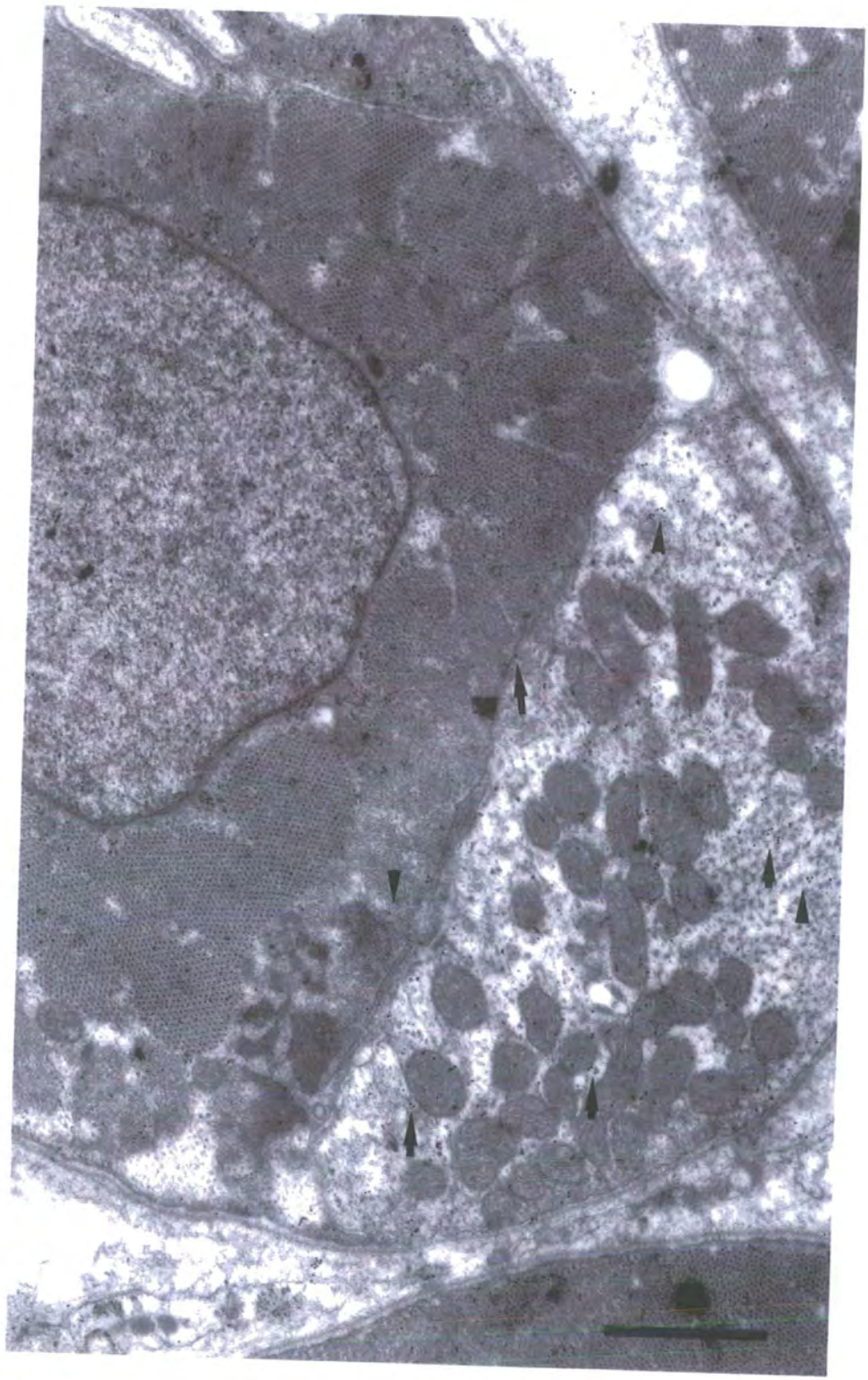

Fig 4.4

1μ

## 4.5 Statistical analysis

Each area was measured in $\mu m^2$ using Scion program and then all gold particles within the area were counted and the data tabulated. Descriptive statistics were calculated and ANOVA was performed on every pair of comparable samples to establish a statistical comparison of glutamate immunoreactivity of different cellular elements in the muscle spindle. Tables 4.1 to table 4.6 are the summaries of the gold particle densities measured in the nerve endings and other subsets of the muscle spindle. Each table is followed by the ANOVA test where P-values are very low indicating real difference in gold-particle densities except in the case of intrafusal nuclei. Table 4.7 is a summary of the average of gold particle counts from the descriptive statistics, together with their standard errors. Chart 4.1 plots the gold particle density according to the average values from the descriptive statistics for the secondary and the primary parts where all secondary parts show a higher density of glutamate except for the nucleus part.

Table 4.1 Immunogold labelled glutamate particles in $\mu m^2$ of the secondary nerve endings vs. primary nerve endings

| sec/nerve.end | prim/nerve.end |
|---|---|
| 21.4 | 6.9 |
| 23.1 | 10.1 |
| 27.1 | 4.3 |
| 19.1 | 10.6 |
| 17.7 | 7.9 |
| 20.1 | 7.9 |
| 26 | 7.8 |
| 14.9 | 10.5 |
| 23.7 | 10.3 |
| 21.6 | 10.7 |
| 20.6 | 6.7 |
| 26.7 | 6.2 |
| 29.4 | 12 |
| 27.2 | 7.4 |
| 14.2 | 8 |
| 2.2 | 13.6 |
| 17.9 | 13.3 |
| 22.8 | 8.9 |
| 17 | 17 |
| 36.1 | 23.3 |
| 34.1 | 13.2 |
| 31.6 | 14.6 |
| | 20 |
| | 19.1 |
| | 15.1 |
| | 20.3 |
| | 20.7 |
| | 18.6 |
| | 18.6 |
| | 12.6 |
| | 12.7 |
| | 3.7 |
| | 6.5 |
| | 11.7 |
| | 3.6 |
| | 8.5 |
| | 2.9 |
| | 19.1 |
| | 8.6 |
| | 3.1 |
| | 2.5 |

Table 4.2 ANOVA for Immunogold labelled glutamate particles per $\mu m^2$ of the secondary nerve endings vs. primary nerve endings

| ANOVA: Two-Factor Without Replication | | | | |
|---|---|---|---|---|
| *SUMMARY* | *Count* | *Sum* | *Average* | *Variance* |
| Row 1 | 2.0 | 28.3 | 14.1 | 104.6 |
| Row 2 | 2.0 | 33.2 | 16.6 | 85.2 |
| Row 3 | 2.0 | 31.4 | 15.7 | 261.4 |
| Row 4 | 2.0 | 29.7 | 14.9 | 35.9 |
| Row 5 | 2.0 | 25.6 | 12.8 | 48.4 |
| Row 6 | 2.0 | 27.9 | 14.0 | 74.0 |
| Row 7 | 2.0 | 33.9 | 16.9 | 165.1 |
| Row 8 | 2.0 | 25.4 | 12.7 | 9.7 |
| Row 9 | 2.0 | 34.0 | 17.0 | 89.3 |
| Row 10 | 2.0 | 32.3 | 16.1 | 59.1 |
| Row 11 | 2.0 | 27.4 | 13.7 | 96.6 |
| Row 12 | 2.0 | 32.8 | 16.4 | 210.9 |
| Row 13 | 2.0 | 41.4 | 20.7 | 151.9 |
| Row 14 | 2.0 | 34.7 | 17.3 | 196.5 |
| Row 15 | 2.0 | 22.2 | 11.1 | 19.5 |
| Row 16 | 2.0 | 15.8 | 7.9 | 65.7 |
| Row 17 | 2.0 | 31.2 | 15.6 | 10.5 |
| Row 18 | 2.0 | 31.7 | 15.8 | 96.5 |
| Row 19 | 2.0 | 34.0 | 17.0 | 0.0 |
| Row 20 | 2.0 | 59.4 | 29.7 | 82.1 |
| Row 21 | 2.0 | 47.3 | 23.7 | 219.3 |
| Row 22 | 2.0 | 46.2 | 23.1 | 143.9 |
| | | | | |
| Column 1 | 22.0 | 494.6 | 22.5 | 55.4 |
| Column 2 | 22.0 | 231.2 | 10.5 | 17.8 |

| ANOVA | | | | | | |
|---|---|---|---|---|---|---|
| *Source of Variation* | *SS* | *df* | *MS* | *F* | *P-value* | *F crit* |
| Rows | 887.7 | 21.0 | 42.3 | 1.4 | 0.240536 | 2.1 |
| **Columns** | **1576.3** | **1.0** | **1576.3** | **50.9** | **4.88E-07** | **4.3** |
| Error | 649.9 | 21.0 | 30.9 | | | |
| | | | | | | |
| Total | 3113.9 | 43.0 | | | | |

Table 4.3 Immunogold labelled glutamate particles per $\mu m^2$ of adjacent intrafusal muscle fibre to the secondary nerve endings vs. the adjacent intrafusal muscle fibre of the primary endings

| intrafusal muscle. | | |
|---|---|---|
| sec/intr.mus | prim/intrf.mus | prim/intrf.mus |
| 6.9 | 2.6 | 3.9 |
| 11.9 | 2.9 | 4.5 |
| 7.2 | 6.2 | 2.5 |
| 6.7 | 6.3 | 2.8 |
| 10.3 | 13.4 | 5.5 |
| 6.3 | 5.7 | 2.0 |
| 7.8 | 7.2 | 5.4 |
| 8.7 | 6.2 | 5.1 |
| 7.7 | 5.6 | 5.6 |
| 10.5 | 5.4 | 4.9 |
| 9.1 | 4.2 | 4.2 |
| 10.2 | 3.0 | 4.7 |
| 8.1 | 6.7 | 6.9 |
| 6.7 | 3.5 | 4.4 |
| 7.6 | 6.5 | 4.7 |
| 9.4 | 3.1 | 7.5 |
| 5.7 | 3.1 | 5.5 |
| 7.3 | 6.0 | 2.3 |
| 5.9 | 10.9 | 17.9 |
| 8.9 | 8.3 | |
| 6.1 | 8.4 | |
| 2.7 | 5.0 | |
| 4.9 | 3.7 | |
| 5.2 | 5.0 | |
| 5.1 | 2.1 | |
| 8.0 | 0.9 | |
| 11.4 | 2.1 | |
| 10.2 | 3.4 | |
| 6.9 | 3.4 | |
| 11.7 | 6.6 | |
| 9.8 | 1.4 | |
| 7.6 | 5.6 | |
| 7.8 | 8.5 | |
| 6.2 | 3.1 | |
| 8.5 | 4.0 | |
| 6.1 | 4.5 | |
| 3.2 | 2.5 | |
| 7.3 | 2.7 | |
| 8.2 | 2.7 | |
| 6.3 | 6.7 | |
| 30.4 | 5.1 | |

Table 4.4 ANOVA of Immunogold labelled glutamate particles per $\mu m^2$ of adjacent intrafusal muscle fibre to the secondary nerve endings vs. the adjacent intrafusal muscle fibre of the primary endings

| ANOVA: Two-Factor Without Replication | | | | |
|---|---|---|---|---|
| *SUMMARY* | *Count* | *Sum* | *Average* | *Variance* |
| Row 1 | 2.0 | 9.6 | 4.8 | 9.3 |
| Row 2 | 2.0 | 14.9 | 7.4 | 40.8 |
| Row 3 | 2.0 | 13.4 | 6.7 | 0.6 |
| Row 4 | 2.0 | 13.1 | 6.5 | 0.1 |
| Row 5 | 2.0 | 23.7 | 11.8 | 5.0 |
| Row 6 | 2.0 | 12.0 | 6.0 | 0.1 |
| Row 7 | 2.0 | 15.0 | 7.5 | 0.2 |
| Row 8 | 2.0 | 14.9 | 7.5 | 3.1 |
| Row 9 | 2.0 | 13.3 | 6.6 | 2.3 |
| Row 10 | 2.0 | 15.9 | 8.0 | 13.5 |
| Row 11 | 2.0 | 13.3 | 6.6 | 11.9 |
| Row 12 | 2.0 | 13.1 | 6.6 | 26.0 |
| Row 13 | 2.0 | 14.8 | 7.4 | 1.0 |
| Row 14 | 2.0 | 10.2 | 5.1 | 5.3 |
| Row 15 | 2.0 | 14.1 | 7.1 | 0.5 |
| Row 16 | 2.0 | 12.5 | 6.2 | 19.8 |
| Row 17 | 2.0 | 8.7 | 4.4 | 3.4 |
| Row 18 | 2.0 | 13.4 | 6.7 | 0.9 |
| Row 19 | 2.0 | 16.7 | 8.4 | 12.6 |
| Row 20 | 2.0 | 17.2 | 8.6 | 0.2 |
| Row 21 | 2.0 | 14.5 | 7.2 | 2.7 |
| Row 22 | 2.0 | 7.8 | 3.9 | 2.6 |
| Row 23 | 2.0 | 8.6 | 4.3 | 0.6 |
| Row 24 | 2.0 | 10.2 | 5.1 | 0.0 |
| Row 25 | 2.0 | 7.2 | 3.6 | 4.6 |
| Row 26 | 2.0 | 8.9 | 4.4 | 25.4 |
| Row 27 | 2.0 | 13.4 | 6.7 | 43.6 |
| Row 28 | 2.0 | 13.6 | 6.8 | 23.1 |
| Row 29 | 2.0 | 10.4 | 5.2 | 6.2 |
| Row 30 | 2.0 | 18.3 | 9.1 | 13.1 |
| Row 31 | 2.0 | 11.2 | 5.6 | 35.5 |
| Row 32 | 2.0 | 13.2 | 6.6 | 1.9 |
| Row 33 | 2.0 | 16.3 | 8.2 | 0.3 |
| Row 34 | 2.0 | 9.3 | 4.7 | 4.9 |
| Row 35 | 2.0 | 12.5 | 6.2 | 9.8 |
| Row 36 | 2.0 | 10.5 | 5.3 | 1.2 |
| Row 37 | 2.0 | 5.7 | 2.8 | 0.3 |
| Row 38 | 2.0 | 10.0 | 5.0 | 10.8 |
| Row 39 | 2.0 | 10.8 | 5.4 | 14.9 |
| Row 40 | 2.0 | 13.0 | 6.5 | 0.1 |
| Row 41 | 2.0 | 35.5 | 17.7 | 322.0 |
| | | | | |
| Column 1 | 41.0 | 336.5 | 8.2 | 17.1 |
| Column 2 | 41.0 | 204.0 | 5.0 | 6.6 |

| ANOVA | | | | | | |
|---|---|---|---|---|---|---|
| *Source of Variation* | *SS* | *df* | *MS* | *F* | *P-value* | *F crit* |
| Rows | 479.2 | 40.0 | 12.0 | 1.0 | 0.464435 | 1.7 |
| **Columns** | **214.1** | **1.0** | **214.1** | **18.4** | **0.000111** | **4.1** |
| Error | 465.8 | 40.0 | 11.6 | | | |
| | | | | | | |
| Total | 1159.1 | 81.0 | | | | |

Table 4.5 Immunogold labelled glutamate particles per $\mu m^2$ of the intrafusal muscle nucleus adjacent to the secondary endings vs. the intrafusal muscle nucleus adjacent to the primary nerve endings

| sec/inte.nuc | prim/interfus/nuc |
|---|---|
| 6.7 | 5.0 |
| 3.9 | 7.1 |
| 4.2 | 4.2 |
| 4.0 | 19.6 |
| 1.2 | 4.3 |
| 3.9 | 3.1 |
| 2.3 | 8.6 |
| 6.6 | 3.0 |
| 5.8 | 3.2 |
| 4.1 | 2.9 |
| 6.4 | 3.1 |
| | 2.3 |

Table 4.6 ANOVA Immunogold labelled glutamate particles per $\mu m^2$ of the intrafusal muscle nucleus adjacent to the secondary endings vs. the intrafusal muscle nucleus adjacent to the primary nerve endings.

| ANOVA: Two-Factor Without Replication | | | | |
|---|---|---|---|---|
| | | | | |
| *SUMMARY* | *Count* | *Sum* | *Average* | *Variance* |
| Row 1 | 2.0 | 11.6 | 5.8 | 1.4 |
| Row 2 | 2.0 | 11.0 | 5.5 | 5.4 |
| Row 3 | 2.0 | 8.3 | 4.2 | 0.0 |
| Row 4 | 2.0 | 23.5 | 11.8 | 121.7 |
| Row 5 | 2.0 | 5.5 | 2.8 | 5.1 |
| Row 6 | 2.0 | 7.0 | 3.5 | 0.3 |
| Row 7 | 2.0 | 11.0 | 5.5 | 20.0 |
| Row 8 | 2.0 | 9.6 | 4.8 | 6.2 |
| Row 9 | 2.0 | 9.1 | 4.5 | 3.4 |
| Row 10 | 2.0 | 6.9 | 3.5 | 0.7 |
| Row 11 | 2.0 | 9.5 | 4.7 | 5.5 |
| | | | | |
| Column 1 | 11.0 | 48.9 | 4.4 | 3.2 |
| Column 2 | 11.0 | 64.2 | 5.8 | 24.2 |

| ANOVA | | | | | | |
|---|---|---|---|---|---|---|
| *Source of Variation* | *SS* | *df* | *MS* | *F* | *P-value* | *F crit* |
| Rows | 114.7 | 10.0 | 11.5 | 0.7 | 0.7 | 3.0 |
| **Columns** | **10.6** | **1.0** | **10.6** | **0.7** | **0.4** | **5.0** |
| Error | 159.1 | 10.0 | 15.9 | | | |
| Total | 284.4 | 21.0 | | | | |

Table 4.7 Summary for glutamate average particles density, in $\mu m^2$ and their standard error for the secondary and the primary parts.

| | nerve.end | intr/mus | inte.nuc |
|---|---|---|---|
| Secn | 22.5 | 8.2 | 4.4 |
| Prim | 11.2 | 5.1 | 5.5 |
| Standard Error.Sec | 1.6 | 0.6 | 0.5 |
| Standard Error.Prim | 0.9 | 0.4 | 1.4 |

Chart 4.1 Glutamate-Like average numbers of gold particles per $\mu m^2$ for the secondary and the primary parts.

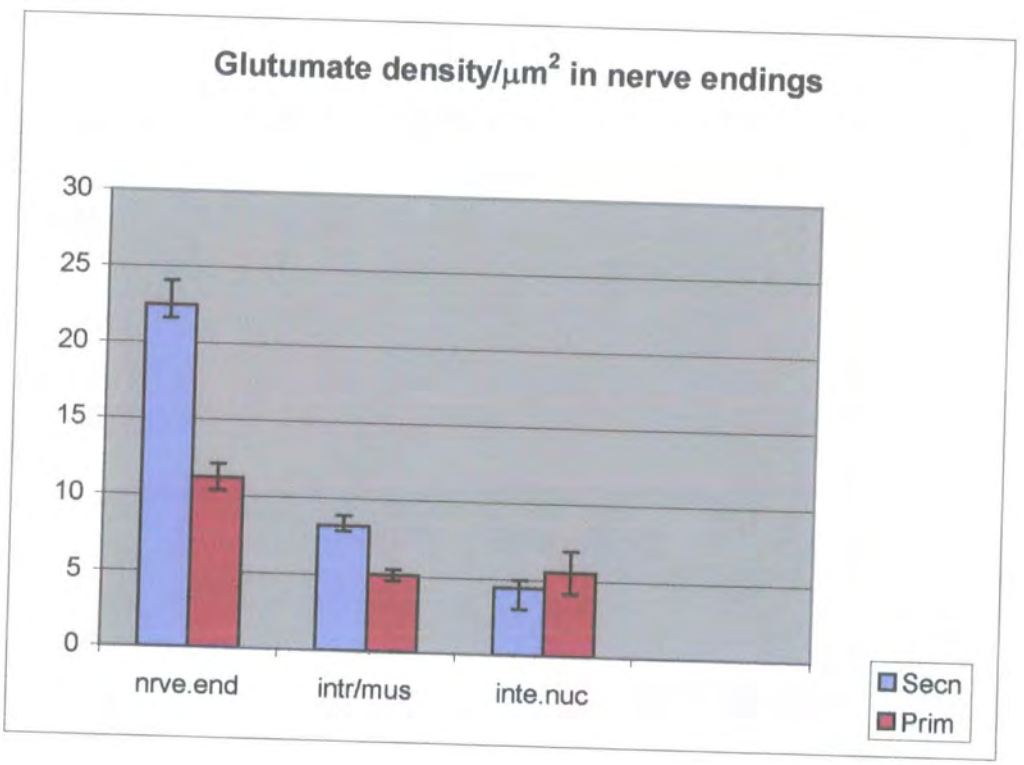

## 4.6 Discussion

Several studies have shown that synaptic vesicles that have been isolated from mammalian brain contain glutamate and aspartate as well as GABA at concentration equal to or higher than those of acetylcholine and other neurotransmitters. (Shank and Campbell, 1983; Fonnum, 1984; De Belleroche, 1973).

Glutamate is widespread throughout the central nervous system and, as an amino acid transmitter, it is considered to have a major excitatory role. It is believed to be important for learning and memory and has been associated with memory-loss disorder, specifically Alzheimer's disease. Moreover, much experimental evidence demonstrates that the release of these excitatory amino acids from both in vivo and isolated neuronal preparation is calcium dependent (Bradford, 1975; Fagg, 1979; Potashner, 1978).

The sensory terminals of muscle spindles also contain similar vesicles, termed synaptic-like vesicles (SLV), but very little is known about their function. Banks and colleagues (Banks *et al*, 2002) presented evidence that SLVs do have a recycling process and that they may release glutamate which has an autogenic excitatory effect on mechanosensory transduction. They also found that this recycling of SLVs is activity dependent and its rate increases in response to high frequency, small-amplitude vibration.

It is known that the removal of extracellular calcium reduces muscle spindle activity (Ottoson, 1976; Westbury, 1985; Turner and Crawford, 1998). Banks' team also found that the SLVs are calcium sensitive and this correlates directly with spindle responsiveness: when external calcium is removed, the SLV recycling is inhibited.

In the same study of rat muscle spindles for evidence of elevated intracellular glutamate levels, post-embedding immunocytochemistry was used to examine the rat extensor digitorum brevis primary endings. This was found to contain much greater levels of

glutamate than the adjacent intrafusal fibres, These findings suggest that SLVs, like synaptic vesicles, contain neuroactive chemicals— in this case glutamate, the major excitatory neurotransmitter of the CNS (Bewick, Reid and Banks, 2000; Banks, Richardson and Bewick, 2000; Banks, Bewick, Reid and Richardson, 2002).

In the present study of glutamate distribution in the cat muscle spindle, post-embedding immunocytochemistry revealed evidence of elevated intracellular glutamate levels in the secondary nerve endings which contain much greater levels of glutamate than their adjacent intrafusal fibres; all these sites contain more glutamate than do the primary nerve endings and their adjacent sites .

# CHAPTER FIVE

## General conclusions and proposal for further study

The muscle spindle is supplied by the Ia afferent which induces the differentiation of the intrafusal muscle fibres. The Ia afferent peripheral terminals occupy the equatorial region of $bag_1$, $bag_2$ and chain fibres over a length of about 350 μm in muscle spindles. The unmyelinated terminals wind around the muscle fibres and in a competitive way occupy the available space, therefore making their own, variable, contribution to the overall form of the primary ending. The $bag_1$ fibre has more terminals, which are most highly branched, their $bag_2$ are intermediate, while chain fibres have fewest and least branched terminals. In 1 μm thin longitudinal sections through the middle of intrafusal muscle fibres the profiles of the sensory terminals appear to be lentiform in shape. The outer and inner (neuromuscular) boundaries of the profiles approximately form segments of circles, with common chord in the plane of the surface of the muscle fibre. In most of the samples measured in this thesis the chords measured approximately 6 μm in $bag_1$ and $bag_2$.

The basal lamina covers the intrafusal muscle fibres and the outer (free) surfaces of the sensory terminals, but there is no intervening basal lamina at the inner (neuromuscular) boundary, so the terminals appear between the cellular and extracellular components of the sarcolemma. Another characteristic of the basal lamina is the absence of dystrophin at the neuromuscular boundary, but it is present elsewhere at the intrafusal muscle-fibre membrane (Nahirney and Ovalle, 1993), in what might be a secondary consequence of the separation of the sarcolemmal components, but an indication to highly localised variations in mechanical properties of both basal lamina and intrafusal fibres.

The profiles of the nerve endings and the structure of the basal lamina suggest a mechanical model of tension transmission from the intrafusal fibres, in which the

terminals are squeezed between inner (cellular) and outer (extracellular) tension-bearing elements. On this hypothesis, the minimum-energy condition (zero tension) would correspond to a circular terminal profile (as the case in the least flexed samples of 869), and that increasing tension would result in an increasingly greater distortion of the nerve ending due the stretch of the surface area of the terminals leading to the lentiform shape (as seen in the stretched control samples of 869). Chapter two of this thesis describes experiments carried out in order to reveal the morphometric changes in the spindles of the cat tenuissimus muscle in particular changes in the sensory nerve endings on the intrafusal fibres of the muscle spindles which might support the above suggestion.

The study examined six tenuissimus muscles from the hind limbs of three cats, which limbs had been placed at different angles thereby producing different degrees of passive stretch of the muscles which were then fixed by perfusion while being secured at these angles. Morphometric changes were noted in the structural features of muscle spindle, including changes in the followings:

- The inner capsule.
- The length of muscle spindle intrafusal sarcomeres.
- The length of adjacent extrafusal sarcomeres.
- The muscle spindle fibre diameters.
- The arrangements of the equatorial nuclei.
- The muscle spindle nerve endings which were the aim of most of investigation in chapter two.

These observations of morphometric changes especially those of the nerve terminals are the first study on cats of such quantitative changes in a big sample.

As the nerve terminals are compressed between longitudinal tension-bearing elements ( i.e. the muscle fibres and their associated basal laminae), so the changes established in the terminals are due to passive stretch of the muscle fibre and the differential

indentation of the sensory terminals into the three type of intrafusal muscle fibres, expressed by the ratios I/C and O/C are in response to passive stretch ( see Fig.2.4), their response to active stretch may be the aim of a future study taking into account the contractile properties of the fibres. The tension-distribution between the inner and outer surfaces of the sensory terminals had resulted in nearly symmetrical development of the lentiform profile of the control (stretched samples) $bag_1$, in comparison with a less symmetrical profile for $bag_2$ where the nerve ending inner boundaries seem to be more indented into the fibre (see 2.5-2.8 diagrams). The arrangement of these sensory terminals in close correlation to the grouping of the underlying myonuclei into nuclear bags and nuclear chains (Banks, Barker and Stacey, 1982) may have to be reconsidered in close association with the nerve endings mechanical model, since it has been observed in this study and previous ones (Karlsson et al., 1970; Banks, 1986) that these accumulations of euchromatic nuclei seem to rearrange themselves as a group in response to the amount of tension exerted on the muscle spindle (see micrographs 2.9 and 2.10). The response was also observed in individual nuclei, which show that they are quite deformable and not rigid.

So the familiarity of these highly unusual accumulations of myonuclei should not obscure the possibility that they might have some role in the overall mechanical properties of the intrafusal fibre.

These findings provide strong support to the suggestion of a mechanical model of transmission from the intrafusal fibre. The evidence for the mechanical model discussed above may lead to the assumption that the mechanical properties of the basal lamina and the sensory terminals are constant throughout the equatorial region. If that is the case, then the range of differential form of the terminals (bulging on the $bag_1$, more indented into the fibre and symmetrical on the $bag_2$, and deeply indented on the chains) must reflect the mechanical properties of the different types of intrafusal muscle fibre.

Evidence of terminal distortion presented in this study and its differential properties, gives a strong indication that longitudinal stretch of the equatorial region leads to a continuously varying receptor potential, generated by the sensory terminals which Hunt and Ottoson (1975) were able to record from single afferent axons (Ia or II) in isolated muscle_spindles of the cat, when the spiking activity of the afferents had been blocked with tetrodotoxin. Hunt and Wilkinson (1978) also showed that the fundamental frequencies of both the receptor potential and the overall tension of the muscle spindle responded similarly to sinusoidal stretch. The depolarization of the sensory terminals presumably results from a conductance change to $Na^+$, produced by stretch deformation and $Ca^{2+}$can partially substitute for $Na^+$. By adopting a systems analytical approach Kruse and Poppele (1991), provided evidence that a $Ca^{2+}$-activated $K^+$ channel contributes to the mid-frequency (0.4 – 4 Hz) dynamics of the primary ending. Under normal conditions, $Ca^{2+}$ makes no significant contribution to the receptor potential, it however does seem to have a key role, which is not yet understood, in regard to the function of the primary ending since the blockage of $Ca^{2+}$ channels by diltiazem or $CoCl_2$ rapidly results in the abolition of spiking activity (Kruse and Poppele, 1991).

The contribution of $Ca^{2+}$ to the receptor potential is further supported by the abundance of $Ca^{2+}$ - binding proteins (CABP) that occur in the nerve endings, including: calbindin D-28k, calretinin, neurocalcin, and in the frog spindles the CABP frequenin, (Hietanen-Peltola *et al.*, 1992; Duc, Barakat-Walter and Droz, 1994; El-Tarhouni and Banks, 1995; Iino, Kobayashi and Hidaka, 1998; Werle, Roder and Jeromin, 2000). CaBPs are a group of homologous proteins that contain a characteristic structure, in the form of pouches for the acceptance of $Ca^{2+}$. All are members of the EF-hand superfamily, representing two families of calcium binding proteins with either 6 or 4 EF-hands, thought to act respectively as $Ca^{2+}$ buffers (calbindin D-28k, calretinin), or $Ca^{2+}$ - activated switches (neurocalcin, frequenin) (Ikura, 1996; Burgoyne and Weiss, 2001).

The distribution of these various proteins differs: all have been found in primary sensory endings; calbindin D-28k also occurs in the intrafusal fibres of rat spindles (Duc *et al* 1994), and calretinin also occurs in the chain fibres of cat spindles, and in cat tendon organs but is absent from secondary endings and from rat tendon organs (Duc *et al.*, 1994; El-Tarhouni and Banks, 1995). The distribution of calretinin in the muscle spindle of the rat soleus muscle was the subject of chapter three of this thesis. The calcium binding-protein calretinin was detected immunohistochemically in the nerve terminals of $bag_1$, $bag_2$ and chain fibres. The soleus muscle of the rat was used with the intention of comparing the outcome with previous results from the study (Duc, Barakat-Walter and Droz, 1994) on the rat and from that study on the cat by El-tarhoni (1996). The results of the present study showed that calretinin is present in the sensory primary nerve endings of all three fibre types, which is in accordance with the results of Duc and colleagues (1994), although differing from the previous observation by El-tarhouni (1996) on the abductor digiti quinti medius (adqm) muscle of the cat by showing no sign of immunostaining of the intrafusal bag or chain fibres themselves. No tendon organs or secondary nerve endings were detected in my samples. Another hint to the role of $Ca^{2+}$ is the detection of glutamate in the muscle spindle in close association with large numbers of small, clear vesicles resembling those of chemical synapses, (Adal, 1969). There is much experimental evidence that the release of excitatory amino acids such as glutamate from both in vivo and isolated neuronal preparations is calcium dependent (Bradford, 1975, Fagg, 1979, Potashner, 1978). The study the dynamics of vesicle release in the (motor) neuromuscular junction using the fluorescent styryl dye FM1-43 to (Betz, Mao and Bewick, 1992) led to the observation that it also stained the sensory endings of muscle spindles, while stimulation of the nerve is necessary to induce uptake of dye into the motor endings, the sensory endings accumulate it spontaneously. The dye appears to be incorporated into the vesicular membranes of

these SLVs in the sensory endings, and it also seems that these vesicles are fusing with the terminal membrane and recycling, and seemingly without any specialized release sites. Evidence has been provided that this process of recycling can be modulated in an activity-dependent manner; and that glutamate is relatively enriched in the sensory terminals; and when applied exogenously glutamate has an excitatory action on muscle-spindle afferents (Banks *et al*, 2002). The SLV recycling shown by FM1-43 correlates directly with spindle responsiveness and itself is $Ca^{2+}$ sensitive hence just like in the synaptic vesicles removal of the external $Ca^{2+}$ inhibited the SLV recycling though it did not block destaining completely so glutamate might be a calcium dependent element in the muscle spindle nerve endings. Chapter 4 describes how glutamate was detected in the nerve terminals of the spindle; the study was carried out using immunogold labelling to evaluate the amount glutamate-like immunoreactivity in the primary and secondary nerve endings, in intrafusal fibres and their nuclei. The study revealed a higher density of gold particles in the secondary nerve endings of the sample chosen from the specimen of extended cat tenuissimus muscle that was used to study morphometric changes. The observation of the nerve endings morphometric changes and the detection of calcium-binding proteins and the great similarity of SLVs to chemical synaptic vesicles, plus the fact that spindle output and SLVs recycling are both enhanced by stretch and sensitive to external calcium level as in the case with synaptic vesicles, which release neurotransmitters by exocytosis, so SLVs also appear to release glutamate by exocytosis, thus enhancing spindle output on mechanical activity. These data may be of use for a future studies to detect an overall mechanism that may involve all the previously mentioned elements and their roles in muscle spindle and sensory endings in general, given the widespread incidence of SLVs.

# REFERENCES


ADAL, M. N. (1969) The fine structure of the sensory region of cat muscle spindles. *J Ultrastruct Res* **26**: 332–354.

AIDLEY, D. J. (1998) *The Physiology of Excitable Cells*. Fourth Edition, chapter 13 pp228-232, chapter **14** pp 254-258 Cambridge University Press.

ANTAL, M., FREUND, T. F., POLGAR, E. (1990) Calcium-binding proteins, parvalbumin and calbindin D 28k-immunoreactive neurons in the rat spinal cord and dorsal root ganglion: a light and electron microscopic study. *J Comp Neurol* **295**: 467–484.

BAIMBRIDGE, K. G., MILLER. J. J., PARKES, C. O. (1982) Calcium-binding protein distribution in the rat brain. *Brain Res* **239**: 519–525.

BAKKER, G. J., RICHMOND, F. J. R. (1981) Two types of muscle spindles in cat neck muscles: a histochemical study of intrafusal fibres composition. *J Neurophysiol* **45**: 973-986.

BAKKER, G. J., RICHMOND, F. J. R. (1982) Muscle spindle complexes in muscles around upper cervical vertebrae in the cat. *J Neurophysiol* **48**: 62–74.

BANKS, R.W. (1983) On the attachment of elastic fibres in cat tenuissimus spindles. *J Physiol* **348**: 16*P*.

BANKS, R. W. (1986) Observations on the primary sensory endings of tenuissimus muscle spindles in the cat. *Cell Tissue Res* **246**: 309–319.

BANKS, R. W., BARKER, D. (1989) Specificities of afferents reinnervating cat muscle spindles after nerve section. *J Physiol* 408: 345–347.

BANKS, R. W., BARKER, D. (2004) The muscle spindle. In *Myology*. 3rd edition (Eds. Engel, A.G., Franzini-Armstrong, C.) McGraw-Hill, New York pp 489-509.

BANKS, R. W., BARKER, D., HARKER, D. W., STACEY, M. J. (1975) Correlations between ultrastructure and histochemistry of mammalian intrafusal muscle fibres. *J Physiol* **252**: 16*P*.

BANKS, R. W., BARKER, D., STACEY, M. J. (1982) Form and distribution of sensory terminals in cat hind limb muscle spindles. *Philos Trans R Soc Lond [Biol]* **299**: 329–364.

BANKS, R.W., BARKER, D., STACEY, M. J. (1985) Form and classification of motor endings in mammalian muscle spindles. *Proc R Soc Lond [Biol] 225*: 195–212.

BANKS, R.W., BEWICK, G. S., REID, B., RICHARDSON, C. (2002) Evidence for activity dependent modulation of sensory terminal excitability in spindles by glutamate release from synaptic-like vesicles. *Advances in Experimental Medicine and Biology.* **508:** 13-18.

BANKS, R. W., EMONET-DENAND, F. (1996) Characteristic properties of superficial lumbrical spindles in the cat hind limb, related to their $bag_1$ fibres. *J Anat* **189**: 65–71.

BANKS, R.W., JAMES, N. T. (1973) The blood supply of rabbit muscle spindles. *J Anat* **114**:7–12.

BANKS, R. W., JAMES, N. T. (1975) Rabbit intrafusal muscle fibres. *J Anat* **119**: 193.

BANKS, R. W., STACEY, M. J, HARKER. D.W. (1977) A study of mammalian intrafusal muscle fibres using a combined histochemical and ultrastructural technique. *J Anat* **123**: 783 –796.

BARKER, D. (1974) The morphology of muscle receptors. In Hunt C. C. (ed): *Muscle Receptors, Handbook of Sensory Physiology,* vol **3**, Pt 2. Berlin, Springer-Verlag, pp 1-190.

BARKER, D., BANKS, R. W. (1994) The muscle spindle. In *Myology* Vol.**1**, 2nd edition (Eds. Engel, A.G., Franzini-Armstrong, C.), McGraw-Hill, NewYork, pp 333–360.

BARKER, D., BANKS, R. W., HARKER, D. W., MILBURN, A., STACEY, M. J. (1976) Studies of the histochemistry, ultrastructure, motor innervation and regeneration of mammalian intrafusal muscle fibres. In Homma, S. (ed), *Understanding the Stretch Reflex, Prog Brain Res,* vol **44**. Amsterdam, Excerpta Medica, pp 67-88.

BARKER, D., EMONET-DENAND, F., HARKER, D.W., JAMI, L., LAPORTE, Y. (1977) Types of intra-and extrafusal muscle fibre innervated by dynamic skeletofusimotor axons in cat peroneus brevis and tenuissimus muscle, as determined by the glycogen-depletion method. *J Physiol* 266: 713–726.

BARKER, D., IP, M. C. (1961) A study of single and tandem types of muscle spindle in the cat. *Proc R Soc Lond [Biol]* **154**: 377–397.

BARKER, D., STACEY, M. J., ADAL, M. N. (1970) Fusimotor innervation in the cat. *Philos Trans R Soc Lond [Biol]* **258**: 315–346.

BEESLEY, J. E. (1995) *Immunohistochemistry A practical Approach 2*: Oxford University Press, Oxford. pp 17–18.

BENDAYAN, M., NANCI, A., KAN, F. W. K. (1987) Effect of tissue processing on colloidal gold cytochemistry. *J Histochem Cytochem* **35:** 983–996.

BENDAYAN, M., ZOLLINGER, M. (1983) Ultrastructural localisation of antigenic sites on osmium–fixed tissues applying the protein A- Gold technique. *J Histochem Cytochem* **31:** 101–109.

BENDEICH, E.G., KARLSSON, U. L., HOOKER, W.M, (1971) Quantitative changes in the frog muscle spindle with passive stretch. *J Ultrastruct Res* **36**: 743–756.

BESSOU, P., LAPORTE, Y. (1962) Responses from primary and secondary endings of the same neuromuscular spindle of the tenuissimus muscle of the cat. In *Symposium on Muscle Receptors*, ed. Barker, D. pp.105-19. Hong Kong, Hong Kong University Press.

BETZ, W. J., MAO, F., BEWICK, G. S. (1992) Activity-dependent fluorescent staining and destaining of living vertebrate motor nerve terminals. *J Neurosci* **12**: 363–375.

BLUMCKE, I., HOF, P. R., MORRISON, J. H., CELIO, M. R. (1990) Distribution of parvalbumin immunoreactivity in the visual cortex of Old World monkeys and humans. *J Comp Neurol* **301**: 417– 432.

BOYD, I. A. (1962) The structure and innervation of the nuclear bag muscle fibre system and the nuclear chain muscle fibre system in mammalian muscle spindles. *Philos Trans R Soc Lond [Biol]* **245**: 81–136.

BOYD, I. A. (1976) The response of fast and slow nuclear bag fibres in isolated cat muscle spindles to fusimotor stimulation, and the effect of intrafusal contraction on the sensory endings. *Quart J Exp Physiol* **61**: 203–254.

BOYD, I. A., GLADDEN, M. H. (eds) (1985) *The Muscle Spindle.* Proceedings of a Symposium on The Mammalian Muscle Spindle held in Glasgow in 1984. London: Macmillan.

BOYD, I. A., GLADDEN, M. H., McWILLIAM, P. N., WARD, J. (1975) "Static" and "dynamic" nuclear bag fibres in isolated cat muscle spindle. *J Physiol* **250**:11*P.*

BOYD, I. A., SMITH, R. S. (1984) The muscle spindle. In Dyck, P. J., Thomas, P. K., Lombert, E. H., Bunge, R. (eds): *Peripheral Neuropathy* 2nd ed. San Francisco, Saunders, pp 171–202.

BRADFORD, H. F. (1975) In *Handbook of Pychopharmacology*, vol. 1, (eds. C. C. Iversen, S. D. Iversen, and S.H. Synder), pp.191-252. Plenum Press, New York.

BRADFORD, H. F. (1989) *Chemical Neurobiology.* Freeman, New York, pp 211–229.

BRAUN, K. (1990) Calcium-binding proteins in avian and mammalian central nervous system: Localization, development and possible function. *Prog Histochem Cytochem* **21**: 1–64.

BRIDGMAN, C. F., SWEENEY, S., ELDRED, E. (1966) The effects of contraction and stretch of a muscle on the morphology of its spindles. *Anat Rec* **156**: 67-81.

BROWN, M. C., CROWE, A., MATTHEWS, P. B. C. (1965) Observations on the fusimotor fibres of the tibialis posterior muscle of the cat. *J Physiol* **177**: 140-159.

BRZEZINSKI, D. K. von (1961) Untersuchungen zur Histochemie der Muskelspindeln.II Mitteilung: Zur Topochemie und Funktion des Spindelraumes und der Spindelkapsel. *Acta Histochem (Jena)* **12**: 277–288.

BURGOYNE, R. D., WEISS, J. L. (2001) The neuronal calcium sensor family of $Ca^{2+}$-binding proteins. *Biochem J* **353**: 1–12.

CELIO, M. R., BAIER, W., SCHARER, L., GREGERSEN, H. J., VIRGAH, PA de, NORMAN, A.W. (1990). Monoclonal antibodies directed against the calcium binding protein calbindin D-28k. *Cell Calcium* **11**: 599-602.

CELIO, M. R., HEIZMANN, C. W. (1981) Calcium-binding protein paravalbumin as a neuronal marker. *Nature* **293**: 300–302.

CHARD, P. S., BLEAKMAN, D., MILLER, R. J. (1991) Parvalbumin is an intracellular $Ca^{+}$ buffering protein. *Soc Neurosci Abstr* **17**: 343.

CHEUNG, W. Y. (1980) Calmodulin plays a pivotal role in cellular regulation. *Science* **207**: 19–27.

CHRISTAKOS, S., FRIEDLANDER, J., FRANDSEN, B. R., NORMAN, A.W. (1979) Studies on the mode of action of calciferol. XIII. Development of radioimmunoassay for vitamin D-dependent chick intestinal calcium –binding protein and tissue distribution. *Endocrinology* **104**:1495–1503.

CLARKE, P. G. H. (1989) Developmental cell death: morphological diversity and multiple mechanisms. *Anat Embryol* **263**:1–19.

COOPER, S. (1961) The response of the primary and secondary endings of muscle spindles with intact motor innervation during applied stretch. *Quart J Exp Physiol* 46: 389-398.

COOPER, S., DANIEL, P. M. (1956) Human muscle spindles. *J Physiol* **133**: 1–3.

COOPER, S., DANIEL, P. M. (1967) Elastic tissue in muscle spindles of man and the rat *J Physiol* **192**: 10–11*P*.

COOPER, S., GLADDEN, M. H. (1974) Elastic fibres and reticulin of mammalian muscle spindles and their functional significance. *Quart J Exp Physiol* **59**: 367–386.

CROUCH, E. (1969) *Text-atlas of Cat Anatomy*, Lea & Febiger. Philadelphia. p 107.

CROWE, A., MATTHEWS, P.B.C. (1964) The effect of stimulation of static and dynamic fusimotor fibres on the response to stretching of the primary endings of muscle spindles. *J Physiol* **174**: 109-131

DAVIDSON, N. (1976) *Amino Acid Neurotransmitters*. Academic Press, London and New York.

DAVIS, H. (1961) Some principles of sensory receptor action. *Phsiol Rev* **41**: 391-416

DE JONG, B. M., ROMIJN, H. J., BUIJS, R. M. (1987) Postembedding immunocytochemical GABA. Labelling in rat neurocortex cultures: applicability in quantitative studies. *Neurosoci Lett* **75**: 23–30.

DE BELLEROCHE, J. S., BRADFORD, H. F. (1973) Amino-acids in synaptic vesicles from mammalian cerebral cortex –reappraisal. *J Neurochem* **21**: 441–445.

de FELIPE, J., HENDRY, S. H. C., HASHIKAWA, T., MOLINARI, M., JONES E. G. (1990) A microcolumnar structure of monkey cerebral cortex revealed by immunocytochemical studies of double bouquet cell axon. *Neuroscience* **37**: 655–673.

DE MEY, J. R. (1983) The preparation of immunoglobulin gold conjugates (ICS reagents and their use as markers for light and electron microscopic immunocytochemistry. In *Immunohistochemistry* (ed. Cuello, A.C.), pp. 347–372. New York, John Wiley & Sons.

DIAMOND, J., GRAY, J. A. B., INMAN, D. R. (1958) The relation between receptor potential and the concentration of sodium ions. *J Physiol* **142**: 382-394.

DIWAN, F. H., MILBURN, A. (1986) The effects of temporary ischaemia on rat muscle spindles. *J Embryol Exp Morph* **92**: 223–254.

DOW, P. R., SHINN, S. L., OVALLE, W. K. (1980) Ultrastructural study of a blood: muscle spindle barrier after systemic administration of horseradish peroxidase. *Am J Anat* **157**: 375–388.

DUC, C., BARAKAT-WALTER, I., DROZ, B. (1994) Innervation of putative rapidly adapting mechanoreceptors by calbindin- and calretinin-immunoreactive primary sensory neurons in the rat. *Europ J Neurosci* **6**: 264–271.

EDWARDS, C., OTTOSON, D., RYDQVIST, B., SWERUP, C. (1981) The permeability of the transducer membrane of the crayfish stretch receptor to calcium and to other divalent cations. *Neuroscience* **6**: 1455-1460.

EL-TARHOUNI, A. (1996) Studies on the mechanosensory innervation of the muscle using organotypic culture, reinnervation and immunohistochemistry. Thesis, University of Durham **4**: 111–112.

EL-TARHOUNI, A., BANKS, R.W. (1995) The distribution of calretinin in muscle receptors of the cat. *J Physiol 487*: 77*P*.

EMONET-DENAND, F., HUNT, C. C., LAPORTE, Y. (1985) Effects of stretch on dynamic fusimotor after-effect in cat muscle spindle .*J Physiol* **360**: 201-213.

ENGBERG, I., TARNAWA, I., DURAND, J., OUARDOUZ, M. (1993) An analysis of synaptic transmission to motoneurons in the cat spinal cord using a new selective receptor blocker. *Acta Physiol Scand* **148**: 97–100.

ERXLEBE, C. (1989) Stretch-activated current through single channels in the abdominal stretch receptor organ of the crayfish. *J Gen Physiol* 94: 1071-1083.

FAGG, G. E., LANE, J. D. (1979) Uptake and release of putative amino-acid neurotransmitters. *Neuroscience* **4**: 1015-1036.

FONNUM, F. (1984) Glutamate-a neurotransmitter in mammalian brain. *J Neurochem* **42**:1–11.

FUKAMI, Y. (1986) Studies of capsule and capsular space of cat muscle spindles. *J Physiol* **376**: 281–297.

FURNESS, J. B., LLEWELLYN, I. J., BORNSTEIN, J. C., COSTA, M. (1988) Chemical neuroanatomy and analysis of neuronal circuitry in the enteric nervous system. In: Bjorklund, A., Hökfelt, T., Owman, C (eds) *Handbook of Chemical Neuroanatomy.* Elsevier, Amsterdam,: pp 161–218.

GARCIA SEGURA, L. M., BAETENS, D., ROTH, J., NORMAN, A. W., ORCI, L. (1984) Immunohistochemical mapping of calcium binding protein immunoreactivity in the rat central nervous system. *Brain Res* **297**: 75–86.

GERFEN, C. R., BAIMBRIDGE, K. G., MILLER, J. J. (1985) The neostriatal mosaic: compartmental distribution of calcium-binding protein and parvalbumin in the basal ganglia of the rat and monkey. *Proc Natl Acad Sci* USA **82**: 8780–8784.

GLADDEN, M. H. (1976) Structural features relative to the function of intrafusal muscle fibres in the cat. In *Understanding the Stretch Reflex* (ed. Homma, S.), *Prog Brain Res* **44**: 51–59. Amsterdam, Excerpta Medica.

GOLGI, C. (1880) Sui nervi di tendini dell'uomo e di altri vertebrati di un nuovo organo nervoso terminale musculo- tendineo . *Mem Rog Accad Sci Torino* **32:** 359-385.

GREGOR, A. (1904) Ueber die Vertheilung der Muskelspindeln in der Musculatur des menschlichen Fötus. *Arch Anat Physiol* Anat Abt: (no volume number given):112-191.

HALATA, Z., RETTIG, T., SCHULTZE, W. (1985) The ultrastructure of sensory nerve endings in the human knee joint capsule. *Anat Embryol* **172**: 265–275.

HEIZMAN, C. W., HUNZIKER, W. (1991) Intracellular calcium-binding proteins: more sites than insights. *Trends Biochem Sci* **16**: 98–103.

HOOKER, W. M., BENDEICH, E. G., KARLSSON, U. (1976) Muscle surface deformation in the stretched sensory zone of the frog muscle spindle. *J Ultrastruct Res* **57**: 204–210.

HÖKFELT, T. (1992) Neuropeptides in perspective: the last ten years. *Neuron* **7**: 867-879.

HIETANEN-PELTOLA, M., PELTO-HUIKKO, M., RECHARDT, L., EMSON, P., HÖKFELT, T. (1992) Calbindin-D-28k-immunoreactivity in rat muscle spindle; a light and electron microscopic study. *Brain Res* **579**: 327–332,

HUNT, C. C., WILKINSON, R. S., FUKAMI, Y. (1978) Ionic basis of the receptor potential in primary endings of mammalian muscle spindles. *J Gen Physiol* **71**: 683–698.

HUNT, C. C., OTTOSON, D. (1975) Impulse activity and receptor potential of primary and secondary endings of isolated mammalian muscle spindles. *J Physiol* **252:** 259 –281.

IINO, S., KOBAYASHI, S., HIDAKA, H. (1998) Neurocalcin-immunopositive nerve terminals in the muscle spindle, Golgi tendon organ and motor endplate. *Brain Res* **808**: 294–299.

IKURA, M. (1996) Calcium binding and conformational response in EF-hand proteins. *Trends Biochem Sci* **21**:14–17.

JAMI, L. (1992) Golgi tendon organs in mammalian skeletal muscle: Functional properties and central actions. *Physiol Rev* **72**: 623–666.

JAMI, L., LAN-COUTON, D., MALMGREN, K., PETIT, J. (1978) 'Fast' and 'slow' skeletofusimotor innervation in cat tenuissimus spindles: a study with the glycogen depletion method. *Acta Physiol Scand* **103**: 284–298.

JAMI, L., LAN-COUTON, D., MALMGREN, K., PETIT, J. (1979) Histophysiological observations on fast skeletofusimotor axons. *Brain Res* **164**: 53–59.

JAMI, L., MURTHY, K. S. K., PETIT, J. (1982) A quantitative study of skeletofusimotor innervation in the rat peroneus tertius muscle. *J Physiol* **325**: 125-144.

JANDE, S. S., MALER, L., LAWSON, D. E. M. (1981) Immunohistochemical mapping of vitamin D-dependant calcium–binding protein in brain. *Nature* **294**: 766–767.

JONES, E. G., HENDRY, S. H. C. (1989) Differential calcium binding protein immunoreactivity distinguishes classes of relay neurons in monkey thalamic nuclei. *Europ J Neurosci* **1**: 222–246.

KARLSSON, U., HOOKER, W. M., BENDEICH. E. G, (1971) Quantitative changes in the frog muscle spindle with passive stretch. *J Ultrastruct Res* **36**: 743-756.

KATZ, B. (1950) Action potentials from a sensory nerve ending. *J Physiol* 111: 248-260.

KRNJEVIC, K. (1974) Chemical nature of synaptic transmission in vertebrates. *Physiol Rev* **54**: 418–540.

KENNEDY, W. R., QUICK, D. C., REESE, T. R. (1979) Freeze-fracture of muscle spindles. *Abs Soc Neurosci* **5**: 304.

KENNEDY, W. R., WEBSTER, H. de F., YOON, K. S. (1975) Human muscle spindle: Fine structure of the primary sensory endings. *J Neurocytol* **4**: 675–695.

KENNEDY, W. R., YOON, K. S. (1979) Permeability of muscle spindle capillaries and capsule. *Muscle Nerve* **2**: 101–108.

KOHR, G., LAMBERT, C. E., MODY, I. (1991) Calbindin –D28K (CaBP) levels and calcium currents in acutely dissociated epileptic neurons. *Exp Brain Res* **85**: 543–551.

KOHR, G., MODY, I. (1991) Endogenous intracellular calcium buffering and the activation / inactivation of HVA Calcium currents in rat dentate gyrus granule cells. *J Gen Physiol* **98**: 941–967.

KRETSINGER, J. H., MONCRIFF, N. D., GOODMAN, M., CZELUSNIAK, J. (1988) Homology of calcium modulated proteins: Their evolutionary and functional

relationships. In Morad, M., Nayler, W., Kazda, S., Schramm (Eds) *The Calcium Channel Structure. Function and Implication*. Berlin: Springer-Verlag, **16**.

KRUSE, M. N., POPPELE, R. E. (1991) Components of the dynamic response of mammalian muscle spindles that originate in the sensory terminals. *Exp Brain Res* **86**: 359-366.

KUCERA, J. (1980) Myofibrillar ATPase activity of intrafusal fibres in chronically de-afferented rat muscle spindles. *Histochemistry* **66**: 221–228.

KUCERA, J. (1982) Morphometric studies on tenuissimus muscle spindles in the cat. *J Morphol* **171**: 137-150.

KUCERA, J., WALRO, J. M. (1987) Postnatal maturation of spindles in deafferented rat soleus muscles. *Anat Embryol* **176**: 449–461.

KUCERA, J., WALRO, J. M., GORZA, L. (1992) Expression of type-specific MHC isoforms in rat intrafusal muscle fibres. *J Histochem Cytochem* **40**: 293–307.

KUCERA, J., WALRO, J. M., REICHLER, J. (1988) Motor and sensory innervation of muscle spindles in the neonatal rat. *Anat Embryol* **177**: 427–436.

LANDON, D. N. (1966a). Electron microscopy of muscle spindles. In *Control and Innervation of Skeletal Muscle* (ed. Andrew, B. L.), pp. 96–111. Edinburgh, Churchill: Livingstone.

LANDON, D. N. (1966b). The fine structure of the annulospiral sensory nerve endings in the muscle spindles of the rat. *J Physiol* **185**: 6–7*P*.

LEHKY, P., BLUM, H. E., STEIN, E. A., FISHER, E. H. (1974) Isolation and characterization of paravalbumin from skeletal muscle of higher vertebrates. *J Biol Chem* **249**: 4332– 4334.

LI, Z., DECAVEL, C., HATTON, G. I. (1995) Calbindin D28k: role in determining intrinsically generating firing patterns in rat supraoptic neurons. *J Physiol* **488**: 601–608.

LOW, F. N. (1976) The perineurium and connective tissue of peripheral nerve. In Landon, D. N. (ed): *The Peripheral Nerve.* London, Chapman & Hall, pp 159–187.

MARIEB, N. (2001) Human *Anatomy and Physiology.* (Fifth edition) p.475 New York, Addison Wesley Longman.

MATTHEWS, P. B. C. (1962) The differentiation of two types of fusimotor fibre by their effects on the dynamic response of muscle spindle primary endings. *Quart J Exp Phsiol* **47**: 324-333.

MATTHEWS, P. B. C. (1972). *Mammalian Muscle Receptors and their Central Action.* Arnold. London.

MERRILLEES, N. C. R. (1960) The fine structure of muscle spindles in the lumbrical muscles of the rat. *J Biophys Biochem Cytol* **7**: 725–740.

MIETTINEN, R., GULYAS, A. I., BAIMBRIDGE, K. G., JACOBWITZ, D. M., FREUND, T. F. (1992) Calretinin is present in non-pyramidal cells of the rat hippocampus. 2. Co-existence with other calcium-binding proteins and GABA. *Neuroscience 48*: 29–43.

MIZE R. R., LUO, Q., BUTLER, G. D., JEON, C. J., NABROS, B. (1992) The calcium binding proteins parvalbumin and calbindin–D 28k form complementary patterns in the cat superior colliculus. *J Comp Neurol* **320**: 243–256.

MOEWS, P G., KRETZENGER, R. H. (1975) Refinement of the structure of carp muscle calcium-binding protein parvalbumin by model building and different Fourier analysis. *J Mol Biol* **91**:201–228.

MORAVEC, M., MORAVEC, J. (1982) Presence of mechanoreceptors in the atrioventricular junction of the rat heart: Microanatomical and ultrastructural evidences. *J Ultrastruct Res* **81**: 47–65.

MORGAN, D. L., PROCHAZKA, A., PROSKE, U. (1984) The after–effects of stretch and fusimotor stimulation on the responses of the primary endings of cat muscle spindles. *J Physiol* **356**: 465-477.

NAHIRNEY, P. C., OVALLE, W. K. (1993) Distribution of dystrophin and neurofilament protein in muscle spindles of normal and mdx-dystrophic mice: an immunocytological study. *Anat Rec* **235**: 501-510.

OHM, T. G., MULLER, H., ULFIG, N., BRAAK, E. (1990) Glutamic-acid-decarboxylase-and parvalbumin–like immunoreactive structure in the olfactory bulb of the human adult. *J Comp Neurol* **291**: 1–8.

OHM, T. G., MULLER, H., ULFIG, N., BRAAK, E. (1991) Calbindin D-28-like immunoreactive structure in the olfactory bulb and the anterior olfactory nucleus of the human adult: distribution and cell typology-partial complementarity with parvalbumin. *Neuroscience* **42**: 823–840.

OTTERSEN, O. P., BRAMHAM, C. R. (1988) Quantitative electron microscopic immunocytochemistry in different cell types and processes in rat cerebellum: an electronic study based on a postembeding immunogold labelling procedure. *Anat Embryol* **178**: 407– 421.

OTTOSON, D. (1976) Morphology and physiology of muscle spindles. In Llinas, R., Precht, W. (Eds) *Frog Neurobiology*, Springer-Verlag, Berlin.

OTTOSON, D., SHEPHERD, G. M. (1968) Changes of length within frog muscle spindle during stretch as shown by stroboscopic photomicroscopy. *Nature* **220**: 912-914.

OVALLE, W. K. (1971) Fine structure of rat intrafusal muscle fibres: the polar region. *J Cell Biol* **52**: 382–396.

OVALLE, W. K., SMITH, R. S. (1972) Histochemical identification of three types of intrafusal muscle fibres in the cat and monkey based on the myosin ATPase reaction. *Can J Physiol Pharmacol* **50**: 195-202.

PARMENTIER, M. (1990) Structure of the human cDNAs and genes coding for calbindin D 28k and Calretinin. In Pochet, R., Lawson, D. E. M., Heizmann, C.W. (Eds) *Calcium Proteins in Normal and Transformed Cell.* New York: Plenum Press pp27-34.

PHILIPPE, E., DROZ, B. (1988) Expression of calbindin by chick dorsal root ganglion cells. Ontogenesis and cytological characteristics of the immunoreactive sensory neurons. *Neuroscience* **26**: 215–224.

POPPELE, R. E., KENNEDY, W. R., QUICK, D. C. (1979) A determination of static mechanical properties of intrafusal muscle in isolated cat muscle spindles. *Neuroscience* **4**: 401-411.

POTASHNER, S. J. (1978).Effects of tetrodotoxin, calcium and magnesium on release of amino-acids from slices of guinea-pig cerebral cortex. *J Neurochem* **31**: 187–195.

PROSKE, U. (1997) The muscle spindle. *News Physiol Sci* **12**: 37–42.

QUICK, D. C. (1984) Freeze-fracture of sensory nerve endings in cat muscle spindles. *J Neurocytol* **13**: 975–987.

REN, K., RUDA, M. A., JACOBOWITZ, D. M. (1993) Immunohistochemical localization of calretinin in the dorsal root ganglion and spinal cord of the rat. *Brain Res Bull* **31**: 13–22.

RESIBOIS, A., BLACHIER, F., ROGERS, J. H., LAWSON, D. E. M., POCHET, R. (1990) Comparison between rat brain calbindin and calretinin immunoreactivity. In *Calcium Binding Proteins in Normal and Transformed Cells.* (Eds Pochet, R., Lowson, D. E. M., Heizmann, C.W.). New York: Plenum Press, pp211–214.

RESIBOIS, A., ROGER, J. H. (1992) Calretinin in rat brain; an immuno-histochemical study. *Neuroscience* **46**: 101–134.

RICHMOND, F. J. R., ABRAHAMS, V. C. (1975) Morphology and distribution of muscle spindles in dorsal muscles of the cat neck. *J Neurophysiol* **38**: 1322-1339.

ROGERS, J. H. (1987) A gene for a novel calcium binding protein expressed principally in neurons. *J Cell Biol* **105**: 1343–1353.

ROGERS, J. H. (1989). Immunoreactivity of calretinin and other calcium-binding proteins in cerebellum. *Neuroscience* **31**: 711–721.

ROGERS, J. H. (1991) Calretinin. In *Novel Calcium Binding Proteins.* (Ed Heizmann, C.W.) Springer, Berlin. pp251–276.

ROGERS, J. H. (1992a). Immunohistochemical marker in rat cortex: colocalization of calretinin and calbindin D28k with neuropeptides and GABA. *Brain Res* **587**: 147-157.

ROGERS, J. H. (1992b). Immunohistochemical marker in rat brain: colocalization of calretinin and calbindin D28k with tyrosine hydroxylase. *Brain Res* **587**: 203–210.

ROGERS, J. H., KHAN. M., ELLIS, J. (1990) Calretinin and other CaBPs in the nervous system. *Adv Exp Med Biol* **269**: 195–203.

RUFFINI, A. (1893) Sur la terminaison nerveuse dans les faisceux musculaires et leur signification physiologique. *Archs Ital Biol* **18**: 106–114.

RUFFINI, A. (1898) On the minute anatomy of the neuromuscular spindles of the cat, and on their physiological significance. *J Physiol* **23**: 190-208.

SCHANNE, F. A. X., KANE, A. B., YOUNG, E. E., FARBER, J. L. (1979) Calcium dependence of toxic cell death: a final common pathway. *Science* **206**: 700–702.

SCHARFMANN, H. E., SCHWARTZKROIN, P. A. (1989) Protection of dentate hilar cells from prolonged stimulation by intracellular calcium chelation. *Science* **246**: 257–260.

SCHWALLER, B., BUCHWALD, P., BLUMCKE, I., CELIO, M. R., HUNZIKER., W. (1993) Characterisation of a polyclonal antiserum against the purified human recombinant calcium binding protein calretinin. *Cell Calcium* **14**: 639–648.

SHANK, R. P., CAMPBELL, G. LEM. (1983). In *Handbook of Neurochemistry* 2d ed, vol. 3 (ed. A. Lajtha,), pp. 381– 404. Plenum Press, New York.

SHEPHERD, G. M. (1983) *Neurobiology*. Oxford, New York.

SLOVITER, R. S. (1989) Calcium binding protein (Calbindin-D28k) and parvalbumin immunocytochemistry: localisation in the rat hippocampus with specific reference to the selective vulnerability of hippocampal neurons to seizure activity. *J Comp Neurol* 280: 183–196.

SOMOGYI, P., HALASY, K., SOMOGYI, J., STORM-MATHISEN, J., OTTERSEN, O. P. (1986) Quantification of immunogold labelling reveals enrichment of glutamate in mossy parallel fibre terminals in cat cerebellum. *Neuroscience* **19**: 1045–1050.

STICHEL, C. C., SINGER, W., HEIZMANN, C. W., NORMAN, A. W. (1987) Immunohistochemical localization of calcium binding proteins, parvalbumin and calbindin –D 28k, in the adult and developing visual cortex of cats: a light and electron microscopy study. *J Comp Neurol* **262**: 563–577.

STORM–MATHISEN, J., LEKENS, A. K., BORE, A. T., VAALAND, J. L., EDMINSON, P., HAUG, F. M. S., OTTERSON O. P. (1983) First visualization of glutamate and GABA in neurons by immunocytochemistry. *Nature* **30**: 517-520.

TAYLOR, A. N. (1974) Chick brain CaBP: comparison with intestinal vitamin D-induced CaBP. *Archs Biochem Biophys.***161**: 100–108.

TURNER, C. R., CRAWFORD, A. C. (1998) Components of the current activated by stretch at the isolated muscle spindle of the frog. *J Physiol* **506**: 82*P*.

VAN BREDERODE, J. F. M., HELLIESEN, M.K., HENDRICKSON, A. E. (1991). Distribution of calcium binding proteins, parvalbumin and calbindin D 28k, in the sensorimotor cortex of the rat. *Neuroscience* **44**: 157–171.

VOSS, H. (1971) Tabelle der absoluten und relativen Muskelspindelzahlen der menschlichen Skelettmuskulatur. *Anat Anz* **129**: 562-572.

WALMSLEY, B., BOLTON, P. S. (1994) An *in vivo* pharmacological study of single group Ia fibre contacts with motoneurones in the cat spinal cord. *J Physiol* **481**: 731–741.

WALRO, J. M., KUCERA, J. (1985a) Motor innervation of intrafusal fibres in rat muscle spindles: incomplete separation of dynamic and static systems. *Am J Anat* **173**: 55–68.

WALRO, J. M., KUCERA, J. (1985b) Rat muscle spindles deficient in elements of static system. *Neuroscience Letters* **59**: 303–307.

WALRO, J. M., KUCERA, J. (1987) Sharing of sensory terminals between the dynamic $bag_1$ and static $bag_2$ fibres in the rat muscle spindle. *Brain Res* **425**: 311-318.

WASSERMAN, R. H., TYLOR, A. N. (1966) Vitamin D3- induced calcium binding – protein in chick intestinal mucosa. *Science* **152**: 791–793.

WATKINS, J.C. (1980) NMDA receptors – new light on amino acid-mediated synaptic excitation. *Trends Neurosci.* **3**: 61–64.

WESTBURY, D. R. (1985) Evidence for the importance of calcium activated potassium conductance in frog muscle spindle sensory endings. In Boyd, I.A., Gladden, M.H. (Eds) *The Muscle Spindle* pp 359–363. Macmillan Press, London.

WEISMAN, A. ( 1861) Uber das wachsen quergestreiften Muskel nac Beobachtungen am Frosch. *Z. Rat Med* **10**: 263–284.

WERLE, M. J., RODER, J., JEROMIN, A. (2000) Expression of frequenin at the frog (Rana) neuromuscular junction, muscle spindle and nerve. *Neuroscience Letters* **284**: 33-36

WHITEAR, M. (1974) The vesicle population in frog skin nerves. *J Neurocytol* **3**: 49-58.

YELLIN, H. (1969) A histological study of muscle spindles and their relationship to extrafusal fibre types in the rat. *Am J Anat* **125**: 31-45.

ZIGMOND, J. M. (1999) *Fundamental Neuroscience*. Academic Press, New York.